FRONTIERS IN OCEAN OBSERVING

MARINE PROTECTED AREAS, WESTERN BOUNDARY CURRENTS, AND THE DEEP SEA

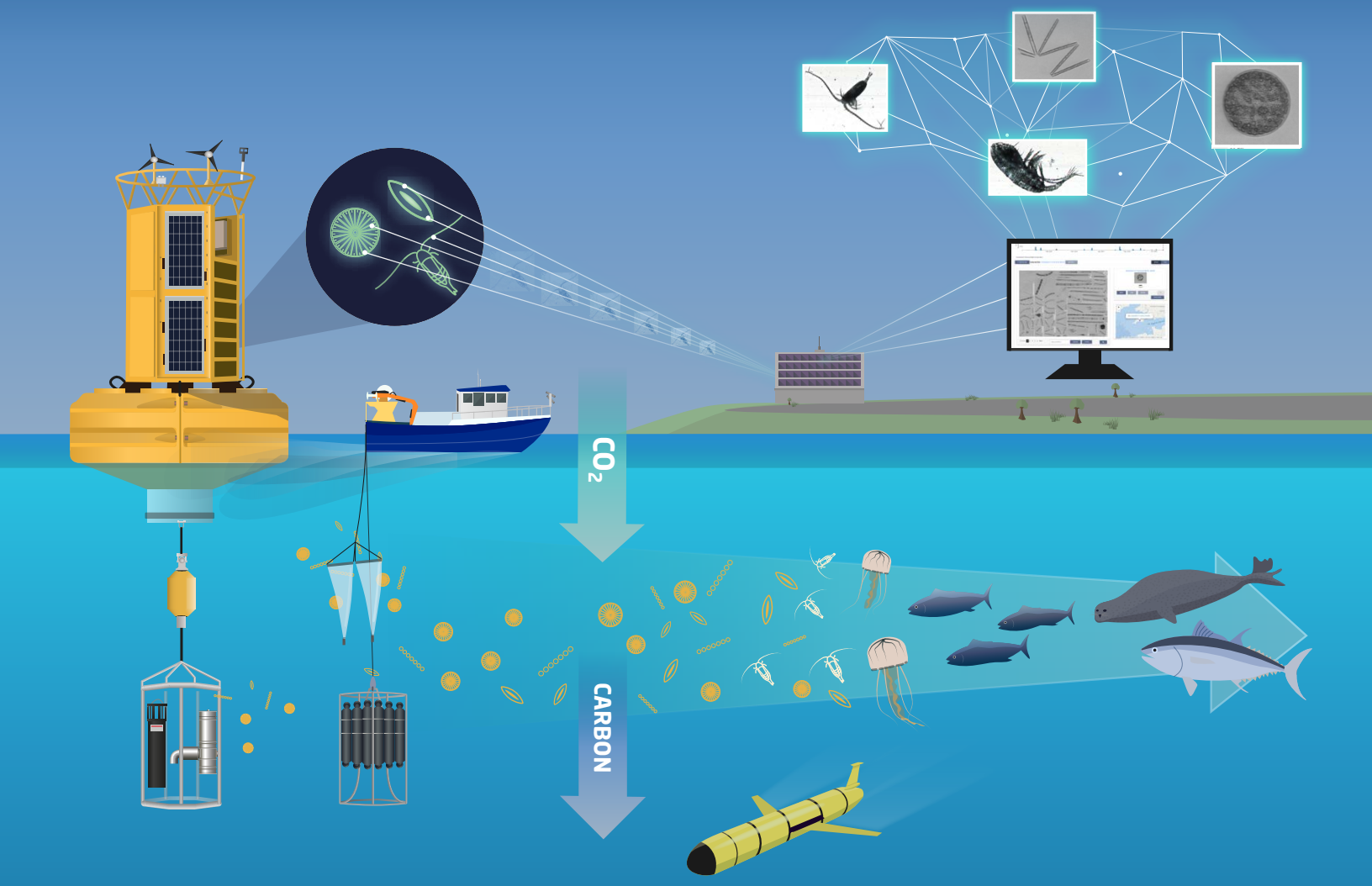

2025 *Oceanography* Supplement

ON THE COVER

Future ocean observing within marine protected areas may include traditional sampling by ships at intervals augmented by continuous data collection of a wide range of variables by a variety of sensors, where the data are transmitted to laboratories in real time for analysis. *Figure modified from Clark et al. (2025, in this issue). Illustration by Jon White, Plymouth Marine Laboratory*

ABOUT THIS PUBLICATION

Support for this publication is provided by Ocean Networks Canada, the National Oceanic and Atmospheric Administration's Global Ocean Monitoring and Observing Program, and the Partnership for Observation of the Global Ocean.

PRINT: ISSN 1042-8275
ONLINE: ISSN 2377-617X
PUBLISHED BY: The Oceanography Society
DATE: April 2025

PREFERRED CITATION

Kappel, E.S., V. Cullen, G. Coward, I.C.A. da Silveira, C. Edwards, T. Morris, and M. Roughan, eds. 2025. *Frontiers in Ocean Observing: Marine Protected Areas, Western Boundary Currents, and the Deep Sea*. *Oceanography* 38(Supplement 1), https://doi.org/10.5670/oceanog.2025.s1.

CONTENTS

WESTERN BOUNDARY CURRENTS AND THEIR IMPACTS ON SHELF SEAS

TECHNOLOGICAL SOLUTIONS FOR AN ACCESSIBLE DEEP OCEAN

INTRODUCTION TO FRONTIERS IN OCEAN OBSERVING

MARINE PROTECTED AREAS, WESTERN BOUNDARY CURRENTS, AND THE DEEP SEA

By Ellen S. Kappel

In this third and final "Frontiers in Ocean Observing" supplement to *Oceanography*, peer-reviewed articles describe data collection and analysis from the surface ocean to the seafloor, spanning the globe from marine protected areas to western boundary currents and the deep sea. They describe a variety of technologies used to collect and analyze ocean observations, including emerging sonar technology for high-resolution mapping and imaging of the seafloor, low-cost tools combined with artificial intelligence to monitor blue carbon in Greenland's deep sea, and the integration of eDNA, acoustic, and trawl data to investigate the diversity, abundance, biomass, and distribution of micronekton in the Western Indian Ocean.

Other articles describe how autonomous vehicles such as gliders now assist with management of marine protected areas, detection and protection of North Atlantic right whales, forecasting of harmful algal blooms, investigation of marine heatwaves, and augmentation of the network for ocean animal tracking. They also detail, for example, how ocean scientists are obtaining long-term data on western boundary currents to augment other more traditional data collection methods with approaches that include partnering with a merchant marine container vessel to collect data on the Gulf Stream and a collaborative project between researchers and industry that uses commercial fishing gear to collect subsurface ocean data in the East Australian Current. Another article considers how the observations collected in western boundary currents, in particular, the East Australian Current, impact ocean forecasts, a useful assessment for improving ocean observing system design.

Similar to the first two ocean observing supplements (see https://tos.org/ocean-observing), we invited potential authors to submit letters of interest associated with topics aligned with the priorities of the UN Decade of Ocean Science for Sustainable Development (2021–2030). The chosen topics for this supplement are described below.

MODEL-BASED DESIGN AND EVALUATION OF OBSERVING NETWORKS

Here, the authors describe and apply model-based methods for methodically evaluating existing integrated ocean observing systems and future extensions by exploring process-focused array design, observation priorities, and sampling strategies; complementarity versus redundancy of multi-platform networks; and detectable changes in key climate metrics.

THE USE OF AUTONOMOUS TOOLS FOR ECOSYSTEM MANAGEMENT AND MONITORING OF MARINE PROTECTED AREAS

Authors addressing this topic demonstrate how sensors on autonomous vehicles are filling critical gaps in ocean biological and spatial conservation knowledge that will help tackle ecosystem-level challenges caused by global environmental changes.

WESTERN BOUNDARY CURRENTS AND THEIR IMPACTS ON SHELF SEAS

These articles showcase long-term, sustained observational efforts in western boundary current shelf sea regions that highlight strengths, weaknesses, and gaps in the system, and/or provide examples of end-user and stakeholder engagement.

TECHNOLOGICAL SOLUTIONS FOR AN ACCESSIBLE DEEP OCEAN

This section provides recent examples of how the intersections among cutting-edge sensors, including low-cost technologies, data analytics, and robotics, are advancing deep-sea exploration and opening avenues for discoveries and a deeper understanding of our planet's least-explored realms.

Many thanks to Ocean Networks Canada, the US National Oceanic and Atmospheric Administration's Global Ocean Monitoring and Observing Program, and the Partnership for Observation of the Global Ocean for generously supporting publication of this supplement to *Oceanography*. I would also like to thank all the supplement's guest editors for their valuable input and guidance on articles submitted to their thematic areas.

AUTHOR

Ellen S. Kappel (ekappel@geo-prose.com), *Oceanography* Editor and Geosciences Professional Services Inc., Bethesda, MD, USA.

ARTICLE DOI. https://doi.org/10.5670/oceanog.2025e120

MODEL-BASED DESIGN AND EVALUATION OF OBSERVING NETWORKS

MODEL-BASED OBSERVING SYSTEM EVALUATION IN A WESTERN BOUNDARY CURRENT: OBSERVATION IMPACT FROM THE COHERENT JET TO THE EDDY FIELD

By Colette Kerry, Moninya Roughan, Shane Keating, and David Gwyther

ABSTRACT

Ocean forecast models rely on observations to provide regular updates in order to correctly represent dynamic ocean circulation. This synthesis of observations and models is referred to as data assimilation. Since initial conditions dominate the quality of short-term ocean forecasts, accurate ocean state estimates, achieved through data assimilation, are key to improving prediction. Western boundary current (WBC) regions are particularly challenging to model and predict because they are highly variable. Understanding how specific observation types, platforms, locations, and observing frequencies impact model estimates is key to effective observing system design.

The East Australian Current (EAC), the South Pacific's WBC, is a relatively well-observed current system that allows us to study the impact of observations on prediction across different dynamical regimes, from where the current flows as a mostly coherent jet to the downstream eddy field. Here we present a review of the impact of observations on model estimates of the EAC using three different methods. Consistent results across the three approaches provide a comprehensive understanding of observation impact in this dynamic WBC. Observations made in regions of greater natural variability contribute most to constraining the model estimates, and subsurface observations have a high impact relative to the number of observations. Significantly, sampling the downstream eddy-rich region constrains the upstream circulation, whereas observing the upstream coherent jet provides less improvement to downstream eddy field estimates. Studies such as these provide powerful insights into both observing system design and modeling approaches that are vital for optimizing observation and prediction efforts.

INTRODUCTION

Accurate estimates of past, present, and future ocean states are crucial to effective management of our ocean environment and marine industries. Short-term ocean predictions (days to weeks) are vital to myriad environmental, societal, and economic applications, including facilitating the adaptive management of marine ecosystems, forecasting extreme weather events, predicting the onset and persistence of marine heatwaves, providing accurate ocean forecasts for shipping and military operations, predicting the fate of pollutants, and guiding search and rescue operations.

Ocean state estimates require the combination of numerical models and ocean observations, referred to as data assimilation (DA). Observations provide sparse data points while the model provides dynamical context. The goal of DA is to combine the model with observations to reduce uncertainty in the model estimate. For forecasting purposes, model estimates are updated through assimilation when observations become available and provide improved initial conditions for the next forecast (Figure 1). Due to the dynamic nature of the ocean circulation, ocean models must be regularly updated through DA to, for example, correctly represent the timing and locations of oceanic eddies (e.g., Thoppil et al., 2021; Chamberlain et al., 2021).

A critical component of the DA problem is the way by

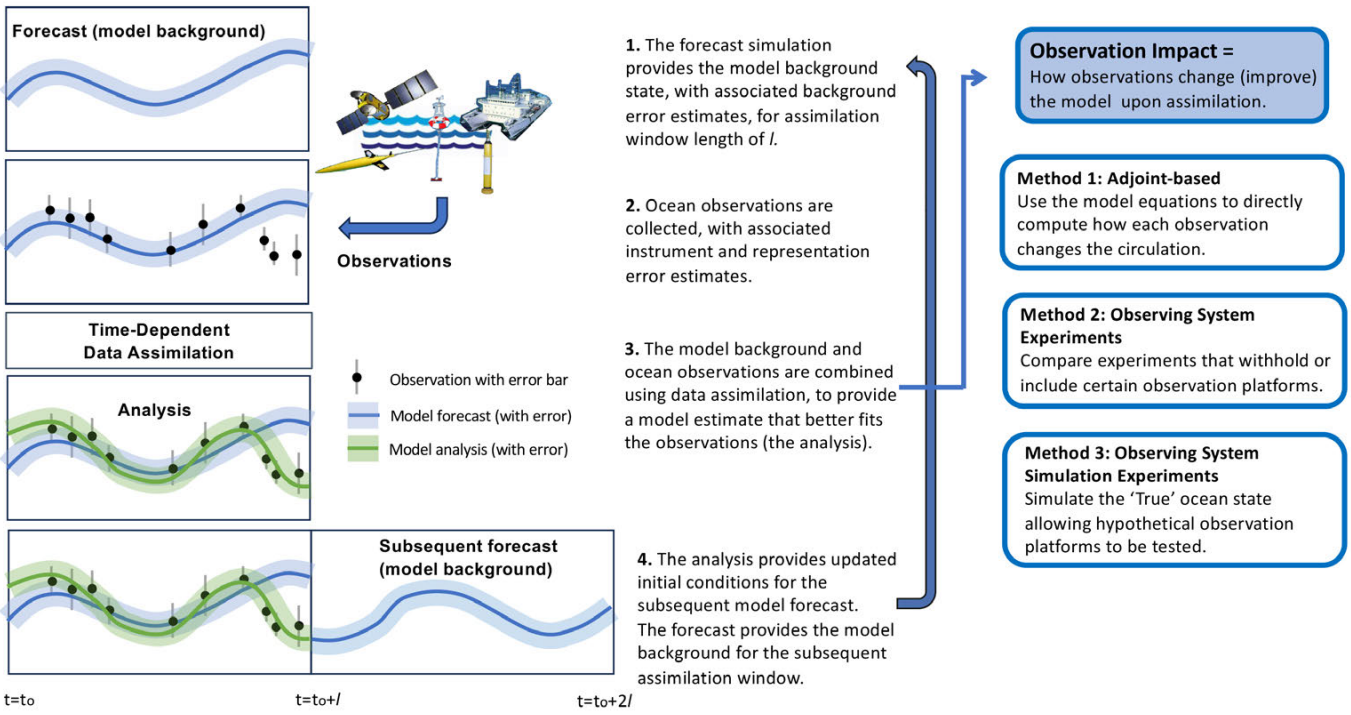

FIGURE 1. Conceptual schematic showing sequential time-dependent data assimilation and a summary of the three methods presented in this study for assessing observation impact.

which the information contained in the observations is projected onto the (unobserved) model state estimate. Advanced DA techniques use time-variable model dynamics to actively interpolate information from observations up- and downstream and forward and backward in time. Observations are assimilated over a time interval, given the temporal evolution of the circulation (e.g., Moore et al., 2020). Identifying observations that best constrain an ocean model can drive improved observing system design for more accurate and more cost-effective prediction. Observation impact studies aim to quantify how specific observation types, locations, and observing frequencies impact model estimates (e.g., Oke et al., 2015).

In this article, we assess observation impact in a dynamic western boundary current (WBC). WBCs are swift, poleward-flowing currents that exist on the western sides of subtropical ocean gyres. They transport warm water from the tropics toward the poles, redistributing heat and modulating global climate. Mesoscale eddies form due to instabilities in the strong boundary current flow, making WBC extension regions hotspots of high eddy variability (Imawaki et al., 2013; Li et al., 2022a). WBCs typically exhibit the highest errors in ocean forecasts (e.g., Brassington et al., 2023) due to their strong flows, the complexities of eddy shedding and evolution (e.g., Kang and Curchitser, 2013; Pilo et al., 2015; Yang et al., 2018), and their complex vertical structures (e.g., Sun et al., 2017; Pilo et al., 2018; Brokaw et al., 2020; Rykova and Oke, 2022). Understanding the interplay of observing system design and modeling approaches is crucial to improving prediction in highly dynamic, eddy-rich oceanographic environments.

The East Australian Current (EAC) is the WBC of the South Pacific subtropical gyre, and its eddies dominate the circulation along the southeastern coast of Australia (Figure 2a; Oke et al., 2019). The southward-flowing current is most coherent off 28°S (Sloyan et al., 2016) and intensifies around 29°–31°S (Kerry and Roughan, 2020). The current typically separates from the coast between 31°S and 32.5°S, turning eastward and shedding large warm-core eddies in the Tasman Sea (Cetina Heredia et al., 2014). The EAC is a relatively well-observed WBC system, with observations collected as part of Australia's Integrated Marine Observing System (IMOS; Figure 2b–d) spanning from the coherent jet to the eddy field (e.g., Roughan et al., 2015). The EAC therefore provides an ideal testbed for assessing observation impact across differing dynamical regimes.

Observing networks, numerical models, and DA schemes make up the key components of ocean prediction systems. Data-assimilating models are useful for evaluating and designing observing networks. Here we synthesize the results from three different model-based approaches in order to assess observation impact across a common system (the EAC). We use three methods for studying observation impact: an adjoint-based approach to directly quantify

observation impact, Observing System Experiments (withholding observations), and Observing System Simulation Experiments (Figure 1). This review summarizes the key results obtained through each method, and synthesizes the consistent results to provide a broad understanding of observation impact along the extent of the WBC system.

ASSESSING OBSERVATION IMPACT

THE SOUTH EAST AUSTRALIAN COASTAL FORECAST SYSTEM

The South East Australian Coastal Forecast System (SEA-COFS) consists of several Regional Ocean Modeling System (ROMS; Shchepetkin and McWilliams, 2005) configurations at a range of resolutions for the southeast Australian oceanic region. The EAC-ROMS regional model (domain shown in Figure 2a) has a 2.5–5 km horizontal resolution, with higher resolution over the continental shelf and slope, and 30 terrain-following vertical layers (Kerry et al., 2016; Kerry and Roughan, 2020).

We constrain the model with observational data from a variety of traditional and novel observation platforms using four-dimensional variational DA (4D-Var). This technique uses variational calculus to solve for increments in model initial conditions, boundary conditions, and forcing such that the differences between the new model solution of the time-evolving flow and all available observations is minimized—in a least-squares sense—over an assimilation window (Figure 1; Moore et al., 2004, 2011). Here we use five-day assimilation windows. The goal is for the model to represent all of the observations in time and space using the physics of the model, and accounting for the uncertainties in the observations and background model state, to produce a description of the ocean state that is a dynamically consistent solution of the nonlinear model equations. For this mesoscale eddy-dominated system, adjustments to the initial conditions dominate over boundary or surface forcing adjustments and forecast errors are dominated by errors in the initial state (Kerry et al., 2020).

Observation impact is studied based on a data-assimilating configuration of the EAC-ROMS model for 2012–2013 (Kerry et al., 2016), when numerous data streams were available through IMOS (Figure 2b,c). These included velocity and hydrographic observations from a deep-water mooring array (the EAC array; Sloyan et al., 2016) and continental shelf moorings (Malan et al., 2021; Roughan et al., 2022), radial surface velocities from a high-frequency (HF) radar array (Archer et al., 2017), and hydrographic observations from ocean gliders (Schaeffer et al., 2016). These observations complemented the more traditional data streams of satellite-derived sea surface height

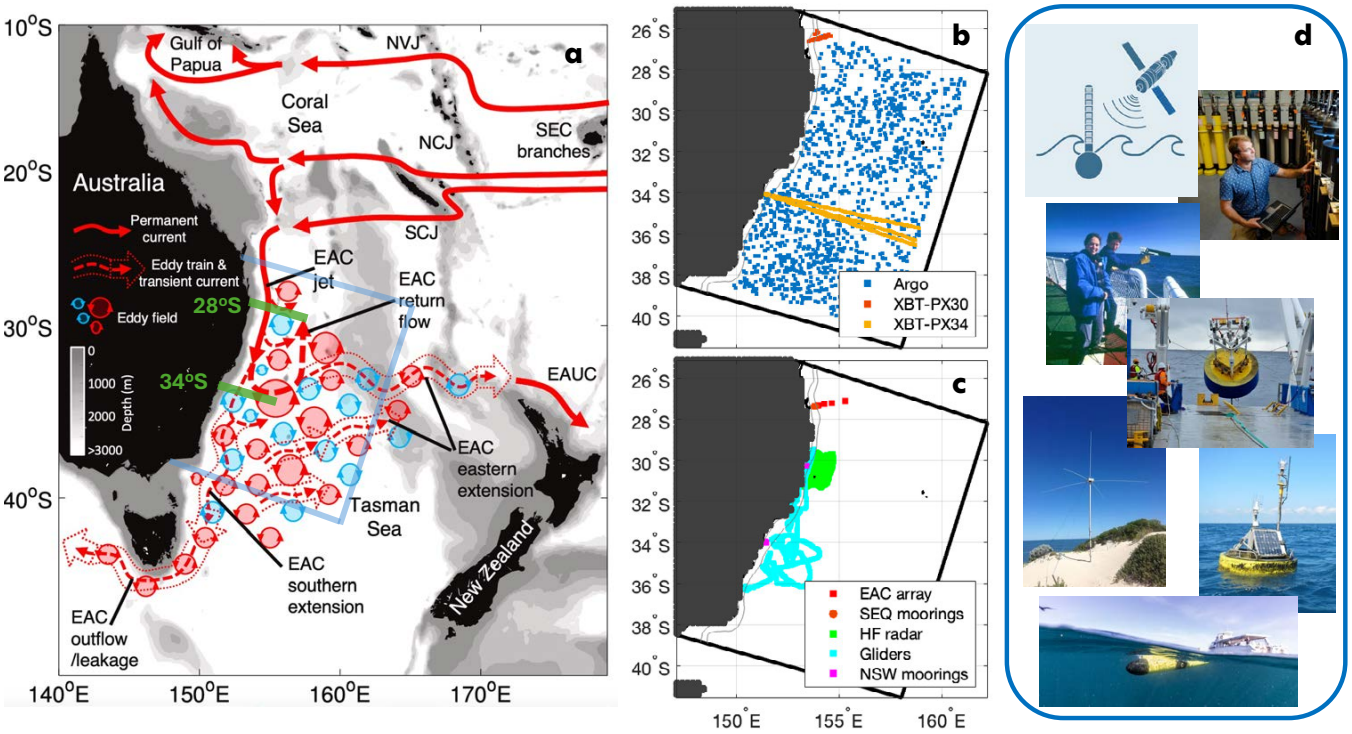

FIGURE 2. The EAC is a fairly well observed western boundary current system. (a) Schematic showing the East Australia Current (EAC; adapted from Oke et al., 2019) with the regional ocean model domain. (b) Locations of Argo and eXpendable BathyThermograph (XBT) observations. (c) Integrated Marine Observing System (IMOS) observations. (d) Photos of observing the EAC. *Photo credits: M. Roughan and IMOS*

(SSH) and sea surface temperature (SST), temperature and salinity from Argo profiling floats, and temperature from eXpendable BathyThermograph (XBT) lines.

METHOD 1: AN ADJOINT-BASED APPROACH

The 4D-Var DA scheme uses sequential iterations of the linearized model equations and their adjoint (Errico, 1997) to minimize the model-observation difference. By defining a scalar measure of the ocean circulation, we can use this mathematical framework to directly compute the impact of each individual observation on the change in the circulation measure (e.g., Langland and Baker, 2004; Powell, 2017). We use this methodology to understand how observations impact estimates of alongshore volume transport through shore-normal sections that span the extent of the EAC, and of spatially averaged eddy kinetic energy (EKE) over the eddy-rich Tasman Sea (Kerry et al., 2018).

The contribution of each observing platform to changes in modeled volume transport and EKE varies considerably over the two-year period, as it depends on the flow regime and the observation coverage for each assimilation window. To gain an overall picture of how observations from across the EAC region impact a particular circulation metric, we group the observation impacts by acquisition latitude (Figure 3a,b). This analysis reveals that both up- and downstream observations impact transport estimates along the extent of the EAC system. While the EAC is mostly coherent off 28°S, volume transport varies due to meandering of the EAC core and intermittent separation events (Oke et al., 2019; Kerry and Roughan, 2020). Glider and XBT observations off 34°S and HF radar observations at 30°S impact EAC transport to the north (28°S, upstream impacts, Figure 3a). The volume transport off 34°S is more variable than upstream due to the eddy-dominated circulation

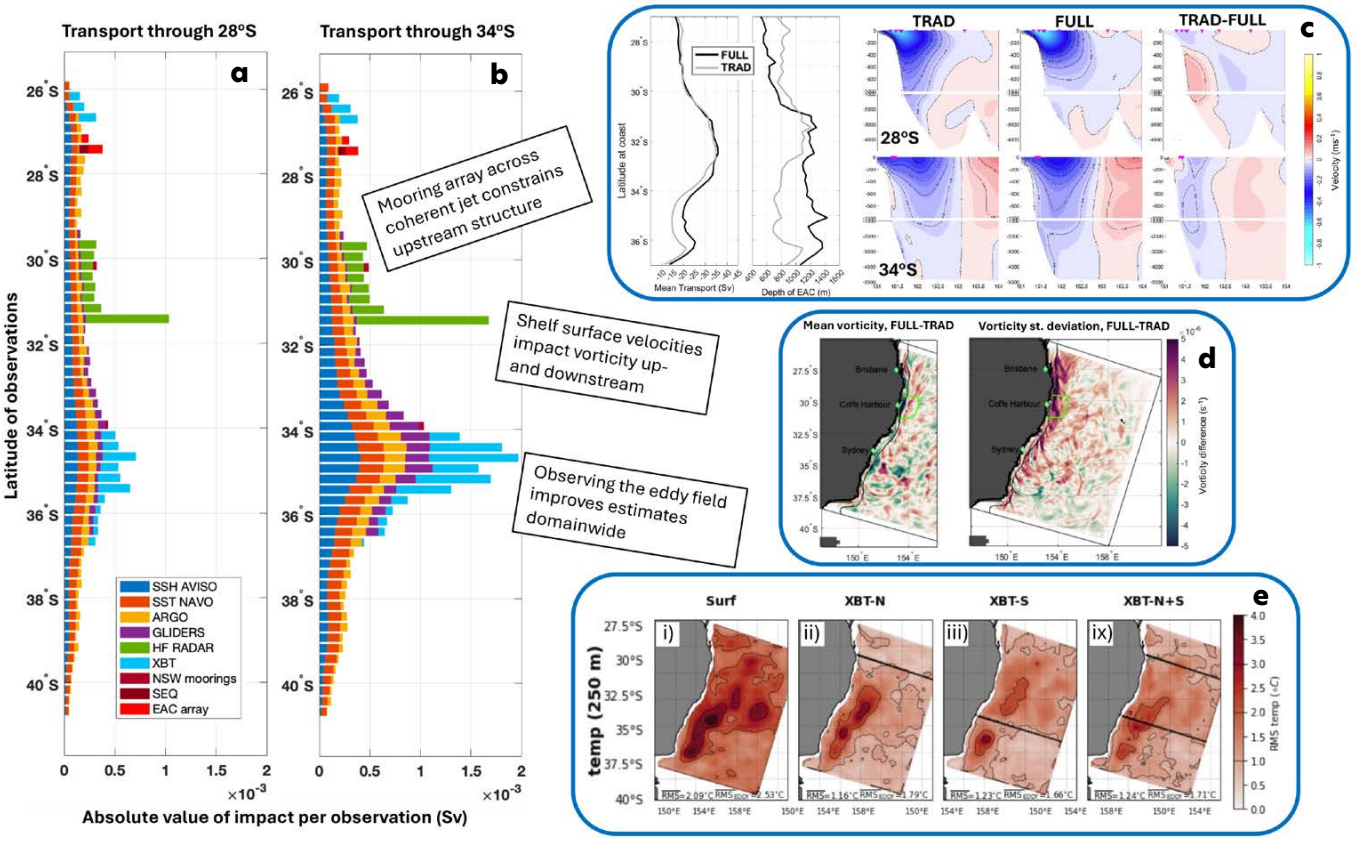

FIGURE 3. Summary of up- and downstream observation impacts. (a) Observation impacts using the adjoint-based method on transport through the shore normal section crossing the coast at 28°S (upstream) grouped into latitude bins of 0.25° and normalized by the number of observations. (b) Same as (a) but for transport through section crossing the coast at 34°S (downstream). *Adapted from Kerry et al. (2018)* (c) Observing System Experiments (OSEs) show the EAC mooring array constraining upstream current structure (Siripatana et al., 2020). (d) Surface radial velocities (from HF radar array at 30°S) impact vorticity up- and downstream (Siripatana et al., 2020). (e) Observing System Simulation Experiments (OSSEs) show that subsurface temperature (250 m) is improved with XBT observations (Gwyther et al., 2022). Text in the black boxes summarizes parallels between the information in panels a–b and that in panels c–e. AVISO = Archiving, Validation, and Interpretation of Satellite Oceanographic data. EAC = East Australia Current. HF = High frequency. SEQ = South East Queensland. SSH = Sea surface height. SST = Sea surface temperature. NAVO = Naval Oceanographic Office. NSW = New South Wales. XBT = eXpendable BathyThermograph. See text for definitions of FULL and TRAD.

regime (Kerry and Roughan, 2020). This downstream transport is constrained primarily by observations over the eddy field but is also impacted by the EAC array, the northern XBT lines, and the HF radar observations (downstream impacts, Figure 3b).

Normalizing the impacts by the number of observations (e.g., Figure 3a,b) reveals that observations over the eddy field make the greatest contribution to volume transport estimates along the coast. SSH, SST, and Argo observations made in the region of high eddy variability (33°–37°S) have more impact than the same observations made elsewhere as they provide information to constrain the variable region. Even for volume transport estimates where the jet is mostly coherent, satellite and Argo observations of the (downstream) eddy field have greater impact than the same observation types upstream (Figure 3a). The eddy field observation impact exceeds the impact of observations local to 28°S.

Subsurface observations that sample hydrography within EAC eddies, such as those from Argo, gliders, and XBTs, are also particularly impactful (Figure 3a,b). Observations made in the upper 500 m of the water column contribute more to changes in the circulation estimates than deeper observations (Figure 4a,b). When glider observations sample eddies offshore of the continental shelf (Figure 2c), they have large impacts on EAC transport and EKE (contributing to 28%–36% of transport increments, and 38% for EKE; Kerry et al., 2018).

METHOD 2: OBSERVING SYSTEM EXPERIMENTS

Observing System Experiments (OSEs) compare the results of a DA system that withholds certain observations with a system that includes them (e.g., Chang et al., 2023). Using the EAC-ROMS configuration for 2012–2013, we compared the impact of assimilating only the more traditional observations (satellite-derived SSH and SST, and vertical profiles from Argo and XBTs: the TRAD experiment), versus also including data from more novel observation platforms (HF radar, deep and shallow moorings, and gliders: the full suite of all available observations, the FULL experiment; Siripatana et al., 2020).

While the overall surface and subsurface properties

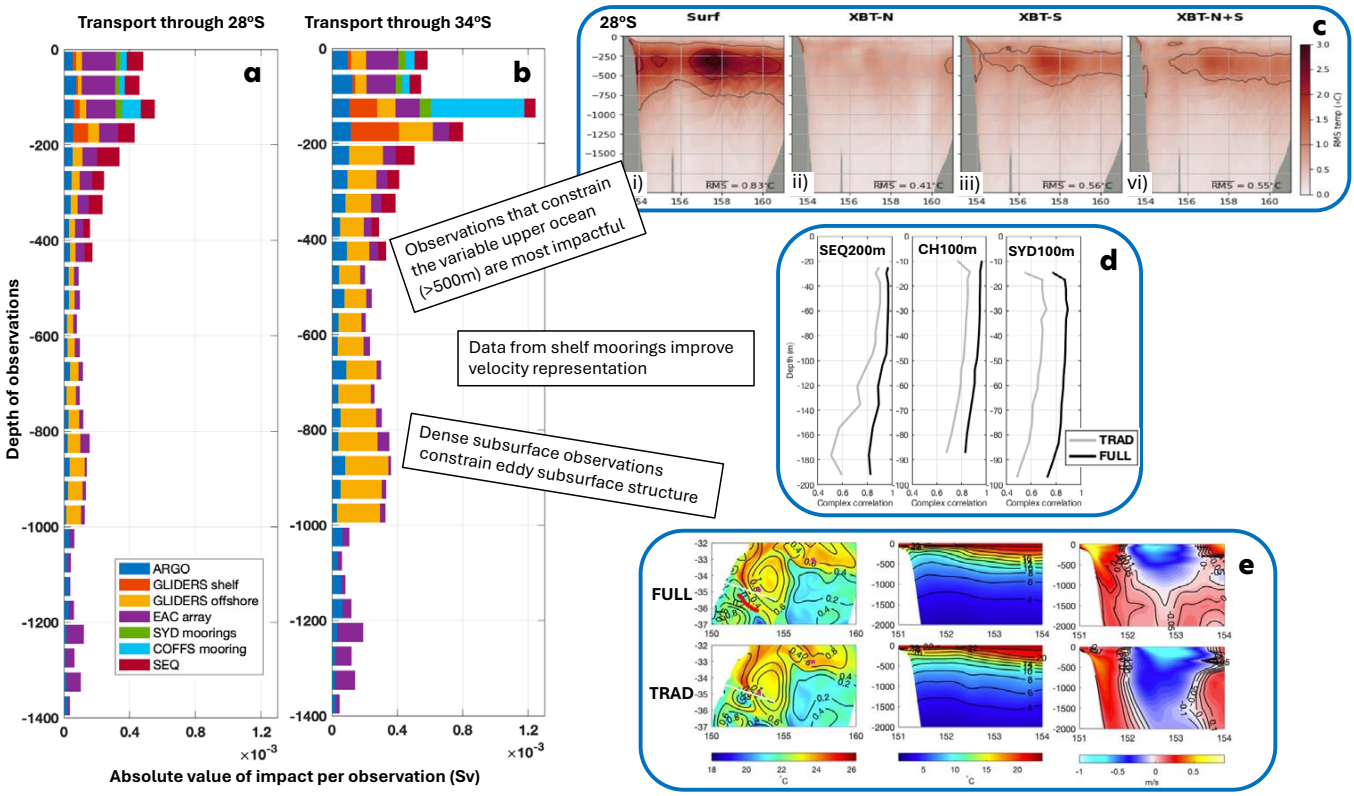

FIGURE 4. Summary of subsurface observation impacts. (a) Observation impacts using the adjoint-based method on transport through the shore normal section crossing the coast at 28°S (upstream) grouped into depth bins and normalized by the number of observations. (b) Same as (a) but for transport through section crossing the coast at 34°S (downstream). *Adapted from Kerry et al. (2018)* (c) OSSEs show the depth region of greatest variability (>500 m) benefits most from subsurface observations (Gwyther et al., 2022). (d) OSEs show improvement in shelf velocities with mooring data assimilated (Siripatana et al., 2020). (e) Example of glider data (glider path shown in red) constraining the subsurface temperature and velocity structure of a cold core eddy off Sydney (Siripatana et al., 2020). Text in the black boxes summarizes parallels between the information in panels a–b and that in panels c–e. SEQ = Southeast Queensland. CH and COFFS = Coffs Harbor. SYD = Sydney.

were well represented with assimilation of surface observations and sparse subsurface profiles (TRAD), including mooring, radar, and glider observations (FULL) further improved ocean state estimates. Specifically, shelf mooring observations improved temperature and velocity estimates inshore of the EAC (e.g., Figure 4d), and HF radar observations covering the continental shelf and slope at 30°S were key to representing vorticity (Siripatana et al., 2020). The inclusion of HF radar data resulted in increased cyclonic vorticity inshore of the EAC both up- and downstream of the HF radar location and increased vorticity variance (Figure 3d). This increase in cyclonic vorticity is confirmed as an improvement under the HF radar footprint (by comparison to the assimilated surface radial velocity observations). Without independent observations, we cannot confirm that this increased vorticity is an improvement in the up- and downstream regions, but it is reasonable to assume that the velocity shear structure inshore of the EAC extends up- and downstream of 30°S and that FULL provides improved representation of this.

Despite the shelf and slope circulation being improved in the FULL analyses, at the end of five-day forecasts, the predictive skill over the shelf was equivalent to that of the TRAD forecasts (Kerry et al., 2024b). For these same experiments, Kerry et al. (2020) show that downscaling to a finer resolution (1 km) coastal/shelf model was more effective at maintaining the vorticity gradient in the five-day forecasts, although correctly predicting the timing and location of fine-scale features, specifically cyclonic eddies that form inshore of the EAC, remains a challenge.

The width of the EAC core and the mean EAC transport with latitude was well constrained across both experiments (TRAD and FULL). Assimilation of observations from the EAC mooring array constrained the core depth over the 27°–30°S region (FULL), while the core extended too deep in their absence (TRAD). However, poleward of 30°S, the average depth of the EAC core extended too deep in the FULL compared to the TRAD experiment (Figure 3c; Siripatana et al., 2020). Glider observations of hydrographic structure were effective in constraining eddy depth when they sampled offshore eddies. When they were available (an approximately three-month period in 2013), eddies constrained by glider data (FULL) showed realistic eddy depths compared to the TRAD case where the eddy depths extended well below the typical level of no motion (e.g., Figure 4e).

METHOD 3: OBSERVING SYSTEM SIMULATION EXPERIMENTS

Assessment of ocean prediction systems is limited as a large portion of the ocean state is unobserved, particularly below the surface. Observing System Simulation Experiments (OSSEs) are designed to replicate a realistic prediction system; by defining a given model solution as the *Truth* (or Nature run), the system can then be evaluated everywhere against a known ocean state (e.g., Gasparin et al., 2019; Kerry and Powell, 2022). Synthetic observations are extracted from the *Truth* and assimilated into a *Baseline* model (or Twin), which represents the background numerical model (refer to Kerry et al., 2024a; Figure 1). Errors are intentionally introduced into the *Baseline* model (e.g., in initial conditions and boundary and surface forcing) to mimic the uncertainties in a realistic prediction system. Often a Nature run is sought with a higher resolution and some degree of independence (e.g., different model physics) from the *Baseline* model (e.g., Halliwell et al., 2017).

In the EAC-ROMS configuration, a series of OSSEs were performed to assess the impact of alternate locations and frequencies of subsurface temperature observations (Gwyther et al., 2022, 2023a, 2023b). These experiments compare the impact of assimilating (synthetic) surface-only observations that mimic satellite derived SSH and SST (SURF) with experiments that also include (synthetic) repeat XBT lines (subsurface temperature profiles) through the upstream EAC region (XBT-N), the downstream region (XBT-S), and both the up- and downstream regions (XBT-N+S; Figure 3e).

The OSSEs show that subsurface temperature observations are key to improved representation of the EAC system below the surface. Observing the downstream, eddy-dominated region has a strong impact on improving EAC subsurface structure both up- and downstream of the observing location (Gwyther et al., 2022, 2023a). Observing the mostly coherent upstream region (XBT-N) gave the best fit across that section but was less effective in improving subsurface estimates in the downstream region, while observing across the downstream section (XBT-S) gave comparatively lower errors across the domain (Figure 3e). Including both observation platforms (XBT-N+S) gave the lowest errors across the domain, but the gain in skill was small relative to XBT-S alone (Figure 3e). A sampling frequency close to the assimilation window length (weekly XBT lines in this case) resulted in considerable improvement in subsurface representation across the eddy field compared to fortnightly and greater periods between samples (Gwyther et al., 2023b).

SYNERGIES ACROSS THE THREE METHODS

Here, we apply three different methods (Figure 1), each with unique advantages and limitations, to assess observation impact in the EAC. The adjoint-based method (Method 1) allows us to quantify the contribution of each individual observation to the change in a given target metric between

the forecast and the analysis. This then allows us to pinpoint exactly which data (from a large set of assimilated constraints) are most valuable in the assimilation system. The impacts relate to changes in the specifically defined circulation metrics, but the degree of improvement is unknown as the true ocean state is not known away from observed locations. The relative impacts of the different observation platforms are specific to the chosen circulation measure. OSEs (Method 2) compare model skill for experiments that withhold or include different platforms, but interpretation is limited as, again, the true state is unknown. OSSEs (Method 3) address this shortcoming by simulating a complete representation of the "true" ocean state. Drawbacks associated with OSSE design include correctly representing background model error so that the system represents a realistic system. By employing all three methods across a common system we can comprehensively assess observation impact across the EAC region. The synergy between the results provides confidence in the overarching findings.

UP- AND DOWNSTREAM IMPACTS

Time-dependent DA methods, like 4D-Var, account for the time-evolving flow so localized observation platforms can have far-reaching impacts. Respecting the model dynamics, information captured by the observations propagates in time and space and influences the unobserved ocean state. For example, changes to surface velocities at a certain time and location (an example of an observed variable) must be balanced by changes to surface and isopycnal tilt, with adjustments both up- and downstream and forward and backward in time.

Surface velocity observations from an HF radar array at 30°S impact EAC volume transport both up- and downstream as well as downstream EKE (Figure 3a,b). OSEs revealed the influence of these observations on vorticity along the extent of the EAC and the vorticity variance (Figure 3d). More generally, observations taken over the latitudinal extent of the EAC system were shown to influence transport estimates both up- and downstream (Figure 3a,b). Measuring the upstream coherent jet impacts downstream transport estimates, and observing the eddies downstream constrains upstream estimates. The propagation of information from the downstream to the upstream is found to be more effective in improving model skill away from the observed location (see the section below).

OBSERVING THE (DOWNSTREAM) EDDY FIELD

The adjoint-based method revealed that observations of the eddy field have higher impacts on transport estimates along the EAC than the same observations taken in the less variable regions. Surface observations of the eddy field impacted upstream transport more than surface observations over the coherent jet (Figure 3a). OSEs showed that while mooring observations across the jet resulted in improved skill in the upstream (27°–30°S) region, EAC transport and subsurface structure in the downstream region were not improved (Figure 3c). The value of observing the downstream region was confirmed by the OSSEs, which show the advantage of subsurface observations through the eddy field compared to observations through the coherent jet (Figure 3e). While the strength of the upstream jet can be a predictor of separation latitude in general (Li et al., 2022b), it provides little skill in predicting the downstream evolution of the current instabilities and resultant eddies. In contrast, observing the location where instabilities are growing into eddies gives information on both the conditions that fed the instability (upstream) and how the eddy will further evolve (downstream).

OBSERVING BELOW THE SURFACE

The value of subsurface observations is revealed across all three observation impact methodologies. EAC transport and eddies (geostrophic flow) should be constrained by both surface observations (that inform surface tilt) and subsurface observations (that inform isopycnal tilt). Given the dynamical context provided by the model, the surface tilt associated with mesoscale eddies should be projected below the surface to alter the isopycnal tilt. However, in practice, the impact of surface observations in constraining the subsurface is limited (e.g., Zavala-Garay et al., 2012). While the adjoint-based method quantifies the relative impact of the surface observations on circulation changes, the OSEs and OSSEs reveal that the depth structure of the EAC is degraded upon assimilation of surface observations alone (Siripatana et al., 2020; Gwyther et al., 2022, 2023a, 2023b; Figure 4c(i)). The adjoint-based method shows that in situ observations in the upper 500 m contribute most to changes in EAC transport and EKE (compared to deeper observations, Figure 4a,b) as they provide information on the structure of the mixed layer and the pycnocline. Glider observations within eddies informed transport estimates some 900 km upstream and 300 km downstream. The OSSEs showed that repeated subsurface temperature observations across the eddy-dominated region improved subsurface temperature estimates over the entire EAC region (Figure 3e). The depth region of greatest variability (>500 m) showed the highest errors upon assimilation of surface only observations and benefited most from subsurface observations (Figure 4c).

FEEDBACK BETWEEN MODELS AND OBSERVATIONS

Observing networks for ocean prediction must be designed with specific goals, and a continuous feedback loop should exist between numerical models and observations (Figure 5). Ocean models, observing systems, and DA schemes must evolve and adapt together for optimal benefit. Observation impact studies are a crucial part of this feedback loop as they can quantify the value of specific observations, identify regions where data gaps are most detrimental to model estimates, and drive improvements in modeling and DA systems.

Observation impact experiments have shown the specific value of various novel observing platforms, motivating their sustained implementation. For example, surface velocity observations from localized HF radar platforms have shown widespread improvement in surface current representation in eddy-rich regions (Siripatana et al., 2020; Kerry et al., 2020; Couvelard et al., 2021). Dense subsurface hydrographic observations (from gliders or profiles) in eddies drove improvements in EAC eddy field and upstream representation (Kerry et al., 2018; Siripatana et al., 2020; Gwyther et al., 2022, 2023a, 2023b). The challenges of piloting gliders in regions of strong and variable currents limit the sustained availability of such observations, and novel opportunistic methods of obtaining subsurface data, such as fishing vessel observation networks (Jakoboski et al., 2024), are emerging.

The value of observing different dynamical regions was shown in the EAC, where observing the downstream instabilities was more useful than observing the upstream jet. This provides valuable information for observing system design in oceanic regions where eddies form from current instabilities, such as WBC regions (e.g., Kang and Curchitser, 2015; Yang et al., 2018) and the North Pacific's subtropical countercurrent (Qiu, 1999). The value of in situ observations of the variable upper ocean was highlighted (Kerry et al., 2018), consistent with findings in other regions (e.g., Powell, 2017; Geng et al., 2020; Kerry et al., 2022). Furthermore, we show that different circulation regimes may require different sampling strategies (Gwyther et al., 2022), motivating adaptive sampling (e.g., Mourre and Alvarez, 2012; Gao et al., 2022).

The value of observations is limited by the spatial and temporal resolution of the model (e.g., Oke and Sakov, 2008), the processes resolved (e.g., Kerry and Powell, 2022), the DA scheme (e.g., Kerry et al., 2024b), observational errors, and redundancy with other elements of the observing system (e.g., Loose and Heimbach, 2021). Observation impact experiments can not only drive

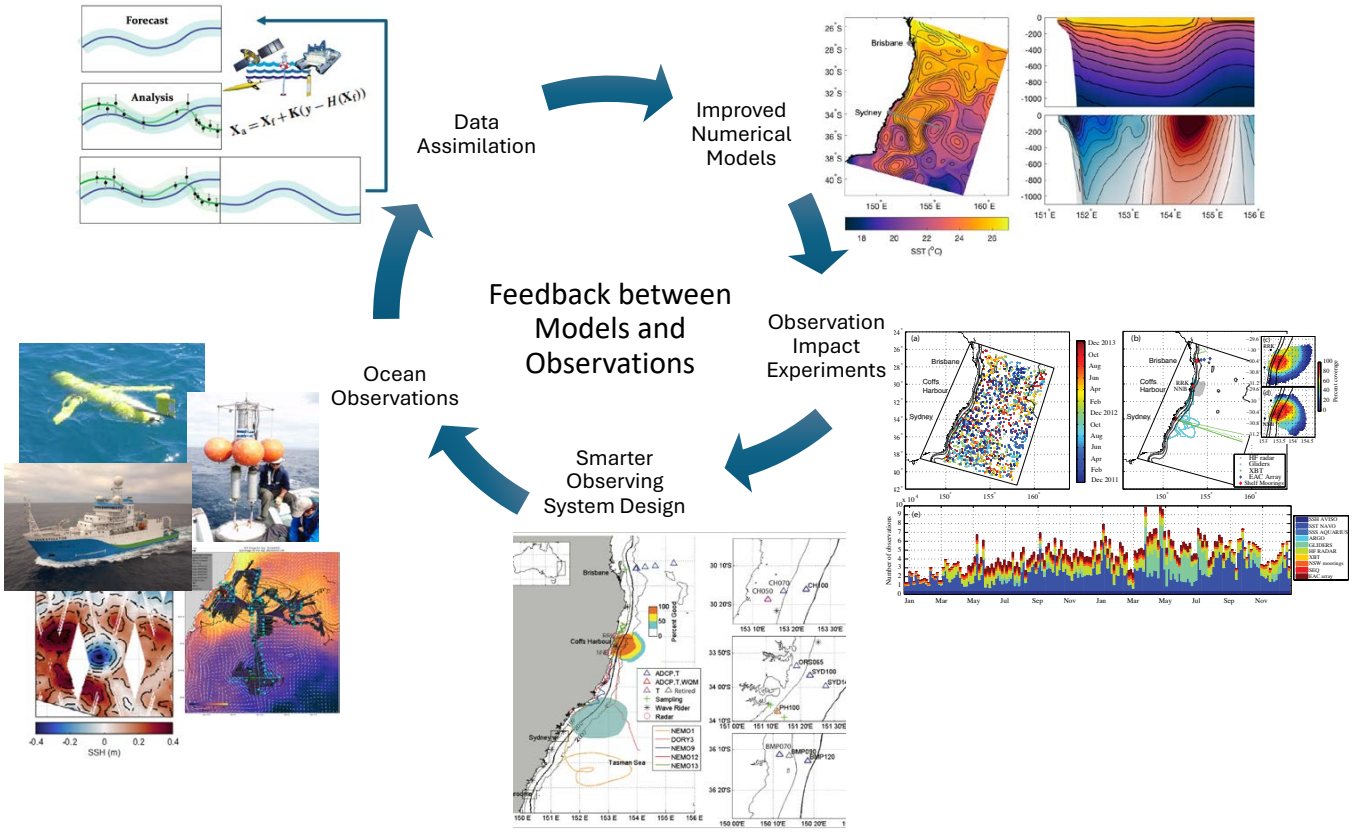

FIGURE 5. Conceptual schematic of the feedback loop between models and observations for continuously evolving ocean prediction systems.

smarter observing system design but also model and DA system improvements. For example, studying the assimilation increments and assessing predictive skill over the continental shelf adjacent to the EAC showed that shelf processes were not adequately resolved in a regional model (Kerry et al., 2020, 2024b). This result revealed that higher resolution models are required to resolve and forecast shelf flows. In a region of strong internal tides and mesoscale eddies, observation impact experiments showed the value of resolving both tides and eddies in the background numerical model for improved prediction of both processes (Kerry and Powell, 2022).

The DA system should be configured to draw optimum benefit from the observations. DA is particularly challenging in regions of complex circulation, such as eddy-rich regions and shelf seas, which are typically under-sampled and where the circulation contains a broad range of temporal and spatial scales. Advanced time-dependent assimilation schemes, such as 4D-Var and the Ensemble Kalman Filter, are crucial for capturing highly intermittent flows with irregularly sampled observations (e.g., Raynaud et al., 2011; Moore et al., 2020; Kerry et al., 2024b). Observation impact studies have shown the importance of the DA system configuration in handling dense, localized observations (e.g., Pasmans et al., 2019; Kerry et al., 2024a). Optimizing DA schemes requires ongoing development, and future advances should include the development of hybrid methods, nested and coupled DA, and the ability to ingest new and emerging observing platforms (Moore et al., 2019; Pasmans et al., 2020).

CONCLUSIONS

Numerical models, observing networks, and data assimilation techniques are the key interconnected components of an ocean prediction system. There is a need for robust and consistent model-based design and evaluation of observing networks that are scale and region appropriate. Such frameworks can inform fit-for-purpose observing strategies, identify gaps in observation systems, and drive improvements in model and data assimilation methodologies. Data-assimilating ocean models need to be evaluated against independent observations and below the surface. Assessment of models against assimilated surface and sparse profile data gives little insight into model performance away from the observed locations.

Here, we present a complementary set of methods that can provide powerful insights into model-based design and evaluation of observing networks. Each method exhibits unique advantages and limitations. By employing all three methods across a common system, we provide a holistic assessment of observation impacts. The results are specific to the numerical model's configuration and resolution, the circulation regime, the distinct observing networks, and the data assimilation system; however, key messages provide parallels to other regions and other systems. Our methods focus on improved ocean state estimates, since initial conditions dominate the quality of short-term ocean forecasts. It is noted that atmospheric forcing errors might be important for longer forecast horizons.

While these and similar methods have been used to guide observing system design in other regions globally, this study is the first of its kind to use three distinct methods to converge toward recommendations. Key outstanding challenges include representing complex subsurface oceanic structures with sparse observations, dealing with localized dense observations, and assimilating data in regions where the circulation varies over a broad range of temporal and spatial scales. Our results point to the importance of feedback between numerical modeling, ocean observing systems, and data assimilation methodology in driving improved estimates of the ocean environment.

REFERENCES

Archer, M., M. Roughan, S. Keating, and A. Schaeffer. 2017. On the variability of the East Australian Current: Jet structure, meandering, and influence on shelf circulation. *Journal of Geophysical Research: Oceans* 122(11):8,464–8,481, https://doi.org/10.1002/2017JC013097.

Brassington, G.B., P. Sakov, P. Divakaran, A. Aijaz, J. Sweeney-Van Kinderen, X. Huang, and S. Allen. 2023. OceanMAPS v4.0i: A global eddy resolving EnKF ocean forecasting system. In *OCEANS 2023 – Limerick*. Conference held June 5–8, 2023, Limerick, Ireland, IEEE, https://doi.org/10.1109/OCEANSLimerick52467.2023.10244383.

Brokaw, R.J., B. Subrahmanyam, C.B. Trott, and A. Chaigneau. 2020. Eddy surface characteristics and vertical structure in the Gulf of Mexico from satellite observations and model simulations. *Journal of Geophysical Research: Oceans* 125:e2019JC015 538, https://doi.org/10.1029/2019JC015538.

Cetina Heredia, P., M. Roughan, E. Van Sebille, and M. Coleman. 2014. Long-term trends in the East Australian Current separation latitude and eddy driven transport. *Journal of Geophysical Research: Oceans* 119(7):4,351–4,366, https://doi.org/10.1002/2014JC010071.

Chamberlain, M., P. Oke, G. Brassington, P. Sandery, P. Divakaran, and R. Fiedler. 2021. Multiscale data assimilation in the Bluelink ocean reanalysis (BRAN). *Ocean Modelling* 166:101849, https://doi.org/10.1016/j.ocemod.2021.101849.

Chang, I., Y.H. Kim, H. Jin, Y.-G. Park, G. Pak, and Y.-S. Chang. 2023. Impact of satellite and regional in-situ profile data assimilation on a high-resolution ocean prediction system in the Northwest Pacific. *Frontiers in Marine Science* 10:1085542, https://doi.org/10.3389/fmars.2023.1085542.

Couvelard, X., C. Messager, P. Penven, S. Smet, and P. Lattes. 2021. Benefits of radar-derived surface current assimilation for South of Africa ocean circulation. *Geoscience Letters* 8(5), https://doi.org/10.1186/s40562-021-00174-y.

Errico, R.M. 1997. What is an adjoint model? *Bulletin of the American Meteorological Society* 78:2,577–2,592, https://doi.org/10.1175/1520-0477(1997)078<2577:WIAAM>2.0.CO;2.

Gao, Z., G. Chen, Y. Song, J. Zheng, and C. Ma. 2022. Adaptive network design for multiple gliders observation of mesoscale eddy. *Frontiers in Marine Science* 9:823397, https://doi.org/10.3389/fmars.2022.823397.

Gasparin, F., S. Guinehut, C. Mao, I. Mirouze, E. Rémy, R.R. King, M. Hamon, R. Reid, A. Storto, P.-Y. Le Traon, and others. 2019. Requirements for

an integrated in situ Atlantic Ocean observing system from coordinated observing system simulation experiments. *Frontiers in Marine Science* 6:83, https://doi.org/10.3389/fmars.2019.00083.

Geng, W., F. Cheng, Q. Xie, X. Zou, W. He, Z. Wang, Y. Shu, G. Chen, D. Liu, D. Ye, and others. 2020. Observation system simulation experiments using an ensemble-based method in the northeastern South China Sea. *Journal of Oceanology and Limnology* 38:1,729–1,745, https://doi.org/10.1007/s00343-019-9119-4.

Gwyther, D.E., C. Kerry, M. Roughan, and S.R. Keating. 2022. Observing system simulation experiments reveal that subsurface temperature observations improve estimates of circulation and heat content in a dynamic western boundary current. *Geoscientific Model Development* 15:6,541–6,565, https://doi.org/10.5194/gmd-15-6541-2022.

Gwyther, D.E., S.R. Keating, C. Kerry, and M. Roughan. 2023a. How does 4DVar data assimilation affect the vertical representation of mesoscale eddies? A case study with observing system simulation experiments (OSSEs) using ROMS v3.9. *Geoscientific Model Development* 162023:157–178, https://doi.org/10.5194/gmd-16-157-2023.

Gwyther, D.E., M. Roughan, C. Kerry, and S.R. Keating. 2023b. Impact of assimilating repeated subsurface temperature transects on state estimates of a western boundary current. *Frontiers in Marine Science* 9:1084784, https://doi.org/10.3389/fmars.2022.1084784.

Halliwell, G.R. Jr., M.F. Mehari, M. Le Hénaff, V.H. Kourafalou, I.S. Androulidakis, H.S. Kang, and R. Atlas. 2017. North Atlantic Ocean OSSE system: Evaluation of operational ocean observing system components and supplemental seasonal observations for potentially improving tropical cyclone prediction in coupled systems. *Journal of Operational Oceanography* 10:154–175, https://doi.org/10.1080/1755876X.2017.1322770.

Imawaki, S., A. Bower, L. Beal, and B. Qiu. 2013. Western boundary currents. Pp. 305–338 in *Ocean Circulation and Climate: A 21st Century Perspective*. G. Siedler, S.M. Griffies, J. Gould, and J.A. Church, eds, Elsevier, https://doi.org/10.1016/B978-0-12-391851-2.00013-1.

Jakoboski, J., M. Roughan, J. Radford, J.M.A.C. de Souza, M. Felsing, R. Smith, N. Puketapu-Waite, M.M. Orozco, K.H. Maxwell, and C. Van Vranken. 2024. Partnering with the commercial fishing sector and Aotearoa New Zealand's ocean community to develop a nationwide subsurface temperature monitoring program. *Progress in Oceanography* 225:103278, https://doi.org/10.1016/j.pocean.2024.103278.

Kang, D., and E.N. Curchitser. 2013. Gulf Stream eddy characteristics in a high-resolution ocean model. *Journal of Geophysical Research: Oceans* 118:4,474–4,487, https://doi.org/10.1002/jgrc.20318.

Kang, D., and E.N. Curchitser. 2015. Energetics of eddy–mean flow interactions in the Gulf Stream region. *Journal of Physical Oceanography* 45:1,103–1,120, https://doi.org/10.1175/jpo-d-14-0200.1.

Kerry, C.G., B.S. Powell, M. Roughan, and P.R. Oke. 2016. Development and evaluation of a high-resolution reanalysis of the East Australian Current region using the Regional Ocean Modelling System (ROMS 3.4) and Incremental Strong-Constraint 4-Dimensional Variational (IS4D-Var) data assimilation. *Geoscientific Model Development* 9:3,779–3,801, https://doi.org/10.5194/gmd-9-3779-2016.

Kerry, C.G., M. Roughan, and B.S. Powell. 2018. Observation impact in a regional reanalysis of the East Australian Current system. *Journal of Geophysical Research: Oceans* 123(10):7,511–7,528, https://doi.org/10.1029/2017JC013685.

Kerry, C., and M. Roughan. 2020. Downstream evolution of the East Australian Current system: Mean flow, seasonal, and intra-annual variability. *Journal of Geophysical Research: Oceans* 125:e2019JC015227, https://doi.org/10.1029/2019JC015227.

Kerry, C., M. Roughan, and B. Powell. 2020. Predicting the submesoscale circulation inshore of the East Australian Current. *Journal of Marine Systems* 204:103286, https://doi.org/10.1016/j.jmarsys.2019.103286.

Kerry, C.G., and B.S. Powell. 2022. Including tides improves subtidal prediction in a region of strong surface and internal tides and energetic mesoscale circulation. *Journal of Geophysical Research: Oceans* 127:e2021JC018314, https://doi.org/10.1029/2021JC018314.

Kerry, C., M. Roughan, and J.M. Azevedo Correia de Souza. 2022. Drivers of upper ocean heat content extremes around New Zealand revealed by Adjoint Sensitivity Analysis. *Frontiers in Climate* 4:980990, https://doi.org/10.3389/fclim.2022.980990.

Kerry, C., M. Roughan, and J.M. Azevedo Correia de Souza. 2024a. Assessing the impact of subsurface temperature observations from fishing vessels on temperature and heat content estimates in shelf seas: A New Zealand case study using Observing System Simulation Experiments. *Frontiers in Marine Science* 11:1358193, https://doi.org/10.3389/fmars.2024.1358193.

Kerry, C.G., M. Roughan, S. Keating, D. Gwyther, G. Brassington, A. Siripatana, and J.M.A.C. Souza, 2024b. Comparison of 4-dimensional variational and ensemble optimal interpolation data assimilation systems using a Regional Ocean Modeling System (v3.4) configuration of the eddy-dominated East Australian Current system. *Geoscientific Model Development* 17:2,359–2,386, https://doi.org/10.5194/egusphere-2023-2355.

Langland, R.H., and N.L. Baker. 2004. Estimation of observation impact using the NRL atmospheric variational data assimilation adjoint system. *Tellus A: Dynamic Meteorology and Oceanography* 56(3):189–201, https://doi.org/10.3402/tellusa.v56i3.14413.

Li, J., M. Roughan, and C. Kerry. 2022a. Drivers of ocean warming in the western boundary currents of the Southern Hemisphere. *Nature Climate Change* 12:901–909, https://doi.org/10.1038/s41558-022-01473-8.

Li, J., M. Roughan, and C. Kerry. 2022b. Variability and drivers of ocean temperature extremes in a warming western boundary current. *Journal of Climate* 35:1,097–1,111, https://doi.org/10.1175/JCLI-D-21-0622.1.

Loose, N., and P. Heimbach. 2021. Leveraging uncertainty quantification to design ocean climate observing systems. *Journal of Advances in Modeling Earth Systems* 13:e2020MS002386, https://doi.org/10.1029/2020MS002386.

Malan, N., M. Roughan, and C. Kerry. 2021. The rate of coastal temperature rise adjacent to a warming western boundary current is nonuniform with latitude. *Geophysical Research Letters* 48:e2020GL090751, https://doi.org/10.1029/2020GL090751.

Moore, A.M., H.G. Arango, E. Di Lorenzo, B.D. Cornuelle, A.J. Miller, and D.J. Neilson. 2004. A comprehensive ocean prediction and analysis system based on the tangent linear and adjoint of a regional ocean model. *Ocean Modelling* 7:227–258, https://doi.org/10.1016/j.ocemod.2003.11.001.

Moore, A.M., H.G. Arango, G. Broquet, B.S. Powell, A.T. Weaver, and J. Zavala-Garay. 2011. The Regional Ocean Modelling System (ROMS) 4-dimensional variational data assimilation systems: Part 1. System overview and formulation. *Progress in Oceanography* 91:34–49, https://doi.org/10.1016/j.pocean.2011.05.004.

Moore, A., M. Martin, S. Akella, H. Arango, M. Balmaseda, L. Bertino, S. Ciavatta, B. Cornuelle, J. Cummings, S. Frolov, and others. 2019. Synthesis of ocean observations using data assimilation for operational, real-time and reanalysis systems: A more complete picture of the state of the ocean. *Frontiers in Marine Science* 6:90, https://doi.org/10.3389/fmars.2019.00090.

Moore, A., J. Zavala-Garay, H.G. Arango, C.A. Edwards, J. Anderson, and T. Hoar. 2020. Regional and basin scale applications of ensemble adjustment Kalman filter and 4D-Var ocean data assimilation systems. *Progress in Oceanography* 189:102450, https://doi.org/10.1016/j.pocean.2020.102450.

Mourre, B., and A. Alvarez. 2012. Benefit assessment of glider adaptive sampling in the Ligurian Sea. *Deep Sea Research Part I* 68:68–78, https://doi.org/10.1016/j.dsr.2012.05.010.

Oke, P.R., and P. Sakov. 2008. Representation error of oceanic observations for data assimilation. *Journal of Atmospheric and Oceanic Technology* 25:1,004–1,017, https://doi.org/10.1175/2007JTECHO558.1.

Oke, P.R., G. Larnicol, E.M. Jones, V. Kourafalou, A. Sperrevik, F. Carse, C.A. Tanajura, B. Mourre, M. Tonani, G. Brassington, and others. 2015. Assessing the impact of observations on ocean forecasts and reanalyses: Part 2. Regional applications. *Journal of Operational Oceanography* 8:s63–s79, https://doi.org/10.1080/1755876X.2015.1022080.

Oke, P.R., M. Roughan, P. Cetina-Heredia, G.S. Pilo, K.R. Ridgway, T. Rykova, M.R. Archer, R.C. Coleman, C.G. Kerry, C. Rocha, and others. 2019. Revisiting the circulation of the East Australian Current: Its path, separation, and eddy field. *Progress in Oceanography* 176:102139, https://doi.org/10.1016/j.pocean.2019.102139.

Pasmans, I., A.L. Kurapov, J.A. Barth, A. Ignatov, P.M. Kosro, and R.K. Shearman. 2019. Why gliders appreciate good company: Glider assimilation in the Oregon-Washington coastal ocean 4DVAR system with and without surface observations. *Journal of Geophysical Research: Oceans* 124:750–772, https://doi.org/10.1029/2018JC014230.

Pasmans, I., A.L. Kurapov, J.A. Barth, P.M. Kosro, and R.K. Shearman. 2020. Ensemble 4DVAR (En4DVar) data assimilation in a coastal ocean circulation model: Part II. Implementation offshore Oregon–Washington, USA. *Ocean Modelling* 154:101681, https://doi.org/10.1016/j.ocemod.2020.101681.

Pilo, G.S., M.M. Mata, and J.L.L. Azevedo. 2015. Eddy surface properties and propagation at Southern Hemisphere western boundary current systems. *Ocean Science* 11:629–641, https://doi.org/10.5194/os-11-629-2015.

Pilo, G.S., P.R. Oke, R. Coleman, T. Rykova, and K. Ridgway. 2018. Patterns of vertical velocity induced by eddy distortion in an ocean model. *Journal of Geophysical Research: Oceans* 123:2,274–2,292, https://doi.org/10.1002/2017JC013298.

Powell, B.S. 2017. Quantifying how observations inform a numerical reanalysis of Hawaii. *Journal of Geophysical Research: Oceans* 122(11):8,427–8,444, https://doi.org/10.1002/2017JC012854.

Qiu, B. 1999. Seasonal eddy field modulation of the North Pacific Subtropical Countercurrent: TOPEX/Poseidon observations and theory. *Journal of Physical Oceanography* 29(10):2,471–2,486, https://doi.org/10.1175/1520-0485(1999)029<2471:SEFMOT>2.0.CO;2.

Raynaud, L., L. Berre, and G. Desroziers. 2011. An extended specification of flow-dependent background error variances in the Météo-France global 4D-Var system. *Quarterly Journal of the Royal Meteorological Society* 137:607–619, https://doi.org/10.1002/qj.795.

Roughan, M., A. Schaeffer, and I.M. Suthers. 2015. Sustained ocean observing along the coast of southeastern Australia: NSW-IMOS 2007–2014. Pp. 76–98 in *Coastal Ocean Observing Systems*. Y. Liu, H. Kerkering, and R.H. Weisberg, eds, Elsevier.

Roughan, M., M. Hemming, A. Schaeffer, T. Austin, H. Beggs, M. Chen, M. Feng, G. Galibert, C. Holden, D. Hughes, and others. 2022. Multi-decadal ocean temperature time-series and climatologies from Australia's long-term National Reference Stations. *Scientific Data* 9:157, https://doi.org/10.1038/s41597hy-022-01224-6.

Rykova, T., and P.R. Oke. 2022. Stacking of EAC eddies observed from Argo. *Journal of Geophysical Research: Oceans* 127:e2022JC018 679, https://doi.org/10.1029/2022JC018679.

Schaeffer, A., M. Roughan, T. Austin, J.D. Everett, D. Griffin, B. Hollings, E. King, A. Mantovanelli, S. Milburn, B. Pasquer, and others. 2016. Mean hydrography on the continental shelf from 26 repeat glider deployments along southeastern Australia. *Scientific Data* 3:160070, https://doi.org/10.1038/sdata.2016.70.

Shchepetkin, A.F., and J.C. McWilliams. 2005. The regional oceanic modeling system (ROMS): A split-explicit, free-surface, topography-following-coordinate oceanic model. *Ocean Modelling* 9:347–404, https://doi.org/10.1016/j.ocemod.2004.08.002.

Siripatana, A., C. Kerry, M. Roughan, J.M.A. Souza, and S. Keating. 2020. Assessing the impact of nontraditional ocean observations for prediction of the East Australian Current. *Journal of Geophysical Research: Oceans* 125:e2020JC016580, https://doi.org/10.1029/2020JC016580.

Sloyan, B.M., K.R. Ridgway, and R. Cowley. 2016. The East Australian Current and property transport at 27°S from 2012 to 2013. *Journal of Physical Oceanography* 46(3):993–1,008, https://doi.org/10.1175/JPO-D-15-0052.1.

Sun, W., C. Dong, R. Wang, Y. Liu, and K. Yu. 2017. Vertical structure anomalies of oceanic eddies in the Kuroshio Extension region. *Journal of Geophysical Research: Oceans* 122:1,476–1,496, https://doi.org/10.1002/2016JC012226.

Thoppil, P.G., S. Frolov, C.D. Rowley, C.A. Reynolds, G.A. Jacobs, E.J. Metzger, P.J. Hogan, N. Barton, A.J. Wallcraft, O.M. Smedstad, and others. 2021. Ensemble forecasting greatly expands the prediction horizon for ocean mesoscale variability. *Communications Earth & Environment* 2:89, https://doi.org/10.1038/s43247-021-00151-5.

Yang, H., B. Qiu, P. Chang, L. Wu, S. Wang, Z. Chen, and Y. Yang. 2018. Decadal variability of eddy characteristics and energetics in the Kuroshio Extension: Unstable versus stable states. *Journal of Geophysical Research: Oceans* 123:6,653–6,669, https://doi.org/10.1029/2018JC014081.

Zavala-Garay, J., J.L. Wilkin, and H.G. Arango. 2012. Predictability of mesoscale variability in the East Australian Current given strong-constraint data assimilation. *Journal of Physical Oceanography* 42:1,402–1,420, https://doi.org/10.1175/JPO-D-11-0168.1.

COMPETING INTERESTS

No competing interests are present.

ACKNOWLEDGMENTS

This research was supported by Australian Research Council grants DP140102337, LP160100162, and LP170100498 to MR. Synthesis of the results was supported by LP220100515 to SK. MR and CK acknowledge funding from the Australian Research Council for the South East Australian Coastal Ocean Forecast System (SEA-COFS), including grants DP230100505, LP220100515, LP170100498, LP160100162, LP150100064, DP140102337, and LP1201005922023. The authors would also like to thank the two anonymous reviewers, whose suggestions improved this manuscript.

AUTHORS

Colette Kerry (c.kerry@unsw.edu.au) and **Moninya Roughan**, Coastal and Regional Oceanography Lab, School of Biological, Earth and Environmental Sciences, University of New South Wales (UNSW), Sydney, Australia. **Shane Keating**, School of Mathematics and Statistics, UNSW, Sydney, Australia. **David Gwyther**, School of the Environment, University of Queensland, Brisbane, Australia.

ARTICLE DOI. https://doi.org/10.5670/oceanog.2025e110

THE USE OF AUTONOMOUS TOOLS FOR ECOSYSTEM MANAGEMENT AND MONITORING OF MARINE PROTECTED AREAS

GLIDER SURVEILLANCE FOR NEAR-REAL-TIME DETECTION AND SPATIAL MANAGEMENT OF NORTH ATLANTIC RIGHT WHALES

By Katherine L. Indeck, Mark F. Baumgartner, Laurence Lecavalier, Frederick Whoriskey, Delphine Durette-Morin, Neal R. Pettigrew, Jacqueline M. McSweeney, Lesley H. Thorne, Katherine L. Gallagher, Catherine R. Edwards, Erin Meyer-Gutbrod, and Kimberley T.A. Davies

ABSTRACT

Successful area-based ocean management relies on long-term, persistent biological monitoring using reliable ocean observation assets. Underwater electric gliders fill a unique monitoring niche compared to other platforms because they can autonomously survey across diverse environments—from shallow coastal waters to remote offshore areas—for weeks to months at a time. Gliders equipped with passive acoustic monitoring (PAM) devices are capable of robust, continuous near-real-time monitoring of numerous species of whales. Here, we highlight five case studies to discuss how gliders are being used for area-based monitoring of the internationally migratory and critically endangered North Atlantic right whale to address several different spatial management objectives. Examples include dynamic management of shipping zones and fishery-area closures in Canadian waters, glider-based monitoring in the United States to mitigate vessel strikes and fishing gear entanglements, surveys to assess whale habitat use near offshore wind energy development areas in the northeastern United States, and surveillance of the coastal calving grounds in the southeastern United States. These examples illustrate how PAM-equipped gliders are being used to monitor an endangered cetacean species with complex conservation management needs across its range. These assets are supporting risk reduction measures across diverse regions, and their use is likely to continue to expand in support of species conservation and threat mitigation.

AUTONOMOUS ACOUSTIC GLIDERS FOR AREA-BASED MANAGEMENT

Area-based ocean management aims to balance human use of the marine environment with biological conservation (Maxwell et al., 2015). There are two primary management frameworks for achieving this: (1) static management areas (e.g., conventional marine protected areas) that are fixed in time (e.g., seasonally) and space based on historical data regarding the occurrence of species needing protection, and (2) dynamic management areas that are triggered in response to recent observations or predictions of species occurrence. Static management is typically applied to known critical habitats or where predictable aggregations of at-risk species frequently overlap with high-threat human activities (i.e., *high risk* areas). Alternatively, dynamic management is increasingly being used to address short-term, localized, changing, or ephemeral risks. This approach is applied in areas with irregular overlap of at-risk species with human activities, but where the impact of potential interaction is significant (i.e., *high threat* areas). Success of either framework relies on long-term, persistent biological monitoring using reliable ocean observation assets.

Electric gliders are mobile, cost-effective underwater surveillance tools that can be equipped with sensors for measuring oceanographic conditions and recording marine soundscapes (Webb et al., 2001). Glider deployments fill a unique whale surveillance niche compared to other standard platforms. Like visual surveys, gliders survey along

transects, but their temporal effort is significantly higher, with deployments lasting up to six months during which monitoring is continuous, including at night and in all types of weather (Baumgartner et al., 2014, 2020). The mobility of gliders allows for regional-scale spatial surveys of habitats or management areas that span hundreds of kilometers and can be remote, a task not easily achievable with individual passive acoustic monitoring (PAM) moorings. Additionally, all profiling electric gliders carry a standard suite of oceanographic sensors for simultaneously monitoring cetacean acoustics and environmental conditions throughout the water column, which is not standard for PAM moorings or visual surveys (e.g., Ruckdeschel et al., 2020). Thus, gliders fill a unique surveillance role that is required to meet whale management objectives that rely on acoustic and environmental monitoring across seasons and variable spatial scales, including in near-real time.

Gliders equipped with PAM devices are capable of robust near-real-time monitoring of numerous whale species (Baumgartner et al., 2013, 2020). One such species is the North Atlantic right whale (*Eubalaena glacialis*, NARW), which is suffering an ongoing unusual mortality event that resulted in 151 documented mortality, serious injury, and morbidity cases from 2017 to 2024: 41 deaths, 39 serious injuries, and 71 sublethal injuries (note that only about one-third of right whale deaths are thought to be documented; NMFS, 2025). The coastal distribution of NARWs spans calving grounds in the southeastern United States to foraging grounds in northern United States and Canadian waters, resulting in frequent overlap with high density vessel traffic, major shipping lanes, and commercial fisheries operations. As a result, the leading causes of death and injury for NARWs are vessel strikes and fishing gear entanglements (Sharp et al., 2019). Unpredictable shifts have occurred in NARW distributions in recent years, likely linked to the consequences of climate change impacts on habitat suitability and feeding conditions (Meyer-Gutbrod et al., 2018). This resulted in changes to NARW co-occurrence with human activities as well as to existing protection measures. Therefore, glider effort is expanding over larger temporal and spatial scales to better understand and respond to the dynamic behavior of and persistent threats to this critically endangered species.

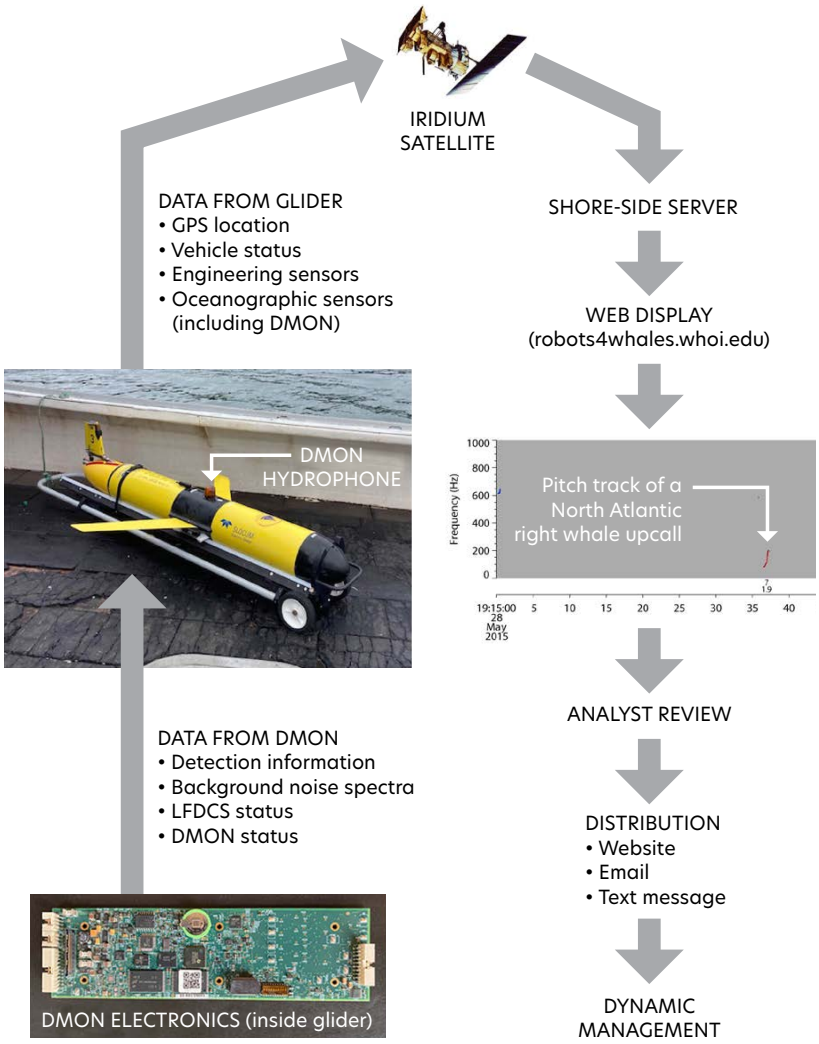

FIGURE 1. Diagram of whale acoustic detection data flow from a digital acoustic monitoring (DMON) instrument running a low-frequency detection and classification system (LFDCS) integrated into a Slocum glider to a shore-side server via the Iridium satellite service and displayed on a publicly accessible website. After analyst review, the presence of North Atlantic right whales is shared with stakeholders via the website and email/text messages. Depending on the area, dynamic management measures may be implemented in response to whale detections.

Glider-derived acoustic detections can provide information on the occurrence and distribution of NARWs in relation to high threat human activities at hourly to daily timescales. Many near-real-time PAM systems deployed to monitor NARWs (i.e., gliders and moored buoys) use a digital acoustic monitoring (DMON) instrument running a low-frequency detection and classification system (LFDCS; Johnson and Hurst, 2007; Baumgartner and Mussoline, 2011; Baumgartner et al., 2013, 2020) that automatically detects and classifies tonal baleen whale sounds in real time. A subset of these detection data is sent to shore periodically (e.g., when a glider surfaces), enabling acoustic analysts to validate detected whale calls in near-real time following a standard protocol (Figure 1; Wilder et al.,

2023). Validated detections are then rapidly disseminated to stakeholders via various automated systems. Here, we highlight five case studies to discuss how DMON/LFDCS-equipped gliders are being used internationally for area-based monitoring of NARWs across habitats and in distinct environments, as well as how the acoustic observations are being used to inform management and/or stakeholder actions to mitigate the impacts of anthropogenic threats (Table 1). The goal of these examples is to illustrate how this platform's unique surveillance niche can help address the complex and multifaceted management needs of a migratory endangered species.

NARW CONSERVATION CASE STUDIES

CANADIAN DYNAMIC SHIPPING ZONES

The Gulf of St. Lawrence (GoSL), Canada, recently became a foraging hotspot for NARWs (Meyer-Gutbrod et al., 2021). The GoSL is an inland sea bisected by shipping lanes that serve as the sole oceanic connection between North America's Great Lakes (including Canada's largest city, Toronto) and global ports. Regional overlap of whales and high vessel density has contributed to the species' unusual mortality event (Daoust et al., 2018). To reduce the risk of vessel strikes to NARWs in this high threat area, the Canadian government developed a significant new dynamic management plan for shipping in 2018 (Transport Canada, 2024). Beginning in 2020, the plan included the implementation of PAM-equipped glider surveys within deep water (>300 m) dynamic shipping zones to trigger mandatory regional speed restrictions of 10 knots in response to NARW acoustic presence (Figure 2). These surveys are conducted annually from April to November and are done in collaboration with the University of New Brunswick and Dalhousie University.

Vessel slowdowns are implemented or can be extended by regulators when a NARW is detected acoustically (via glider) or visually (via aerial surveillance) within or near a dynamic shipping zone. Slowdowns are initially triggered for a period of 15 days and apply to all vessels >13 m transiting within the active slow zone. If a speed limit is already implemented when a new detection is made, the speed limit is reset for an additional 15-day period starting on the day of the new detection, given that it occurs in the last seven days after the start of the previous slowdown

TABLE 1. Summary of area-based monitoring of North Atlantic right whales (NARWs) across Canada and the United States, highlighting how glider-derived acoustic detections are being used to trigger management actions and/or inform stakeholder decisions to mitigate the impacts of various anthropogenic threats.

THREAT	REGION	FRAME-WORK	COMPLIANCE	ACTION	STAKEHOLDERS*
Vessel strike	Atlantic Canada	Dynamic	Mandatory	15-day, 10-knot slowdown of all vessels >13 m transiting the speed-restricted dynamic shipping zone; this is extended an additional 15 days if a second detection occurs during days 8–15.	• Transport Canada • Shipping industry
Fishing gear entanglement	Atlantic Canada	Dynamic	Mandatory	15-day area closure, including a 72-hour gear removal period; if a second detection occurs during days 9–15, the area is put under a seasonal closure.	• Fisheries and Oceans Canada • Snow crab and lobster fisheries
Fishing gear entanglement	Northeast United States	Static	Mandatory	Annual static closure in Lobster Management Area 1 from October 1 to January 31, where traditional fixed-gear fishing with vertical lines is prohibited, based on seasonal presence of NARWs.	• National Oceanic and Atmospheric Administration (NOAA) • Lobster fishery
Noise exposure, habitat degradation	Northeast United States	N/A	N/A	Comparison of pre-and post-construction data in offshore wind energy development areas will allow their potential impacts on NARWs to be assessed and provide information on the environmental drivers of NARW habitat use.	• Bureau of Ocean Energy Management (BOEM) • Wind energy developers
Vessel strike	Northeast United States	Dynamic	Voluntary	15-day, 10-knot slowdown of all vessels >19.8 m as part of NOAA's Slow Zones for Right Whales program.	• NOAA • Northeast US mariners
Vessel strike	Southeast United States	Dynamic	Voluntary	Early Warning System and communication network for vessel strike mitigation, which alerts nearby vessel traffic of NARW presence shortly after a detection.	• NOAA • Southeast US mariners

*All projects include state/provincial agencies and/or academic institutions that are integral to the success of monitoring and management objectives.

(Transport Canada, 2024). When no speed restrictions are in place in the dynamic shipping zones, vessels can transit at a safe operating speed, which may vary depending on the type of vessel. Most commercial vessels normally transit at speeds over 10 knots.

Over the first four years of this dynamic management plan, there were 30 days with near-real-time acoustic detections of NARWs made during 580 glider survey days in the GoSL, triggering 194 days of dynamic shipping zone slowdowns. We found a high degree of interannual and seasonal variation in NARW acoustic occurrence that likely reflected their transitory use of the shipping lanes, as well as within- and between-season shifts in distribution across the region (recent work of author Indeck and colleagues).

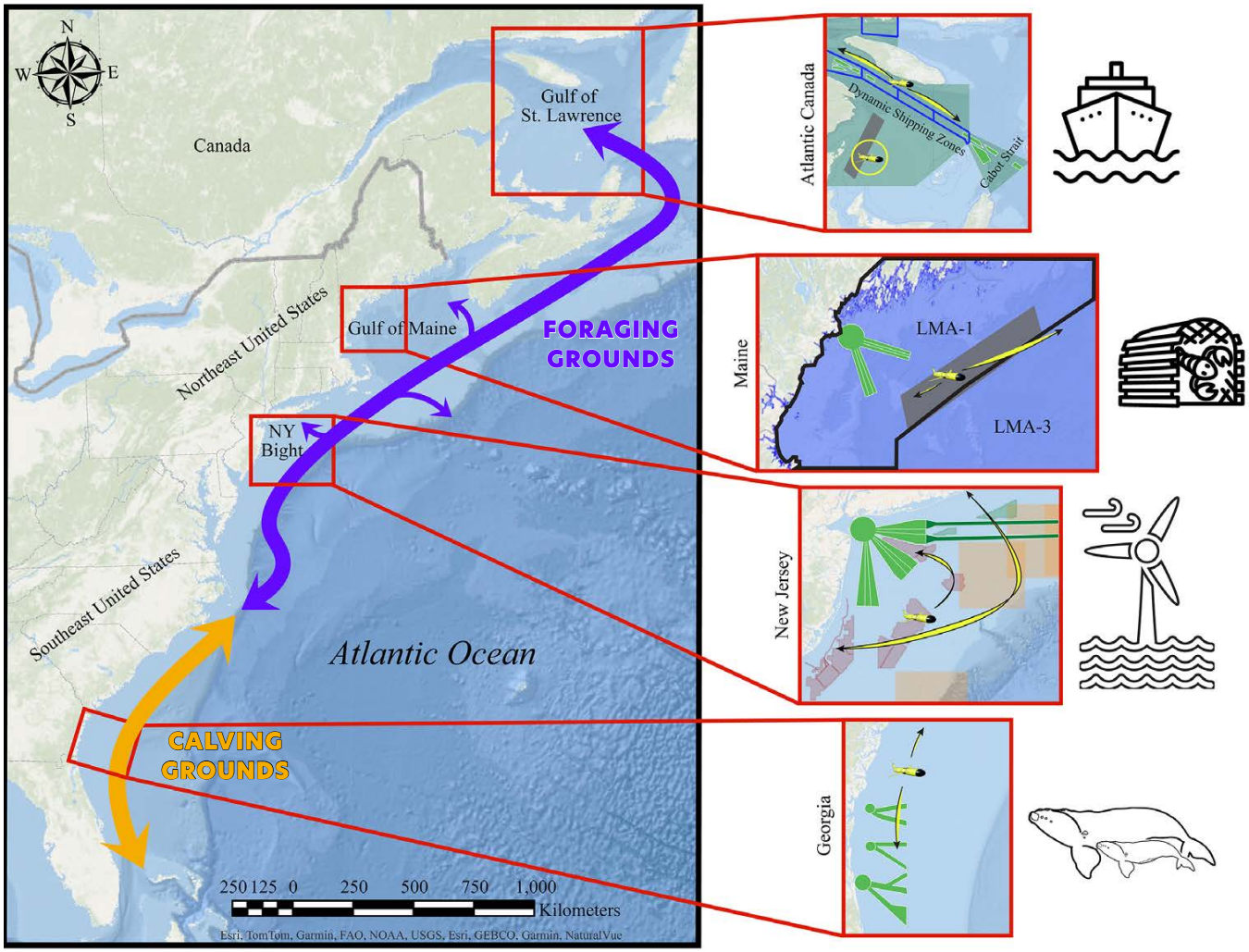

FIGURE 2. Map of the eastern United States and Canada, illustrating North Atlantic right whale (NARW) calving grounds off the southeastern United States and a foraging grounds/migratory corridor that extends along the northeastern United States into Canadian waters. Insets highlight the different regions where gliders are being used for area-based monitoring of NARWs. In Atlantic Canada, glider-derived NARW detections are used in the dynamic management of shipping zones (outlined in blue) and contribute to fishery area closures in the southern Gulf of St. Lawrence (GoSL, yellow circle); the green shading indicates all of Transport Canada's vessel traffic management areas, which include a restricted area in the southern GoSL (gray shading), a voluntary seasonal slowdown zone in the Cabot Strait to the southeast of the dynamic shipping zones, and static 10-knot speed zones to the north and south of the dynamic shipping zones. In the Gulf of Maine, nine years of glider deployments provided insight on seasonal patterns of NARW presence, which informed the establishment of the region's seasonal restricted area (gray shading) within Lobster Management Area 1 (LMA-1, outlined in black), where ongoing missions continue to monitor NARW occurrence. Glider missions in the New York Bight play an important role in assessing NARW habitat use relative to offshore wind energy development in the northeastern United States, with deployments in wind planning areas (shaded green polygons), wind lease areas (shaded red polygons), and busy shipping lanes (green outlines), as acoustic detections supplement visual observations in triggering dynamic voluntary slow zones (shaded orange squares). Lastly, in US southeast waters, glider deployments off the coast of Georgia contribute to an early warning system in and around heavily trafficked shipping lanes (green outlines) to mitigate the threat of vessel strike for female NARWs and their newborn calves. Yellow arrows in each inset panel indicate the general geographic span of glider missions conducted in that region.

Gliders triggered more slowdowns than aerial surveillance by a factor of two to five during fall and summer but were less effective during spring, as whales migrating into the GoSL tend to call at lower rates and occur at lower densities than during other behavioral states (Parks et al., 2011; Matthews and Parks, 2021).

CANADIAN DYNAMIC FISHING AREAS

In 2018, Fisheries and Oceans Canada (DFO) initiated a new fishery management plan to mitigate entanglement harm to NARWs from fixed-gear fisheries (primarily snow crab, *Chionoecetes opilio*, and lobster, *Homarus americanus*) in Canadian NARW habitats. Measures included mandatory static zones starting in 2018 and 2019, and dynamic fishery-area closures that began in 2020, supplemented by increased visual and acoustic survey efforts to detect NARW presence, including the use of Slocum acoustic gliders (Fisheries and Oceans Canada, 2023).

Under the current plan, the GoSL is subdivided into 10 minutes latitude × 10 minutes longitude grids. If any NARW is detected within a grid by any monitoring platform (vessel, airplane, buoy, glider, or validated opportunistic sighting), a temporary closure area is triggered for a period of 15 consecutive days, including a minimum 48-hour gear removal period (Fisheries and Oceans Canada, 2024). Each closure area is a 3 × 3 grid unit that includes the surveyed cell (i.e., the grid containing the NARW detection) and eight surrounding buffer grids, totaling approximately 2,000 km^2. Buffer grids are included in the trigger to account for NARW movement after the detection is made, because NARWs can travel 80 km d^{-1} on average (Baumgartner and Mate, 2005). DFO is then responsible for surveying the closure area with an aerial platform during the 15-day closure. If an NARW is not detected again, visually or acoustically, within the closure area during days 9–15 and after two clearance flights (on separate days) with two trained Marine Mammal Observers on board have been completed, then the area is reopened to fishing on day 16. However, if an NARW is detected within the closure area during days 9–15, the area is put under a seasonal closure, effectively ending fishing in that area for the rest of the monitoring season on November 15 (Fisheries and Oceans Canada, 2024).

Gliders have been used to trigger fishery-area closures in the GoSL each year since 2020. During the first four years (2020–2023), the gliders triggered 13, 46, 21, and 48 grid closures, respectively, comprising a total closed area of approximately 8,700 nm^2 (30,000 km^2) across years. Both the DFO fisheries and the Transport Canada shipping management plans have been reviewed and adapted every year, as more has been learned about NARW presence and distribution in the GoSL.

US MONITORING TO MITIGATE FISHING GEAR ENTANGLEMENTS AND VESSEL STRIKES

Glider-based monitoring of NARWs in US waters serves several purposes, including informing mitigation efforts for fishing gear entanglements and vessel strikes. Near-real-time acoustic detections of NARWs from gliders began in the Gulf of Maine in 2012 (Baumgartner et al., 2013), in a region that in 2021 was designated a seasonal restricted area within Lobster Management Area 1, where traditional fixed-gear fishing with vertical lines is now prohibited annually from October 1 to January 31 because of the seasonal presence of NARWs (**Figure 2**). Glider-based detections from regular surveys of NARWs conducted by the Woods Hole Oceanographic Institution and The University of Maine were used, in part, to justify this restricted area, as well as to defend its existence in US federal court (Bowling, 2022).

Vessel strike mitigation in the United States currently consists of mandatory vessel speed restrictions in relatively small static management areas for vessels with lengths over 19.8 m, and voluntary vessel speed restrictions dynamically triggered by visual or acoustic detections of NARWs outside of the static management areas. Speed in both areas is limited to 10 knots, and dynamic management areas persist for 15 days. The program to encourage cooperation with voluntary vessel speed restrictions based on near-real-time acoustic detections was established in late 2020 and is called the National Oceanic and Atmospheric Administration's Slow Zones for Right Whales. In the four years since its inception, 154 Slow Zones have been triggered or extended by acoustic detections of NARWs, and 51 (33%) of those Slow Zones were triggered or extended by gliders operated by the Woods Hole Oceanographic Institution, Rutgers University, Stony Brook University, and The University of Maine during 57 separate glider missions. The remaining Slow Zones were triggered by moored buoys operated by the Woods Hole Oceanographic Institution and carrying the same DMON/LFDCS system as the gliders (Baumgartner et al., 2019).

US OFFSHORE WIND DEVELOPMENT AREAS

In pursuit of ambitious renewable energy targets, the United States plans to develop its eastern seaboard with offshore wind energy farms over the upcoming decade. Lease areas in northeastern US waters are in various stages of turbine installation, and there is a coordinated effort between the Bureau of Ocean Energy Management (BOEM), state agencies, wind energy developers, and the scientific community to address the ecological impacts of offshore wind energy development (OWD; Van Parijs et al., 2021). These impacts are anticipated to span the marine food chain through

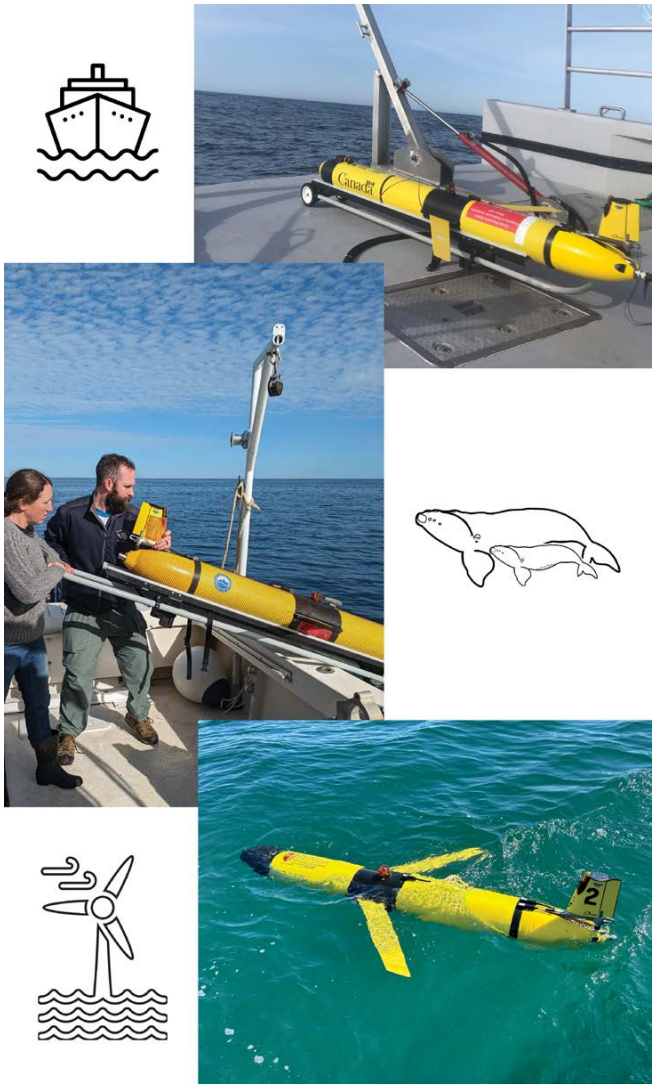

FIGURE 3. Photos of gliders in the field show them, from the top, ready for deployment in the Gulf of St. Lawrence, Canada, being deployed by field personnel on the coastal calving grounds of Georgia, USA, and in the water during deployment in the New York Bight, USA.

nuanced linkages between the hydrodynamics and food web ecology at turbine, wind energy area, and regional scales (NASEM, 2024).

Within the US Northeast, increases in NARW occurrence have been observed south of traditional foraging grounds in the Gulf of Maine since approximately 2010, in regions where considerable OWD is ongoing or upcoming (Davis et al., 2017; Meyer-Gutbrod et al., 2022). Further, OWD is occurring in regions such as the New York Bight, which has historically received limited survey effort and has lacked density estimates and detailed distributional data for large whales until recently (Zoidis et al., 2021). PAM-equipped gliders operated by Rutgers and Stony Brook Universities are playing a key role in assessing the habitat use of NARWs and other large whales relative to OWD in the northeastern United States.

Since 2020, gliders have surveyed for over 700 days and have transited more than 14,000 km in and adjacent to wind lease areas in New York and New Jersey (Figures 2 and 3). These surveys have documented detections of NARWs on 10%–20% of survey days from November to March, and <5% of survey days from March to October. Continued monitoring, and the comparison of pre- and post-development occurrence data in OWD areas, will allow potential impacts of OWD on NARWs to be assessed. Further, by providing NARW detections, along with concurrently sampled subsurface oceanographic data, glider surveys will help to improve our understanding of the environmental drivers of NARW habitat use in these previously understudied regions. Given the rapid environmental change occurring in the northeastern United States, this information will be critical to distinguishing impacts of OWD on habitat use from effects of environmental variability.

US COASTAL CALVING GROUND SURVEILLANCE

Pregnant NARWs migrate to nearshore southeast US calving grounds, spanning the states of Florida, Georgia, and South Carolina, to give birth and nurse their newborn calves between the months of November and April (Gowan and Ortega-Ortiz, 2014). Non-reproductive individuals also migrate to this calving ground during the winter months (Gowan et al., 2019). Although gliders have been used for near-real-time detections of NARWs in northern foraging grounds off the coast of the United States and Canada for more than a decade, gliders were not used until 2023 for PAM in the southeast US calving ground, where glider-based PAM faces two major challenges. First, vocalization rates of lactating females compared to other demographic groups are lower in the calving ground (Parks et al., 2019b), and these calls tend to be low amplitude (Parks et al., 2019a). This reduces the likelihood of acoustically detecting a mother-calf pair in this region. Second, the calving ground is situated close to the coast over a shallow portion of the inner continental shelf. Typical depth occupancy in the calving ground is between 10 m and 25 m, which provides limited vertical space for a glider to operate its dive-climb flight pattern. The frequent shift between ascending and descending status requires more frequent engagement of the buoyancy pump, which is both energetically costly and produces self-noise that may mask whale vocalizations. Further, strong gradients in temperature, salinity, and thus sound speed, may further limit detection range.

Despite these challenges, a pilot program using gliders for NARW PAM was recently implemented through a collaboration between the University of South Carolina and the Skidaway Institute of Oceanography. So far, these

efforts consisted of a two-week mission in January 2023, and two four-week missions from January through March 2024 (Figures 2 and 3). During these three missions, which operated in water as shallow as 11 m, three definite NARW detections were made. The NARW detection on January 20, 2024, was the first definite glider-based acoustic detection in southeast US waters, and it triggered an alert from the Southeast Early Warning System notifications program for vessel strike mitigation. These pilot missions indicate that glider-based PAM may be a useful tool for supplementing aerial-based detections of NARWs in the calving ground, especially providing coverage when aerial surveillance is not feasible due to weather or other logistical constraints.

CONSERVATION IMPLICATIONS

North Atlantic right whales are at risk of extinction before the end of the century, as climate change continues to initiate distributional and behavioral changes that inadvertently increase mortality due to vessel strikes and entanglements (Meyer-Gutbrod et al., 2021). As a result, the Canadian and US governments are investing millions of dollars in technologies to support species monitoring, research to better predict future whale distributions, and mitigation efforts to address complex threats to vulnerable species. In the last five years, glider efforts have rapidly expanded, with cumulative deployments totaling thousands of days across the NARW migratory range for conservation applications (Figure 3). Here, we highlighted several examples of how PAM-equipped underwater gliders are being used for vessel strike and entanglement mitigation by enhancing risk reduction for dynamic management areas, regional fisheries, and offshore wind energy projects (Table 1). Going forward, this technology has the capacity to contribute to more spatial conservation strategies, such as marine protected areas. These areas tend to encompass vast and/or remote areas that are logistically difficult for personnel to survey, which can hamper authorities' ability to enforce protective measures. Therefore, the use of gliders is likely to continue expanding into the future and across the marine domain in support of species conservation and threat mitigation.

Glider-based PAM offers key spatial monitoring capabilities for NARW threat management but is typically used in conjunction with other, complementary monitoring platforms, such as aerial surveillance and PAM moorings. Because NARWs are an internationally mobile cetacean species that spans diverse habitats and protection measures, surveillance assets must fulfill different requirements (e.g., temporal effort, spatial scale, deployment location, data type) across the NARW range, depending on the goal(s) of each individual monitoring program. Because the space-time needs of successful range-wide management are so complex, no one tool could possibly achieve all monitoring imperatives. As one example, gliders were deployed in the Cabot Strait voluntary seasonal slowdown zone in the GoSL for two years. Despite being a known high-use migratory corridor, we did not acoustically detect any NARWs in near-real time. This may have been because of behaviorally influenced calling rates, missed whales traveling close to shore (i.e., deployment location vs. whale movements), or platform type (e.g., mid-endurance mobile glider vs. long-endurance stationary array). Thus, glider-based PAM is being used alongside a suite of other tools, including moored PAM, visual monitoring, and distribution modeling, to aid conservation goals.

We have presented several different area-based threats, management goals, and mitigation plans across glider survey regions. These highlight the need for continued research/support for additional and/or new monitoring platforms (including gliders) to be incorporated into existing and future management plans for the conservation of NARWs. However, the efficacy of glider detections at achieving conservation goals depends largely on the regional regulatory measures in place being informed by these detections. For example, in a recent study, the average percentage of mariners found to be cooperating with 10-knot speed requests in US dynamic management areas was less than 50%, compared to higher compliance in some, but not all, mandatory seasonal management areas (>85% in most areas, but <25% for the largest commercial vessels outside four ports in the southeastern United States; NMFS, 2020). In contrast, Canada has made mitigation measures in the dynamic shipping zones of the GoSL mandatory and achieved 99% compliance during the 2023 monitoring season (Bilodeau, 2023). Furthermore, slowdowns in eastern Canadian waters affect vessels down to 13 m, whereas US speed restrictions currently only apply to vessels that are greater than or equal to 19.8 m. This difference is significant, as four of 13 vessel-related NARW deaths in US waters since 2008 were attributable to boats less than 20 m and, therefore, not subject to slowdown measures (Redfern, 2023). No matter how capable a technology or monitoring system, its overall conservation impact is intertwined with the prevailing management policies.

REFERENCES

Baumgartner, M.F., and B.R. Mate. 2005. Summer and fall habitat of North Atlantic right whales (*Eubalaena glacialis*) inferred from satellite telemetry. *Canadian Journal of Fisheries and Aquatic Sciences* 62(3):527–543, https://doi.org/10.1139/f04-238.

Baumgartner, M.F., and S.E. Mussoline. 2011. A generalized baleen whale call detection and classification system. *The Journal of the Acoustical Society of America* 129(5):2,889–2,902, https://doi.org/10.1121/1.3562166.

Baumgartner, M.F., D.M. Fratantoni, T.P. Hurst, M.W. Brown, T.V. Cole, S.M. Van Parijs, and M. Johnson. 2013. Real-time reporting of baleen whale passive acoustic detections from ocean gliders. *The Journal of the Acoustical Society of America* 134(3):1,814–1,823, https://doi.org/10.1121/1.4816406.

Baumgartner, M.F., K.M. Stafford, P. Winsor, H. Statscewich, and D.M. Fratantoni. 2014. Glider-based passive acoustic monitoring in the Arctic. *Marine Technology Society Journal* 48(5):40–51, https://doi.org/10.4031/MTSJ.48.5.2.

Baumgartner, M.F., J. Bonnell, S.M. Van Parijs, P.J. Corkeron, C. Hotchkin, K. Ball, L.P. Pelletier, J. Partan, D. Peters, J. Kemp, and others. 2019. Persistent near real-time passive acoustic monitoring for baleen whales from a moored buoy: System description and evaluation. *Methods in Ecology and Evolution* 10(9):1,476–1,489, https://doi.org/10.1111/2041-210X.13244.

Baumgartner, M.F., J. Bonnell, P.J. Corkeron, S.M. Van Parijs, C. Hotchkin, B.A. Hodges, J. Bort Thornton, B.L. Mensi, and S.M. Bruner. 2020. Slocum gliders provide accurate near real-time estimates of baleen whale presence from human-reviewed passive acoustic detection information. *Frontiers in Marine Science* 7:100, https://doi.org/10.3389/fmars.2020.00100.

Bilodeau, M. 2023. Transport Canada (TC) update on North Atlantic right whale vessel management measures. Presentation given at the annual North Atlantic Right Whale Consortium, October 24–25, 2023, Halifax, NS, Canada.

Bowling, T. 2022. Court reinstates seasonal closure of Maine lobster fishery to protect whales. *The SandBar* 21(1):4–5.

Daoust, P.Y., E.L. Couture, T. Wimmer, and L. Bourque. 2018. *Incident Report: North Atlantic Right Whale Mortality Event in the Gulf of St. Lawrence, 2017.* Collaborative report produced by Canadian Wildlife Health Cooperative, Marine Animal Response Society, and Fisheries and Oceans Canada, 256 pp.

Davis, G.E., M.F. Baumgartner, J.M. Bonnell, J. Bell, C. Berchok, J. Bort Thornton, S. Brault, G. Buchanan, R.A. Charif, D. Cholewiak, and others. 2017. Long-term passive acoustic recordings track the changing distribution of North Atlantic right whales (*Eubalaena glacialis*) from 2004 to 2014. *Scientific Reports* 7(1):13460, https://doi.org/10.1038/s41598-017-13359-3.

Fisheries and Oceans Canada. 2023. "Protecting North Atlantic Right Whales: Canada's Fishing Measures by Year Launched," https://www.dfo-mpo.gc.ca/about-notre-sujet/publications/infographics-infographies/narw-bnan-by-year-par-annee-eng.html.

Fisheries and Oceans Canada. 2024. "2024 Fishery Management Measures," https://www.dfo-mpo.gc.ca/fisheries-peches/commercial-commerciale/atl-arc/narw-bnan/management-gestion-eng.html.

Gowan, T.A., and J.G. Ortega-Ortiz. 2014. Wintering habitat model for the North Atlantic right whale (*Eubalaena glacialis*) in the southeastern United States. *PLoS ONE* 9(4):e95126, https://doi.org/10.1371/journal.pone.0095126.

Gowan, T.A., J.G. Ortega-Ortiz, J.A. Hostetler, P.K. Hamilton, A.R. Knowlton, K.A. Jackson, R.C. George, C.R. Taylor, and P.J. Naessig. 2019. Temporal and demographic variation in partial migration of the North Atlantic right whale. *Scientific Reports* 9(1):353, https://doi.org/10.1038/s41598-018-36723-3.

Johnson, M., and T. Hurst. 2007. The DMON: An open-hardware/open-software passive acoustic detector. Paper presented at the 3rd International Workshop on the Detection and Classification of Marine Mammals Using Passive Acoustics, July 24–26, 2007, Boston, MA, USA.

Matthews, L.P., and S.E. Parks. 2021. An overview of North Atlantic right whale acoustic behavior, hearing capabilities, and responses to sound. *Marine Pollution Bulletin* 173(Pt B):113043, https://doi.org/10.1016/j.marpolbul.2021.113043.

Maxwell, S.M., E.L. Hazen, R.L. Lewison, D.C. Dunn, H. Bailey, S.J. Bograd, D.K. Briscoe, S. Fossette, A.J. Hobday, M. Bennett, and others. 2015. Dynamic ocean management: Defining and conceptualizing real-time management of the ocean. *Marine Policy* 58:42–50, https://doi.org/10.1016/j.marpol.2015.03.014.

Meyer-Gutbrod, E., C. Greene, and K. Davies. 2018. Marine species range shifts necessitate advanced policy planning: The case of the North Atlantic right whale. *Oceanography* 31(2):19–23, https://doi.org/10.5670/oceanog.2018.209.

Meyer-Gutbrod, E.L., C.H. Greene, K.T.A. Davies, and D.G. Johns. 2021. Ocean regime shift is driving collapse of the North Atlantic right whale population. *Oceanography* 34(3):22–31, https://doi.org/10.5670/oceanog.2021.308.

Meyer-Gutbrod, E.L., K.T.A. Davies, C.L. Johnson, S. Plourde, K.A. Sorochan, R.D. Kenney, C. Ramp, J.F. Gosselin, J.W. Lawson, and C.H. Greene. 2022. Redefining North Atlantic right whale habitat-use patterns under climate change. *Limnology and Oceanography* 68:S71–S86, https://doi.org/10.1002/lno.12242.

NASEM (National Academies of Science, Engineering, and Medicine). 2024. *Potential Hydrodynamic Impacts of Offshore Wind Energy on Nantucket Shoals Regional Ecology: An Evaluation from Wind to Whales*. The National Academies Press, Washington, DC, https://doi.org/10.17226/27154.

NMFS (National Marine Fisheries Service). 2020. *North Atlantic Right Whale (*Eubalaena glacialis*) Vessel Speed Rule Assessment*. National Marine Fisheries Service, Office of Protected Resources, Silver Spring, MD, 53 pp.

NMFS. 2025. "2017–2025 North Atlantic Right Whale Unusual Mortality Event," https://www.fisheries.noaa.gov/national/marine-life-distress/2017-2025-north-atlantic-right-whale-unusual-mortality-event.

Parks, S.E., A. Searby, A. Célérier, M.P. Johnson, D.P. Nowacek, and P.L. Tyack. 2011. Sound production behavior of individual North Atlantic right whales: Implications for passive acoustic monitoring. *Endangered Species Research* 15(1):63–76, https://doi.org/10.3354/esr00368.

Parks, S.E., D.A. Cusano, S.M. Van Parijs, and D.P. Nowacek. 2019a. Acoustic crypsis in communication by North Atlantic right whale mother-calf pairs on the calving grounds. *Biology Letters* 15(10):20190485, https://doi.org/10.1098/rsbl.2019.0485.

Parks, S.E., D.A. Cusano, S.M. Van Parijs, and D.P. Nowacek. 2019b. North Atlantic right whale (*Eubalaena glacialis*) acoustic behavior on the calving grounds. *The Journal of the Acoustical Society of America* 146(1):EL15–EL21, https://doi.org/10.1121/1.5115332.

Redfern, J.V. 2023. *Examining the Impacts of the National Oceanic and Atmospheric Administration's Proposed Changes to the North Atlantic Right Whale Vessel Strike Reduction Rule*. United States House of Representatives Natural Resources Subcommittee on Water, Wildlife, and Fisheries, Washington, DC, 12 pp.

Ruckdeschel, G.S., K.T.A. Davies, and T. Ross. 2020. Biophysical drivers of zooplankton variability on the Scotian Shelf observed using profiling electric gliders. *Frontiers in Marine Science* 7:627, https://doi.org/10.3389/fmars.2020.00627.

Sharp, S.M., W.A. McLellan, D.S. Rotstein, A.M. Costidis, S.G. Barco, K. Durham, T.D. Pitchford, K.A. Jackson, P.Y. Daoust, T. Wimmer, and others. 2019. Gross and histopathologic diagnoses from North Atlantic right whale *Eubalaena glacialis* mortalities between 2003 and 2018. *Diseases of Aquatic Organisms* 135(1):1–31, https://doi.org/10.3354/dao03376.

Transport Canada. 2024. "Protecting North Atlantic right whales from collisions with vessels in the Gulf of St. Lawrence," https://tc.canada.ca/en/marine-transportation/navigation-marine-conditions/protecting-north-atlantic-right-whales-collisions-vessels-gulf-st-lawrence.

Van Parijs, S.M., K. Baker, J. Carduner, J. Daly, G.E. Davis, C. Esch, S. Guan, A. Scholik-Schlomer, N.B. Sisson, and E. Staaterman. 2021. NOAA and BOEM minimum recommendations for use of passive acoustic listening systems in offshore wind energy development monitoring and mitigation programs. *Frontiers in Marine Science* 8, https://doi.org/10.3389/fmars.2021.760840.

Webb, D.C., P.J. Simonetti, and C.P. Jones. 2001. SLOCUM: An underwater glider propelled by environmental energy. *IEEE Journal of Oceanic Engineering* 26(4):447–452, https://doi.org/10.1109/48.972077.

Wilder, J., G. Davis, A. DeAngelis, S. Van Parijs, and M. Baumgartner. 2023. *Low-Frequency Detection and Classification System (LFDCS) Reference Guide*. National Oceanic and Atmospheric Administration, National Marine Fisheries Service, Northeast Fisheries Science Center, Woods Hole, Massachusetts, 142 pp.

Zoidis, A.M., K.S. Lomac-MacNair, D.S. Ireland, M.E. Rickard, K.A. McKown, and M.D. Schlesinger. 2021. Distribution and density of six large whale species in the New York Bight from monthly aerial surveys 2017 to 2020. *Continental Shelf Research* 230:104572, https://doi.org/10.1016/j.csr.2021.104572.

ACKNOWLEDGMENTS

We would like to thank the following for funding support: Transport Canada, Fisheries and Oceans Canada, the Ocean Tracking Network, Marine Environmental Observation, Prediction and Response Network, the Murphy Family Foundation, the Broad Reach Fund, NOAA Northeast Fisheries Science Center, the Northeastern Regional Association of Coastal Ocean Observing Systems, the New York State Environmental Protection Fund Ocean and Great Lakes Program via the New York State Department of Environmental Conservation, the New York State Energy Research and Development Authority, the Mid-Atlantic Regional Association Coastal Ocean Observing System, the Tides Foundation, and the Southeast Coastal Ocean Observing Regional Association.

We would also like to express our sincere appreciation to the following individuals, who were key to glider operations and mission support: A. Comeau, J. van der Meer, Z. Viva, B. Hodges, M. Meier, J. Wilder, C. Flagg, D. Aragon, N. Waite, J. Kohut, T. Miles, A. Kreuser, A. Sefah-Twerefour, K. Dreger, J. Bird, F. McQuarrie, and A. Vincent.

AUTHORS

Katherine L. Indeck (katherine.indeck@unb.ca), University of New Brunswick, Saint John, NB, Canada. **Mark F. Baumgartner**, Woods Hole Oceanographic Institution, Woods Hole, MA, USA. **Laurence Lecavalier**, Transport Canada Innovation Centre, Ottawa, ON, Canada. **Frederick Whoriskey**, Ocean Tracking Network, Halifax, NS, Canada. **Delphine Durette-Morin**, Canadian Whale Institute, Welshpool, NB, Canada. **Neal R. Pettigrew**, School of Marine Sciences, The University of Maine, Orono, ME, USA. **Jacqueline M. McSweeney**, **Lesley H. Thorne**, and **Katherine L. Gallagher**, Stony Brook University, Stony Brook, NY, USA. **Catherine R. Edwards**, Skidaway Institute of Oceanography, University of Georgia, Savannah, GA, USA. **Erin Meyer-Gutbrod**, School of the Earth, Ocean, and Environment, University of South Carolina, Columbia, SC, USA. **Kimberley T.A. Davies**, University of New Brunswick, Saint John, NB, Canada.

ARTICLE DOI. https://doi.org/10.5670/oceanog.2025e111

OBSERVING MARINE HEATWAVES USING OCEAN GLIDERS TO ADDRESS ECOSYSTEM CHALLENGES THROUGH A COORDINATED NATIONAL PROGRAM

By Jessica A. Benthuysen, Charitha Pattiaratchi, Claire M. Spillman, Pallavi Govekar, Helen Beggs, Hugo Bastos de Oliveira, Arani Chandrapavan, Ming Feng, Alistair J. Hobday, Neil J. Holbrook, Fabrice R.A. Jaine, and Amandine Schaeffer

MARINE HEATWAVES THREATEN MARINE ECOSYSTEMS

As the ocean has warmed, in recent decades marine heatwaves (MHWs) have emerged as a major threat to marine ecosystems and ecosystem services, presenting challenges for management of marine fisheries, aquaculture, tourism, and conservation, including for marine protected areas (MPAs). An MHW is a period of unusually high ocean temperatures, often defined as ocean temperatures that are warmer than 90% of the previous observations for a given time of year. MHWs along Australia's coastal regions have led to mass coral bleaching on the Great Barrier Reef, damage to kelp forests and seagrass meadows in Western Australia, shifts in species, and fish and invertebrate mortality, all creating pressures on fisheries management (as reviewed in Smith et al., 2023). Understanding how climate change influences ocean extremes and impacts societal and natural values is key for evaluating future risks. Growing concerns around the effects of MHWs on marine industries, food security, ecosystem dynamics, and conservation efforts led to the development of MHW response plans for Tasmania and New South Wales during the summer of 2023/24 (Hobday et al., 2024).

While satellite sea surface temperature (SST) products reveal an MHW's surface expression, its subsurface structure remains unknown without in situ monitoring. The ability to investigate subsurface properties in near-real time is critical for understanding MHWs' impacts on vulnerable habitats and species and can support evidence-based decision-making.

EVENT BASED SAMPLING: A NATIONAL INITIATIVE

Ocean gliders are agile instruments that can be deployed relatively easily to transmit data in near-real time. Gliders measure a range of subsurface oceanographic variables, including water temperature and salinity, and other data important for characterizing the marine environment, such as chlorophyll fluorescence as an estimate of phytoplankton biomass, and light, which is important for photosynthesis. Since 2007, Australia's Integrated Marine Observing System (IMOS) Ocean Gliders Facility has repeatedly conducted routine missions in specific regions around Australia (Pattiaratchi et al., 2017). Since December 2018, when IMOS enabled an Event Based Sampling program, glider missions have rapidly responded to and sampled emerging MHWs over the Australian continental shelf, creating a step change in our capacity to understand the dynamics and impacts of MHWs on marine ecosystems.

Sampling extreme events is challenging, as their occurrence is rare and somewhat unpredictable. A nationally coordinated strategy guides the selection of glider missions to target MHW events during their growth, peak, and decay phases. A national advisory committee composed of experts from universities, government and science institutions, and stakeholders, including marine park managers, meets every one to two months. The committee reviews risk criteria on emerging MHWs (**Figure 1**), such as current SST observations and seasonal forecasts, to determine how conditions are likely to change (Smith and Spillman, 2024). Based on available evidence, deployment locations are prioritized according to an event's severity and duration, likely impacts, consequences for decision-makers, and technical feasibility as well as the availability of existing observations and models for analyzing the event.

Once an emerging MHW has been identified, gliders can be deployed within one to three weeks in most areas around Australia. A glider mission typically lasts for three to four weeks and can be redeployed rapidly if required. Near-real-time data are openly available through the IMOS Australian Ocean Data Network Portal and visualized at the IMOS Ocean Gliders Facility website and the IMOS OceanCurrent glider website, allowing direct access to the latest information on an MHW's subsurface characteristics. Using their links to different sectors, the multi-partner national committee disseminates the glider mission's status and findings to stakeholders and data users.

REVEALING SUBSURFACE MARINE HEATWAVES

MHWs can span hundreds to thousands of kilometers along the continental shelf and last from weeks to months. Hence, understanding the physical processes that underpin their occurrences, depths, and influence on other biophysical variables is necessary for assessing the risks they pose to marine systems and MPAs, thereby aiding in effective

STRATEGIES FOR EVENT BASED SAMPLING
DEPLOYING OCEAN GLIDERS TO MONITOR EXTREME EVENTS

DECISION-MAKING CRITERIA

INDICATORS AND PREDICTORS
Is an event developing, such as a marine heatwave based on current ocean temperatures and seasonal predictions?

EVENT TEMPORAL EXTENT
Will a deployment be able to sample the full event?

EVENT SPATIAL EXTENT
Will the event affect a large region and the area of interest?

PHYSICAL PROCESSES
What processes are causing the event and how will observations improve our understanding?

AVAILABLE OBSERVATIONS
What other datasets are being collected and in near-real time?

ECOLOGICAL IMPACTS
What will be the consequences of the event, and will observations improve our understanding?

STAKEHOLDER NEEDS
Will the observations provide the information required for analysis, assessment, and decision-making?

DEPLOYMENT

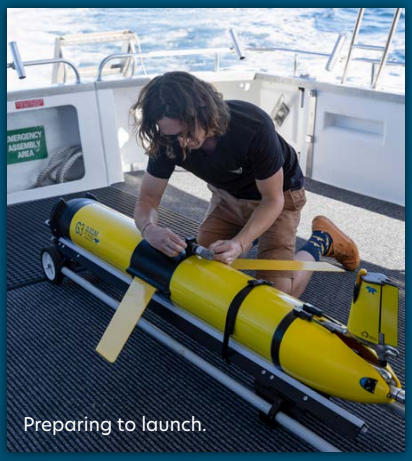
Preparing to launch.


Deployment underway.

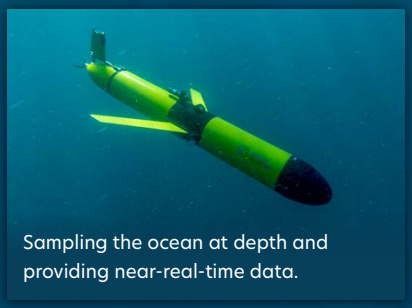
Sampling the ocean at depth and providing near-real-time data.

DATA DELIVERY FOR IMPACT

NEAR-REAL-TIME DATA STREAMS
Visualizations show the glider's location and measurements once it has surfaced every several hours. Found at the Integrated Marine Observing System (IMOS) Ocean Glider Facility.

DISPLAYING DATA WITH OTHER OCEAN OBSERVATIONS
While sampling, the glider's position is shown with sea surface temperatures, anomalies, and percentiles, which reveal the surface marine heatwave. Found at IMOS OceanCurrent.

ACCESSIBLE DATA
Quality-controlled near-real-time and delayed mode data are available through the Australian Ocean Data Network (AODN) Portal and visualized through the IMOS OceanCurrent's glider webpage.

SHARING FINDINGS
During an event, glider data visualizations and findings are shared via a national committee with stakeholders and through briefings and in newsletters.

FIGURE 1. The steps are shown here for planning an Event Based Sampling glider mission, deploying a glider, and providing the resulting data to researchers, marine managers, industry, and the broader community. *Photo credits: Nick Thake*

management and conservation. The IMOS Event Based Sampling program has deployed 15 glider missions targeting MHWs, one for a tropical cyclone and one for a cold eddy that occurred post-tropical cyclone (Figure 2a). Since 2019, an additional 11 routine glider missions have sampled MHWs, and they have been instrumental in capturing an MHW generation phase, and 24 missions total have intersected MPAs (Figure 2a).

Repeat glider missions have been conducted off Tasmania, as this region's long-term warming trend has been associated with long-lasting and intense MHWs (Kajtar et al., 2021). During summer 2022, in response to an MHW off Tasmania's east coast, a glider mission revealed the vertical extent of extremely warm temperatures (Figure 2c) beyond those observed at the sea surface by satellite remote sensing (Figure 2b). The high salinity signature of warm water (Figure 2d) was indicative of the East Australian Current extension flowing southward through Freycinet Marine Park. A deep chlorophyll maximum was observed from fluorescence measurements (Figure 2e). MHWs can occur in this region due to enhanced and deep poleward movement of heat from an intensified East Australian Current extension or enhanced air-sea heat flux. During the warmest months of the year, near-real-time subsurface data from gliders can be useful for detecting southward shifts in waters that likely influence marine species unable to cope with poleward relocation. A 2019 mission highlighted a larger-scale MHW offshore

and cooler coastal waters that created a buffer zone for coastal resources and industries. The findings from these glider missions were communicated to representatives from the seafood industry so they could anticipate MHW conditions and potential impacts on this sector. During winter to spring, MHWs can cause harmful algal blooms, and regular communication with those conducting sampling has enhanced understanding of whether anomalously warm water conditions were causing such events.

Glider missions around the Great Barrier Reef have provided valuable near-real-time subsurface measurements during coral bleaching events. Mission locations were planned in collaboration with researchers enacting coral bleaching response plans and representatives from the Great Barrier Reef Marine Park Authority. As events unfolded, interpretations of the glider observations were communicated broadly to researchers and government agencies. In some cases, cooler waters were found to be present at depth in reef passages that connect the lagoon to the continental slope, offering corals and other organisms potential refugia from hot surface waters.

RESPONDING TO MARINE ECOSYSTEM CHALLENGES

To date, strategic sampling with IMOS glider deployments has captured ocean conditions associated with a diversity of MHWs to support marine research, management, industry, and the broader community. Event Based Sampling missions provided stakeholders with near-real-time subsurface data at high spatial and temporal resolution at

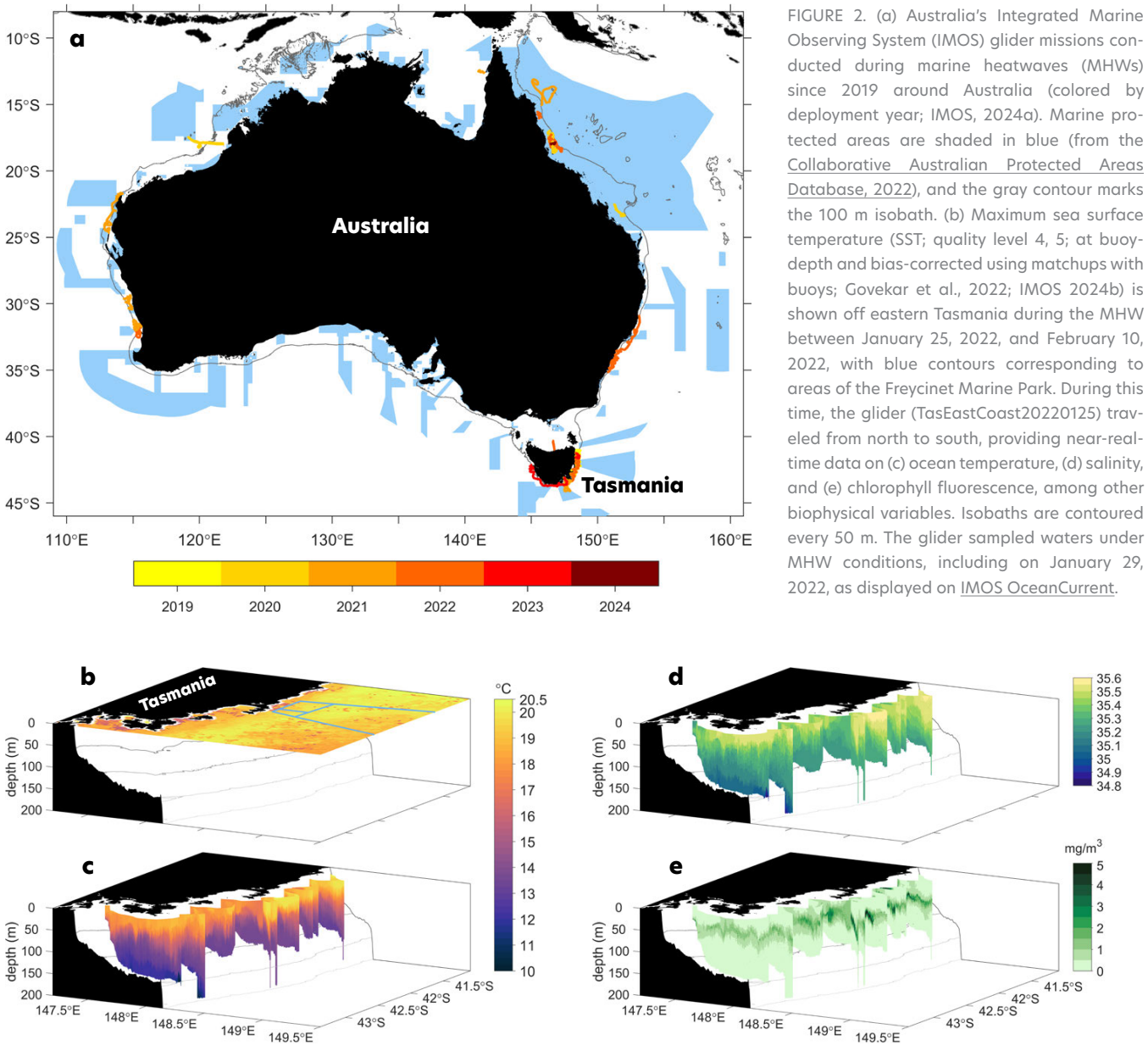

FIGURE 2. (a) Australia's Integrated Marine Observing System (IMOS) glider missions conducted during marine heatwaves (MHWs) since 2019 around Australia (colored by deployment year; IMOS, 2024a). Marine protected areas are shaded in blue (from the Collaborative Australian Protected Areas Database, 2022), and the gray contour marks the 100 m isobath. (b) Maximum sea surface temperature (SST; quality level 4, 5; at buoy-depth and bias-corrected using matchups with buoys; Govekar et al., 2022; IMOS 2024b) is shown off eastern Tasmania during the MHW between January 25, 2022, and February 10, 2022, with blue contours corresponding to areas of the Freycinet Marine Park. During this time, the glider (TasEastCoast20220125) traveled from north to south, providing near-real-time data on (c) ocean temperature, (d) salinity, and (e) chlorophyll fluorescence, among other biophysical variables. Isobaths are contoured every 50 m. The glider sampled waters under MHW conditions, including on January 29, 2022, as displayed on IMOS OceanCurrent.

critical times for understanding MHW persistence and biological impacts in coastal areas. The missions have offered opportunities to assess the impacts of MHWs on habitats and species while also improving our understanding of the ocean processes that drive their occurrence. They have helped to address the challenge of data scarcity, reducing uncertainties in characterizing these events in the subsurface where observations are limited but crucial for conservation and management decisions. Scientific data generated through these targeted missions have underpinned research advances that will potentially inform policy related to climate change and environmental adaptation (e.g., Hobday et al., 2024).

The integration of glider data with other near-real-time data streams through web platforms (e.g., IMOS OceanCurrent) offers a valuable one-stop source for stakeholders to monitor the development of extreme weather events in their regions of interest and increases public accessibility of available data. Ocean water temperature and salinity data from gliders are currently compared against coarse resolution climatologies, and work is underway to develop glider-derived subsurface climatologies over the continental shelf and improve understanding of subsurface MHWs. Furthermore, ocean glider measurements offer validation of high-resolution satellite observations in coastal areas and can detect fronts, where sharp changes in oceanographic variables occur and regular buoy data at fixed locations are not sufficient.

With projected changes to Australia's climate, including rising ocean temperatures, increased tropical cyclone intensity, and extreme rainfall events and subsequent outflows, marine extremes are increasingly recognized as high-priority issues. Looking forward, the scope of IMOS Event Based Sampling will be broadened to monitor those extremes along with marine heatwaves and cold spells. Continued efforts will provide insights into how events affect MPAs, supporting assessment of their impacts on the marine environment, including habitat degradation and changes in species distribution and abundance, the food web, and biodiversity. Now, more than ever before, ocean gliders offer a powerful capability for rapid mobilization and near-real-time monitoring to respond to challenges in marine ecosystems and their management.

REFERENCES

Govekar, P.D., C. Griffin, and H. Beggs. 2022. Multi-sensor sea surface temperature products from the Australian Bureau of Meteorology. *Remote Sensing* 14:3785, https://doi.org/10.3390/rs14153785.

Hobday, A.J., C.M. Spillman, J. Allnutt, M.A. Coleman, F. Bailleul, L.K. Blamey, S. Brodie, A. Chandrapavan, J.R. Hartog, D. Maynard, and others. 2024. Forecasting a summer of extremes: Building stakeholder response capacity to marine heatwaves. *Oceanography* 37(3):42–51, https://doi.org/10.5670/oceanog.2024.508.

IMOS (Integrated Marine Observing System). 2024a. IMOS Australian National Facility for Ocean Gliders (ANFOG) – Delayed mode glider deployments, https://portal.aodn.org.au/search?uuid=c317b0fe-02e8-4ff9-96c9-563fd58e82ac.

IMOS. 2024b. IMOS 6-day Night-time Multi-Sensor L3S gridded multiple-sensor multiple-swath Australian region skin SST (L3SM-6d), https://portal.aodn.org.au/search?uuid=e1908591-b3cf-42aa-a32f-424322b28165.

Kajtar, J.B., N.J. Holbrook, and V. Hernaman. 2021. A catalogue of marine heatwave metrics and trends for the Australian region. *Journal of Southern Hemisphere Earth Systems Science* 71(3):284–302, https://doi.org/10.1071/ES21014.

Pattiaratchi, C., L.M. Woo, P.G. Thomson, K.K. Hong, and D. Stanley. 2017. Ocean glider observations around Australia. *Oceanography* 30(2):90–91, https://doi.org/10.5670/oceanog.2017.226.

Smith, K.E., M.T. Burrows, A.J. Hobday, N.G. King, P.J. Moore, A. Sen Gupta, M.S. Thomsen, T. Wernberg, and D.A. Smale. 2023. Biological impacts of marine heatwaves. *Annual Review of Marine Science* 15:119–145, https://doi.org/10.1146/annurev-marine-032122-121437.

Smith, G.A., and C.M. Spillman. 2024. Global ocean surface and subsurface temperature forecast skill over subseasonal to seasonal timescales. *Journal of Southern Hemisphere Earth Systems Science* 74:ES23020, https://doi.org/10.1071/ES23020.

ACKNOWLEDGMENTS

Glider and SST data were produced as part of Australia's Integrated Marine Observing System (IMOS). IMOS is enabled by the National Collaborative Research Infrastructure Strategy (NCRIS). It is operated by a consortium of institutions as an unincorporated joint venture, with the University of Tasmania as lead agent. We thank the IMOS Ocean Gliders Facility team for their contributions to this program. The satellite imagery data were acquired from the Suomi-NPP and NOAA-20 satellites by NOAA, from the MetOp-B satellite by EUMETSAT OSI-SAF, and from the NOAA spacecraft by the Bureau of Meteorology, Australian Institute of Marine Science, Australian Commonwealth Scientific and Industrial Research Organization, Geoscience Australia, and Western Australian Satellite Technology and Applications Consortium. The satellite data were processed by the Bureau of Meteorology to produce the IMOS Multi-sensor L3S SST data.

AUTHORS

Jessica A. Benthuysen (j.benthuysen@aims.gov.au), Australian Institute of Marine Science, Crawley, Western Australia, Australia. **Charitha Pattiaratchi**, School of Engineering and the UWA Oceans Institute, The University of Western Australia, Perth, Western Australia, Australia. **Claire M. Spillman**, **Pallavi Govekar**, and **Helen Beggs**, Bureau of Meteorology, Docklands, Victoria, Australia. **Hugo Bastos de Oliveira**, South Australian Research and Development Institute (Aquatic Sciences), Henley Beach, South Australia, Australia. **Arani Chandrapavan**, Western Australian Fisheries and Marine Research Laboratories, and Department of Primary Industries and Regional Development, Hillarys, Western Australia, Australia. **Ming Feng**, CSIRO Environment, Crawley, Western Australia, Australia. **Alistair J. Hobday**, CSIRO Environment, Hobart, Tasmania, Australia. **Neil J. Holbrook**, Institute for Marine and Antarctic Studies, and ARC Centre of Excellence for Climate Extremes, University of Tasmania, Hobart, Tasmania, Australia. **Fabrice R.A. Jaine**, Integrated Marine Observing System, University of Tasmania, Hobart, Tasmania, Australia. **Amandine Schaeffer**, School of Mathematics and Statistics, and Centre for Marine Science and Innovation, University of New South Wales, Sydney, New South Wales, Australia.

ARTICLE DOI. https://doi.org/10.5670/oceanog.2025e101

MONITORING OCEAN BIOLOGY AND NATURAL RESOURCES AUTONOMOUSLY AND EFFICIENTLY USING UNDERWATER GLIDERS

By Heather Broadbent, Alex Silverman, Randy Russell, Garrett Miller, Sean Beckwith, Edmund Hughes, and Chad Lembke

The University of South Florida (USF) College of Marine Science operates a fleet of six Teledyne Webb Research Slocum gliders as cost-effective research platforms for sampling the water column. Underwater gliders are autonomous robots that traverse the water to collect a suite of physical (e.g., temperature and salinity) and chemical (e.g., nutrients and dissolved oxygen) data to better understand the environment of coastal and open oceans. Over the past decade, the USF glider group has added sensors to obtain biological data (e.g., fluorometers, acoustic telemetry receivers, echosounders, and passive acoustic monitors) to help survey and monitor marine organisms. The data collected on these glider missions has been used in the forecasting of red tide blooms, detection of tagged aquatic animals, collection of biomass data, and recording of fish and marine mammal sounds in the Gulf of Mexico (GoM) and the Atlantic Ocean. Here we describe how our glider fleet has obtained critical biological data and is continuously evolving to better assist in addressing ecosystem-level challenges associated with global environmental changes.

Most of the USF glider missions in the GoM are cross-shelf deployments that sample the water column to directly measure or derive salinity, temperature, density, oxygen, chlorophyll-*a*, and colored dissolved organic matter (CDOM; Figure 1). Each of these parameters has been used to monitor water column variables to assist in forecasting blooms of the toxic alga *Karenia brevis*, also known

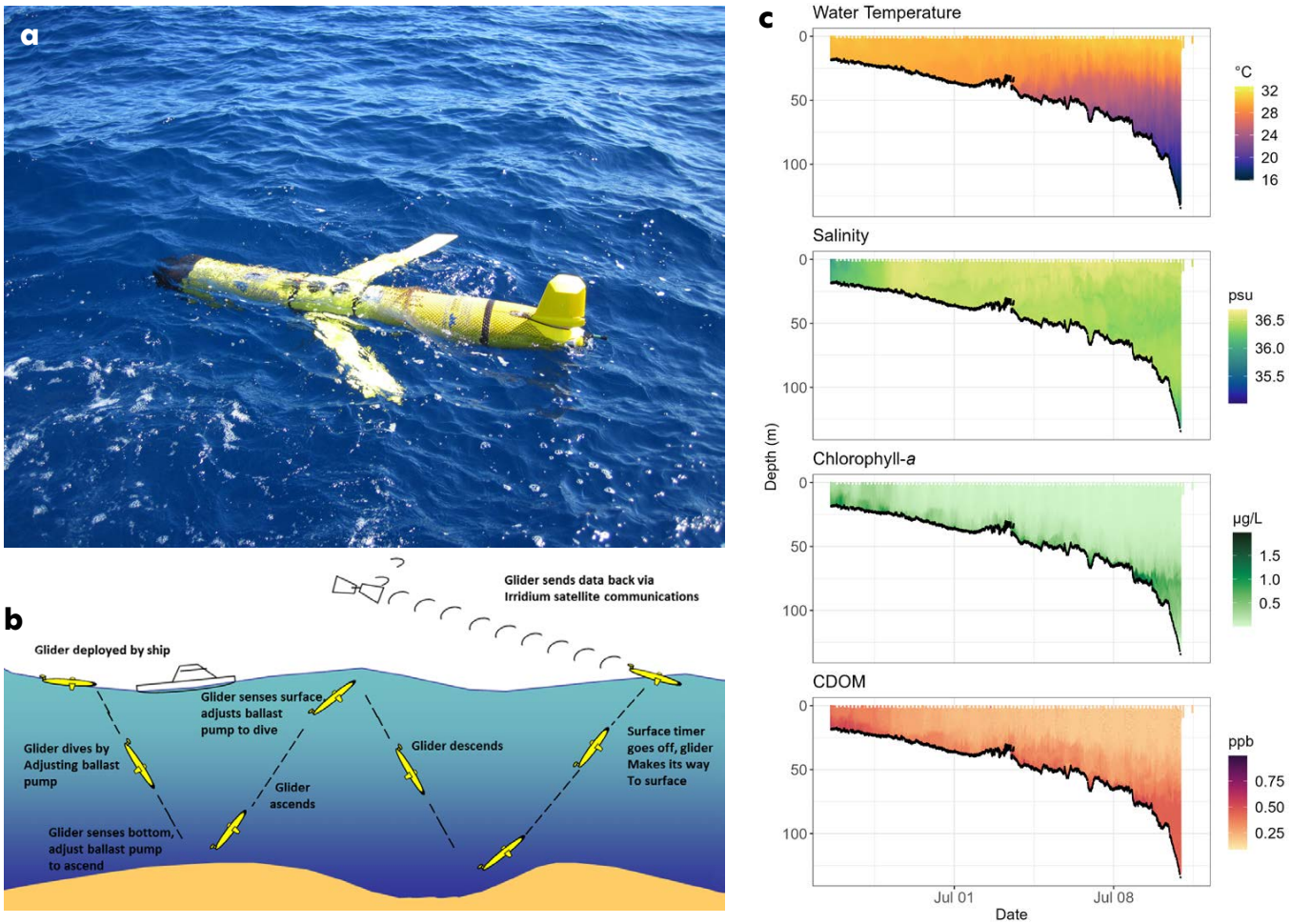

FIGURE 1. Gliders (a) are autonomous tools that (b) systematically profile the ocean water column while collecting (c) important data such as temperature, salinity, chlorophyll-*a*, and colored dissolved organic matter (CDOM).

as red tide. Our group collaborates with the Florida Fish and Wildlife Conservation Commission (FWC) harmful algal bloom monitoring and research program as part of the College of Marine Science's Center for Red Tide Tracking and Forecasting to acquire continuous water column observations in support of modeling and nutrient analyses. Water property glider observations, such as those listed above, confirm water column dynamics predicted by eastern GoM models. For example, a 2018 across-shelf transect identified upwelling circulation favorable for transporting deep-water nutrients that likely contributed to the intensity and location of a red tide outbreak on the west Florida shelf (Weisberg et al., 2019). Since 2018, USF gliders have totaled over 1,500 glider days, contributing to tracking red tide blooms and their effects.

Acoustic telemetry receivers have become a regular part of USF glider fleet deployments, with loaned or donated receivers detecting marine organisms that are implanted with acoustic transmitting tags. Since 2014, detected tag identification numbers and associated data have been submitted to the Ocean Tracking Network (OTN) and Integrated Tracking of Aquatic Animals in the Gulf of Mexico (iTAG) groups for research, monitoring, and management. By working directly with the FWC Fish and Wildlife Research Institute, we have successfully detected 231 red snappers tagged and released in the GoM by the Movement Ecology and Reproductive Resilience Lab, providing key contextual environmental data for these fish detections, including location, depth, and water temperature. In addition, these glider-based receivers have detected another 211 unknown tags owned by other members of the network, such as academic, state, and federal institutions. By working with OTN and iTAG, 56 of these detections have been identified and the managing researchers notified of the detection location, time, and corresponding water column environmental data collected. These data are critical to understanding the tagged animal's migration and residency activity needed to improve and reach management targets (Figure 2).

Passive acoustic monitoring (PAM) devices on gliders that record ambient ocean sounds, including fish and

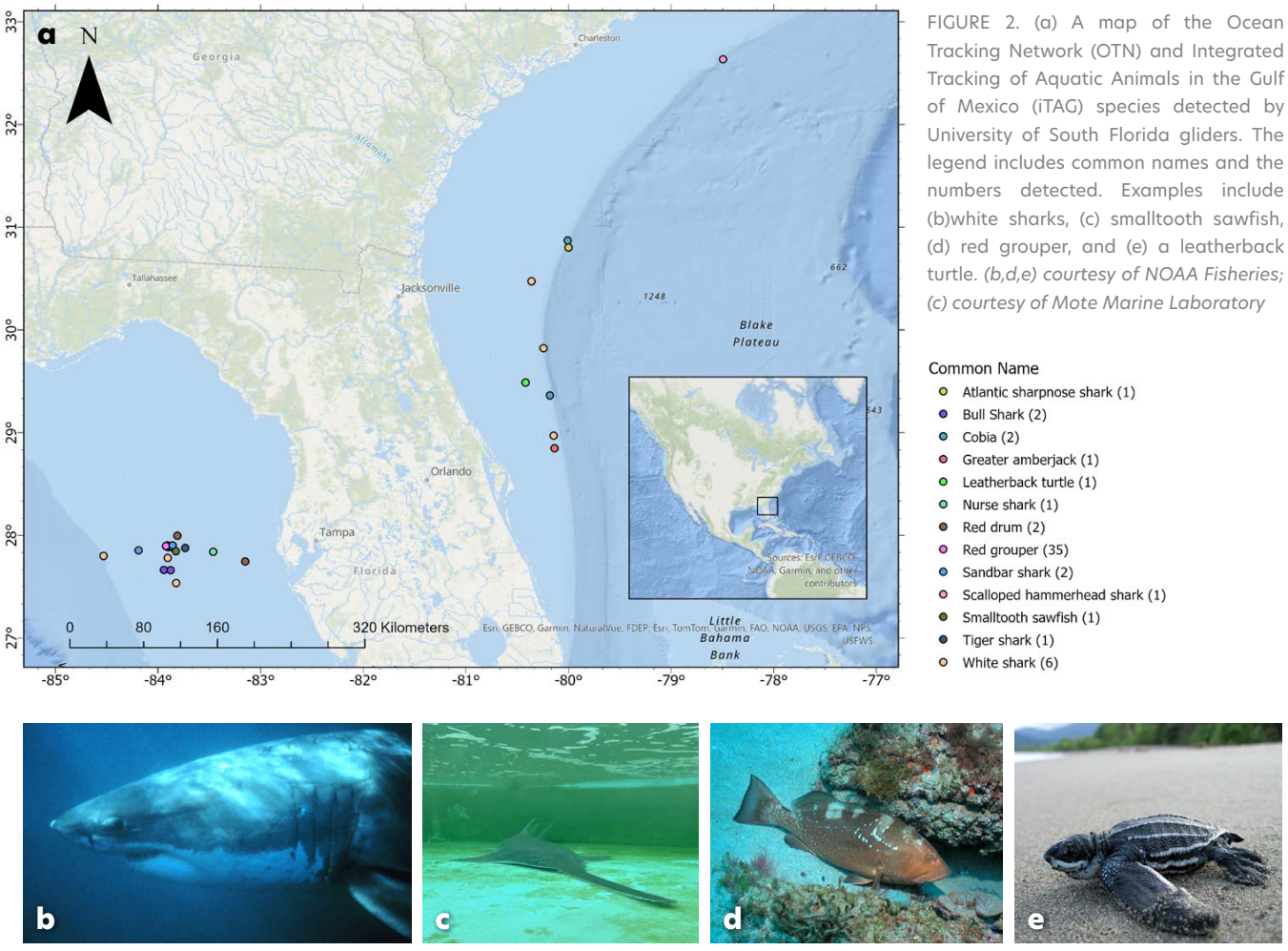

FIGURE 2. (a) A map of the Ocean Tracking Network (OTN) and Integrated Tracking of Aquatic Animals in the Gulf of Mexico (iTAG) species detected by University of South Florida gliders. The legend includes common names and the numbers detected. Examples include (b)white sharks, (c) smalltooth sawfish, (d) red grouper, and (e) a leatherback turtle. *(b,d,e) courtesy of NOAA Fisheries; (c) courtesy of Mote Marine Laboratory*

marine mammals, have been used extensively. Since 2009, USF recordings have detected red grouper, toadfish, marine mammals, and anthropogenic sounds (Wall et al., 2017). During a 2023 GoM glider mission, a PAM device detected the endangered Rice's whale, whose numbers are likely fewer than 100 individuals throughout the GoM (Soldevilla et al., 2024). Collaborating with the NOAA Southeast Fisheries Marine Mammal and Turtle Division, we detected hundreds of calls from these protected whales over a two-month glider deployment. These critically important data help management organizations to better understand Rice's whale distribution and to plan for a recovery of their population.

More recently, we have worked with acoustic manufacturers and NOAA's National Center for Coastal Ocean Science researchers to equip gliders with compact fisheries echosounders that have the potential to provide information about fish and zooplankton biomass within their field of view. These glider-based echosounders are being evaluated as a cost-effective method for surveying broad spatiotemporal ranges to augment the work of traditional acoustic methods on oceanographic research vessels. Initial observations have demonstrated that these combined oceanographic tools can detect plankton and fish biomass in the pelagic and near-benthic environments, thus expanding fishery ecosystem assessment and management to remote places (Taylor and Lembke, 2017). Adapting sensors to new platforms typically results in benefits and compromises, in this case using a mobile platform makes analysis more challenging, but glider mission endurance and the ability to concurrently sample the entire water column with a suite of sensors provide unique capabilities. For example, the ability to energize the echosounder below a thermocline allows the glider to potentially achieve higher echo detection quality than if the echosounder were energized from the ocean surface aboard a ship. Moreover, a glider is always equipped with physical sensors that enable calculation of critical sound speed information for precise correction and enhancement of the echosounder's biomass detections.

While originally developed as physical oceanographic tools for monitoring the water column to validate and improve circulation models, diverse payload-capable gliders collect a suite of measurements on oceanographic properties, providing a wealth of data analysis opportunities. The examples highlighted above allow a glimpse at the potential for sustained monitoring or for sentinel exploration to add insight into biological processes. The ability to concurrently collect biological, physical, and chemical data on a single, high-endurance, cost-effective platform is invaluable to fisheries and other natural resource monitoring programs.

USF's growing fleet of underwater gliders is made possible through support and collaboration of federal and state organizations as well as regional ocean observing networks like the Southeast Coastal Ocean Observing Regional Association and the Gulf Coast Ocean Observing System. While scientists who go to sea are the foundation of oceanographic research, autonomous robots, such as gliders, are cost-effective, risk-reducing tools capable of sampling in all seasons and in all weather types and from the surface to near the seafloor, while traversing large distances over periods of weeks to months. This unique format has firmly established the critical role of gliders as ocean observing tools and demonstrated their diverse applicability in monitoring marine organisms.

REFERENCES

Soldevilla, S., A. Debich, I. Perez-Carballo, S. Jarriel, K. Frasier, L. Garrison, A. Gracia, J. Hildebrand, P. Rosel, and A. Serrano. 2024. Rice's whale occurrence in the western Gulf of Mexico from passive acoustic recordings. *Marine Mammal Science* 40:e13109, https://doi.org/10.1111/mms.13109.

Taylor, J.C., and C. Lembke. 2017. Echosounder for biological surveys using ocean gliders. *Sea Technology* 58(7):35–38, https://digitalcommons.usf.edu/msc_facpub/469.

Wall, C., D. Mann, C. Lembke, C. Taylor, R. He, and T. Kellison. 2017. Mapping the soundscape off the southeastern USA by using passive acoustic glider technology. *Marine and Coastal Fisheries* 9(1):23–37, https://doi.org/10.1080/19425120.2016.1255685.

Weisberg, R., Y. Liu, C. Lembke, C. Hu, K. Hubbard, and M. Garrett., 2019. The coastal ocean circulation influence on the 2018 West Florida Shelf *K. brevis* red tide bloom. *Journal of Geophysical Research: Oceans* 124:2,501–2,512, https://doi.org/10.1029/2018JC014887.

ACKNOWLEDGMENTS

Funding for this work is provided by the Florida Fish and Wildlife Conservation Commission (FWC Agreement # 20035-A1), the Gulf of Mexico Coastal Ocean Observing System (NOAA Award # M2201260-410041-09001), the Southeast Coastal Ocean Observing Regional Association (NOAA Award # NA21NOS0120097), and the Florida RESTORE Act Centers of Excellence Program (RCEGR020002-01-00).

AUTHORS

Heather Broadbent (hbroadbent@usf.edu), **Alex Silverman**, **Randy Russell**, **Garrett Miller**, **Sean Beckwith**, **Edmund Hughes**, and **Chad Lembke**, University of South Florida, College of Marine Science, St. Petersburg, FL, USA.

ARTICLE DOI. https://doi.org/10.5670/oceanog.2025e102

THE WESTERN CHANNEL OBSERVATORY AUTOMATED PLANKTON IMAGING AND CLASSIFICATION SYSTEM

By James R. Clark, Elaine S. Fileman, James Fishwick, Saskia Rühl, and Claire E. Widdicombe

Marine plankton are an important and diverse group of organisms that make up the lower trophic levels of the marine food web. They play several critical roles in the ocean that have direct or indirect societal benefits, including supporting food security, oxygen production, and carbon sequestration via the biological carbon pump. Plymouth Marine Laboratory (PML) has been making weekly measurements of zooplankton and phytoplankton at Western Channel Observatory (WCO) Station L4 (50°15'N, 4°13'W) since 1988 and 1992, respectively, using traditional ship-based sampling and light microscopy techniques. Thus, Station L4 has become one of the longest-running, continuous plankton time series in the world and a key marine biodiversity reference site for studies into both short- and long-term environmental changes.

Short generation timescales and the potential for rapid changes in community composition make plankton good indicators of environmental change and of the health of the marine environment (McQuatters-Gollop et al., 2024). In the United Kingdom, a *Changes in Phytoplankton and Zooplankton Communities* indicator has been adopted within the UK Marine Monitoring and Assessment Strategy, which holds to account the UK Marine Strategy for creating a marine protected area (MPA) network and maintaining "clean, healthy, safe, productive and biologically diverse oceans and seas." The indicator is based on the abundances of distinct planktonic life-forms and their relationships to environmental pressures (Bedford et al., 2020). The same indicator was also used at the regional level in the most recent Convention for the Protection of the Marine Environment of the North-East Atlantic (OSPAR) 2023 Quality Status Report (OSPAR, 2023). Plankton data from the WCO feed directly into both UK and OSPAR reporting. The WCO record is also long enough to support climate change impact assessments. A recent report on long-term changes in plankton communities across the North Atlantic, which included data from the WCO, indicated wide-spread declines in Northeast Atlantic plankton, but more stable levels in the rapidly warming North Sea (Holland et al., 2023).

Traditional plankton sampling techniques include net hauls using standard mesh sizes and water sample collection using Niskin bottles. Samples are preserved

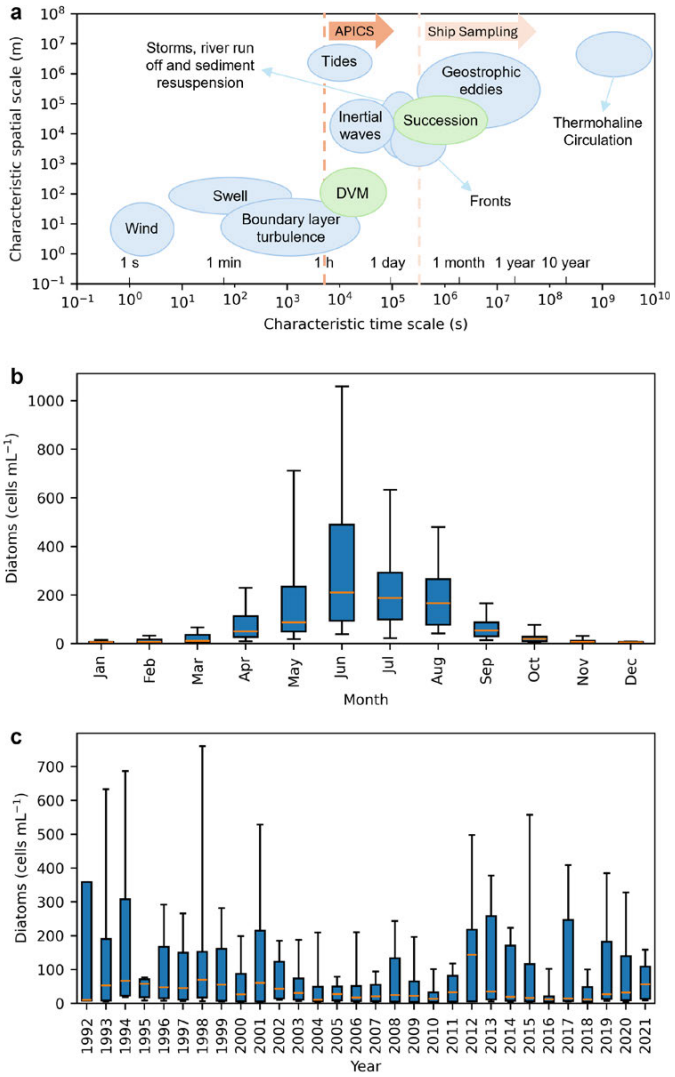

FIGURE 1. Processes impacting plankton communities at various temporal scales. (a) Physical (blue) and biological (green) processes that impact plankton communities are ordered according to their characteristic temporal and spatial scales. The light orange dashed line marks the period (weekly) at which ship-based samples are collected at the WCO's Station L4. The dark orange dashed line marks the period (~ hourly) at which samples can be collected using the Automated in situ Plankton Imaging and Classification System (APICS). *Figure adapted from Cushman-Roisin and Beckers, 2011, Figure 1.7* (b) Box plots show monthly variations in diatom cell concentrations at Station L4 between 1992 and 2021, as derived from traditional weekly ship-based sampling. The orange lines indicate the median concentrations across all years, while the blue boxes give the interquartile ranges. Whiskers (lines extending from the blue boxes) are drawn at 5% and 95%. Fliers (data that extend beyond the whiskers) have been excluded from the plot. (c) Box plots show annual variations in diatom cell concentrations at Station L4. The orange lines indicate median concentrations across all months in that year. The blue box and whiskers are the same as in b.

and taxonomically identified and counted in the laboratory using light microscopy. This process has several drawbacks. For example, standard mesh sizes can be biased toward certain plankton sizes, and fragile or gelatinous organisms can be damaged or fragmented during the sampling and preservation process, making identification difficult. Further, there is no opportunity to observe behavioral interactions among organisms (Remsen et al., 2004; Greer et al., 2021).

Ship-based sampling is also time-consuming and restricted to periods when there is good weather, limiting the frequency at which data can be collected. Historically, plankton samples from Station L4 have been collected once a week (weather permitting), enabling important seasonal and interannual changes to be quantified and studied. However, numerous processes that influence plankton population numbers and community composition have shorter characteristic timescales and thus are either missed or aliased by weekly sampling. These include successional changes in the plankton community that characterize bloom events or the recovery of the community following passage of a storm (Topor et al., 2022), diel vertical migrations (DVMs) that are undertaken by many larger zooplankton (Parra et al., 2019), and changes due to the tide (Figure 1). Fine-scale spatial heterogeneity, for example, caused by the presence of fronts, can also result in large apparent changes in community composition as water masses hosting different communities are advected over the sampling site. Collectively, these processes complicate the interpretation of weekly time series.

In an attempt to address these issues, several groups around the world have now pioneered the use of underwater cameras to monitor plankton communities (Lombard et al., 2019). Building on these efforts, a new WCO Automated in situ Plankton Imaging and Classification System (APICS) is being operationalized. Distinguishing features of the system include (1) the use of *two* autonomous submersible camera units—an Imaging FlowCytobot (IFCB) and a Moonpool Plankton Imager (PI-10)—that provide broad size spectrum imaging capability, and (2) a configuration that facilitates deployment under a remotely operated, moored buoy (Figure 2). The system will image both phytoplankton and zooplankton (size range <10 µm–20 mm) at a depth of 10 m. APICS will enable a ~100-fold improvement in sampling frequency, which allows many of the processes missed by weekly sampling to be resolved (Figure 1a). The cameras sample a known volume of water, with the IFCB imaging a 5 mL sample every 20 minutes and the PI-10

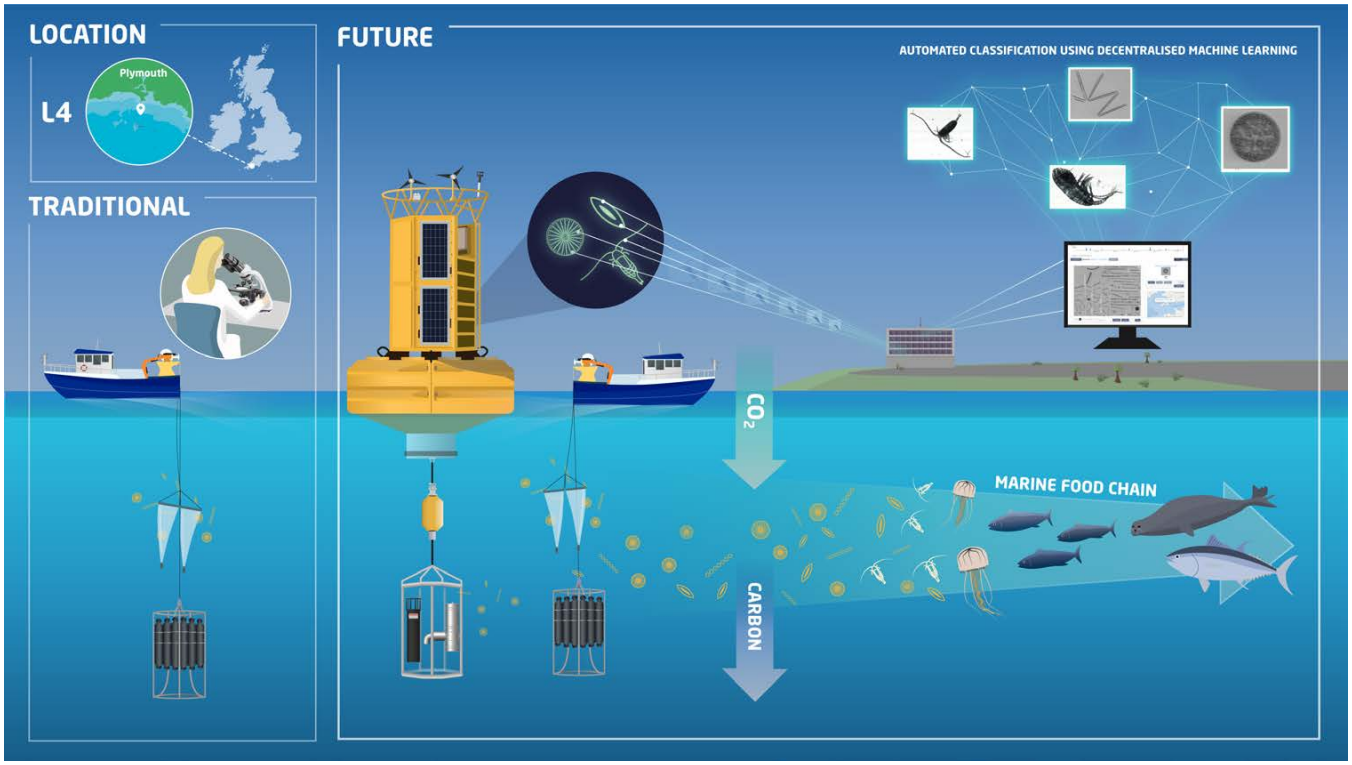

FIGURE 2. Traditional ship-based plankton sampling methods that have been deployed at Station L4 in the Western Channel Observatory. They are contrasted with future methods that include the addition of APICS and the automated, high-frequency imaging of plankton. With APICS, images are automatically transmitted back to the laboratory. The laboratory operates a node within a decentralized network that allows the team to collaborate with external partners on the automated classification of data using machine learning techniques.

actively pumping water through the camera unit at a rate of 34 L min^{-1} to ensure organisms present at lower concentrations (~100 individuals per m^3) can be accurately enumerated. Real-time data processing will be facilitated using swarm learning (Warnat-Herresthal et al., 2021)—a machine learning methodology that allows multiple owners of biological image data to participate in decentralized, collaborative networks where they can leverage the data and expertise of external partners to obtain better, higher efficacy classification results (**Figure 2**).

The WCO's APICS and similar systems offer advantages over traditional sampling methods for both assessing candidate MPAs and monitoring existing ones. Cameras deployed in situ facilitate the collection of high frequency data over an extended time period, allowing a more detailed picture of the environment to be assembled. In general, it is financially and logistically impossible to collect a similar volume of data using traditional, ship-based sampling methods. Further, the real-time processing of data from autonomous camera systems directly facilitates operational monitoring, including for harmful algal blooms and invasive species, which in turn facilitates more rapid decision-making by marine managers.

Within the WCO, APICS will complement the traditional sampling methods that support the current multiyear time series by allowing short-period processes and controls on biodiversity to be studied and understood. In addition, the continuation and expansion of long-term observations based on traditional methods will remain paramount for studying the long-term impacts of climate change.

REFERENCES

Bedford, J., C. Ostle, D.G. Jones, A. Atkinson, M. Best, E. Bresnan, M. Machairopoulou, C.A. Graves, M. Devline, A. Milligen, and others. 2020. Lifeform indicators reveal large-scale shifts in plankton across the North-West European shelf. *Global Change Biology* 26:3,482–3,497, https://doi.org/10.1111/gcb.15066.

Cushman-Roisin, B., and J.-M. Beckers, eds. 2011. *Introduction to Geophysical Fluid Dynamics: Physical and Numerical Aspects*. International Geophysics book series, vol. 101, Elsevier, 828 pp.

Greer, A.T., L.M. Chiaverano, L.M. Treible, C. Briseño-Avena, and F.J. Hernandez. 2021. From spatial pattern to ecological process through imaging zooplankton interactions. *ICES Journal of Marine Science* 78:2,664–2,674, https://doi.org/10.1093/icesjms/fsab149.

Holland, M.M., A. Louchart, L.F. Artigas, C. Ostle, A. Atkinson, I. Rombouts, C.A. Graves, M. Devlin, B. Heyden, M. Machairopoulou, and others. 2023. Major declines in NE Atlantic plankton contrast with more stable populations in the rapidly warming North Sea. *Science of the Total Environment* 898:165505, https://doi.org/10.1016/j.scitotenv.2023.165505.

Lombard, F., E. Boss, A.M. Waite, M. Vogt, J. Uitz, L. Stemmann, H.M. Sosik, J. Schulz, J.-B. Romagnan, M. Picheral, and others. 2019. Globally consistent quantitative observations of planktonic ecosystems. *Frontiers in Marine Science* 6:196, https://doi.org/10.3389/fmars.2019.00196.

McQuatters-Gollop, A., R.F. Stern, A. Atkinson, M. Best, E. Bresnan, V. Creach, M. Devlin, M. Holland, C. Ostle, K. Schmidt, and others. 2024. The silent majority: Pico- and nanoplankton as ecosystem health indicators for marine policy. *Ecological Indicators* 159:111650, https://doi.org/10.1016/j.ecolind.2024.111650.

OSPAR. 2023. Pelagic habitats thematic assessment. In *Quality Status Report 2023*, OSPAR Commission, London, https://oap.ospar.org/en/ospar-assessments/quality-status-reports/qsr-2023/thematic-assessments/pelagic-habitats/.

Parra, S.M., A.T. Greer, J.W. Book, A.L. Deary, I.M. Soto, C. Culpepper, F.J. Hernandez, and T.N. Miles. 2019. Acoustic detection of zooplankton diel vertical migration behaviors on the northern Gulf of Mexico shelf. *Limnology and Oceanography* 64:2,092–2,113, https://doi.org/10.1002/lno.11171.

Remsen, A., T.L. Hopkins, and S. Samson. 2004. What you see is not what you catch: A comparison of concurrently collected net, Optical Plankton Counter, and Shadowed Image Particle Profiling Evaluation Recorder data from the northeast Gulf of Mexico. *Deep Sea Research Part I* 51(1):129–151, https://doi.org/10.1016/j.dsr.2003.09.008.

Topor, Z.M., A.M. Genung, and K.L. Robinson. 2022. Multi-storm analysis reveals distinct zooplankton communities following freshening of the Gulf of Mexico shelf by Hurricane Harvey. *Scientific Reports* 12:8721, https://doi.org/10.1038/s41598-022-12573-y.

Warnat-Herresthal, H. Schultze, K.L. Shastry, S. Manamohan, S. Mukherjee, V. Garg, R. Sarveswara, K. Händler, P. Pickkers, N.A. Aziz, and others. 2021. Swarm learning for decentralized and confidential clinical machine learning. *Nature* 594:265–270, https://doi.org/10.1038/s41586-021-03583-3.

ACKNOWLEDGMENTS

The authors acknowledge the Natural Environmental Research Council (UK) for funding APICS (NE/X006018/1) and the WCO time series (NE/R015953/1). The team thanks PML's Smart Sound Plymouth technical support team and the crew of R/V *Plymouth Quest* for supporting both projects. We thank Jonathon White for assistance in creating graphics used in this article.

AUTHORS

James R. Clark (jcl@pml.ac.uk), **Elaine S. Fileman**, **James Fishwick**, **Saskia Rühl**, and **Claire E. Widdicombe**, Plymouth Marine Laboratory, Plymouth, UK.

ARTICLE DOI. https://doi.org/10.5670/oceanog.2025e106

COLLABORATING WITH MARINE BIRDS TO MONITOR THE PHYSICAL ENVIRONMENT WITHIN COASTAL MARINE PROTECTED AREAS

By Rachael A. Orben, Adam Peck-Richardson, Alexa Piggott, James Lerczak, Greg Wilson, Jessica C. Garwood, Xiaohui Liu, Sabir Bin Muzaffar, Alexa D. Foster, Humood A. Naser, Mohamed AlMusallami, Tycho Anker-Nilssen, John P.Y. Arnould, Michael L. Berumen, Thomas Cansse, Susana Cárdenas-Alayza, Signe Christensen-Dalsgaard, Abdul Qader Khamis, Tegan Carpenter-Kling, Nina Dehnhard, Mindaugas Dagys, Annette Fayet, Rebecca M. Forney, Stefan Garthe, Scott A. Hatch, Michael E. Johns, Miran Kim, Kate Layton-Matthews, Ariel K. Lenske, Gregory T.W. McClelland, Julius Morkūnas, Areen O. Nasif, Gayomini Panagoda, Jong-Hyun Park, Victor R.A. Pimenta, Flavio Quintana, Matt J. Rayner, Tone Kristin Reiertsen, Sampath S. Seneviratne, Mariëlle van Toor, Pete Warzybok, Eleanor A. Weideman, Jinhee Yi, Yat-Tung Yu, and Carlos B. Zavalaga

ABSTRACT

Animal telemetry is maturing into a viable method for observing the ocean as it can be used to monitor both environmental conditions and biological metrics along the movement trajectories of marine animals. As part of the Cormorant Oceanography Project, we have augmented a biologging tag with an external fast response temperature sensor to collect ocean temperature profiles from the backs of foraging marine birds. Cormorants dive between 50 and 250+ times a day to forage for prey so they can provide hard-to-match temporal and spatial coverage of coastal ocean conditions within their foraging areas. We process tag measurements to obtain fundamental oceanographic data (e.g., temperature profiles, bottom soundings, surface current measurements). Together, we have tracked 17 marine bird species (including two *Spheniscus* penguins spp. and a sea duck), originating from 17 countries and foraging along the edges of all major oceans. Tagged birds' distribution included 191 MPAs in 26 countries, offering a unique ocean monitoring method to complement more widely used methods.

BACKGROUND

Coastal oceans are complex dynamic environments, and the neritic zone supports high levels of biodiversity. It is these very complexities that make coastal ecosystems challenging to monitor at the resolutions required. Coastal ecosystems also sustain high human use and impacts, placing changes in these ecosystems at a nexus for societal relevance. Marine spatial planning and coastally located marine protected areas (MPAs) are management tools that promote the sustainable use of marine ecosystems. While most coastal MPAs are too small to encompass the year-round range of highly mobile megafauna species, small MPAs may include portions of individual ranges at key periods during the year (Conners et al., 2022). Furthermore, understanding the efficacy of an MPA to provide spatial protection for a dynamic marine environment requires monitoring of changes in both biotic and physical environmental conditions. Marine bird diet composition and demographic metrics (such as reproductive success and population trajectories) are well documented metrics of ecosystem health. Though foraging behavior is the process by which an animal expends energy to gain energy, it has not often been distilled into ocean monitoring variables (e.g., essential ocean variables [EOVs]; Harcourt et al., 2019). An understanding of environmental conditions associated with foraging is therefore a powerful ocean monitoring approach that can aid in MPA monitoring (McMahon et al., 2021).

BIOLOGGING AS AN OCEAN MONITORING TOOL

Animal telemetry, or biologging, has become a viable ocean observation tool that can be used to monitor both environmental conditions and biological metrics along the movement paths of animals (overview in Harcourt et al., 2019). Larger bodied marine animals provide free-ranging autonomous platforms and inherently visit and revisit areas that are of importance for meeting self-maintenance and life-history needs. Biologging employs miniaturized electronic devices to track animal movement and behavior through the use of multiple sensors (e.g., GPS, accelerometry, temperature, pressure). These same sensors can be tailored to collect relevant data on the marine physical environment. Biologging sampling offers fine-scale spatiotemporal resolution, lower costs, and the potential to sample dynamic or hard to reach areas (e.g., under sea ice; Ribeiro et al., 2021) that are challenging for other currently applied ocean monitoring methods (e.g., shipboard sampling, a single autonomous vehicle, moorings, drifters).

The type of environmental data available from biologging devices depends on the movement capacity and behavior of the animal carrying the device. For instance, deep diving southern elephant seals (*Mirounga leonina*) have collected temperature and salinity profiles necessary

to model deep ocean currents in the Southern Ocean (reviewed in McMahon et al., 2021), while Brandt's cormorants (*Phalacrocorax penicillatus*) resting on the surface between dives have documented surface currents in the Columbia River estuary that subsequently improved multivariate bathymetric modeling (Ardağ et al., 2023). Biologgers attached to benthic diving animals including seals and cormorants allow mapping of the seafloor during animals' foraging dives (e.g., Padman et al., 2010; McMahon et al., 2023), and given how little of the ocean floor has been mapped (Tozer et al., 2019), offer a valuable, if unconventional, observing method.

Animal welfare concerns are paramount when applying a biologging approach, including species-tailored attachment, placement, and device shape, weight, and overall size. Especially for both flying and diving marine birds, tag miniaturization is key to accomplishing these goals. Over the last few decades, miniaturization has occurred in tandem with increases in the technical capabilities of tags, including their power capacities. This allows multiple data streams to be collected by one device in order to couple animal ecology studies with simultaneous collection of high-quality information on the physical and biological environment encountered by an individual animal. Flying-diving marine birds offer multiple environmental sampling opportunities, including temperature profiling during dives, seafloor mapping from benthic diving species, and surface currents and wave metrics collected when birds are resting on the surface. Furthermore, additional development of sensors will enhance the sampling capability of bird-borne biologging that could be expanded to other water column properties (e.g., fluorescence, pH, salinity) and temperature measurements (e.g., air-sea contrast).

THE CORMORANT OCEANOGRAPHY PROJECT

As part of the Cormorant Oceanography Project, we have collaborated with a biologging company, Ornitela (Vilnius, Lithuania), to develop a customized external fast response temperature sensor to collect ocean temperature profiles from the backs of foraging marine birds (Orben et al., 2021). Additionally, customized tag programming options have allowed us to improve power management by selectively sampling during periods of activity that are both biologically relevant and key for oceanographic monitoring (e.g., dives and surface drift periods). Specifically, a GPS location fix is triggered when the bird resurfaces as the tag crosses a 1 m depth threshold. This results in a GPS fix following each dive event. Data are transferred at programmable intervals over the cell phone network (3G or 4G), allowing megabytes of data to be transmitted with each connection. Our tagging efforts focused on cormorants and shags to ensure good cell phone connectivity, as these species usually forage within 15 km of the coast and regularly return to land to roost at night. Depending on the species, we use variations of the tag type to meet the threshold of <3% animal body mass; however, typically the tag is 26 g (60 mm plus a 12 mm sensor housing × 25.7 mm x 15.4 mm) and is powered by a battery that is recharged with solar cells (Figure 1). For most cormorant species, tags are attached with a Teflon backpack harness; however, in some cases, tags were attached to feathers for shorter durations with Tesa tape (back attachment: *Spheniscus* penguins spp. and sea duck [velvet scoter, *Melanitta fusca*]; tail attachment: European shag [*Gulosus aristotelis*] and Cape cormorant [*Phalacrocorax capensis*]).

Tags were customized with an external temperature sensor (TMP117, Texas Instruments, USA; ±0.1°C (maximum) from -20°C to +50°C) to measure water temperatures during dives. To estimate in situ sampling performance across a range of temperatures (10°–24.4°C), we conducted water column profiles of tags paired with a calibrated CTD (RBR Concerto CTD; Ottawa, Canada) in the Yaquina River and Estuary, in central Oregon, at five different sites along the estuary with different temperature characteristics. At each site, the CTD and biologging tags (n = 33), attached to a

FIGURE 1. (a) A Brandt's cormorant (*Phalacrocorax penicillatus*) carrying a biologging device rests on a piling in the Columbia River Estuary, USA. *Photo credit: A. Peck-Richardson* (b) A biologging tag fitted with a fast-response temperature sensor and housing has proven useful. *Photo credit: A. Peck-Richardson*

stainless steel frame, were lowered on a handline to depths ranging roughly from 3 m to 12 m, depending on water depth. Sensors were held near the bottom for 10–90 sec and then raised to mimic marine bird diving behavior. Five to 10 casts were made at each site. We estimated water surface temperature (SST) using the final temperature measurement of both CTD and biologging tag (1.58 ± SD 0.52 m depth). Resulting SST measurements (n = 1,160) were similar with a root-mean-squared difference of 0.21°C.

GLOBAL MONITORING OF MARINE PROTECTED AREAS

Together, we have tracked 17 species (14 cormorants and shags, two penguin species, and one sea duck) originating from 17 countries, and documented marine birds foraging along the coasts of all continents except Antarctica (Figure 2, as of September 2024). Some of these countries have well-developed networks of coastal MPAs (e.g., Peru, Norway, South Korea, west coast of the United States, and Canada), and while these data were collected for more general coastal ocean monitoring, tagged birds were found to occur within 191 MPAs in 26 countries (UNEP-WCMC, 2024; refined for non-overlapping management units). Most MPAs (68%) sampled in our study were small (<100 km^2), but on average the protected area size was 659 ± SD 2,675 km^2. The largest MPAs were used by Imperial cormorants (*Leucocarbo atriceps*) and located in Patagonia Azul (30,697 km^2) and Frente Valdez (19,479 km^2) in Argentina. The species tracked in Sri Lanka, the Indian cormorant (*Phalacrocorax fuscicollis*) and the little cormorant (*Microcarbo niger*), did not encounter MPAs. On average, birds encountered MPAs 115 ± SD 208 km from where they were originally fitted with biologging devices; the longest distance to an MPA (1,471 km) was traveled by a Brandt's cormorant tagged in the Columbia River Estuary and tracked to southern California the following winter.

The regional distribution of the vulnerable Socotra cormorant (*Phalacrocorax nigrogularis)* within the Arabian Gulf, and its tendency for short-distance migratory movements (Muzaffar et al., 2017), presents a case study for how this species seasonally uses and consequently can provide samples from the physical environment within multiple

FIGURE 2. Marine bird tracking data from the Cormorant Oceanography Project (2019–2024, colored by species) surrounded by photos of birds tracked. *Photo credits: Top (left to right): Nina Dehnhard, Julius Morkūnas, JinHee Lee, JinHee Lee, William Kennerley, Mike Johns, Hugo Cliff, Jose Cabello. Bottom (left to right): Eleanor Weideman, Eleanor Weideman, Sabir Bin Muzaffar, Gayomini Panagoda, Gayomini Panagoda, Thomas Cansse, Edin Whitehead, Victor Pimenta, Flavio Quintana*

MPAs. The Arabian Gulf is a shallow estuary that supports a uniquely productive tropical ecosystem fueled by nutrients supplied by seasonal dust storms and river systems running through Iraq and Iran (Piontkovski et al., 2019). Socotra cormorants are obligate marine birds and depend on the availability of schooling prey fishes (e.g., anchovy, sailfin flying fish, and blue-stripe sardines), and their movements track regional productivity (Muzaffar et al., 2017). From 2019 to 2023, we fitted Socotra cormorants with biologging devices at four colony locations within the Arabian Gulf (Figure 3a). Sixty-five birds carried devices for 231 ± SD 146 days, with 12 birds continuing to transmit data (as of August 2024). As expected, the resulting Socotra cormorant distribution was along the southern coast of the Gulf; however, individuals ranged farther than anticipated and spent time in 16 MPAs in Oman, the United Arab Emirates, Qatar, Saudi Arabia, Bahrain, and Kuwait (Figure 3a). Thus, the MPAs used by individual birds can change seasonally, and the temperatures the birds can be equipped to measure document the seasonal cycle of sea surface temperatures in their regions (Figure 4a). The number of dives made per day by each bird is an ecological variable that integrates prey availability, foraging success, and life-history needs (e.g., breeding stage; Cook et al., 2017), and it offers a metric of MPA use throughout the southern Arabian Gulf (Figure 4b), reflecting the cooler temperatures during the breeding period when birds tend to dive more frequently.

CONCLUSION

Our efforts demonstrate that the coastal movements of marine diving birds can effectively sample large areas while collecting high-quality data via bird-borne biologging devices. The data derived are already proving useful for dynamic coastal ocean models (e.g., Ardağ et al., 2023). Systematic deployments in the future will make biologging devices important additions to global coastal ocean observation efforts and provide managers with another tool for monitoring ecosystem variables. Capacity building to use biologging data depends on developing user-friendly ways to transfer data. Through an automated data pipeline, we plan to provide biologging data in near-real time as well as archived data products to promote the use

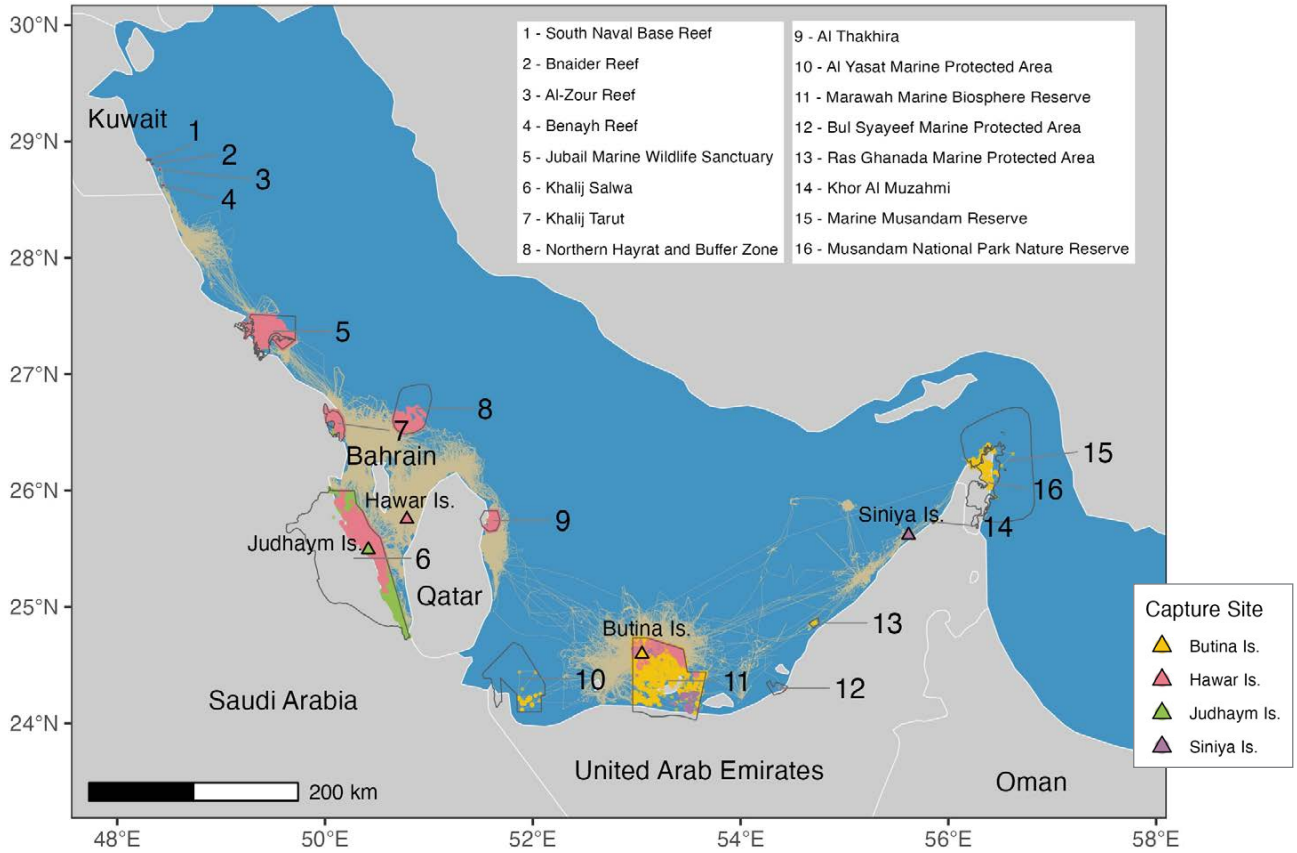

FIGURE 3. Use of marine protected areas (MPAs) by Socotra cormorants (*Phalacrocorax nigrogularis*) in the Arabian Gulf. All bird tracks are depicted (tan) to show movements between MPAs. Each MPA is delineated by a solid gray line and identified by number. Bird locations within each MPA are colored by the colony where birds were tagged: Butina (n = 12, yellow), Hawar Islands (n = 44, pink), Judhaym Island (n = 8, green), and Siniya Island (n = 1, purple).

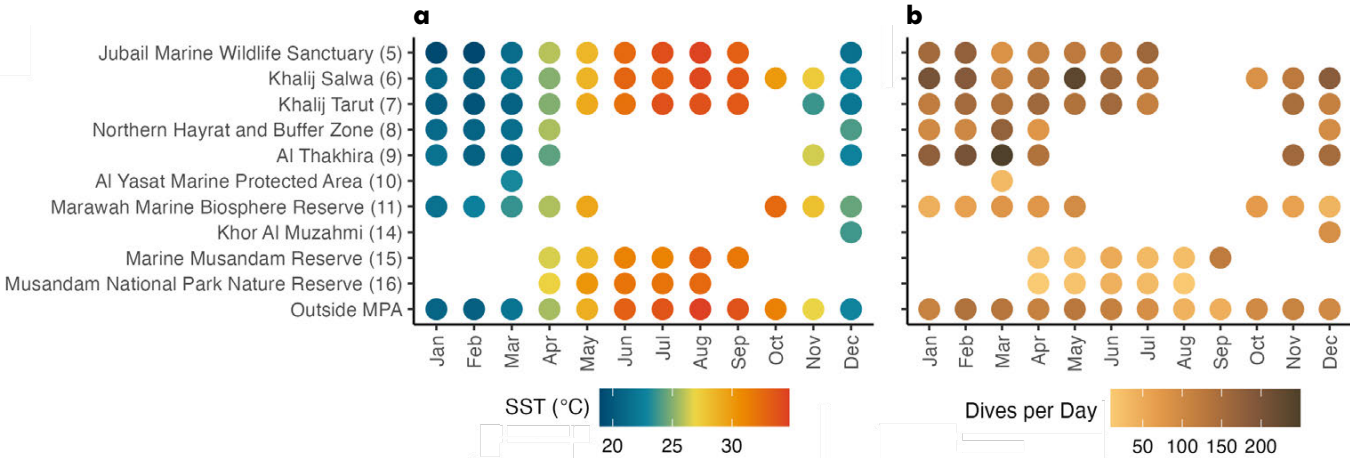

FIGURE 4. Data collected during environmental and biotic monitoring by Socotra cormorants (*Phalacrocorax nigrogularis*) in Arabian Gulf MPAs. (a) Average monthly sea surface temperature (SST) within and outside these MPAs calculated from biologging devices. (b) Average dives per day per bird within and outside the MPAs. Numbers following MPA names correspond to the map in Figure 3. Due to bird behavior and tag performance, dives were not recorded within all MPAs visited.

and reuse of these data streams. Human-wildlife conflict is problematic for many species of cormorants, as these colonial waterbirds are seen as competitors with fisheries and fish farms, can outcompete other arboreal nesting species (e.g., herons, egrets), and are often considered dirty due to intense guano deposition. More generally, marine birds are one of the most threatened groups of birds. Here, six of our 17 study species are listed by the International Union for Conservation of Nature as near threatened or higher. Biologging is one of many tools that researchers can use to provide insights for conservation and management. Continued development of high-quality, multi-sensor tags, coupled with innovative data distribution pipelines, is needed to fully benefit from and apply animal-borne sensor technology.

REFERENCES

Ardağ, D., G. Wilson, J.A. Lerczak, D.S. Winters, A. Peck-Richardson, D.E. Lyons, and R.A. Orben. 2023. Multivariate data assimilation at a partially mixed estuary. *Journal of Atmospheric and Oceanic Technology* 40(9):1,007–1,022, https://doi.org/10.1175/JTECH-D-22-0101.1.

Conners, M.G., N.B. Sisson, P.D. Agamboue, P.W. Atkinson, A.M.M. Baylis, S.R. Benson, B.A. Block, S.J. Bograd, P. Bordino, W.D. Bowen, and others. 2022. Mismatches in scale between highly mobile marine megafauna and marine protected areas. *Frontiers in Marine Science* 9:897104, https://doi.org/10.3389/fmars.2022.897104.

Cook, T.R., R. Gubiani, P.G. Ryan, and S.B. Muzaffar. 2017. Group foraging in Socotra cormorants: A biologging approach to the study of a complex behavior. *Ecology and Evolution* 7(7):2,025–2,038, https://doi.org/10.1002/ece3.2750.

Harcourt, R., A.M.M. Sequeira, X. Zhang, F. Roquet, K. Komatsu, M. Heupel, C. McMahon, F. Whoriskey, M. Meekan, G. Carroll, and others. 2019. Animal-borne telemetry: An integral component of the ocean observing toolkit. *Frontiers in Marine Science* 6:326, https://doi.org/10.3389/fmars.2019.00326.

McMahon, C.R., F. Roquet, S. Baudel, M. Belbeoch, S. Bestley, C. Blight, L. Boehme, F. Carse, D.P. Costa, M.A. Fedak, and others. 2021. Animal borne ocean sensors – AniBOS – An essential component of the Global Ocean Observing System. *Frontiers in Marine Science* 8:751840, https://doi.org/10.3389/fmars.2021.751840.

McMahon, C.R., M.A. Hindell, J.B. Charrassin, R. Coleman, C. Guinet, R. Harcourt, S. Labrousse, B. Raymond, M. Sumner, and N. Ribeiro. 2023. Southern Ocean pinnipeds provide bathymetric insights on the East Antarctic continental shelf. *Communications Earth & Environment* 4(1):266, https://doi.org/10.1038/s43247-023-00928-w.

Muzaffar, S.B., C. Clarke, R. Whelan, R. Gubiani, and T.R. Cook. 2017. Short distance directional migration in the threatened Socotra cormorant: Link to primary productivity and implications for conservation. *Marine Ecology Progress Series* 575:181–194, https://doi.org/10.3354/meps12209.

Orben, R.A., A.G. Peck-Richardson, G. Wilson, D. Ardağ, and J.A. Lerczak. 2021. Cormorants are helping characterize coastal ocean environments. *Eos* 102, https://doi.org/10.1029/2021EO163427.

Padman, L., D.P. Costa, S.T. Bolmer, M.E. Goebel, L.A. Huckstadt, A. Jenkins, B.I. McDonald, and D.R. Shoosmith. 2010. Seals map bathymetry of the Antarctic continental shelf. *Geophysical Research Letters* 37(21):L21601, https://doi.org/10.1029/2010GL044921.

Piontkovski, S.A., W.M. Hamza, N.M. Al-Abri, S.S.Z. Al-Busaidi, and K.A. Al-Hashmi. 2019. A comparison of seasonal variability of Arabian Gulf and the Sea of Oman pelagic ecosystems. *Aquatic Ecosystem Health & Management* 22(2):108–130, https://doi.org/10.1080/14634988.2019.1621133.

Ribeiro, N., L. Herraiz-Borreguero, S.R. Rintoul, C.R. McMahon, M. Hindell, R. Harcourt, and G. Williams. 2021. Warm modified Circumpolar deep water intrusions drive ice shelf melt and inhibit dense shelf water formation in Vincennes Bay, East Antarctica. *Journal of Geophysical Research: Oceans* 126:e2020JC016998, https://doi.org/10.1029/2020JC016998.

Tozer, B., D.T. Sandwell, W.H.F. Smith, C. Olson, J.R. Beale, and P. Wessel. 2019. Global bathymetry and topography at 15 arc sec: SRTM15+. *Earth and Space Science*, 6(10):1847–1864, https://doi.org/10.1029/2019EA000658.

UNEP-WCMC. 2024. "February 2024 update of the WDPA and WD-OECM," https://www.protectedplanet.net/en/resources/february-2024-update-of-the-wdpa-and-wd-oecm.

ACKNOWLEDGMENTS

This work was supported by the Office of Naval Research (ONR) grant N00014-19-1-2218. Under Award N00014-13-1-0369, the ONR-funded initial work using cormorants as sampling platforms was part of the Inlet and River Mouth Dynamics DRI at the mouth of the Columbia River (MCR). Environment and Climate Change Canada provided funding for tags and fieldwork in Canada. We thank the Punta San Juan Program of Centro para la Sostenibilidad Ambiental (CSA), at Universidad Peruana Cayetano Heredia for the photographs provided by Hugo Cliff and Jose Cabello. Work with birds was approved by the Animal Care and Use Committee of Oregon State University. Permits were obtained from the respective national governments and local jurisdictions.

AUTHORS

Rachael A. Orben (rachael.orben@oregonstate.edu), Department of Fisheries, Wildlife, and Conservation Sciences, Hatfield Marine Science Center, Oregon State University, Newport, OR, USA. **Adam Peck-Richardson** and **Alexa Piggott**, Department of Fisheries, Wildlife, and Conservation Sciences, Oregon State University, Corvallis, OR, USA. **James Lerczak**, **Greg Wilson**, **Jessica C. Garwood**, and **Xiaohui Liu**, College of Earth, Ocean, and Atmospheric Sciences, Oregon State University, Corvallis, OR, USA. **Sabir Bin Muzaffar**, Department of Biology, College of Science, United Arab Emirates University, Al Ain, UAE. **Alexa D. Foster**, Reef Ecology Lab, Division of Biological and Environmental Science and Engineering, King Abdullah University of Science and Technology, Thuwal, Saudi Arabia. **Humood A. Naser**, Department of Biology, University of Bahrain, Kingdom of Bahrain. **Mohamed AlMusallami**, Department of Biology, College of Science, United Arab Emirates University, Al Ain, UAE, and Fisheries Management, Terrestrial and Marine Biodiversity, Environment Agency-Abu Dhabi, UAE. **Tycho Anker-Nilssen**, Norwegian Institute for Nature Research (NINA), Trondheim, Norway. **John P.Y. Arnould**, School of Life and Environmental Sciences, Faculty of Science, Engineering and Built Environment, Deakin University, Burwood, Victoria, Australia. **Michael L. Berumen**, Reef Ecology Lab, Division of Biological and Environmental Science and Engineering, King Abdullah University of Science and Technology, Thuwal, Saudi Arabia. **Thomas Cansse**, School of Life and Environmental Sciences, Faculty of Science, Engineering and Built Environment, Deakin University, Burwood, Victoria, Australia. **Susana Cárdenas-Alayza**, Departamento Académico de Ciencias Biológicas y Fisiológicas, Facultad de Ciencias e Ingeniería, Universidad Peruana Cayetano Heredia, Lima, Peru. **Signe Christensen-Dalsgaard**, NINA, Trondheim, Norway. **Abdul Qader Khamis**, Arab Regional Center for World Heritage, Bahrain. **Tegan Carpenter-Kling**, Institute for Coastal and Marine Research, Nelson Mandela University, Gqeberha, South Africa. **Nina Dehnhard**, NINA, Trondheim, Norway. **Mindaugas Dagys**, Nature Research Centre, Vilnius, Lithuania. **Annette Fayet**, NINA, Trondheim, Norway. **Rebecca M. Forney**, Point Blue Conservation Science, Petaluma, CA, USA. **Stefan Garthe**, Research and Technology Centre, Kiel University, Büsum, Germany. **Scott A. Hatch**, Institute for Seabird Research and Conservation, Anchorage, AK, USA. **Michael E. Johns**, Point Blue Conservation Science, Petaluma, CA, USA. **Miran Kim**, Seabirds Lab of Korea, Wonju, Gangwon State, Republic of Korea. **Kate Layton-Matthews**, NINA, Oslo, Norway. **Ariel K. Lenske** and **Gregory T.W. McClelland**, Canadian Wildlife Service, Environment and Climate Change Canada, Delta, British Columbia, Canada**. Julius Morkūnas**, Marine Research Institute, Klaipėda University, Klaipėda, Lithuania. **Areen O. Nasif**, Reef Ecology Lab, Division of Biological and Environmental Science and Engineering, King Abdullah University of Science and Technology, Thuwal, Saudi Arabia. **Gayomini Panagoda**, Avian Sciences and Conservation, Department of Zoology and Environment Sciences, University of Colombo, Colombo, Sri Lanka. **Jong-Hyun Park**, HAE-IN Ecological Research Institute, Busan, Republic of Korea. **Victor R.A. Pimenta**, Department of Fisheries Engineering and Biological Sciences, State University of Santa Catarina, Laguna, Brazil. **Flavio Quintana**, Instituto de Biología de Organismos Marinos, CONICET, Puerto Madryn, Chubut, Argentina. **Matt J. Rayner**, Auckland War Memorial Museum, Tāmaki Paenga Hira, The Domain, Auckland, New Zealand, and School of Biological Sciences, The University of Auckland, Auckland, New Zealand. **Tone Kristin Reiertsen**, NINA, Tromsø, Norway. **Sampath S. Seneviratne**, Avian Sciences and Conservation, Department of Zoology and Environment Sciences, University of Colombo, Colombo, Sri Lanka. **Mariëlle van Toor**, Centre for Ecology and Evolution in Microbial Model Systems, Linnaeus University, Kalmar, Sweden. **Pete Warzybok**, Point Blue Conservation Science, Petaluma, CA, USA. **Eleanor A. Weideman**, Seabird Conservation Programme, BirdLife South Africa, Cape Town, South Africa. **Jinhee Yi**, Wildlife Ecological Conservation Institute, Gongju-si, Chungcheongnam-do, Republic of Korea. **Yat-Tung Yu**, Hong Kong Bird Watching Society, Hong Kong SAR, China. **Carlos B. Zavalaga**, Unidad de Investigación en Ecología y Conservación de Aves Marinas - Universidad Científica del Sur, Peru.

ARTICLE DOI. https://doi.org/10.5670/oceanog.2025e115

OCEAN GLIDERS FOR PLANNING AND MONITORING REMOTE CANADIAN PACIFIC MARINE PROTECTED AREAS

By Tetjana Ross, Hayley V. Dosser, Jody M. Klymak, Wiley Evans, Alex Hare, Jennifer M. Jackson, and Stephanie Waterman

THE CHALLENGE: PLANNING AND THEN MONITORING MARINE PROTECTED AREAS IN REMOTE LOCATIONS

Given the United Nations' ambitious goal—endorsed by more than 100 nations, including Canada—of protecting 30% of the world's marine ecosystems by 2030 (UN, 2023), the need to establish, expand, and track the effectiveness of protected areas is becoming more pressing each year. Effective planning for and monitoring of marine protected areas (MPAs) rely on the availability of quality baseline ecological and oceanographic information. Many of the sites in the Canadian Pacific Ocean best suited for protection, due to the confluence of ecological, cultural, and political significance, are remote. This poses two challenges: (1) there is little baseline information to guide planning, and (2) they are challenging to monitor once established.

THE TOOL: OCEAN GLIDERS

Autonomous sampling technologies, such as ocean gliders and floats, are providing new opportunities to collect oceanographic and ecological information more frequently, at times of year not typically sampled, and in remote regions. These autonomous platforms can sample in harsher conditions, are less costly to operate, and have much lower carbon footprints than ship-based operations.

The Canadian-Pacific Robotic Ocean Observing Facility (C-PROOF) has been collecting glider data in understudied areas of interest to inform marine conservation efforts in the Canadian Pacific since 2019 as part of its mission to create a world-class autonomous ocean-observing facility in the Northeast Pacific Ocean and adjacent Canadian coastal waters. C-PROOF is a partnership involving the Universities of Victoria and British Columbia, Fisheries and

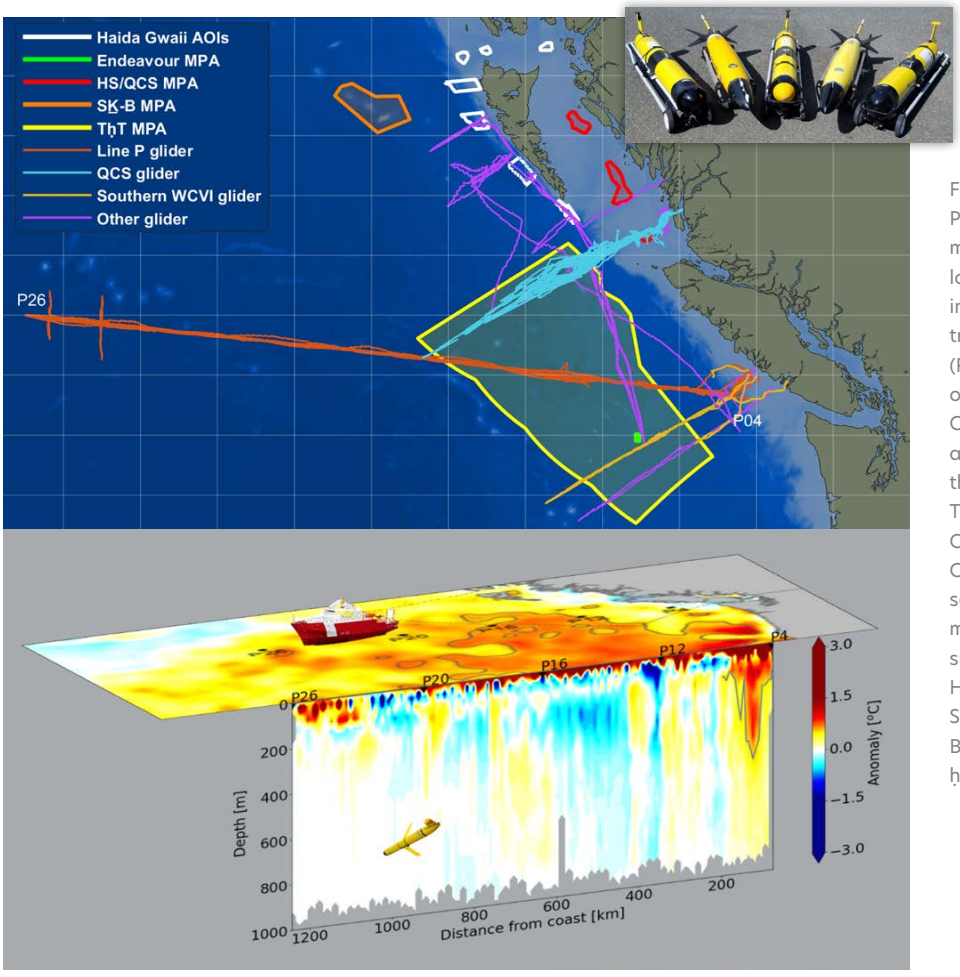

FIGURE 1. (top) A map of the Northeast Pacific Ocean showing C-PROOF glider mission tracks (to August 20, 2024) and locations of marine protected areas (MPAs) in British Columbia waters. The glider tracks are colored by the monitoring lines (Red: Line P. Orange: Southern West Coast of Vancouver Island, WCVI. Cyan: Queen Charlotte Sound, QCS). The existing MPAs are shaded throughout their areas while the proposed MPAs are only outlined. The inset shows some of the gliders in the C-PROOF fleet. (bottom) An example of how C-PROOF glider data can be combined with satellite sea surface temperature data to map marine heatwaves below the ocean's surface. AOI = Area of Interest. HS/QCS = Hecate Strait/Queen Charlotte Sound Glass Sponge Reefs. SK̲-B = SG̲áan K̲ínghlas-Bowie Seamount MPA. TḥT = Tang.g̲wan - ḥačxwiqak - Tsig̲is MPA.

Oceans Canada, and the Hakai Institute, a not-for-profit organization committed to long-term ecological research on the British Columbian coast. In addition to making an important contribution to regional ocean observing in the Northeast Pacific (Barth et al., 2019), the C-PROOF glider lines pass through or near many remote MPAs in the Canadian Pacific (Figure 1). Ocean gliders traverse these lines at high spatiotemporal resolution in all seasons, gathering comprehensive physical and biogeochemical oceanographic data that provide invaluable insights into the health and dynamics of these marine ecosystems.

THE SUCCESSES: FIRST, REGULAR, AND TIMELY

C-PROOF glider data have successfully contributed to MPA planning and monitoring in three main ways: (1) providing the first baseline oceanographic data in some proposed MPAs, (2) frequent monitoring of oceanographic and ecological variables, including ecosystem stressors (such as ocean acidification and deoxygenation), in remote MPAs, and (3) delivering this oceanographic and ecological context in near-real time, key to tracking marine heatwaves.

Baselines for Proposed MPAs. Even regions of high ecological importance, such as the generation site for Haida eddies that connect the coastal margins to the deep Northeast Pacific, have only been visited about a dozen times by oceanographic expeditions. An MPA planning process is now underway for seven sites along the west and north coasts of Haida Gwaii (white outlines, Figure 1), and five C-PROOF glider missions over the last three years have sampled the sites. The data collected have been incorporated into the official governmental planning process, with a recommendation for repeat glider surveys as part of the eventual monitoring plan (DFO, 2024).

Monitoring in Remote MPAs. All C-PROOF regularly sampled glider monitoring lines pass through or near already designated protected areas. Providing ecosystem stressor data has required extensive quality control of the glider oxygen data and the development and verification of two regionally tuned multiple linear regression models to provide ocean acidification metrics useful to MPA management (e.g., Queen Charlotte Sound: Hare et al., 2023; Line P: Dosser et al., 2024). However, for effective uptake in MPA

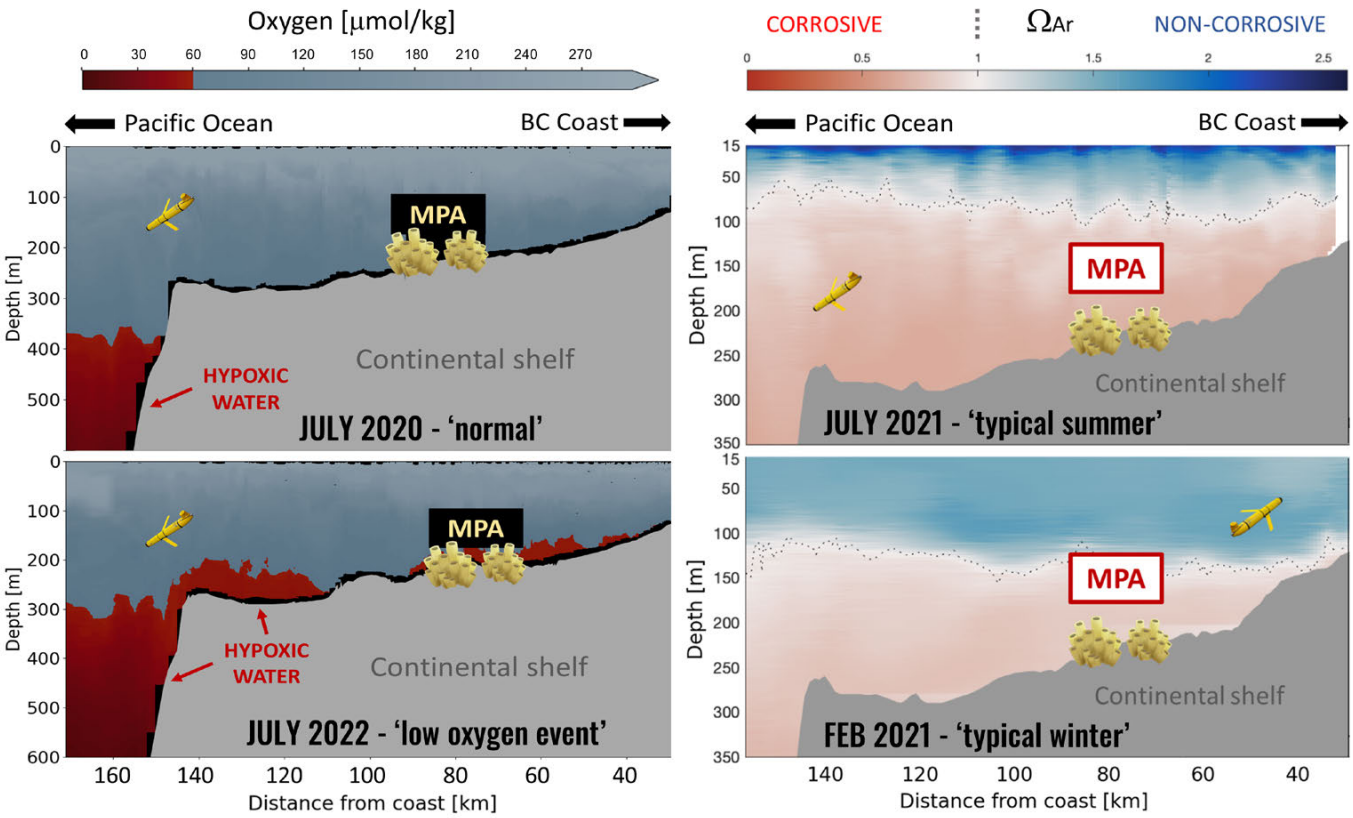

FIGURE 2. Section plots of oxygen and aragonite saturation state (Ω_{Ar}) on the Queen Charlotte Sound (QCS) continental shelf as observed by C-PROOF gliders (i.e., data from cyan lines in Figure 1). The left panels compare a normal oxygen summer (2020, upper left) to a low oxygen summer (2022, lower left). Note how values below 60 µmol kg^{-1}—a biologically meaningful hypoxia limit in the region—are highlighted for ease of interpretation by MPA managers. The right panels show the putatively normal seasonal variation in aragonite saturation horizon between summer (upper right) and winter (lower right), determined from glider proxy measurements. Again, the biologically and chemically important level of $\Omega_A = 1$ is highlighted visually. In all sections, the location of the QCS glass sponge reef MPA is highlighted.

management, the results must be further refined and simplified to effectively communicate with non-scientist management team members (e.g., Figure 2). With respect to marine heatwaves, intuitive visualizations that merge satellite and glider data (inset in Figure 1) have been instrumental in communicating the importance of looking beneath the surface; deep marine heatwaves last longer and have greater impacts on marine ecosystems than heatwave events confined to the surface (Fragkopoulou et al., 2023).

Providing Near-Real Time Context. The value of ocean gliders' capacity to provide oceanographic context in near-real time to serve MPA management needs is exemplified by the ability to adaptively redirect gliders to identify and map extreme events. In the summer of 2021, an unusually large deoxygenation event occurred in the bottom waters on the continental shelf along the west coast of Vancouver Island (Ross et al., 2022). A C-PROOF glider monitoring mission in October 2021 detected this event, and the glider sampling strategy was adapted on-the-fly to better map the event's evolution. This event was proximate to several existing and proposed MPA sites, and its mapping by adaptive glider sampling illustrates how glider-based monitoring of low oxygen water could provide early warnings of potentially lethal low-oxygen events propagating into an MPA.

In sum, ocean gliders hold significant promise to become key tools in MPA managers' toolboxes, providing important oceanographic and ecological data critical to understanding and protecting valuable marine ecosystems in a timely and cost-effective manner.

REFERENCES

Barth, J.A., S.E. Allen, E.P. Dever, R.K. Dewey, W. Evans, R.A. Feely, J.L. Fisher, J.P. Fram, B. Hales, D. Ianson, and others. 2019. Better regional ocean observing through cross-national cooperation: A case study from the Northeast Pacific. *Frontiers in Marine Science* 6:93, https://doi.org/10.3389/fmars.2019.00093.

DFO (Fisheries and Oceans Canada). 2024. *Proceedings of the Pacific Regional Peer Review on the Biophysical and Ecological Overview of the Pacific Region Offshore Haida Gwaii Network Zones; November 8-9, 2022*. DFO Canadian Science Advisory Secretariat, Proceedings Series 2024/002, 36 pp., https://waves-vagues.dfo-mpo.gc.ca/library-bibliotheque/41225132.pdf.

Dosser, H., T. Ross, and D. Ianson. 2024. Quantifying variability in the Northeast Pacific Ocean hypoxic boundary and saturation horizons from ocean glider data along Line P. Paper presented at the Canadian Meteorological and Oceanographic Society 58th Congress, June 3–6, 2024.

Fragkopoulou, E., A. Sen Gupta, M.J. Costello, T. Wernberg, M.B. Araújo, E.A. Serrão, O. De Clerck, and J. Assis. 2023. Marine biodiversity exposed to prolonged and intense subsurface heatwaves. *Nature Climate Change* 13(10):1,114–1,121, https://doi.org/10.1038/s41558-023-01790-6.

Hare, A., W. Evans, S.R. Alin, H. Dosser, J. Jackson, C. Hannah, and T. Ross. 2023. Empirical relationships allow autonomous monitoring of the carbonate system in Queen Charlotte Sound, British Columbia. Paper presented at the Canadian Meteorological and Oceanographic Society 57th Congress, May 28–June 1, 2023.

Ross, T., A.C. Franco, J.A. Barth, A. Sastri, M. Robert, D. Ianson, C. Hannah, F. Chan, R. Feely, R. Dewey, and A. Peña. 2022. Northeast Pacific update: Summer 2021 low oxygen event on the west coast of North America. *PICES Press* 30(1):38–42, https://meetings.pices.int/publications/pices-press/volume30/PPJan2022.pdf#page=38.

UN (United Nations). 2023. *Report of the Conference of the Parties to the Convention on Biological Diversity on the Second Part of its Fifteenth Meeting*. UN Environment Programme, 292 pp., https://www.cbd.int/doc/c/f98d/390c/d25842dd39bd8dc3d7d2ae14/cop-15-17-en.pdf.

AUTHORS

Tetjana Ross (tetjana.ross@dfo-mpo.gc.ca), Fisheries and Oceans Canada, Institute of Ocean Sciences, Sidney, BC, Canada. **Hayley V. Dosser**, Environment and Climate Change Canada, Canadian Centre for Climate Services, Victoria, BC, Canada, and Fisheries and Oceans Canada, Institute of Ocean Sciences, Sidney, BC, Canada. **Jody M. Klymak**, School of Earth and Ocean Sciences, University of Victoria, Victoria, BC, Canada. **Wiley Evans** and **Alex Hare**, Hakai Institute, Campbell River, BC, Canada. **Jennifer M. Jackson**, Fisheries and Oceans Canada, Institute of Ocean Sciences, Sidney, BC, Canada, and Hakai Institute, Campbell River, BC, Canada. **Stephanie Waterman**, Department of Earth, Ocean and Atmospheric Sciences, University of British Columbia, Victoria, BC, Canada.

ARTICLE DOI. https://doi.org/10.5670/oceanog.2025e104

OPTICAL SEDIMENT TRAP FOR IN SITU MONITORING OF SINKING MARINE PARTICLES

By Kirby Simon, Wayne Slade, Margaret Estapa, Ole Mikkelsen, and Chuck Pottsmith

INTRODUCTION

The ocean's biological carbon pump (BCP) comprises a set of physical and biological processes that impact how carbon is exchanged between the atmosphere, the land, and the ocean. Sinking particles, such as "marine snow," are a key mechanism of the BCP, where the depth of remineralization of carbon from these particles governs the extent to which carbon releases back into the atmosphere or sequesters in the deep ocean (Siegel et al., 2021). In addition, this sinking flux is a key energy source for deep water and benthic ecosystems. Studying these particles remains challenging, however, making it difficult to quantify carbon flux on a global scale. Global climate change further decreases the predictability of oceanic carbon flux due to the indirect changes induced by warming, ecosystem shifts, and acidification. Other human-induced alterations of the ocean's carbon cycle, such as proposed marine carbon dioxide removal (mCDR) techniques like ocean alkalinity enhancement or nutrient fertilization, stand to further complicate carbon quantification and the ability to establish a carbon flux baseline from which future measurements can be compared and contextualized.

Marine protected areas (MPAs) are ideal locations for studying the natural carbon cycle in the ocean. Although indirect influences such as climate change, acidification, and pollution still impact them, MPAs (especially those designated as no-entry and no-take) are largely protected from harmful direct human activities. By protecting relatively intact ecosystems from human interference, these sites provide ideal "control" environments for studying and establishing an independent baseline of carbon flux from natural oceanic and biological processes. An observationally constrained BCP baseline will enable scientists to better quantify human-induced direct (e.g., nutrient fertilization) and indirect (e.g., global climate change) perturbations to the carbon cycle, and to better understand the responses of pelagic-benthic energy transfer and benthic ecosystems. Measurements of carbon flux in MPAs also serve as indicators of ecosystem health, as long-term and real-time monitoring of sinking particles can provide data that enable (1) expedited intervention when perturbations are detected, and (2) implementation of more sustainable management practices.

MEASURING SINKING PARTICLES

Typical methods for measuring sinking particles in the ocean include deployment of sediment traps throughout the water column to capture particles to be brought back to the ship (or lab) for analysis. They are time-consuming, labor intensive, and costly, which hinders the widespread study of sinking particles throughout the ocean. While sample collection remains a critical part of oceanographic research, the development and advancement of autonomous platforms, such as autonomous underwater vehicles (AUVs), instrumented moorings, and profiling floats, has enabled more research to be conducted with in situ instrumentation through globally distributed platform and sensor networks. Instrumentation for studying sinking particles in situ on autonomous platforms is limited, however, with requirements on size, weight, power, cost, and data bandwidth/storage hindering the types of sensors permissible for integration with underwater platforms.

Transmissometers show promise in meeting these constraints for studying sinking particles in situ, as the measured beam attenuation coefficient due to particles (c_p) serves as an established proxy for suspended particulate organic carbon (POC; Bishop, 1999). In fact, the earliest studies of sinking particles from autonomous platforms employed transmissometers aboard floats, where researchers observed an increasing trend in measured c_p and attributed it to particles settling and accumulating on the instrument's upward-facing window over time (Bishop et al., 2004). While this demonstrates the potential for transmissometers to measure sinking particles, existing transmissometers do not suit this application because the instrument housing interferes with capturing naturally settling particles and the small beam cross section results in a small sampling capacity compared to sediment traps (Estapa et al., 2024). Therefore, transmissometer design advancements are necessary in order to optimize the sensor for measuring sinking particles in situ and enable widespread adoption and implementation on autonomous platforms.

OPTICAL SEDIMENT TRAP CONCEPT

We are developing a modified transmissometer, called the LISST-OST (Laser In-Situ Scattering and Transmissometry Optical Sediment Trap), to directly address instrumentation shortcomings for straightforward measurements of sinking

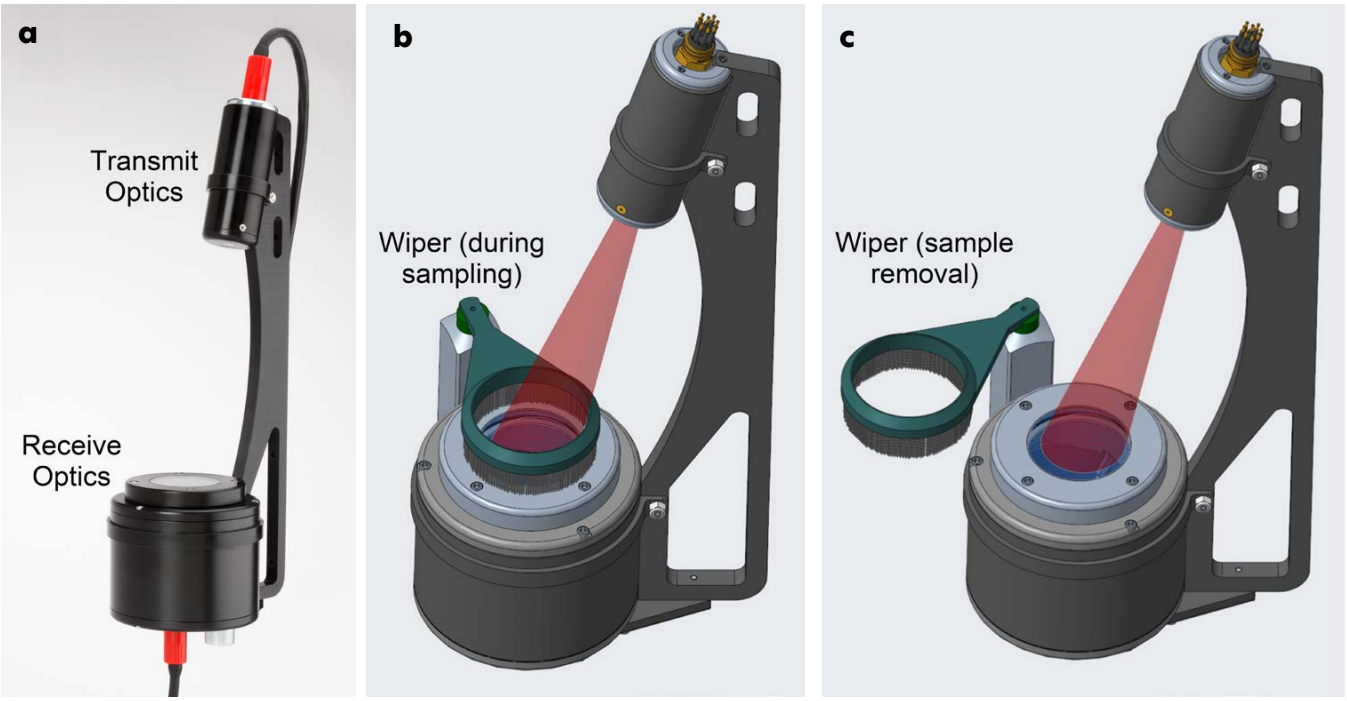

FIGURE 1. (a) The LISST-OST (Optical Sediment Trap) is a modified transmissometer designed for monitoring sinking particles. (b, c) The large clear aperture and reduced obstruction of naturally settling particle fluxes constitute improvements over transmissometers historically employed for measuring sinking particles. The LISST-OST is intended for deployment on autonomous platforms such as profiling floats; however, an optional brush can be integrated for stationary platform deployments to clear particles post-sampling and reduce biofouling.

particles on autonomous platforms (Figure 1). The LISST-OST measures diffuse attenuation in an off-axis optical geometry that enables the sensor to collect sinking particles while minimizing the disruption of their natural settling pathways. Although originally conceptualized for Lagrangian floats (e.g., Biogeochemical-Argo) to collect and measure particles at parking depths up to 2,000 meters, the LISST-OST can also be deployed on stationary platforms with a wiper that reduces biofouling and effectively "refreshes" the measurement at regular intervals.

The sensor consists of two pressure housings: (1) the transmit optics, which includes a single wavelength (approximately 650 nm) source with a diverging beam geometry, and (2) the receive optics, which includes an upward-facing sapphire collection window, focusing optics, and a detector to measure the transmitted optical signal. The large (approximately 5 cm) optical beam cross section at the collection window enables the collection and measurement of a statistically representative sample of sinking particles. As Figure 2 shows, as particles settle on the upward-facing window, the sensor measures changes in diffuse attenuation, which is similarly correlated with POC like c_p (Estapa et al., 2024). The LISST-OST measures diffuse attenuation at a rate of 1 Hz using light modulation and synchronous detection to reject ambient light.

CURRENT AND FUTURE DIRECTIONS

A LISST-OST prototype recently completed its first successful field tests in Monterey Bay, California, USA. The instrument was deployed with other in situ optical sensors on a profiling/drifting platform at depths up to 100 m to explore the trade-offs between, and capabilities of, in situ optical sensors to monitor sinking particles and estimate POC flux. The deployment demonstrated (1) the LISST-OST can successfully collect particles and monitor particle accumulation through changes in diffuse attenuance on an autonomous profiling platform, and (2) sufficient upward motion of the platform can clear particles from the collection window to "refresh" the measurement. Quantitative results and correlations with POC flux are in progress; however, this successful deployment serves as a critical demonstration before large-scale sensor deployments to support MPA management and study of spatiotemporal changes in carbon flux.

The LISST-OST has broad applicability to future MPA management and monitoring efforts. Deploying distributed networks of these sensors in MPAs can provide data to quantify ecosystem health and productivity. Long-term deployments in MPAs can improve management efforts by enabling faster response times to human-induced perturbations that disrupt localized carbon cycles from their

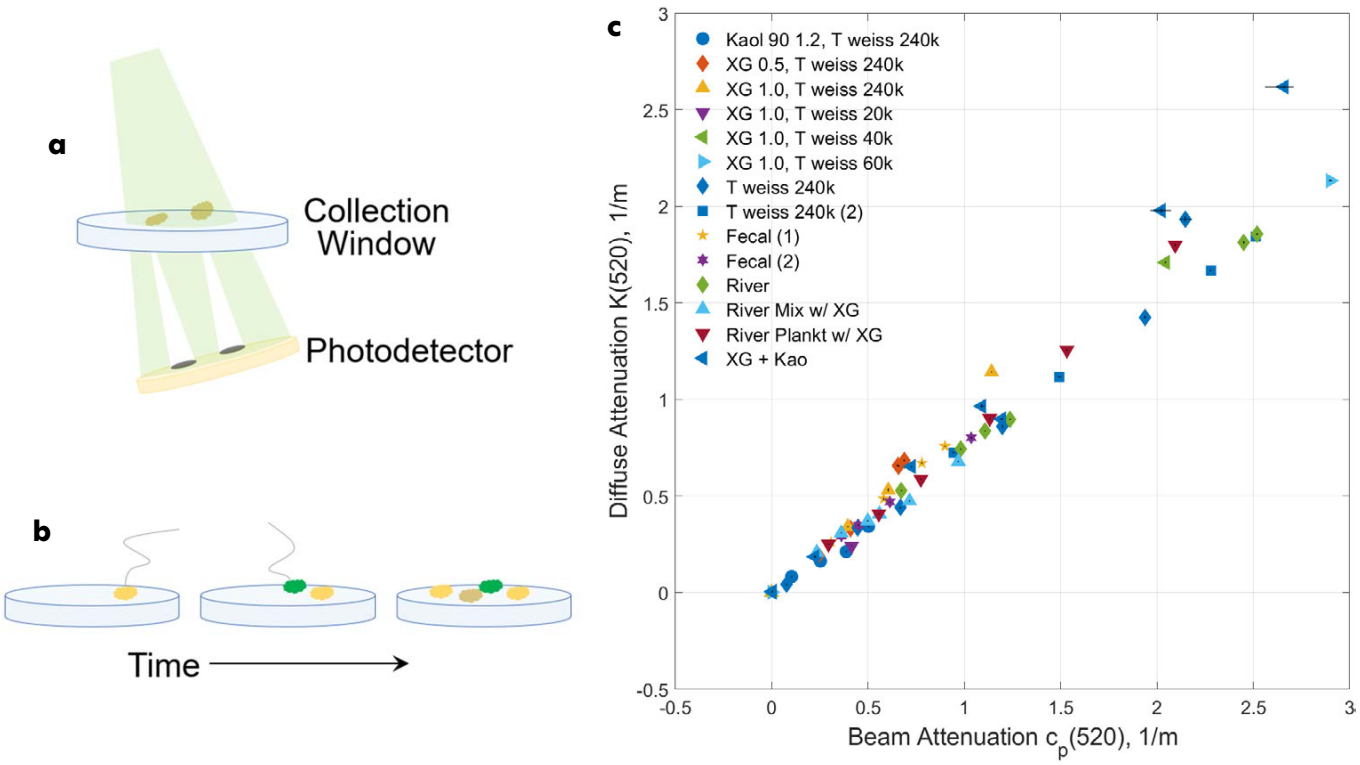

FIGURE 2. (a, b) As sinking particles accumulate on the collection window over time, they reduce the transmitted optical signal to the photodetector. (c) As shown through laboratory testing of a LISST-OST prototype comparing two transmissometer optical geometries, diffuse attenuation (measured in the off-axis geometry) strongly correlates with beam attenuation, which is a proxy for particulate organic carbon (Estapa et al., 2024).

baseline fluxes. On a broader scale, we can improve our quantification of global ocean carbon flux and enhance our understanding of how climate change and human activities impact flux by conducting comparative analysis between LISST-OST data collected from within MPAs versus the open ocean. These data can also be used to support the establishment of new MPAs, as localized measurements that indicate an area exhibits high productivity or carbon export potential could be used to argue for protection of the area from human interventions.

REFERENCES

Bishop, J.K.B. 1999. Transmissometer measurement of POC. *Deep Sea Research Part I* 46(2):353–369, https://doi.org/10.1016/s0967-0637(98)00069-7.

Bishop, J.K.B., T.J. Wood, R.E. Davis, and J.T. Sherman. 2004. Robotic observations of enhanced carbon biomass and export at 55°S during SOFeX. *Science* 304(5669):417–420, https://doi.org/10.1126/science.1087717.

Estapa, M.L., C.A. Durkin, W.H. Slade, C.L. Huffard, S.P. O'Neill, and M.M. Omand. 2024. A new, global optical sediment trap calibration. *Limnology and Oceanography: Methods* 22(2):77–92, https://doi.org/10.1002/lom3.10592.

Siegel, D.A., T. DeVries, S.C. Doney, and T. Bell. 2021. Assessing the sequestration time scales of some ocean-based carbon dioxide reduction strategies. *Environmental Research Letters* 16(10):104003, https://doi.org/10.1088/1748-9326/ac0be0.

ACKNOWLEDGMENTS

The sensor development was funded by the National Science Foundation through the Small Business Technology Transfer (STTR) program under award number 2136735. The views and opinions of authors expressed here do not necessarily state or reflect those of the US government or any agency thereof.

AUTHORS

Kirby Simon (kirby.simon@sequoiasci.com), Sequoia Scientific Inc., Bellevue, WA, USA. **Wayne Slade**, OceanSense, LLC, Vero Beach, FL, USA. **Margaret Estapa**, Darling Marine Center, University of Maine, Walpole, ME, USA. **Ole Mikkelsen** and **Chuck Pottsmith**, Sequoia Scientific Inc., Bellevue, WA, USA.

ARTICLE DOI. https://doi.org/10.5670/oceanog.2025e109

BUILDING OCEAN BIODIVERSITY MONITORING CAPACITY: TRACKING MARINE ANIMALS WITH ACOUSTIC TELEMETRY AND THE ROLE OF THE OCEAN TRACKING NETWORK

By Frederick G. Whoriskey

Critical gaps exist in the ocean science community's biological observation capabilities (e.g., Canonico, 2024; Hassoun et al., 2024). Defining exactly what to monitor and how to obtain the necessary resources to do so are subjects of ongoing debates.

Many highly valued marine species migrate seasonally over long distances and cross international borders as they seek the resources needed to complete their life cycles (Matley et al., 2022). These species drive ecosystem processes, influence carbon cycling, and are critically important for food security and socioeconomic well-being of Indigenous peoples and coastal communities.

Mobile species' ocean distribution and abundance patterns are changing rapidly and unpredictably, primarily due to anthropogenic impacts, including climate warming effects on fisheries, that make monitoring these changes and the factors driving them critically important (e.g., Pershing et al., 2021). As the migration patterns of valued species change, altering ecosystem structure and function and putting at risk the benefits that the migratory species bring to people in coastal communities, there is an increasing need to document these changes and the factors driving them in a timely manner to provide mitigation and adaptation capabilities. The relatively recent development of electronic telemetry technology has enabled researchers to address this need.

There are three principal types of marine animal tracking telemetry systems: satellite tags, data loggers, and acoustic telemetry. For cost and other logistical reasons, acoustic telemetry has become the most widely used (Matley et al., 2022). This technique involves fitting a tag that emits an acoustic signal carrying an animal's unique ID (and in some tag models, secondary signals from tag sensors provide such measurements such as temperature or salinity). These signals are logged by acoustic receivers placed at different points in the ocean. Globally, >20,000 receivers are currently deployed (Figures 1 and 2) by many different research groups. Each receiver (Figure 3) has an omnidirectional detection range of about 800 m. Receivers frequently detect other researchers' tagged animals, so a grass-roots

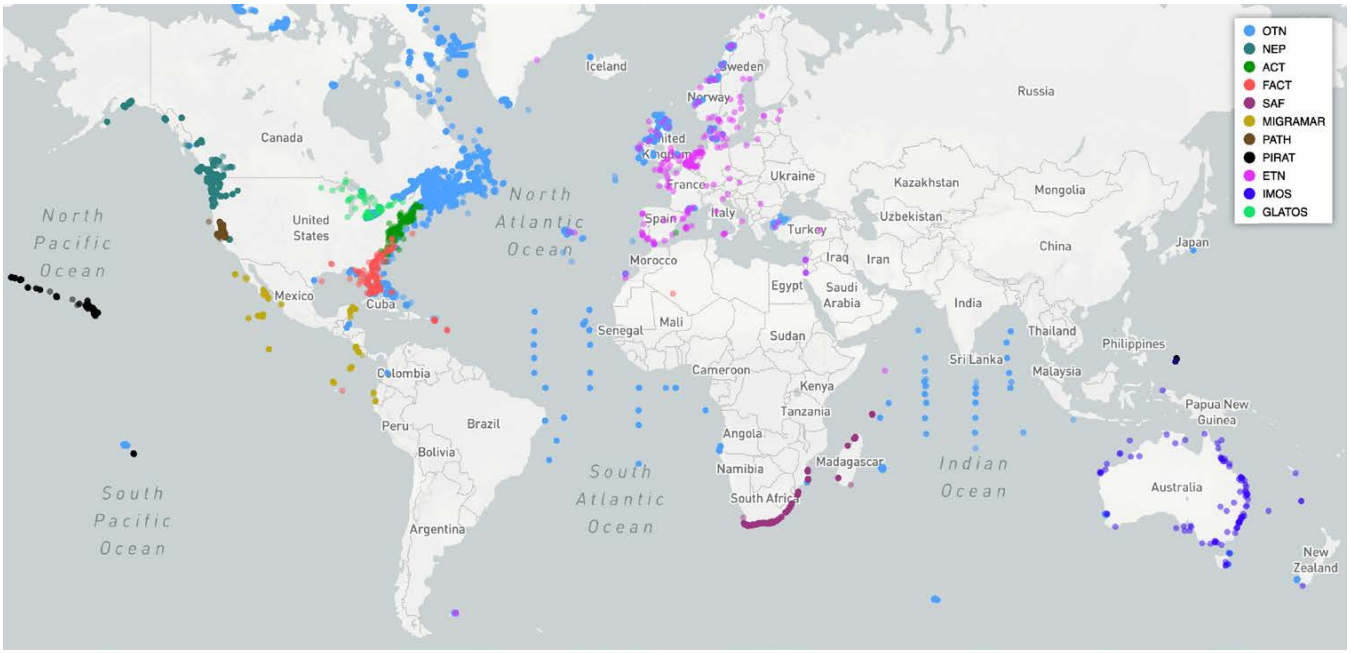

FIGURE 1. Global distribution of current Ocean Tracking Network (OTN) and partner node moored acoustic receiver deployments. Partner nodes are: the North East Pacific (NEP), the Atlantic Cooperative Telemetry network (ACT), the FACT network, the South Africa Acoustic Tracking Array Platform (SAF), MigraMar, the Pacific Aquatic Telemetry Hub (PATH), the Pacific Islands Region Acoustic Telemetry network (PIRAT), the European Tracking Network (ETN), the Integrated Marine Observing System (IMOS), and the Great Lakes Acoustic Telemetry Observing System (GLATOS). *Figure drafted by J. Pye and B. Delo*

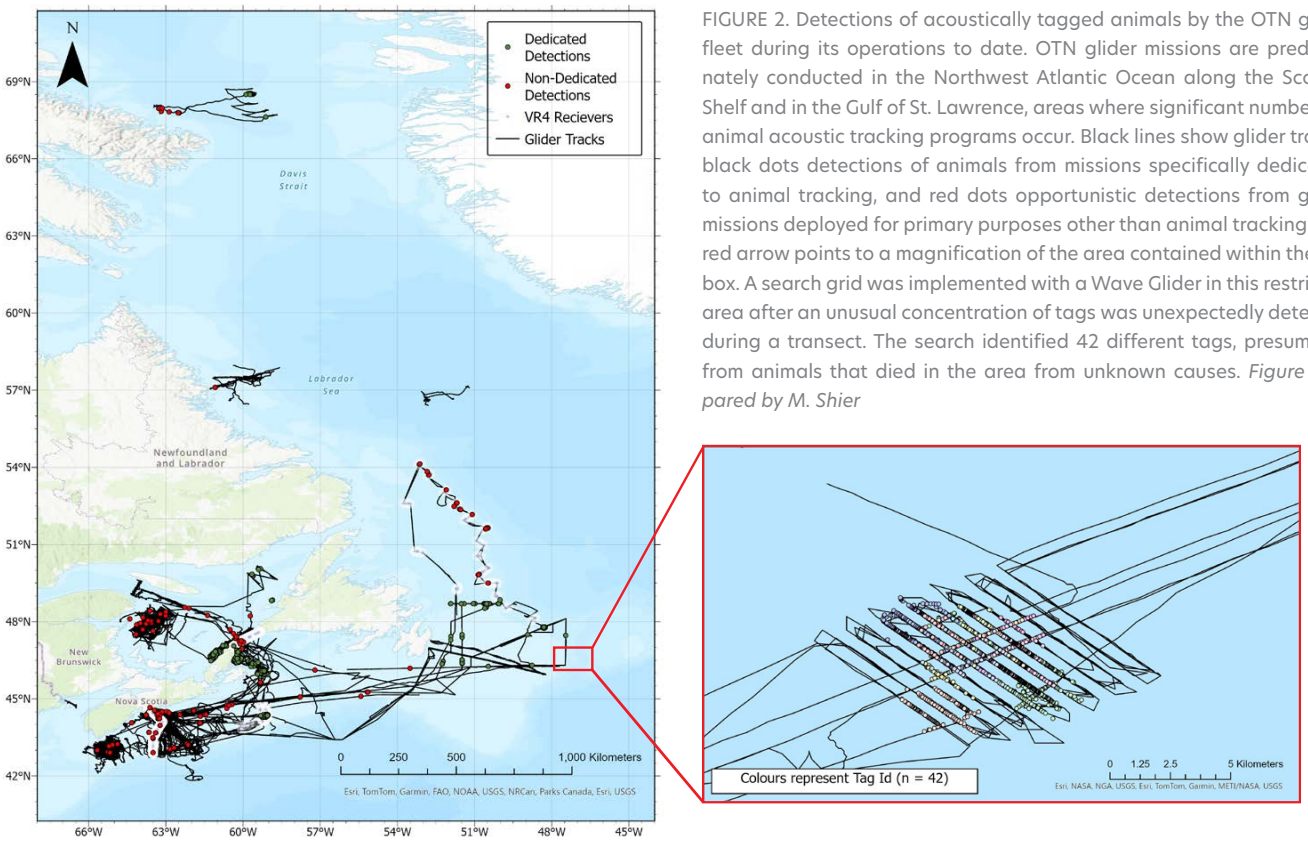

FIGURE 2. Detections of acoustically tagged animals by the OTN glider fleet during its operations to date. OTN glider missions are predominately conducted in the Northwest Atlantic Ocean along the Scotian Shelf and in the Gulf of St. Lawrence, areas where significant numbers of animal acoustic tracking programs occur. Black lines show glider tracks, black dots detections of animals from missions specifically dedicated to animal tracking, and red dots opportunistic detections from glider missions deployed for primary purposes other than animal tracking. The red arrow points to a magnification of the area contained within the red box. A search grid was implemented with a Wave Glider in this restricted area after an unusual concentration of tags was unexpectedly detected during a transect. The search identified 42 different tags, presumably from animals that died in the area from unknown causes. *Figure prepared by M. Shier*

effort developed within the telemetry community to share detections, thereby creating a global monitoring network (Matley et al., 2022), with the Ocean Tracking Network (OTN) playing a leading role.

OTN is a global aquatic animal tracking, technology, data management, and partnership platform headquartered at Dalhousie University in Canada. Funded by the Canada Foundation for Innovation as a Major Sciences Initiative, OTN operates an international network of acoustic receivers (up to 3,000 at any given time) that supports and leverages the efforts of the global science community. OTN has staffed, designed, and implemented a data system to collate, provide quality assurance and control for, curate, and distribute the acoustic telemetry data generated by participants in the OTN network. The system is a certified Associate Data Unit of UNESCO's Intergovernmental Oceanographic Committee's International Oceanographic Data and Information Exchange (ADU-IODE) and a thematic node of the global Ocean Biodiversity Information System (OBIS). More than 7,000 users have registered with the broader OTN data system, which is responsible for over 2 billion detection records.

The OTN network-of-networks federates data from 10 international partners (nodes; see **Figure 1**) who use the same database structure and workflows to manage data from their home regions. This node structure enables the efficient exchange of data among these networks, and an investigator seeking information about tagged animals can enter through any of these nodes and pull detections from all the participating nodes. OTN has additional international data partners that maintain independent data systems and enable exchanges with the family of OTN nodes.

OTN operates a fleet of Slocum electric profiling gliders and Liquid Robotics Wave Gliders to augment its animal tracking activities (**Figures 2 and 3**). Glider sensors (e.g., temperature, conductivity, dissolved oxygen concentration, chlorophyll, and others) provide data on environmental conditions that can be used to determine whether animals are attracted to or avoid particular ocean areas. The gliders can serve as dedicated mobile receiver platforms in places where it is too costly or logistically infeasible (e.g., heavy fishing pressure) to moor fixed receivers. They also routinely carry acoustic receivers to provide opportunistic detection of tagged animals. The Slocum gliders can carry passive acoustic monitoring (PAM) systems that can detect whale and other cetacean calls, enabling the monitoring of their presence (**Figure 3**).

Scientists monitor the presence and movements of marine animals for many different reasons. Examples include:

EFFECTIVENESS OF MPAs. For marine protected areas, acoustic telemetry is a valuable tool for determining whether animals remain within the MPA borders and receive the intended protection. OTN acoustic receivers have been deployed within protected areas in Canada and the United States to document the use of the MPAs by a suite of tagged

FIGURE 3. (a) Deployed acoustic receiver mooring (with sacrificial disc anchor, acoustic release, and yellow flotation collar housing the acoustic receiver) before deployment. (b) Recovery of a Slocum electric glider fitted at the bow with a Digital Acoustic Monitoring (DMON) external hydrophone to record whale calls. (c) Close up of DMON. *Photo credits: Nicolas Winkler Photos courtesy of the Ocean Tracking Network*

species, including commercially important snow crab (*Chionoecetes opilio*), Atlantic cod (*Gadus morhua*), highly migratory bluefin tuna (*Thunnus thynnus*), and protected (US) or endangered (Canada) white sharks (*Carcharodon carcharias*). In Canada, where long-term monitoring plans for MPAs are now under development, current data from acoustically tagged species in MPAs is being used to help design future MPA monitoring strategies.

RIGHT WHALES IN THE GULF OF ST. LAWRENCE. A calling whale is perhaps the largest and most powerful "acoustic tag" imaginable. OTN's PAM-equipped gliders are supported by Transport Canada as part of a Canadian whole-of-government effort to protect migrating endangered right whales, many of which suddenly shifted their summer feeding distribution from the Bay of Fundy to the Gulf of St. Lawrence around 2016. In the Gulf, the whales encountered threats from entanglement in fishing gear and ship strikes, and in the 2017–2019 period an exceptional mortality event occurred, with 21 dead whales reported. OTN gliders are now patrolling the shipping lanes in the Gulf of St. Lawrence listening for whales, complementing aerial and other monitoring systems. Whale call detections by the gliders trigger management decisions that include mandatory ship slow-downs and closure of fishing areas. Since the monitoring program began, there have been no reports of right whale deaths in the Gulf of St. Lawrence.

PROMOTING CONSERVATION OF PACIFIC SALMON. Declines of multiple species of Pacific salmon (genus *Oncorhynchus*) in North America are of great concern because they support extensive Indigenous, commercial, and recreational fisheries. A variety of measures are being applied to help conserve Pacific salmon, including live release of specific species or strains taken in recreational fisheries. Many factors, including water temperature, fight time, aerial exposure, and hook wounding, could affect whether the released fish survive. In a comprehensive study that used acoustic telemetry to link fish survival to these factors, Hinch et al. (2024) identified the prime mortality drivers for caught-and-released chinook (*O. tshawytscha*) and coho salmon (*O. kisutch*). Their work has generated 15 actionable recommendations for managers and policymakers regarding ways anglers can modify their fishing practices to improve the conservation effectiveness of live release.

REFERENCES

Canonico, G., J.E. Duffy, M. Edmonson, K. Fillingham, A. Benson, K. Bisson, A. Demopoulos, B. Hinchey, K. Matsumoto, C. Meyer, and others. 2024. *The National Ocean Biodiversity Strategy*. Report of the Interagency Working Group on Biodiversity, 18 pp., https://www.whitehouse.gov/wp-content/uploads/2024/06/NSTC_National-Ocean-Biodiversity-Strategy.pdf.

Hinch, S.G., S.D. Johnston, E.L. Lunzmann-Cooke, K. Zinn, and B.J.L. Hendriks. 2024. *Enhancing the Sustainability of Capture and Release Marine Recreational Pacific Salmon Fisheries Using New Tools and Novel Technologies*. Final Report on Project 2019_058 submitted to the British Columbia Salmon Restoration and Innovation Fund, July 12, 2024.

Hassoun, A.E.R., T. Tanhua, I. Lips, E. Heslop, G. Petihakis, and J. Karstensen. 2024. The European Ocean Observing Community: Urgent gaps and recommendations to implement during the UN Ocean Decade. *Frontiers in Marine Science* 11:1394984, https://doi.org/10.3389/fmars.2024.1394984.

Matley, J.K., N.V. Klinard, A.P. Barbosa Martins, K. Aarestrup, E. Aspillaga, S.J. Cooke, P.D. Cowley, M.R. Heupel, G.C. Lowe, S.K. Lowerre-Barbieri, and others. 2022. Global trends in aquatic animal tracking with acoustic telemetry. *Trends in Ecology and Evolution* 7:79–94, https://doi.org/10.1016/j.tree.2021.09.001.

Pershing, A.J., M.A. Alexander, D.C. Brady, D. Brickman, E.N. Curchitser, A.W. Diamond, L. McClenachan, K.E. Mills, O.C. Nichols, D.E. Pendleton, and others. 2021. Climate impacts on the Gulf of Maine ecosystem: A review of observed and expected changes in 2050 from rising temperatures. *Elementa: Science of the Anthropocene* 9:1, https://doi.org/10.1525/elementa.2020.00076.

AUTHOR

Frederick G. Whoriskey (fwhoriskey@dal.ca), Ocean Tracking Network, Dalhousie University, Halifax, NS, Canada.

ARTICLE DOI. https://doi.org/10.5670/oceanog.2025e103

WESTERN BOUNDARY CURRENTS AND THEIR IMPACTS ON SHELF SEAS

ADVANCING OBSERVATIONS OF WESTERN BOUNDARY CURRENTS: INTEGRATING NOVEL TECHNOLOGIES FOR A COORDINATED MONITORING APPROACH

By Moninya Roughan, Junde Li, and Tamaryn Morris

ABSTRACT

Western boundary currents (WBCs) play a crucial role in global ocean circulation, regulating climate, influencing weather patterns, driving marine ecosystems, and transporting heat, momentum, and biogeochemical properties across ocean basins. Despite their importance, their strong variability and deep structures make them challenging to observe. Here, we synthesize the physical properties of the five major subtropical WBCs and highlight the need for improved and sustained observations. We present dynamically driven priorities for observation, emphasizing novel and cost-effective methods. Advances in satellite altimetry, autonomous vehicles, and ship-based measurements have enhanced monitoring efforts, but gaps remain, particularly in subsurface observations and cross-system comparisons. Emerging technologies such as the fishing vessel observation network and uncrewed surface vehicles provide new opportunities for broad-scale, high-frequency data collection. Modified Argo float deployments (more frequent profiling) and repeat glider missions offer improved resolution of eddy structures and upper-ocean heat content estimates. We emphasize the need for consistent observational strategies across WBC systems to enable direct comparisons and improve predictive modeling. Integrating satellite data with in situ observations and high-resolution models is essential for refining estimates of WBC variability, heat transport, and climate-driven changes. A coordinated, multi-platform approach for observation and analysis is critical to understanding WBC dynamics and their long-term impacts on regional and global climate.

INTRODUCTION

Western boundary currents (WBCs) are crucial components of the global ocean circulation, responsible for transporting water (momentum), heat, and nutrients from the tropics to higher latitudes. They play a vital role in regulating regional weather and global climate patterns. The world's five major WBCs: the Gulf Stream (GS), the Kuroshio Current (KC), the East Australian Current (EAC), the Brazil Current (BC), and the Agulhas Current (AC) exhibit distinct characteristics influenced by a variety of processes, including large velocity and temperature gradients, variable wind stress, topographic steering, high oceanic heat content, intrinsic variability, and large-scale climate variability. These ocean regions are also undergoing rapid environmental change, for example, warming at above-average rates. Combined, these elements make it essential to measure, observe, and predict WBCs. Therefore, understanding their short-term and long-term variability and their drivers is fundamental. However, observation and prediction in these regions is challenging, and efforts internationally are not coherent. Here, we provide an overview of some of the main WBC characteristics and pose dynamically driven suggestions for observation priorities.

MEAN STATE AND DRIVERS OF FIVE MAJOR WBCs IN THE GLOBAL OCEAN

Velocities and volume transport vary considerably across the five WBCs, ranging from approximately 1.3 to 150 Sv (1 Sv = 10^6 m^3 s^{-1}; Imawaki et al., 2013; Table 1). The GS, one of the most extensively studied WBCs, has a maximum surface

velocity of 2.5 m s^{-1} (Wei et al., 2008) and a volume transport of 18.9–150 Sv (Imawaki et al., 2013). The KC in the North Pacific shows similar strength, with maximum velocities reaching 2 m s^{-1} (Nagai et al., 2019) and a volume transport of 21.5–130 Sv from a lowered acoustic Doppler current profiler survey conducted across the Kuroshio Extension southeast of Japan (Imawaki et al., 2013). The AC in the Indian Ocean is slightly weaker, with peak velocities of 1.5–2 m s^{-1} and a mean transport of 84 ± 24 Sv (Beal and Elipot, 2016) based on a three-year time series of moored observations. Its mean transport is 70 Sv at 32°S, making it the strongest WBC in either hemisphere at this latitude (Imawaki et al., 2013). The BC in the South Atlantic is comparatively weaker, with maximum velocities of 1.1 m s^{-1} (Biló et al., 2014) and a transport of 1.3–30.9 Sv (Schmid et al., 2018). The EAC, while less powerful than its northern counterparts, still exhibits significant flow, with surface velocities up to 2 m s^{-1}. From a ~10-year moored time series, Sloyan et al. (2024) found a maximum southward transport of approximately 60 Sv, with periods of net northward transport (maximum of 20 Sv) and a calculated mean of 18 Sv (from 0–1,500 m depth at 28°S). Chandler et al. (2022) made estimates of transport across three of the WBCs (AC, KC, and EAC) using a consistent methodology that combined several observation types, allowing direct comparison of the transports in the systems; however, the latitudes of the observations were not consistent, and estimates were not made for the BC or the GS.

These currents are also highly variable. Fluctuations driven by meandering of the currents, the formation and shedding of mesoscale eddies, and variability in local and remote wind forcing result in changes in transport of up to 20%–30% over short periods. On longer timescales, they are driven by seasonally driven shifts and decadal oscillations often influenced by large-scale climate patterns and wind stress variations over their respective ocean basins.

The KC and the GS are deep reaching, with strong velocities (0.3 m s^{-1}) down to at least 1,000 m depth. The EAC is generally considered the shallowest of the WBCs, extending to about 1,200 m depth at 28°S, with a core at ~400 m. The BC is also generally shallower than its Northern Hemisphere counterparts, typically extending to depths of 500–1,000 m. The AC extends to depths of 1,500 m and has a more complex vertical structure with a distinct undercurrent (Imawaki et al., 2013). Vertical and horizontal velocity shear is greatest on the coastal (cyclonic) side of the jets, which are the core of the WBCs, accompanying a strong sea surface temperature (SST) gradient. These strong, variable, and deep currents make them inherently difficult to observe.

Temperature gradients (Figure 1b–f) are largest in the WBC extension regions, but they are weak within the jets themselves. Temperature gradients reach a maximum of up to 0.1°C per km in the GS extension region (north of the GS proper) and in the AC extension region (south of the AC).

Broader climatic patterns such as the Pacific Decadal Oscillation, the North Atlantic Oscillation, and the El Niño-Southern Oscillation influence long-term variability in the Northern Hemisphere WBCs. Additionally, recent observations indicate that for some WBCs, like the AC, there have been increases in width (eddying) without significant strengthening (Beal and Elipot, 2016) or shifting (Li et al., 2022), while others, such as the EAC and the BC, have shown a poleward shift and intensification in response to global climate change (Yang et al., 2016). The Global eXpendable BathyThermograph (XBT) program has observed the northward shift of the GS since the early 1990s (Andres et al., 2025, in this issue) and the BC's structure and variability over the period of 2004–2023 (Ferreira et al., 2025, in this issue). The dynamic variations documented highlight the complex interplay among these powerful currents and the evolving climate system.

OCEAN HEAT TRANSPORT, TEMPERATURE VARIABILITY, AND TRENDS

WBCs transport warm tropical water poleward along the western boundaries of each ocean basin. Warm mesoscale eddies shed from the WBCs also advect heat as the eddies propagate. WBCs are easily observed from space in satellite SST data, and their poleward extensions are readily monitored by observations of warm water intrusions. Temperatures vary seasonally due to warming at

TABLE 1. Characteristics of the five major subtropical western boundary currents in the global ocean (where negative transport is southward).

NAME	VOLUME TRANSPORT RANGE (Sv)	MAXIMUM VELOCITY (m s^{-1})	GEOGRAPHIC RANGES	CITATIONS
Gulf Stream	18.9 to 150	2.5	25°N–35°N, 75°W–81.5°W	Imawaki et al., 2013; Wei et al., 2008
Kuroshio Current	21.5 to 130	2.0	22°N–36°N, 124°E–141°E	Imawaki et al., 2013; Nagai et al., 2019
Agulhas Current	–60 to –108	2.0	27°S–37°S, 20°E–35°E	Imawaki et al., 2013; Beal and Elipot, 2016
East Australian Current	–60 to 20	2.0	24°S–34°S, 151°E–155°E	Sloyan et al., 2024
Brazil Current	–1.3 to 30.9	1.1	21°S–38°S, 55°W–40°W	Biló et al., 2014; Schmid et al., 2018

the upstream (equatorward) origins of WBCs (Figure 1a) and cooling through loss of heat to the atmosphere along their poleward transits. Temperature gradients across WBC fronts can be large (Figure 1b–f) and contribute to the generation of instabilities as the WBCs extend poleward. In the EAC, temperature gradients can be up to 0.07°C per km, with much larger temperature gradients (>0.1°C per km) in the other WBC extension regions (Figure 1b–f).

Marine heatwaves (extremely high temperatures) are readily calculated and quantified using satellite data due to the 30-year record and broad spatial coverage; however, satellite observations do not provide the subsurface structures of marine heatwaves in WBC regions, which are often related to the advection of heat in eddies. Recent mooring observations in the KC and Mindanao Current region (Hu et al., 2020) and the EAC (Sloyan et al., 2016) indicate the complexity of vertical structures of the currents. Additionally, models driven by sparse observations tend to poorly represent the subsurface structures of the WBCs and mesoscale and submesoscale eddies. Hence, it is essential that we measure vertical temperature structure throughout the water column, including the mixed layer depth, the thermocline, and the full-depth structure in WBC regions. This also has implications for estimates of upper ocean heat content, which are fundamental for both short- and long-term weather and climate prediction.

WBC extension regions are global ocean warming hotspots (Figure 1g–k), with the surface ocean warming over the paths of WBCs and their extension regions two to three times faster than the global mean (Wu et al., 2012), along with increased poleward penetration of heat in the EAC, BC, KC, and GS. This is further motivation to measure and monitor heat content in WBCs below the surface.

Additionally, due to global warming, the major subtropical ocean gyres have consistently shifted poleward over recent decades. The WBCs (except the GS) are not only shifting poleward but are also intensifying (Yang et al., 2016), with more warm waters being transported into the WBC extension regions. The barotropic and baroclinic instabilities that generate eddies (see below) in the WBC regions are also increasing (Li et al., 2022), and eddy-rich regions are forming even more eddies and getting warmer

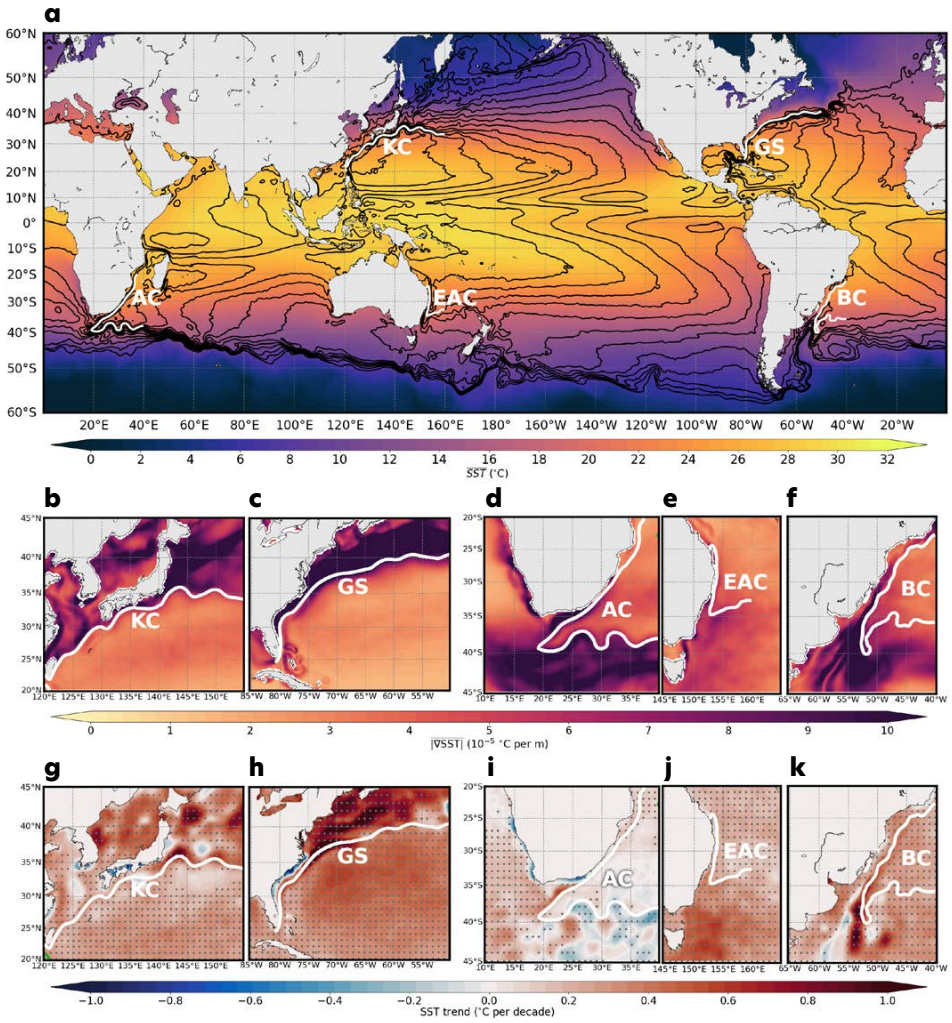

FIGURE 1. Spatial distributions of (a) mean sea surface temperature (SST), (b–f) mean SST gradients, and (g–k) SST trends from Optimum Interpolation Sea Surface Temperature (OISST) observations from satellites, ships, buoys, and Argo floats between 1993 and 2020. The black contours in (a) indicate the climatological mean sea surface height from AVISO satellite observations between 1993 and 2020. The white lines in (a–k) illustrate the paths of the global ocean's five major western boundary currents. The gray stippling in (g–k) indicates that the trends are statistically significant above the 95% confidence level. KC = Kuroshio Current. GS = Gulf Stream. AC = Agulhas Current. EAC = East Australian Current. BC = Brazil Current.

(Martínez-Moreno et al., 2021). Hence, it is essential that we monitor and observe effectively below the surface in these eddy-rich regions to understand the full extent of the impacts of ocean warming and environmental change.

EDDY FIELDS IN THE FIVE WBCs

Mesoscale eddies (large rotating bodies of water, with diameters ranging from tens to hundreds of kilometers) are important features in all the WBCs and play a crucial role in their dynamics by influencing heat transport, nutrient distribution, and mixing processes. The eddy fields associated with WBCs are characterized by high variability and are influenced by factors such as ocean topography, local and remote wind patterns, and large-scale ocean circulation.

Eddies can form through WBC meanders that pinch off from the WBCs themselves (also known as warm core rings) but also from instabilities that propagate across the ocean basins. Eddies are essential for the transport of heat and nutrients and play a key role in modulating the strength and variability of the WBC jets themselves, as well as having an influence on regional climate and marine ecosystems.

Compared to short-lived eddies, long-lived eddies have larger diameters and higher impacts on the ocean's dynamical processes, biological productivity, and marine ecosystems. The AC rings are notably larger (200–400 km diameter) and longer-lived (6–18 months) compared to eddies in the other WBCs, while the BC eddies tend to be smaller (50–150 km) and shorter-lived (1–3 months). The GS, KC, and EAC eddies share similar characteristics (100–300 km diameter) and last 3–6 months.

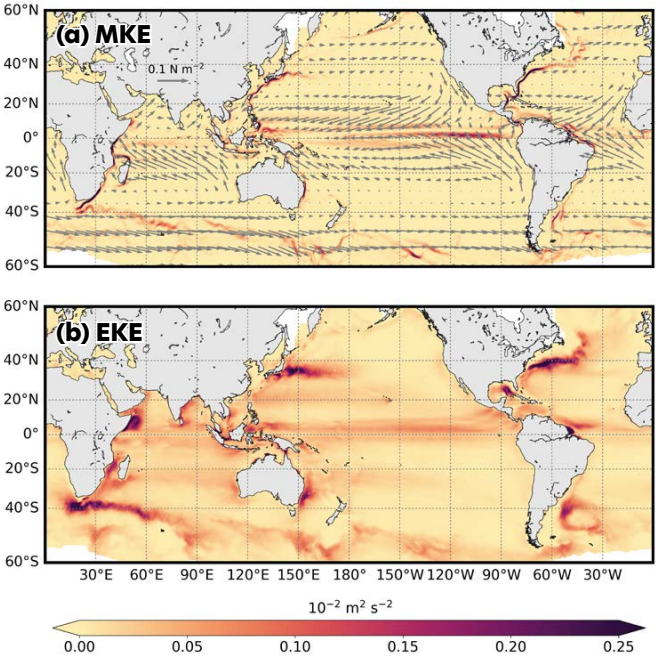

FIGURE 2. Spatial distributions of (a) mean kinetic energy (MKE), and (b) eddy kinetic energy (EKE) from AVISO observations between 1993 and 2020. The gray vectors in (a) indicate the wind stress from ERA5 reanalysis between 1993 and 2020.

Although kinetic energy in WBCs is high in the main core of the jets (Figure 2a), mesoscale eddies account for around 90% of the total surface kinetic energy in the global ocean. In the eddy-rich areas, such as the WBC extension regions, the eddy kinetic energy is much larger than the global mean (Figure 2b) and shows a significant increase of 2%–5% per decade (Martínez-Moreno et al., 2021).

Due to their dynamic nature, eddies are difficult to measure, model, and predict; hence, observational strategies are challenging. Recent work shows that the subsurface structures of WBC eddies are not well represented in ocean models (Gwyther et al., 2022, 2023a, 2023b). For example, eddy-permitting models typically have eddies that are too barotropic and extend too deep through the water column (Gwyther et al., 2023a). Thus, temperature stratification, mixed layer depth, and thermocline and eddy-driven vertical processes are not well represented, resulting in poor estimates of ocean heat content. This observational gap needs to be addressed to improve eddy prediction (Gwyther et al., 2022, 2023a, 2023b).

CROSS-SHELF EXCHANGE AND COASTAL UPWELLING

Cross-shelf exchange and coastal upwelling are key processes associated with WBCs that influence the distribution of heat, nutrients, and biota in coastal regions. These processes are driven by interaction between the strong WBCs and the coastal topography, as well as by local wind patterns. Additionally, the width of the continental shelf plays a role. For example, the EAC, AC, and KC flow within close proximity to the coast along narrow shelves (ranging from 15 km to 30 km) compared to the GS and BC where the shelf ranges from 20 km to 100 km wide and the WBC core can be well offshore. In the EAC (Roughan and Middleton, 2002) and BC (Calado et al., 2010) regions, where the strong jets can flow close to the coast, current-driven upwelling plays a key role in bringing nutrient-rich waters to the coast. Similarly, the interaction between the KC and the continental shelf plays a critical role in cross-shelf exchange and coastal upwelling. WBC-induced coastal upwelling also strongly impacts chlorophyll and oxygen concentrations, vertical migrations of zooplankton, and primary production. Across the broad GS shelf, river outflow and buoyancy forcing play roles in driving the shelf circulation. Cyclonic (cold core) eddies also form on the inside edges of WBCs (as frontal eddies) and can spin up and grow. They are important ecological features that can drive the retention,

advection, and connectivity of coastal species. These cross-shelf exchange processes are essential for sustaining the productivity of coastal ecosystems.

The broadening of the AC has implications for cross-shelf exchange processes, potentially enhancing the transport of warm, nutrient-poor waters onto the continental shelf (Beal and Elipot, 2016). Intensified warming of the Southern Hemisphere WBCs (Li et al., 2022) could lead to changes in cross-shelf exchange and coastal upwelling patterns and a reduction in upwelling intensity. This could have significant impacts on local marine ecosystems, particularly in terms of nutrient availability and primary productivity. Thus, as cross-shelf exchange processes are sensitive to changes in the strength and variability of the WBCs, with potential consequences for coastal ecosystems and fisheries.

PRESENT AND FUTURE OBSERVATIONS

Understanding the dynamics of WBCs and their responses to climate change requires continuous and comprehensive observations. Advances in satellite technology, oceanographic measurements, and numerical modeling have provided valuable insights into the behavior of WBCs, but challenges remain in capturing their full complexity and predicting future changes. Their deep extents and strong currents make them an observational challenge.

Expendable BathyThermographs (XBTs) have provided some of the longest and most sustained repeat observations of WBC regions, starting in the 1960s (Goni et al., 2019). Due to their simple and robust nature, they provide an excellent means with which to get widespread observations along routine shipping routes. However, they typically only measure temperature in the top 700–900 m of the water column, leaving much of the depth structures of the WBCs and their eddies unobserved. Additionally, as the observations are reliant on repeat shipping routes, the latitude at which the vessels cross the WBC core varies in each system (Chandler et al., 2022). This means that analogous repeat observations of WBC jets do not yet exist. Having analogous observations across similar dynamical regimes (e.g., Archer et al., 2018) would allow for robust comparison between the WBCs and help to eliminate uncertainty in the comparisons of estimates of volume transport and heat content.

The increasing intensity of eddy activity in WBCs observed over the satellite altimetry record (Martínez-Moreno et al., 2021; Li et al., 2022) highlights the importance of continued monitoring to understand the drivers and impacts of these changes. Data from new satellites such as Surface Water and Ocean Topography (SWOT) that fully resolve mesoscale and some submesoscale processes will play an important role in resolving the structure and variability of WBCs and their mesoscale eddies, particularly when their data is combined with in situ observations (e.g., Beal and Elipot, 2016, extended a three-year moored time series in combination with satellite altimetry).

In the EAC and GS, efforts have been made to use repeat glider missions along the length of the currents (as opposed to endurance lines in eastern boundary currents) for sustained monitoring of heat content (and in the GS also velocities) (Todd et al., 2019). These efforts provide broad-scale but sporadic observations below the surface, but with enough repetition, they are valuable for observing mean and extreme hydrographic states (e.g., Schaeffer and Roughan, 2015).

Argo floats (Wijffels et al., 2024) and surface drifters (Lumpkin et al., 2017; Matisons et al., in press) provide Lagrangian estimates of the WBCs; however, they are readily advected out of the swift currents, and ejected from eddies; hence, regular seeding of floats into WBCs is important to maintain coverage of the jet and eddy regions. Modified Argo float sampling strategies have shown that daily profiles are useful not only for resolving eddy structure but also for retaining the floats within eddies (e.g., by changing park depths to 300–500 m), and this deserves further exploration.

The importance of long-term moored observational data was highlighted in Beal and Elipot (2016) for understanding changes in AC structure and variability below the surface. They emphasize combining satellite altimetry and in situ measurements in calculating variability and change, and their results underscore the need for sustained in situ observations to monitor these changes and their impacts on WBC circulation. While long-term moored observations are essential for obtaining full-depth structure, they are costly and challenging to maintain long term; for example, see Sloyan et al. (2016 and 2024) for a description of ~10 years of full-depth observations in the EAC.

New methods to observe broadly at low cost include the use of ships of opportunity, for example, the emerging Fishing Vessel Observation Network (FVON; Jakoboski et al., 2024), that allows broad-scale coverage. These ships offer opportunistic observations largely in shelf seas, where fishing occurs, to complement existing observation methods (e.g., the high temporal resolution but single point moored observations and broad scale, but sporadic glider missions). The use of fishing vessel observations to explore marine heatwaves and high-resolution subsurface ocean structure has been demonstrated successfully in the EAC (Lago et al., 2025, in this issue), and this low-cost technology should be considered an essential part of a WBC observing system, particularly in data poor regions.

There is increasing use of uncrewed surface vehicles to measure ocean-atmosphere exchanges. The usefulness of

these vehicles in exploring the role of WBCs on short-term weather and longer-term seasonal and climatic dynamics is also noteworthy. Like glider missions, these observations are autonomous (with piloting and technical teams located ashore) and play a crucial role in understanding fluxes and cross-shelf exchanges (Cronin et al., 2023).

There is no clear and consistent guidance for observations in WBCs, which makes comparisons between them difficult. Archer et al. (2018) showed the value of using similar observational datasets for direct comparisons between systems (they used high-resolution high-frequency radar to compare upstream circulation in the EAC and the GS at similar latitudes). While the global XBT program comes close to meeting this objective, the observation lines are determined by shipping routes, not ocean dynamics, which makes direct comparisons more difficult (Chandler et al., 2022).

In order to make direct comparisons among systems (e.g., like those in Table 1), there is a pressing need for analogous observations in dynamically similar locations in each of the WBC systems. This would enable accurate comparisons among the systems, for example, of upstream transport and heat content, or eddy variability and retention. Similarly, consistent methodologies for analysis of the analogous datasets allow for direct comparisons of WBC variability (Archer et al., 2018; Chandler et al., 2022). A readily accessible suite of tools to interrogate ocean models and WBC datasets in similar ways would also be welcome.

Continuous and comprehensive in situ surface and subsurface observations in the upstream areas of WBCs and their extension regions are critical for us to better understand the dynamics, changes, and drivers of WBCs. Additionally, the full integration of satellite observations and in situ real-time measurements with high-resolution models is essential in order to improve state estimates and predictions of future changes in WBCs and to better understand the drivers of ocean warming and their impacts on regional and global climates.

REFERENCES

Andres, M., T. Rossby, E. Firing, C. Flagg, N.R. Bates, J. Hummon, D. Pierrot, T.J. Noyes, M.P. Enright, J.K. O'Brien, and others. 2025. Monitoring impacts of the Gulf Stream and its rings on the physics, chemistry, and biology of the Middle Atlantic Bight shelf and slope from CMV *Oleander*. In *Frontiers in Ocean Observing: Marine Protected Areas, Western Boundary Currents, and the Deep Sea*. E.S. Kappel, V. Cullen, G. Coward, I.C.A. da Silveira, C. Edwards, T. Morris, and M. Roughan, eds, *Oceanography* 38(Supplement 1):54–60, https://doi.org/10.5670/oceanog.2025e108.

Archer, M.R., S.R. Keating, M. Roughan, W.E. Johns, R. Lumpkin, F.J. Beron-Vera, and L.K. Shay. 2018. The kinematic similarity of two western boundary currents revealed by sustained high-resolution observations. *Geophysical Research Letters* 45:6,176–6,185, https://doi.org/10.1029/2018GL078429.

Beal, L., and S. Elipot. 2016. Broadening not strengthening of the Agulhas Current since the early 1990s. *Nature* 540:570–573, https://doi.org/10.1038/nature19853.

Calado, L., I.C.A. Da Silveira, A. Gangopadhyay, and B.M. De Castro. 2010. Eddy-induced upwelling off Cape São Tomé (22°S, Brazil). *Continental Shelf Research* 30(10-11):1,181–1,188, https://doi.org/10.1016/j.csr.2010.03.007.

Chandler, M., N.V. Zilberman, and J. Sprintall. 2022. Seasonal to decadal western boundary current variability from sustained ocean observations. *Geophysical Research Letters* 49:e2022GL097834, https://doi.org/10.1029/2022GL097834.

Cronin, M.F., N.D. Anderson, D. Zhang, P. Berk, S.M. Wills, Y. Serra, C. Kohlman, A.J. Sutton, M.C. Honda, Y. Kawai, and others. 2023. PMEL Ocean Climate Stations as reference time series and research aggregate devices. *Oceanography* 36(2–3):46–53, https://doi.org/10.5670/oceanog.2023.224.

Ferreira, T.P., P. Marangoni G.M.P., M. Cirano, A.M. Paiva, S.B.O. Cruz, P.P. Freitas, M. Goes, and M.M. Mata. 2025. Twenty years monitoring the Brazil Current along the NOAA AX97 high-density XBT transect. In *Frontiers in Ocean Observing: Marine Protected Areas, Western Boundary Currents, and the Deep Sea*. E.S. Kappel, V. Cullen, G. Coward, I.C.A. da Silveira, C. Edwards, T. Morris, and M. Roughan, eds, *Oceanography* 38(Supplement 1):61–66, https://doi.org/10.5670/oceanog.2025e113.

Goni, G.J., J. Sprintall, F. Bringas, L. Cheng, M. Cirano, S. Dong, R. Domingues, M. Goes, H. Lopez, R. Morrow, and others. 2019. More than 50 years of successful continuous temperature section measurements by the Global Expendable Bathythermograph Network, its integrability, societal benefits, and future. *Frontiers in Marine Science* 6:452, https://doi.org/10.3389/fmars.2019.00452.

Gwyther, D., C. Kerry, M. Roughan, and S. Keating. 2022. Observing system simulation experiments reveal that subsurface temperature observations improve estimates of circulation and heat content in a dynamic western boundary current. *Geoscientific Model Development* 15:6,541–6,565, https://doi.org/10.5194/gmd-15-6541-2022.

Gwyther, D., S. Keating, C. Kerry, and M. Roughan. 2023a. How does 4DVar data assimilation affect the vertical representation of mesoscale eddies? A case study with OSSEs using ROMS v3.9. *Geoscientific Model Development* 16:157–178, https://doi.org/10.5194/gmd-16-157-2023.

Gwyther, D., M. Roughan, C. Kerry, and S. Keating. 2023b. Impact of assimilating repeated subsurface temperature transects on state estimates of a western boundary current. *Frontiers in Marine Science* 9:1084784, https://doi.org/10.3389/fmars.2022.1084784.

Hu, S., L. Liu, C. Guan, L. Zhang, J. Wang, Q. Wang, J. Ma, F. Wang, F. Jia, J. Feng, and others. 2020. Dynamic features of near-inertial oscillations in the northwestern Pacific derived from mooring observations from 2015 to 2018. *Journal of Oceanology and Limnology* 38:1,092–1,107, https://doi.org/10.1007/s00343-020-9332-1.

Imawaki, S., A.S. Bower, L. Beal, and B. Qiu. 2013. Western boundary currents. Pp. 305–338 in *Ocean Circulation and Climate: A 21st Century Perspective*. G. Siedler, S. Griffies, J. Gould, and J. Church, eds, Academic Press.

Jakoboski, J., M. Roughan, J. Radford, J. de Souza, M. Felsing, R. Smith, N. Puketapu-Waite, M. Montano Orozco, K.H. Maxwell, and C. Van Vranken. 2024. Partnering with the commercial fishing sector and Aotearoa New Zealand's ocean community to develop a nationwide subsurface temperature monitoring program. *Progress in Oceanography* 225:103278, https://doi.org/10.1016/j.pocean.2024.103278.

Lago, V., M. Roughan, C. Kerry, and I. Knuckey. 2025. Fishing for ocean data in the East Australian Current. In *Frontiers in Ocean Observing: Marine Protected Areas, Western Boundary Currents, and the Deep Sea*. E.S. Kappel, V. Cullen, G. Coward, I.C.A. da Silveira, C. Edwards, T. Morris, and M. Roughan, eds, *Oceanography* 38(Supplement 1):67–71, https://doi.org/10.5670/oceanog.2025e105.

Li, J., M. Roughan, and C. Kerry. 2022. Drivers of ocean warming in the western boundary currents of the Southern Hemisphere. *Nature Climate Change* 12:901–909, https://doi.org/10.1038/s41558-022-01473-8.

Lumpkin, R., T. Ozgokmen, and L. Centurioni. 2017. Advances in the application of surface drifters. *Annual Review of Marine Science* 9:59–81, https://doi.org/10.1146/annurev-marine-010816-060641.

Martínez-Moreno, J., A.M. Hogg, M.H. England, N.C. Constantinou, A.E. Kiss, and A.K. Morrison. 2021. Global changes in oceanic mesoscale currents over the satellite altimetry record. *Nature Climate Change* 11:397–403, https://doi.org/10.1038/s41558-021-01006-9.

Matisons, L., M. Roughan, and A.S. Schaeffer. In press. Dispersion characteristics in the East Australian Current System: Insights from 20 years of Lagrangian drifter data. *Progress in Oceanography*.

Nagai, T., G.S. Durán, D.A. Otero, Y. Mori, N. Yoshie, K. Ohgi, D. Hasegawa, A. Nishina, and T. Kobari. 2019. How the Kuroshio Current delivers nutrients to sunlit layers on the continental shelves with aid of near-inertial waves and turbulence. *Geophysical Research Letters* 46:6,726–6,735, https://doi.org/10.1029/2019GL082680.

Roughan, M., and J.H. Middleton. 2002. A comparison of observed upwelling mechanisms off the east coast of Australia. *Continental Shelf Research* 22(17):2,551–2,572, https://doi.org/10.1016/S0278-4343(02)00101-2.

Schaeffer, A., and M. Roughan. 2015. Influence of a western boundary current on shelf dynamics and upwelling from repeat glider deployments. *Geophysical Research Letters* 42(1):121–128, https://doi.org/10.1002/2014GL062260.

Schmid, C., and S. Majumder. 2018. Transport variability of the Brazil Current from observations and a data assimilation model. *Ocean Science* 14:417–436, https://doi.org/10.5194/os-14-417-2018.

Sloyan, B.M., K.R. Ridgway, and R. Cowley. 2016. The East Australian Current and property transport at 27°S from 2012 to 2013. *Journal of Physical Oceanography* 46(3):993–1,008, https://doi.org/10.1175/JPO-D-15-0052.1.

Sloyan, B.M., R. Cowley, and C.C. Chapman. 2024. East Australian Current velocity, temperature and salinity data products. *Scientific Data* 11:10, https://doi.org/10.1038/s41597-023-02857-x.

Todd, R.E., F.P. Chavez, S. Clayton, S. Cravatte, M. Goes, M. Graco, X. Lin, J. Sprintall, N.V. Zilberman, M. Archer, and others. 2019. Global perspectives on observing ocean boundary current systems. *Frontiers in Marine Science* 6:423, https://doi.org/10.3389/fmars.2019.00423.

Wei, J., D.-P. Wang, and C.N. Flagg. 2008. Mapping Gulf Stream warm core rings from shipboard ADCP transects of the Oleander Project. *Journal of Geophysical Research: Oceans* 113(C10), https://doi.org/10.1029/2007JC004694.

Wijffels, S.E., G. Gebbie, and P.E. Robbins. 2024. Resolving the ubiquitous small-scale semipermanent features of the general ocean circulation: A multiplatform observational approach. *Journal of Physical Oceanography* 54:2,503–2,521, https://doi.org/10.1175/JPO-D-23-0225.1.

Wu, L., W. Cai, L. Zhang, H. Nakamura, A. Timmermann, T. Joyce, M.J. McPhaden, M. Alexander, B. Qiu, M. Visbeck, and others. 2012. Enhanced warming over the global subtropical western boundary currents. *Nature Climate Change* 2:161–166, https://doi.org/10.1038/nclimate1353.

Yang, H., G. Lohmann, W. Wei, M. Dima, M. Ionita, and J. Liu. 2016. Intensification and poleward shift of subtropical western boundary currents in a warming climate. *Journal of Geophysical Research: Oceans* 121:4,928–4,945, https://doi.org/10.1002/2015JC011513.

ACKNOWLEDGMENTS

This research is supported by an Australian Research Council Discovery Project (DP230100505), the Fundamental Research Funds for the Central Universities, China (B240201133), the Open Fund Project of Key Laboratory of Marine Environmental Information Technology, Ministry of Natural Resources of the People's Republic of China (523060012), and the Jiangsu Specially-Appointed Professor (B1203524).

AUTHORS

Moninya Roughan, Coastal and Regional Oceanography Lab, School of Biological Earth and Environmental Sciences, University of New South Wales, Sydney, NSW, Australia. **Junde Li** (junde.li@unsw.edu.au), College of Oceanography, Hohai University, Nanjing, China, and Coastal and Regional Oceanography Lab, School of Biological Earth and Environmental Sciences, University of New South Wales, Sydney, NSW, Australia. **Tamaryn Morris**, Egagasini Node, South African Environmental Observation Network, Cape Town, South Africa.

ARTICLE DOI. https://doi.org/10.5670/oceanog.2025e116

MONITORING IMPACTS OF THE GULF STREAM AND ITS RINGS ON THE PHYSICS, CHEMISTRY, AND BIOLOGY OF THE MIDDLE ATLANTIC BIGHT SHELF AND SLOPE FROM CMV *OLEANDER*

By Magdalena Andres, Thomas Rossby, Eric Firing, Charles Flagg, Nicholas R. Bates, Julia Hummon, Denis Pierrot, Timothy J. Noyes, Matthew P. Enright, Jeffery K. O'Brien, Rebecca Hudak, Shenfu Dong, D. Christopher Melrose, David G. Johns, and Lance Gregory

ABSTRACT

Sustained observation is key to measuring physical and ecological variability in the Northwest Atlantic. Here we illustrate how a partnership with a merchant marine container vessel in service between New Jersey and Bermuda twice per week gives scientists a unique window into upper ocean currents, water properties, and marine ecology. Scientific observations collected from CMV *Oleander*, operated by Bermuda Container Line/Neptune Group, enable cross-disciplinary research, complement satellite measurements, and contribute to global observing programs—including the Global eXpendable BathyThermograph (XBT) Network, the Surface Ocean CO_2 Atlas (SOCAT), and the Continuous Plankton Recorder (CPR) Survey. Recent co-located measurements along the Oleander Line document that fronts in temperature, salinity, and carbon dioxide concentrations align with the (sub)mesoscale circulation patterns. The sustained observations show warming and shrinking of the Slope Sea, a northward shift of the Gulf Stream, and warming of the "18°C water" (subtropical North Atlantic mode water) to 19°C.

THE NORTHWEST ATLANTIC

Circulation in the Northwest Atlantic is dominated by the Gulf Stream, a subtropical western boundary current whose warm, salty waters course along the continental slope of the southeastern United States in a narrow (~100 km width), intense jet that serves both to close the wind-driven gyre and to carry the warm limb of the Atlantic Meridional Overturning Circulation poleward. After passing Cape Hatteras, North Carolina, the deep-reaching Gulf Stream begins to meander, serving both as a moving boundary between the water masses, ecosystems, and chemical regimes of the Slope and Sargasso Seas (Figure 1a) and as a locus of air-sea exchange that drives intense regional wintertime cooling (Joyce et al., 2013) and uptake of atmospheric carbon dioxide (Nickford et al., 2024).

Warm and cold core rings are intermittently shed from Gulf Stream meander crests and troughs, respectively, and drive transport across the sharp front that separates the deep thermocline (~800 m depth) and salty, warm oligotrophic Sargasso Sea waters to the south from the shallow thermocline (~200 m depth) and relatively cooler, fresher

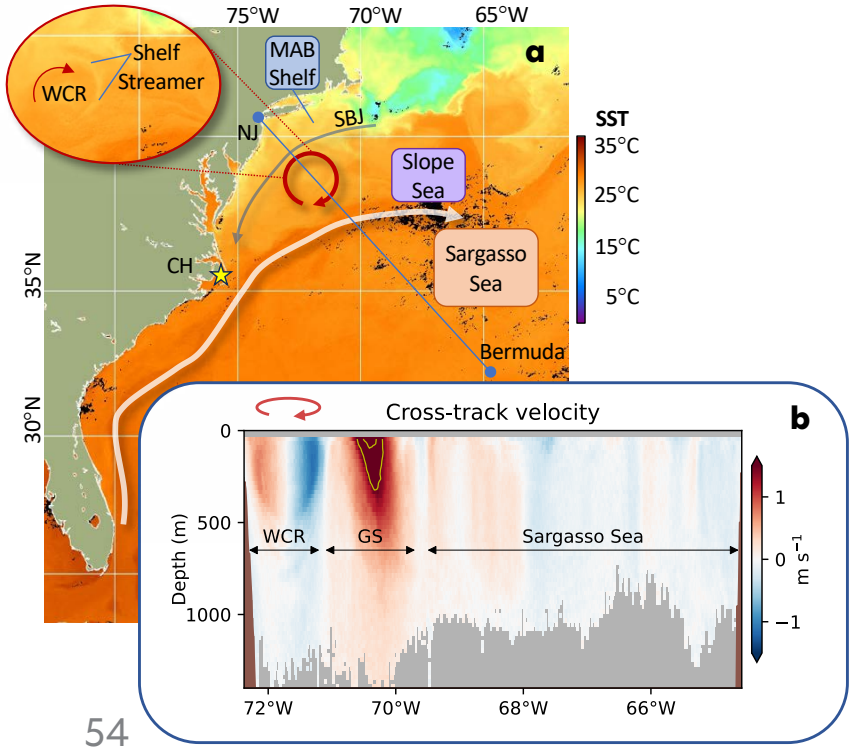

FIGURE 1. (a) Schematic of Northwest Atlantic circulation superimposed on a composite sea surface temperature (SST) map produced by NOAA from the Advanced Very High Resolution Radiometer and the Visible Infrared Imaging Radiometer Suite (AVHRRR/VIIRS) merged from July 23–26, 2021. The inset shows a close-up of a warm core ring (WCR) with a streamer of cooler (and fresher) waters from the Middle Atlantic Bight (MAB) shelf wrapping around the anticyclonic ring. (b) Cross-track component of ocean velocity (heading 47°) measured during the concurrent Bermuda-bound CMV *Oleander* transit with an Ocean Surveyor 38 kHz ADCP (OS38), with the 1.5 m s^{-1} and 2.0 m s^{-1} isolines (yellow) and bathymetry (shaded brown). Gray shaded regions have less than 30% good data returns. The WCR is deep reaching and surface intensified: ~16 Sv is being circulated within the upper 1,000 m of the ring, and most of this (88%) is concentrated in the upper 500 m. The Gulf Stream is carrying ~81.6 Sv (integrated from the surface to 1,000 m depth and from 71.1°W to 69.6°W).

Slope Sea waters to the north. Rings influence biological (Hare et al., 2002) and chemical (Conway et al., 2018) distributions as well as air-sea fluxes (Silver et al., 2021).

Warm core rings, which carry Sargasso Sea waters into the Slope Sea, are deep-reaching and cannot move directly onto the shallow Middle Atlantic Bight (MAB) shelf (Figure 1b). They do, however, interact with the upper slope and outer shelf through ageostrophic processes that impact the Shelfbreak Jet (Forsyth et al., 2022) and that exchange waters across the shelf break (e.g., Zhang and Gawarkiewicz, 2015; Gawarkiewicz et al., 2022). The Gulf Stream also sheds warm filaments called "shingles" (von Arx et al., 1955) into the Slope Sea. The formation, evolution, and impacts of individual shingles, rings, the Shelfbreak Jet, and other (sub)mesoscale circulation features can be difficult to capture with the limited temporal and spatial resolution of satellite observations and intermittent cloud cover. Underway in situ measurements from ships can complement satellites with their high along-track resolution and critical subsurface measurements.

Since the 1970s, scientific equipment has been hosted on three different container ships operating consecutively on the "Oleander Line," a longstanding route between Elizabeth, New Jersey, and Hamilton, Bermuda. The operation on the first two vessels and key results from 25 years of velocity and 40 years of temperature measurements are summarized in Rossby et al. (2019), with the historical data (see The Oleander Project website) and derived products (Forsyth et al., 2020a, 2020b) available.

SCIENTIFIC SENSORS ON THE NEW CMV *OLEANDER*

The newest CMV *Oleander* came into service in 2019 with some scientific infrastructure and sensors already installed, and additional equipment was installed and commissioned upon the ship's first drydock in early 2024. The vessel is now providing water column, sea surface, and atmospheric measurements along the Oleander Line (Figure 2).

Measurements include discrete profiles of upper ocean temperatures along the transect. Since late 2020, 48 eXpendable BathyThermograph (XBT) probes have been launched monthly using an Autonomous eXpendable Instrument System (AXIS; Fratantoni et al., 2017). Near-real-time profiles are transmitted via the Iridium satellite network, and after quality control, complete temperature sections are posted on the project's ERRDAP server and on the XBT project's website.

Velocity profiles and acoustic backscatter intensity to ~200 m depth are continuously recorded during each crossing with a 150 kHz acoustic Doppler current profiler (ADCP). Individual pings are five-minute averaged to give profiles with along-track resolution of about 2 km. A sample of the ADCP data is sent to shore daily via Starlink to monitor system performance, and the full dataset is downloaded during each port call. Velocity sections have been collected biweekly since October 2023 and are available here.

CMV *Oleander* is equipped with an underway scientific seawater line. The intake, located at ~5.8 m depth, supplies flow-through instrumentation that measures near-surface temperature and salinity. There is a newly installed (since 2024) carbon dioxide (CO_2) system for measuring partial pressure and fugacity of CO_2 (pCO_2 and fCO_2) in surface seawater and boundary layer air, with other sensors occasionally measuring alkalinity and pH. In addition, underway near-surface atmospheric data are recorded with a weather station. The underway data are recorded at 1–4 Hz (except for pCO_2, which is recorded every two minutes) and are transmitted to shore via Starlink at 10-minute intervals.

Each month, the ship tows a Continuous Plankton Recorder (CPR) at ~10 m depth to sample plankton in the upper water column with a 280-micron mesh gauze. CPR cartridges are returned to shore after three or four months and are analyzed to identify and count organism taxa and, where possible, species. The gauze is cut into slices representing ~10 nautical miles of tow, with each slice sampling roughly 3 m^3 of seawater. To avoid potential interference between the XBT probes and the towed body, the monthly CPR and XBT sections are generally conducted during separate crossings.

Two recently funded pilot programs will expand the underway biological sampling. A biomolecular autosampler, the Robotic Cartridge Sampling Instrument (RoCSI), and an Imaging FlowCytobot (IFCB) will be connected to the scientific seawater line in 2025. The autosampler will preserve water samples for environmental DNA metabarcoding to assess biodiversity and monitor ecosystems across marine gradients (Adams et al., 2023). The IFCB will provide size- and taxon-resolved concentrations of phytoplankton and their biomasses (Sosik and Olsen, 2007).

USING *OLEANDER* DATA TO STUDY PROCESSES ACROSS SPATIAL AND TEMPORAL SCALES

ALONG-TRACK VARIABILITY

Concurrent measurements from CMV *Oleander*'s scientific sensors underscore the interplay of ocean physics, chemistry, and biology at temporal scales spanning events to seasons and spatial scales spanning shingles to regional recirculation cells. For example, velocity profiles recorded during the transit on August 3–4, 2024, provide context for the along-track property distributions (Figure 3). The vessel crossed a ~200 m thick Gulf Stream shingle in the Slope Sea and a deep-reaching cyclonic cold core ring (CCR) in

the Sargasso Sea. In this late summer section, heating has muted near-surface temperature contrasts, so the shingle is only slightly warmer than the ambient Slope Sea waters, and the CCR does not stand out as particularly cold relative to the Sargasso Sea. However, near-surface salinities combined with the subsurface temperature profiles (with the 12°C isotherm used to identify the depth of the thermocline) clearly delineate fronts that align with the submesoscale (shingle) and mesoscale (CCR and Gulf Stream) circulation features.

The correspondence between these circulation features and the along-track variability in fCO_2 is striking. The core of the fresh, cyclonic CCR stands out as a region of elevated fCO_2 (450 µatm) within the otherwise lower fCO_2 waters of the surrounding Sargasso Sea (i.e., the oligotrophic subtropical gyre of the North Atlantic Ocean). The salty shingle in the Slope Sea, which grows westward as it continues to draw waters from the eastward-flowing Gulf Stream, has lower fCO_2 (440 µatm) and, like the Gulf Stream, is more saline than the ambient Slope Sea. The addition of other CO_2 sensors will clarify whether the CCR is similar to Slope Sea waters, with higher fCO_2 resulting from a higher dissolved inorganic carbon (DIC) to alkalinity ratio, and potentially the contribution of vertical mixing upward of DIC water into the CCR. Concurrent satellite ocean color measurements (see inset to Figure 3a) of chlorophyll *a* (chl-*a*) show that—in contrast to the core of the Gulf Stream, which has low chl-*a* (~0.1 mg m^{-3})—the shingle is associated with a filament of elevated chl-*a* (~0.3 mg m^{-3}), suggesting biophysical interactions rather than simple horizontal advection of

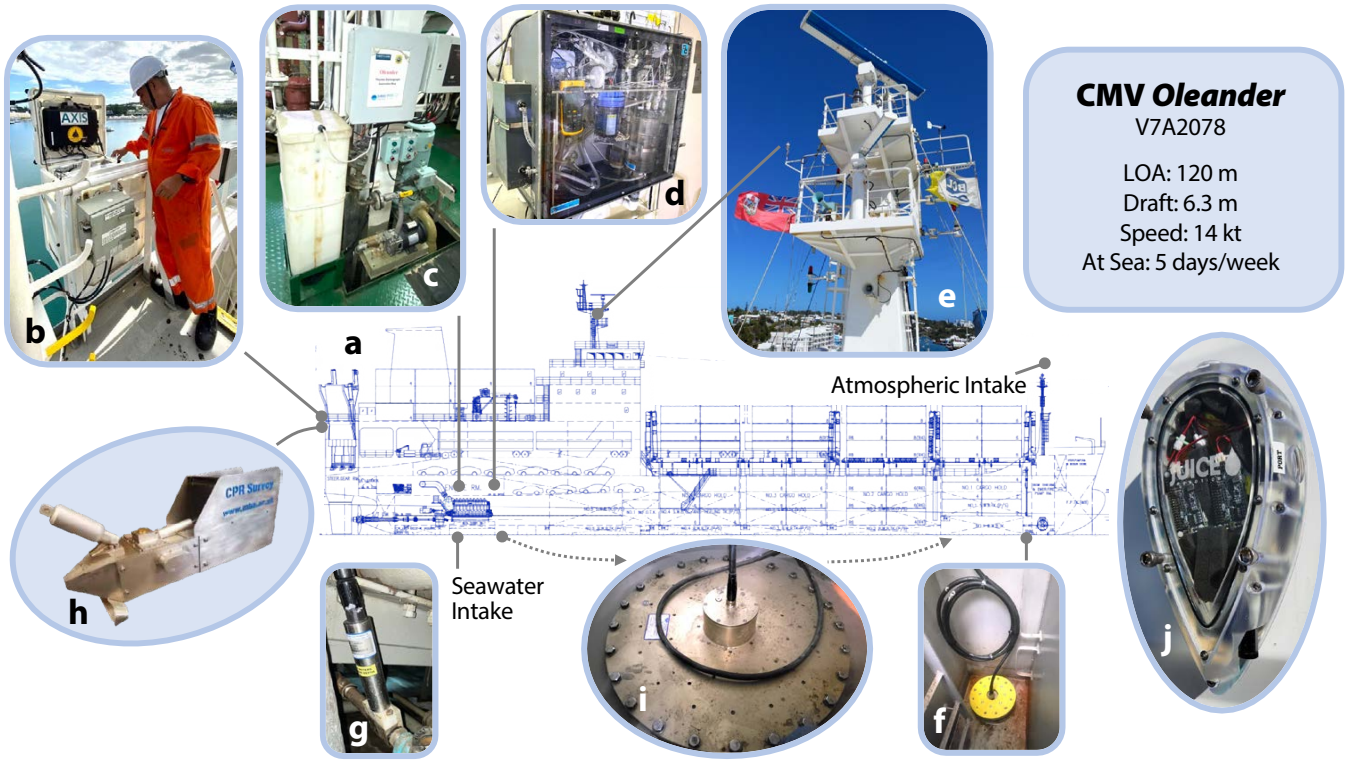

FIGURE 2. (a) General arrangement drawing of the new CMV *Oleander* showing ship configuration and oceanographic sensors. (b) The Autonomous eXpendable Instrument System (AXIS) on the stern being reloaded with Global eXpendable BathyThermograph (XBT) probes. (c) Underway scientific seawater system in the engine room. (d) Sea-Bird SBE45 TSG for recording seawater salinity (left) and General Oceanics 8050 pCO_2 Measuring System (right), with a LICOR 7000 analyzer calibrated every two to three hours with four standard gases with concentrations ranging from 0 ppm to 470 ppm traceable to the World Meteorological Organization (WMO) scale. (e) Vaisala WXT536 weather sensor mounted on the flybridge mast to measure air temperature, humidity, sea level pressure, rainfall, and wind speed and direction. (f) Hull-mounted Teledyne RD Instruments 150 kHz Ocean Surveyor ADCP (OS150) with a 3/8-inch-thick polycarbonate acoustic window for protection. (g) Sea-Bird SBE38 temperature probe near the seawater intake to provide near-surface ocean temperature before the seawater pipes pass through the hot engine room. (h) Continuous Plankton Recorder (CPR), which is lowered by the crew using the ship's mooring winch for towing behind the vessel. Not shown are the GPS and ABXTWO antennas used for accurate ship position and heading to calculate ocean velocities. (i) The Ocean Surveyor 38 kHz ADCP (OS38), installed during the ship build, has only rarely given good velocity sections, with some profiles reaching beyond 1,000 m depth (e.g., Figure 1b). The OS38 was removed during the January 2024 drydock and will be reinstalled in a forward location with less bubble noise and with a 1½ inch acoustic window for protection. The new site was chosen based on analysis of videos of the bubble field using (j) the commercially available, hull-mounted Remora system with programmable forward- and side-facing cameras built by Juice Robotics LLC. This magnetically mounted camera system was installed by commercial divers for two transits in fall 2023 to help identify the locations of bubble clouds entrained under the vessel that can cause noise in ADCP measurements.

Gulf Stream water masses by the shingle. Because these features are long-lived compared to *Oleander* sampling intervals, it will be possible to examine the plankton distributions within these features as sampled by the CPR, which was towed on the previous Bermuda-bound transit on July 27–28, 2024, once the cartridge is returned to shore. The concurrent underway data (near-surface salinity and velocity profiles) will help identify the exact locations of the fronts and circulation features during that transect (which marked the 535th CPR tow from an *Oleander*).

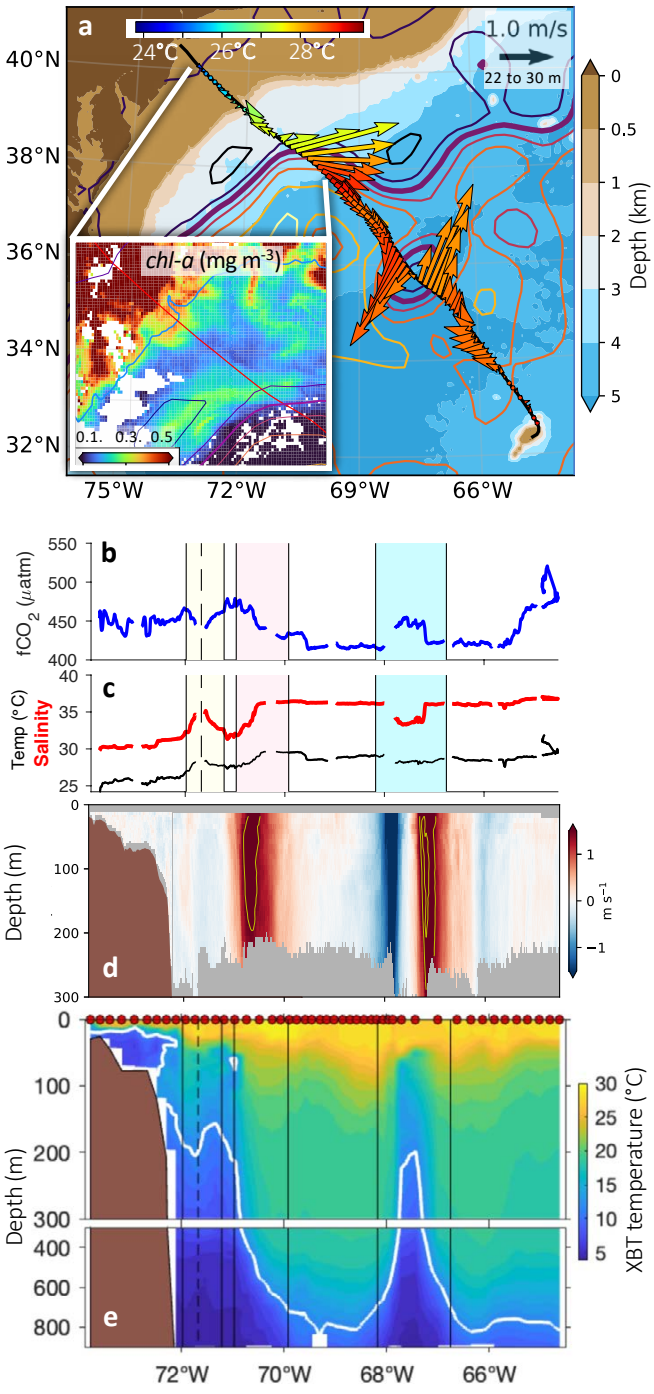

The (sub)mesoscale variability of fCO_2 in the along-track data is superimposed on strong regional-scale contrasts between waters of the coastal Middle Atlantic Bight (~450 µatm), the Slope Sea (~470 µatm), the Sargasso Sea (~420 µatm), and those north of Bermuda (~430–470 µatm) with the waters on the Bermuda reef and lagoon (>490 µatm). While it is known that the assemblages of plankton species in the Sargasso Sea and Slope Sea vary, and that rings can host species not found in surrounding waters, a thorough comparison of the circulation features with the plankton survey and with underway near-surface data (including fCO_2) in this and other sections remains to be undertaken.

LONG-TERM CHANGES

The observations along the Oleander Line resolve seasonal and interannual variability superimposed on long-term changes on the Middle Atlantic Bight shelf and within the Shelfbreak Jet (Forsyth et al., 2015). Here we show that the measurements also capture significant changes in the open ocean, including warming and low frequency shifts in Gulf Stream position. These changes are in contrast to Gulf Stream transport, which is relatively stable at the Oleander Line (e.g., Rossby et al., 2019), consistent with sustained observations of this western boundary current 1,500 km upstream in the Florida Straits (Volkov et al., 2024).

In the Slope Sea, warming from the surface to 750 m depth spanning the last 86 years (1937–2023) is evident from temperature profiles along the Oleander Line between 39.2°N and 38.4°N, averaged over three different epochs (Figure 4a). Profiles that sampled a warm core ring or a Gulf Stream meander crest can be identified by

FIGURE 3. Observations spanning August 3–4, 2024. (a) Near-surface velocity vectors (averaged from 22 m to 30 m depth) from the Teledyne RD Instruments 150 kHz Ocean Surveyor ADCP (OS150). Colors, superimposed on bathymetry (shading), indicate temperature as measured internally. The inset shows chl-*a* from NOAA's Sentinel-3A-OLCI for August 2, 2024, with the CMV *Oleander* route plotted in red and the 200 m isobath in blue. Sea surface height contours for August 3, 2024, are also plotted based on mapped satellite altimetry from Copernicus Marine Service product SEALEVEL_GLO_PHY_L4_NRT_008_046 contoured at 0.25 m intervals, with the 0.25 m contour highlighted as a proxy for the Gulf Stream core (thick purple). (b) Underway fCO_2 with the shingle (yellow), Gulf Stream (pink), and cold core ring (blue) highlighted. (c) Underway near-surface salinity (thick, red) and temperature (thin, black) with shading as in (b). (d) Cross-track velocity profiles (heading 47°) with the 1.5 m s^{-1} and 2.0 m s^{-1} isolines (yellow) highlighted. (e) Temperature section in the upper (surface to 300 m depth) and mid-depth (300–900 m) water column, as observed with XBT probes launched by AXIS at the locations indicated by red dots at the surface, with the 12°C (white) and boundaries of the circulation features noted above (vertical lines).

the shape of the temperature profile and are excluded from the averaging to isolate changes within ambient Slope Sea waters. The mean temperature profiles demonstrate significant, surface-intensified warming of the Slope Sea that is consistent with other studies and is concentrated in the last three decades. Because the number of warm core rings shed annually by the Gulf Stream doubled after 2000 (Gangopadhyay et al., 2019), this upper-ocean warming likely reflects the cumulative effect of mixing of Gulf Stream and Sargasso Sea waters into the ambient Slope Sea by dissipation of warm core rings, which, as noted earlier (Figure 1b), extend to ~750 m depth.

In concert with this warming, the Slope Sea is also shrinking. Oleander velocity sections demonstrate that its southern boundary, the Gulf Stream, has shifted northward by about 50 km (0.5° latitude) since the early 1990s (Figure 4b), with its position identified in each ADCP transect by the latitude of the velocity maximum at 55 m depth. This gradual northward shift and the strong lateral position changes evident in the 1990s and early 2000s may reflect variations in dense water formation and export from the Labrador Sea (e.g., Bisagni et al., 2017).

Temperature profiles from the Sargasso Sea along the Oleander Line between 33°N and 35°N show warming at 300 m depth, with a rather sudden 0.5ºC increase in the mean around 2015 (red, Figure 4c). Warming at this depth reflects change in the subtropical mode water, which used to be called "18°C water" (e.g., Joyce et al., 2013), but which is now 19°C. This change may reflect warmer winters in the mode water formation regions. In contrast, temperatures at 800 m depth show no trend or step change but do show substantial scatter. This scatter, possibly due to internal waves, is not unexpected, as this is the depth of the main thermocline in the Sargasso Sea, and the 1°C standard deviation in temperature here corresponds to about 40 m of thermocline heave.

GLOBAL OBSERVING PROGRAMS

The Global XBT Network provides repeated upper ocean (0–900 m) temperature measurements along fixed transects at eddy-resolving scales in regions critical for monitoring and understanding upper ocean dynamical and thermodynamic processes. Deployment of XBTs began in the 1960s, and data collected from XBTs became the largest contributor to the upper ocean thermal record during the 1970s–1990s. Since initiation of the Argo array in 1999 to sample the ocean interior, the focus of the XBT network has been to monitor boundary currents, gyre circulation, and meridional transport of heat and mass from trans-basin sections (e.g., Goni et al., 2019). Some XBT transects have been occupied continuously for more than 30 years, providing an unprecedented long-term climate record at spatial

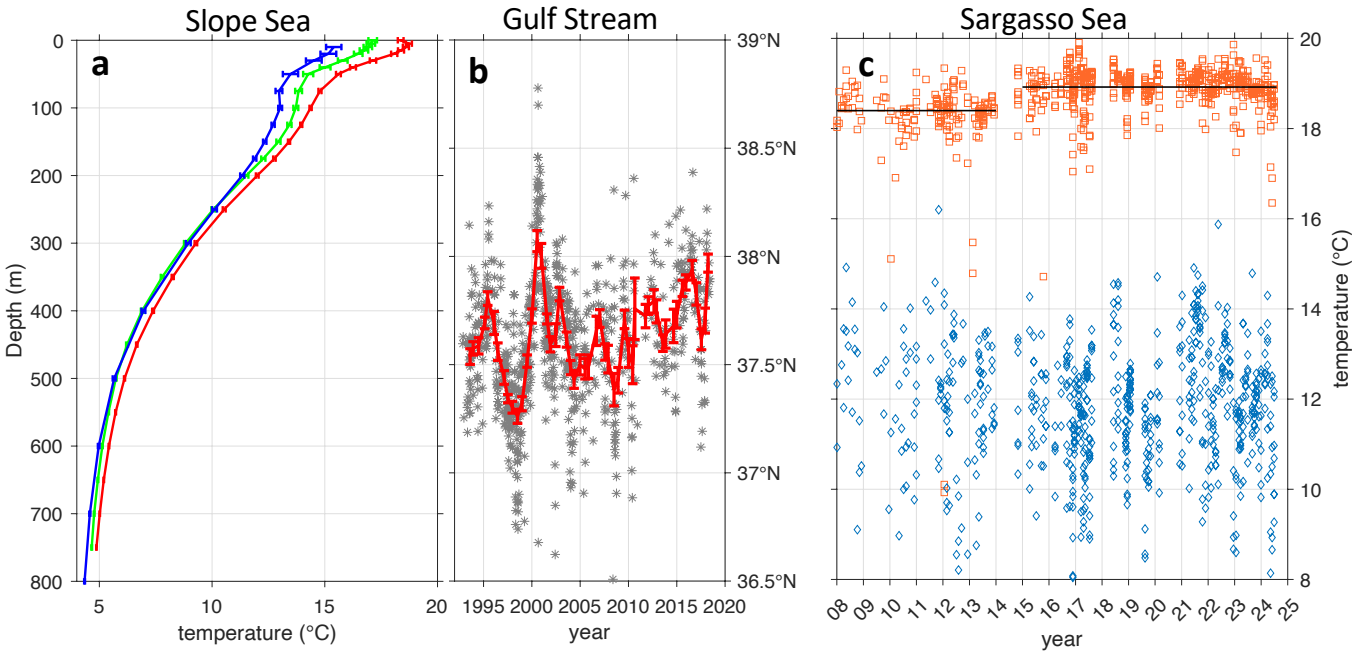

FIGURE 4. Long-term changes in the Northwest Atlantic. (a) Deseasoned and spatially averaged temperature profiles and mean standard errors (horizontal bars) from the Slope Sea for 1937–1940, (blue) from 35 hydrocasts (Iselin, 1940), (green) from 147 XBT profiles collected from 1994 to 2003, and (red) from 284 XBT profiles made during 2014–2023. (b) Latitude of maximum velocity of the meandering Gulf Stream as measured during individual transits (gray stars), with the annual average stepped every six months superimposed (red). (c) Temperature at 300 m depth (red squares) and 800 m depth (blue diamonds) from XBT profiles taken within the Sargasso Sea. Horizontal black lines show time averages at 300 m depth.

and temporal scales that remains unmatched by other observing platforms. XBT profiles have been collected from CMV *Oleander* (referred to as transect AX32) for nearly 50 years. Starting in 1977, data were mainly collected in the Middle Atlantic Bight shoreward of the Gulf Stream. Since 2009, XBTs have been deployed along the entire section with resolution varying from 15 km within the Gulf Stream to 25–50 km in the ocean interior.

The pCO_2 system and associated sensors aboard CMV *Oleander* allow for evaluation of surface seawater CO_2-carbonate chemistry and air-sea CO_2 gas exchange over weekly, seasonal, and longer timescales, and across different ocean regions. Such data collection is important for understanding physical and biogeochemical variability at the Bermuda Atlantic Time-series Study (BATS) site (1988 to present; Bates and Johnson, 2023) near the island of Bermuda. The pCO_2 data contribute to the international Surface Ocean CO_2 Atlas (SOCAT) effort, which provides the scientific community with a global, quality-controlled dataset and gridded product every year (e.g., Bakker et al., 2022). This product in turn contributes to annual global carbon budget analyses (Friedlingstein et al., 2023). It is also the source of multiple other products and publications. The CMV *Oleander* dataset provides unmatched coverage (100 transects/year) that is uniquely suited to help quality control other regional data sets.

The CPR Survey, established in 1931, seeks to observe the location and abundance of plankton globally. Sampling from ships running southeastward from New Jersey toward Bermuda—referred to as the MB route—began in 1976, with CMV *Oleander* recruited in 1981 (Jossi et al., 2003). Operations, initially managed by NOAA Fisheries, are now carried out by the Marine Biological Association (e.g., Helaouet et al., 2024).

FUTURE OCEAN OBSERVING

The long-standing cooperation between scientists and the Bermuda Container Line/Neptune Group serves as a model for advancing a sustained global observing system that also resolves local and regional processes. Science Research on Commercial Ships (Science RoCS) aims to emulate this enduring partnership on a broad scale (Macdonald et al., 2024), including with the use of ADCPs (Ocean Scope Working Group, 2012), by engaging ship owners and operators. The industry has signaled that it is willing to help as scientists seek to expand their ability to collect sustained observations of the atmosphere and upper ocean waters to advance science and address pressing global challenges. With its integrated system of scientific sensors, CMV *Oleander* serves as an interdisciplinary observatory in the Northwest Atlantic that can be replicated elsewhere to aid oceanographers who have only limited access to the seas. The successes of *Oleander*'s operation over the last 50 years demonstrate that partnering with the merchant marine can greatly increase this access.

REFERENCES

Adams, C.I.M., G.-J. Jeunen, H. Cross, H.R. Taylor, A. Bagnaro, K. Currie, C. Hepburn, N.J. Gemmell, L. Urban, F. Balter, and others. 2023. Environmental DNA metabarcoding describes biodiversity across marine gradients. *ICES Journal of Marine Science* 80:953–971, https://doi.org/10.1093/icesjms/fsad017.

Bakker, D.C.E., S.R. Alin, M. Becker, H.C. Bittig, R. Castaño-Primo, R.A. Feely, T. Gkritzalis, K. Thanos, K. Koji, A. Kozyr, and others. 2022. Surface Ocean CO_2 Atlas Database Version 2022 (SOCATv2022) (NCEI Accession 0253659), NOAA National Centers for Environmental Information, https://par.nsf.gov/biblio/10409726.

Bates, N.R., and R.J. Johnson. 2023. Forty years of ocean acidification observations (1983–2023) in the Sargasso Sea at the Bermuda Atlantic Time-series Study site. *Frontiers in Marine Science* 10:1289931, https://doi.org/10.3389/fmars.2023.1289931.

Bisagni, J.J., A Gangopadhyay, and A. Sanches-Franks. 2017. Secular change and inter-annual variability of the Gulf Stream position, 1993–2013, 70°– 55°W. *Deep Sea Research Part I* 125:1–10, https://doi.org/10.1016/j.dsr.2017.04.001.

Conway, T.M., J.B. Palter, and G.F. de Souza. 2018. Gulf Stream rings as a source of iron to the North Atlantic subtropical gyre. *Nature Geosciences* 11:594–598, https://doi.org/10.1038/s41561-018-0162-0.

Forsyth, J.S.T., M. Andres, and G.G. Gawarkiewicz. 2015. Recent accelerated warming of the continental shelf off New Jersey: Observations from the CMV *Oleander* expendable bathythermograph line. *Journal of Geophysical Research Oceans* 120:2,370–2,384, https://doi.org/10.1002/2014JC010516.

Forsyth, J., M. Andres, and G. Gawarkiewicz, 2020a. Gridded Oleander ADCP Data [Velocity Data set]. Zenodo, https://doi.org/10.5281/zenodo.3935983.

Forsyth, J., M. Andres, and G. Gawarkiewicz. 2020b. Gridded Oleander XBT Data [Temperature Data set]. Zenodo, https://doi.org/10.5281/zenodo.3967332.

Forsyth, J., G. Gawarkiewicz, and M. Andres. 2022. The impact of warm core rings on Middle Atlantic Bight shelf temperature and shelf break velocity. *Journal of Geophysical Research: Oceans* 127:e2021JC017759, https://doi.org/10.1029/2021JC017759.

Fratantoni, D., J. O'Brien, C. Flagg, and T. Rossby. 2017. AXIS: An Autonomous eXpendable Instrument System. *Journal of Atmospheric and Oceanic Technology* 34:2,673–2,682, https://doi.org/10.1175/JTECH-D-17-0054.1.

Friedlingstein, P., M. O'Sullivan, M.W. Jones, R.M. Andrew, D.C.E. Bakker, J. Hauck, P. Landschützer, C. Le Quéré, I.T. Luikxz, G.P. Peters, and others. 2023. Global carbon budget 2023. *Earth System Science Data* 15:5,301–5,369, https://doi.org/10.5194/essd-15-5301-2023.

Gangopadhyay, A., G. Gawarkiewicz, E.N.S. Silva, M. Monim, and J. Clark. 2019. An observed regime shift in the formation of warm core rings from the Gulf Stream. *Scientific Reports* 9:12319, https://doi.org/10.1038/s41598-019-48661-9.

Gawarkiewicz, G., P. Fratantoni, F. Bahr, and A. Ellertson. 2022. Increasing frequency of mid-depth salinity maximum intrusions in the Middle Atlantic Bight. *Journal of Geophysical Research: Oceans* 127:e2021JC018233, https://doi.org/10.1029/2021JC018233.

Goni, G., J. Sprintall, F. Bringas, L. Cheng, M. Cirano, S. Dong, R. Domingues, M. Goes, H. Lopez, R. Morrow, and others. 2019. More than 50 years of successful continuous temperature section measurements by the Global Expendable Bathythermograph Network, its integrability, societal benefits, and future. *Frontiers in Marine Science* 6:452, https://doi.org/10.3389/fmars.2019.00452.

Hare, J.A., J.H. Churchill, R.K. Cowen, T.J. Berger, P.C. Cornillon, P. Dragos, S.M. Glenn, and J.J. Govini. 2002. Routes and rates of larval fish transport from the southeast to the northeast United States continental

shelf. *Limnology and Oceanography* 47:1,774–1,789, https://doi.org/10.4319/lo.2002.47.6.1774.

Helaouet, P., L. Sheppard, and D. Johns. 2024. Continuous Plankton Recorder phytoplankton and zooplankton occurrence and count data from The CPR Survey in the Western North Atlantic Ocean from 1958 to 2021 (Version 4) [Data set]. Biological and Chemical Oceanography Data Management Office (BCO-DMO), https://doi.org/10.26008/1912/BCO-DMO.765141.4.

Iselin, C.O'D. 1940. Preliminary report on long-period variations in the transport of the Gulf Stream system. *Papers in Physical Oceanography and Meteorology* 8(1), https://doi.org/10.1575/1912/1048.

Joyce, T.M., L.N. Thomas, W.K. Dewar, and J.B. Girton. 2013. Eighteen degree water formation within the Gulf Stream during CLIMODE. *Deep Sea Research Part II* 91:1–10, https://doi.org/10.1016/j.dsr2.2013.02.019.

Jossi, J.W., A.W.G. John, and D. Sameoto. 2003. Continuous Plankton Recorder sampling off the east coast of North America: History and status. *Progress in Oceanography* 58:313–325, https://doi.org/10.1016/j.pocean.2003.08.010.

Macdonald, A.M., L. Hiron, L. McRaven, L. Stolp, K. Strom, R. Hudak, S. Smith, J. Hummon, and M. Andres. 2024. A framework for multidisciplinary science observations from commercial ships. *ICES Journal of Marine Science*, fsae011, https://doi.org/10.1093/icesjms/fsae011.

Nickford, S., J.B. Palter, and L. Mu. 2024. The importance of contemporaneous wind and pCO_2 measurements for regional air-sea CO_2 flux estimates. *Journal of Geophysical Research: Oceans* 129:e2023JC020744, https://doi.org/10.1029/2023JC020744.

Ocean Scope Working Group. 2012. *OceanScope: A Proposed Partnership Between the Maritime Industries and the Ocean Observing Community to Monitor the Global Ocean Water Column*. Report of Scientific Committee on Ocean Research (SCOR)/International Association for the Physical Sciences of the Oceans (IAPSO) Working Group 133. SCOR, Paris, https://scor-int.org/Publications/OceanScope_Final_report.pdf.

Rossby, T., C.N. Flagg, K. Donohue, S. Fontana, R. Curry, M. Andres, and J. Forsyth. 2019. *Oleander* is more than a flower: Twenty-five years of oceanography aboard a merchant vessel. *Oceanography* 32(3):126–137, https://doi.org/10.5670/oceanog.2019.319.

Silver, A., A. Gangopadhyay, G. Gawarkiewicz, E. Silva, and J. Clark. 2021. Interannual and seasonal asymmetries in Gulf Stream ring formations from 1980 to 2019. *Scientific Reports* 11:2207, https://doi.org/10.1038/s41598-021-81827-y.

Sosik, H.M., and R.J. Olson. 2007. Automated taxonomic classification of phytoplankton sampled with imaging-in-flow cytometry. *Limnology and Oceanography Methods* 5:204–216, https://doi.org/10.4319/lom.2007.5.204.

Volkov, D.L., R.H. Smith, R.F. Garcia, D.A. Smeed, B.I. Moat, W.E. Johns, and M.O. Baringer. 2024. Florida Current transport observations reveal four decades of steady state. *Nature Communications* 15:7780, https://doi.org/10.1038/s41467-024-51879-5.

von Arx, W.S., D.F. Bumpus, and W.S. Richardson. 1955. On the fine-structure of the Gulf Stream front. *Deep Sea Research* 3(1):46–65, https://doi.org/10.1016/0146-6313(55)90035-6.

Zhang, W.G., and G.G. Gawarkiewicz. 2015. Dynamics of the direct intrusion of Gulf Stream ring water onto the Mid-Atlantic Bight shelf. *Geophysical Research Letters* 42:7,687–7,695, https://doi.org/10.1002/2015GL065530.

ACKNOWLEDGMENTS

The National Science Foundation (NSF) Division of Ocean Sciences (OCE)-funded Oleander Program supports the operation of the ADCPs, weather station, TSG, and associated infrastructure, as well as the operation of AXIS, with the XBT probes supplied by NOAA/AOML and analysis support from OCE-2122726. Operation of the fCO_2 system is funded by NOAA AOML, and the operation of the CPR and analysis of the samples are presently supported by NOAA through the Northeastern Regional Association of Coastal Ocean Observing Systems (NERACOOS). The US Office of Naval Research funded the purchase of a Remora hull-mounted camera system. The expanded biological sampling is supported in part by the Arizona State University/Bermuda Institute of Ocean Sciences Cawthorn Innovation Fund and the Woods Hole Oceanographic Institution Ocean Vital Signs Network Initiative. CMV *Oleander* science is made possible by the continued generosity of the Bermuda Container Line/Neptune Group and the invaluable expertise and support of the ship's captains, chief engineers, and crew.

AUTHORS

Magdalena Andres (mandres@whoi.edu) Physical Oceanography Department, Woods Hole Oceanographic Institution, Woods Hole, MA, USA. **Thomas Rossby**, Graduate School of Oceanography, University of Rhode Island, Narragansett, RI, USA. **Eric Firing**, Department of Oceanography, University of Hawai'i at Mānoa, Honolulu, HI, USA. **Charles Flagg**, School of Marine and Atmospheric Sciences, Stony Brook University, Stony Brook, NY, USA. **Nicholas R. Bates**, School of Ocean Futures, Julie Ann Wrigley Global Futures Laboratory, Arizona State University (ASU), Tempe, AZ, USA, and ASU-Bermuda Institute of Ocean Sciences, St. George's, Bermuda. **Julia Hummon**, Department of Oceanography, University of Hawai'i at Mānoa, Honolulu, HI, USA. **Denis Pierrot**, NOAA Atlantic Oceanographic and Meteorological Laboratory (AOML), Miami, FL, USA. **Timothy J. Noyes**, School of Ocean Futures, Julie Ann Wrigley Global Futures Laboratory, ASU, Tempe, AZ, USA, and ASU-Bermuda Institute of Ocean Sciences, St. George's, Bermuda. **Matthew P. Enright**, ASU-Bermuda Institute of Ocean Sciences, St. George's, Bermuda. **Jeffery K. O'Brien** and **Rebecca Hudak**, Woods Hole Oceanographic Institution, Woods Hole, MA, USA. **Shenfu Dong**, NOAA AOML, Miami, FL, USA. **D. Christopher Melrose**, NOAA Northeast Fisheries Science Center, Narragansett, RI, USA. **David G. Johns** and **Lance Gregory**, Marine Biological Association, Plymouth, UK.

ARTICLE DOI. https://doi.org/10.5670/oceanog.2025e108

TWENTY YEARS MONITORING THE BRAZIL CURRENT ALONG THE NOAA AX97 HIGH-DENSITY XBT TRANSECT

By Tayanne P. Ferreira, Paula Marangoni G.M.P., Mauro Cirano, Afonso M. Paiva, Samantha B.O. Cruz, Pedro P. Freitas, Marlos Goes, and Maurício M. Mata

ABSTRACT

The NOAA/Atlantic Oceanographic and Meteorological Laboratory (AOML) AX97 High Density eXpendable Bathy-Thermograph (XBT) transect constitutes the longest sustained monitoring system of the Brazil Current (BC), having so far provided two decades of observational data. The BC plays an important role in oceanic variability and related processes, as it significantly influences regional and global climate dynamics. The BC is also the main pathway by which subtropical waters are carried to high latitudes. The AX97 data integration into assimilation schemes enhances the accuracy of short-term ocean predictions and long-term reanalyses, benefiting global forecasting centers by improving ocean models at regional, basin, and global scales. Moreover, the AX97 data contribute to global datasets used to quantify ocean heat content, and they are pivotal in assessing high-resolution ocean forecast systems and Earth system models, including those employed by the Intergovernmental Panel on Climate Change. This bimonthly sampling effort, a collaboration between Brazilian universities, the Brazilian Navy, and NOAA/AOML, successfully completed 100 cruises between August 2004 and August 2024, deploying 4,704 XBTs along the transect from Rio de Janeiro to Trindade Island near 22°S. Here, we analyze the BC's structure and variability over the period 2004–2023, examining its behavior under extreme warm and cold oceanic conditions, including positive and negative anomalies in sea surface height and temperature.

THE BRAZIL CURRENT REGION AND ITS PARTICULARITY

Surface circulation in the western part of the South Atlantic Subtropical Gyre is dominated by the poleward-flowing Brazil Current (BC), a warm and saline western boundary current (WBC). The BC originates at the bifurcation of the South Equatorial Current around 14°S and extends to approximately 500 m deep in the water column. At ~20°S, the BC encounters the Vitoria-Trindade Ridge, a chain of submerged seamounts that acts as a barrier, forcing the current to flow through narrow channels (see **Figure 1a**) before reorganizing into a more coherent WBC further south. Near 22°–23°S, the BC exhibits intense mesoscale variability (Mill et al., 2015) associated with eddy formation and recirculating gyres, and interacts with localized coastal upwelling and equatorward-propagating coastal trapped waves (Freitas et al., 2021), resulting in highly complex hydrodynamics.

This region is a crucial area for research and monitoring. Most of Brazil's oil and gas production originates in the Espírito Santo, Campos, and Santos sedimentary basins, located around these same latitudes, and includes recently discovered pre-salt oil reserves in deep waters. The associated risks of oil spills and the continuous development of adjacent coastal areas pose severe environmental challenges, demanding forecast capabilities and continuous monitoring of the circulation in shelf and deep waters. In addition, this region is characterized by high coastal productivity and unique ecosystems, influenced by the Cabo Frio upwelling system to the south and the Abrolhos Bank coral reef complex to the north. Studies indicate that cross-shelf fluxes that may impact coastal productivity are strongly affected by BC meandering and eddy formation (Aguiar et al., 2014). The BC also plays an important role in extreme events such as the marine heatwaves by advecting anomalies across different latitudes (Goes et al., 2024), with possible ecological impacts along the Brazilian coast.

Historical sparsity of in situ data in the Western South Atlantic Ocean poses challenges for studying the climate dynamics of the BC region. The longest sustained monitoring system of the BC, the US NOAA/Atlantic Oceanographic and Meteorological Laboratory (AOML) AX97 high density XBT transect (hereafter AX97), was initiated in 2004. Part of a global network of XBT transects (Goni et al., 2019), AX97 is conducted in cooperation with the Brazilian regional office of the Global Ocean Observing System (GOOS) and a partnership that includes Brazilian universities (Federal University of Rio de Janeiro and Federal University of Rio Grande), the Brazilian Navy, and the Brazilian Ministry of Science, Technology, and Innovation (MCTI), with additional support from the National Council for Scientific and Technological Development (CNPq).

Since August 2004, AX97 has conducted bimonthly sampling, measuring the upper ocean temperature structure between Rio de Janeiro (22.9°S, 43°W) and Trindade Island (20°S, 30°W) (**Figure 1a**). AX97 is part of the Ship of Opportunity Program and is generally executed in even months (**Figure 1b**) following the supply schedule of the Brazilian Navy ships to the Trindade Island. The sampling route crosses the BC region and the 200 m isobath around

22.8°S. This area is noted for intense mesoscale activity, typically associated with cyclonic (clockwise) meanders that give rise to recurring eddy formation (generally referred to as the São Tomé eddy). This study aims to assess the vertical structure and variability of the BC under extreme warm and cold scenarios, spanning the 20-year period, where composites of sea surface temperature (SST), anomalies of sea surface height (SSH), and the BC structure were analyzed.

DATA AND METHODS

Our analysis is restricted to the region west of 38°W, comprising most of the BC mean flow and mesoscale variability for the period August 2004 to August 2023. Five cruises with spurious data were excluded after quality control, resulting in a total of 80 cruises. The AX97 transect starts offshore of the 200 m isobath and monitors upper ocean temperatures from the surface to approximately 800 m, with an average spatial resolution of 27 km, and increased resolution of 18 km near the shelf-slope regions. Salinity was estimated from a historical temperature-salinity relationship for the region (Goes et al., 2018).

Geostrophic velocities were calculated, and the absolute dynamic height (DH(z)) was estimated following the methodology described by Goes et al. (2019). This approach begins with the computation of relative dynamic height from temperature and salinity profiles using a reference depth of z = 500 m. Subsequently, DH(z) was refined by combining the monthly climatological absolute dynamic topography (ADT) with the relative dynamic height at the reference level. The ADT data were sourced from the International Pacific Research Center (IPRC), which integrates gridded satellite altimetry with Argo float data. Once the DH along the AX97 transect was determined, it was extrapolated to shallower depths (<200 m, as indicated by the red line in the upper panel of Figure 1) using altimetry data. This approach enabled the computation of extrapolated DH for the entire AX97 transect.

Altimetry was further used, together with SST data, to visualize circulation features, including the BC front and mesoscale eddies sampled by the XBT data. SSH and sea level anomaly (SLA) relative to mean dynamic topography data, available at 1/4° horizontal resolution, were

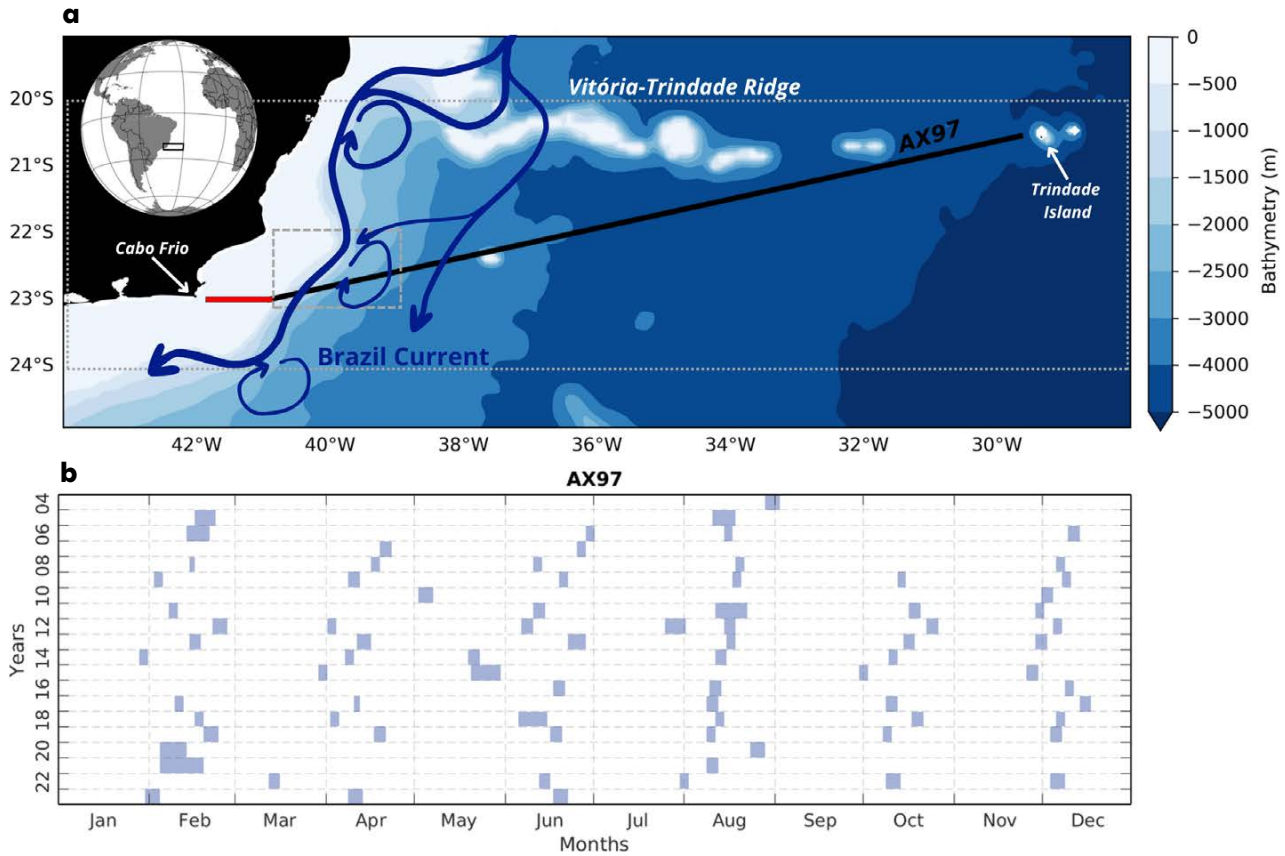

FIGURE 1. (a) Circulation scheme in the Brazil Current (BC) region, according to studies available in the literature. The thick blue line shows the BC mean path. The black line indicates the AX97 eXpendable BathyThermograph (XBT) reference transect overlaid on the contours of the local bathymetry in meters. The red line indicates a zonal coastal transect extension that connects the western end of the AX97 reference transect to the vicinity of Cabo Frio. The gray dashed and dotted boxes mark the area used to identify eddy occurrence and sea surface temperature anomalies, respectively, during 2004–2023. (b) Monthly distribution of cruises over the 20 years.

obtained from the Archiving, Validation, and Interpretation of Satellite Oceanographic data (AVISO), produced by SSALTO/DUACS and distributed by the Copernicus Marine and Environment Monitoring Service (CMEMS). Altimetry, and absolute geostrophic velocity derived from SSH were used to identify eddies in the region using the Okubo-Weiss parameter (OW; Okubo, 1970), which expresses the strain-vorticity balance in the horizontal flow field. Eddies were considered to occur for OW ≤ 2×10^{-12} s^{-2}, in the region bounded by longitudes 41°W and 39°W and latitudes 22°S and 23°S (gray dashed box in Figure 1a).

The SST data used in this study were sourced from the Operational Sea Surface Temperature and Sea Ice Analysis (OSTIA) dataset (Good et al., 2020) for 2004 to 2023. The Global Ocean OSTIA SST data, provided by CMEMS and accessible through the Marine Data Store (MDS), offers high-resolution (1/20°) daily global SST maps. In addition to identifying eddies, SST data were used to detect extreme temperature anomalies in the AX97 region, from 20°S to 24°S and 44°W to 28°W (gray dotted box in Figure 1a). Warm (cold) anomalies were computed, taking into account the 90th (10th) percentiles, and warm (cold) composites were generated for the entire region.

RESULTS AND DISCUSSION

Figure 2a presents the average SSH over the period 2004–2023, along with the corresponding mean surface geostrophic velocity from AVISO during the days of the AX97 cruises. The averaged SSH is very similar to the mean dynamic topography, indicating that the AX97 sampling strategy is capable of representing the region's mean dynamics. This similarity allows us to interpret the processes observed during the AX97 cruises as proxies for the local BC conditions. Analogous to the BC scheme (Figure 1a), the mean path of the BC is observed to follow the shelf break, with slight variations in areas such as Cabo São Tomé (~22.5°S) and Cabo Frio (~23.5°S). As previously mentioned, this region is characterized by high BC variability and eddy genesis, with the São Tomé eddy being the prevailing mesoscale feature in the AX97 region that could contribute to a reduction in the overall mean SSH.

The vertical structure of the mean geostrophic velocity (Figure 2b) reflects the surface signal of the BC and features two distinct cores, one that corresponds to the mean flow of the BC (located west of 40°W) and the other that is associated with cyclonic meanders (around 40°W). The vertical velocity structure of these mesoscale features extend through the first 400 m of the water column, influencing and modulating exchanges between the oceanic region and the continental shelf. The dynamics of these processes will be discussed in detail later.

Comparison of panels a and b in Figure 2 indicates that the BC primarily flows where SSH gradients are most pronounced. This observation is further supported by the DH calculated from AX97 transect profiles. The DH derived from XBT data aligns closely with the SSH obtained from altimetry (Figure 2c), a consistency that is also evident in the extrapolation to the shelf, indicating the effectiveness

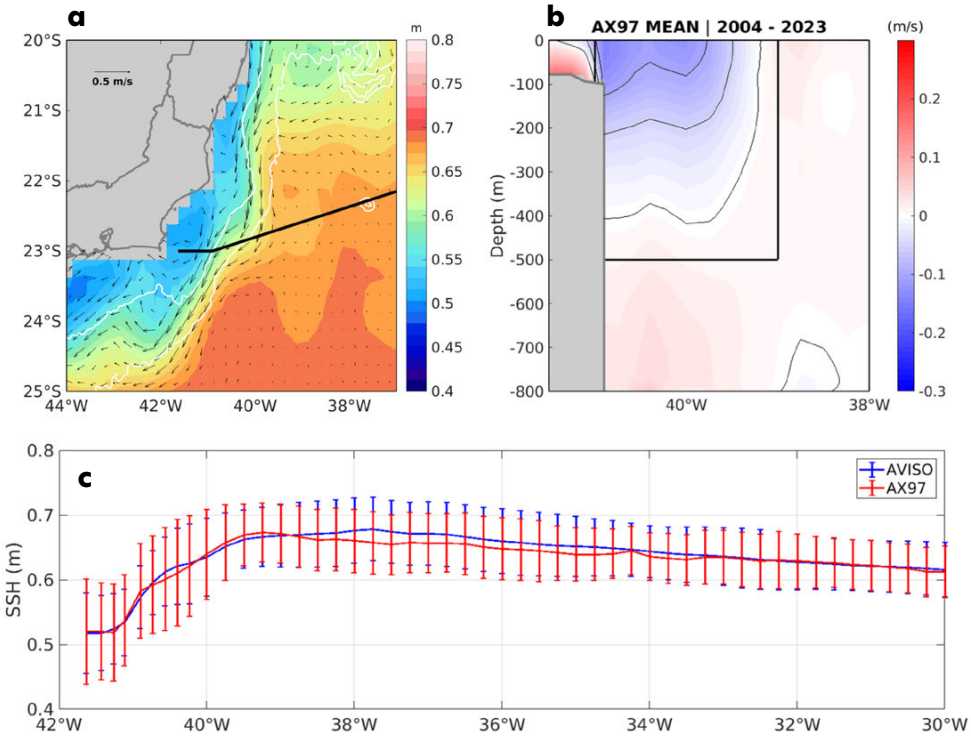

FIGURE 2. (a) Mean sea surface height (SSH) for the 20-year period analyzed considering only dates that coincide with the AX97 cruises. The black arrows illustrate the associated mean geostrophic velocity from AVISO. (b) The mean geostrophic velocity derived from XBT data for the BC region. Negative values (blue) indicate southward velocities. The black box marks the area used to evaluate the transport in Figure 3b. (c) Mean SSH along the AX97 reference transect and its standard deviation (blue line) compared to the mean dynamic height evaluated from AX97 cruises and its standard deviation (red line).

of the methodology. The highest values of SSH and DH, along with the most pronounced variations, are observed in the BC region between 41°W and 39°W. Within this area, there is a difference of approximately 15 cm between maximum and minimum values, which reflects the distinct signature of the BC pathway (Figure 2c).

The mean BC volume transport and its associated standard deviation observed from AX97 was -4.96 ± 2.69 Sv (horizontal gray line in Figure 3a), in line with previous estimates made by Goes et al. (2019). This transport was evaluated based on the southward (negative) geostrophic velocities in an area between 41°W and 39°W, from the surface to a depth of 500 m (black box in Figure 2b). The transport data were organized by season, and subsequent average values were calculated in order to highlight seasonal variations in BC transport. The highest transport of -6.51 ± 1.91 Sv was observed in austral spring (SON), while the lowest transport of -4.02 ± 2.54 Sv occurred in austral winter (JJA). Transport values for austral summer (DJF) and autumn (MAM) were -5.67 ± 2.64 Sv and -4.37 ± 2.87 Sv, respectively. The different scenarios (positive/negative SST anomalies and SSH eddy track) analyzed in this study are identified on the transport time series (Figure 3a).

From the total of the 80 cruises analyzed between 2004 and 2023, 25 cruises or 31.2% reported the presence of eddies, identified by black dots on the southward transport time series in Figure 3a. More than half of these eddies (52%) occurred during summer, and the rest were evenly spread among the other three seasons (16% each). This indicates that mesoscale activity is most intense during summer, given that the cruises were evenly distributed throughout the seasons.

Figure 3b illustrates one eddy event, where BC meandering generated a São Tomé eddy during the summer of 2019 (pink dot on the transport series in Figure 3a). A depression in the SSH signal characterizes the São Tomé eddy as a cyclonic eddy whose vertical velocity structure indicates two opposing cores that modulate the water column to a depth of 500 m (Figure 3c). The offshore core represents the BC front when displaced from the shelf break, characterized by an intense southward geostrophic velocity that exhibited a maximum near the surface (~0.6 m s^{-1}). The inner core of the cyclonic recirculation is less intense (~0.4 m s^{-1}) and directed northward. Considering only southward transport, BC transport observed during this cruise was -8 Sv, almost double the average. Some of the eddies identified in this study were also analyzed by Mill et al. (2015), who used a similar method over a larger area. They found that six São Tomé eddies detached from the main BC flow and formed isolated rings between 2005 and 2013. Two of these eddies followed the BC southward, while six moved northward toward the Tubarão Bight (20°S, 39°W). The authors also highlighted the potential of these eddies to transport shelf and slope water properties along or across the BC.

The extreme cold and warm events in the region were identified using a percentile-based methodology, where area-averaged temperature values for 10th (P10) and 90th (P90) percentiles were -2.11°C and 2.30°C, respectively.

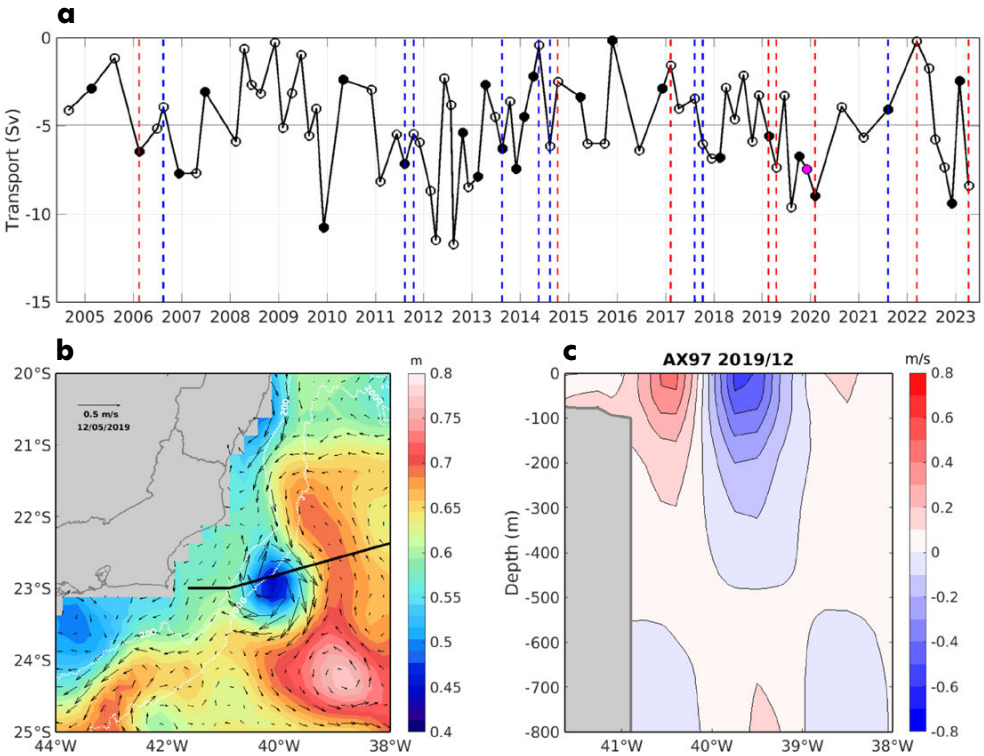

FIGURE 3. (a) Volume transport estimated across the reference transect indicated in Figure 2b. Different scenarios are indicated as follows: presence of eddy (black dots), negative anomalies (dashed blue line), and positive anomalies (dashed red line) in sea surface temperature. The pink dot indicates the eddy event in December 2019 highlighted in panels b and c. (b) Regional sea surface height and associated geostrophic velocities (arrows) illustrate a BC cyclonic eddy examined during the December 2019 cruise. (c) Absolute geostrophic velocity (m s^{-1}) estimated from AX97 data for the December 2019 cruise. Negative velocities (blue) have a southward flow, and positive velocities (red) have a northward flow. The black contours are shown every 0.1 m s^{-1}.

Among the 80 cruises analyzed, eight of them (four in February, two in March, and two in April) exhibited P90 anomalies (warm) and nine (five in August and four in October) showed P10 anomalies (cold). Not surprisingly, more than 50% of the warm anomalies were observed after 2019. In contrast, only one negative anomaly was recorded after 2019. This suggests a general warming trend in the AX97 region over the recent years.

The composite of positive anomalies exhibits a spatially warm distribution in the region, with the northern part of the domain being warmer than the southern part (Figure 4a). Additionally, a negative signal is concentrated closer to the coast between 22°S and 23°S, and north of 21°S. To some extent, this agrees with the negative anomalies (Figure 4b), where the major anomalies are concentrated near the coast. These areas are associated with coastal upwelling previously identified in the literature to be driven by northeasterly winds and to be stronger in summer (Aguiar et al., 2014; Goes et al., 2019). As mentioned above, this region is also known for continuous generation of cold-core cyclonic eddies that could contribute to this negative anomaly.

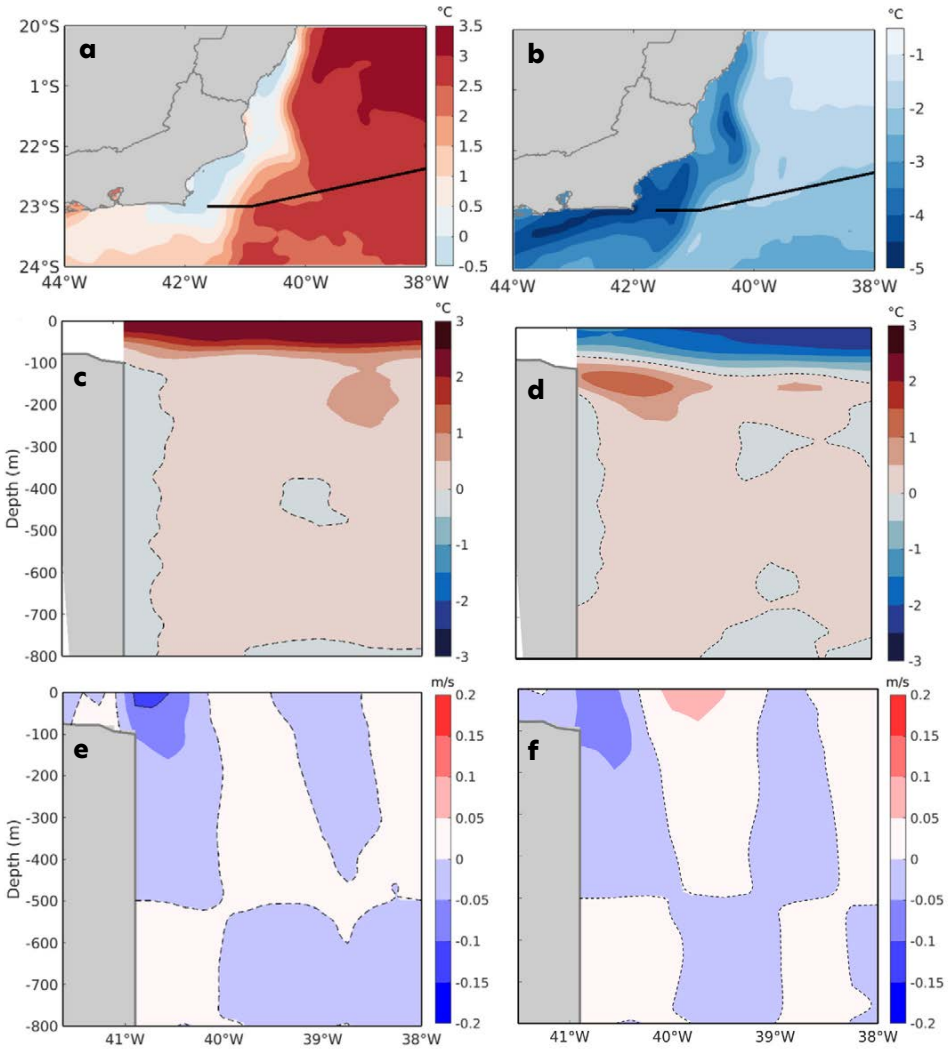

FIGURE 4. (a) Composite of positive sea surface temperature (SST) anomalies (the warmest 10% of cruises). (b) Composite of negative SST anomalies (the coldest 10% of cruises). (c) Vertical structure of temperature anomalies for the warmest 10% of cruises estimated from AX97 data. (d) Vertical structure of temperature anomalies for the coldest 10% of cruises. (e) Vertical structure of geostrophic velocity anomalies for the warmest cruises. (f) Vertical structure of geostrophic velocities anomalies for the coldest cruises estimated from AX97 data. The dashed black lines in panels c–f indicate the zero values in both temperature anomalies and velocities.

The vertical distribution of temperature anomalies varied along the section and with depth. The composite of warm anomalies (Figure 4c) shows significant warming throughout much of the water column, with positive anomalies extending to 800 m during warmer periods. In contrast, the composite of cold anomalies indicates cooling mainly within the upper 100 m (Figure 4d) and warming at the subsurface. At the surface, a positive anomaly of up to 3°C was observed, accompanied by an intensified temperature gradient near the shelf during warm events. During cold events, this gradient was less pronounced, with anomalies dropping to as low as -2.5°C.

Regarding the vertical structure of velocity anomalies, the BC was observed to intensify during warm events (Figure 4e), consistent with the increased temperature gradient between inshore and offshore areas that results in a more pronounced density gradient. During warmer cruises, a velocity anomaly of 0.2 m s^{-1} was recorded in the BC region, with its core being shallower and more intense. In contrast, during colder cruises (Figure 4f), the velocity anomaly was less pronounced, peaking at 0.1 m s^{-1}.

CONCLUSIONS

AX97 is the only long-term XBT monitoring system for the BC, having operated continuously for the past 20 years. The data are freely available from NOAA. This study analyzed temperature profiles to assess the BC's transport and explore its variability, especially in relation to mesoscale eddies and temperature anomalies. The average BC transport was found to be -4.96 ± 2.69 Sv, consistent

with previous studies. Seasonal variations were observed, with the highest transport levels occurring in austral spring and the lowest in austral winter. Eddies were detected on approximately 30% of the 80 cruises, mainly during austral summer, and they altered the vertical structure of the BC by creating opposing flows that extended to 500 m depth. Temperature anomalies were classified as either warming or cooling events, revealing extreme thermal patterns. Of the eight warm events observed, five occurred after 2019, indicating a potential regional warming trend. Notably, warm anomalies affected deeper water layers, while cold anomalies were confined to the upper 100 m, suggesting that warming events could have more widespread effects on ocean conditions.

These findings have significant implications for society, as they contribute to a better understanding of ocean processes that influence global climate and weather patterns. The 20 years of AX97 data are being used in key areas such as: (1) improving the accuracy of ocean forecasts through data assimilation by global operational centers, thus enhancing the prediction skill of short-term weather events and long-term climate trends that can inform policy decisions, disaster preparedness, and resource management; (2) study of upper-ocean heat content and the transport of heat in the Atlantic Meridional Overturning Circulation (AMOC), which plays a crucial role in regulating global climate systems that affect agriculture, energy production, and water resources; and (3) assessment of high-resolution ocean forecast systems and Earth system models that provide vital insights for climate change mitigation and adaptation strategies.

Moreover, the ongoing expansion of the AX97 program to include shelf waters and the collection of atmospheric data during cruises ensures the continued enhancement of the dataset, directly benefiting climate science and strengthening the resilience of coastal communities. By improving our understanding of the BC's behavior, this research supports efforts to predict and manage the impacts of climate variability, contributing to the well-being of society and the protection of vulnerable ecosystems.

REFERENCES

Aguiar, A.L., M. Cirano, J. Pereira, and M. Marta-Almeida. 2014. Upwelling processes along a western boundary current in the Abrolhos–Campos region of Brazil. *Continental Shelf Research* 85:42–59, https://doi.org/10.1016/j.csr.2014.04.013.

Freitas, P.P., A. de Moraes Paiva, M. Cirano, G.N. Mill, V.S. Costa, M. Gabioux, and B.R.L. França. 2021. Coastal trapped waves propagation along the Southwestern Atlantic Continental Shelf. *Continental Shelf Research* 226:104496, https://doi.org/10.1016/j.csr.2021.104496.

Goes, M., J. Christophersen, S. Dong, G. Goni, and M.O. Baringer. 2018. An updated estimate of salinity for the Atlantic Ocean sector using temperature-salinity relationships. *Journal of Atmospheric and Oceanic Technology* 35(9):1,771–1,784, https://doi.org/10.1175/JTECH-D-18-0029.1.

Goes, M., M. Cirano, M.M. Mata, and S. Majumder. 2019. Long-term monitoring of the Brazil Current transport at 22°S from XBT and altimetry data: Seasonal, interannual, and extreme variability. *Journal of Geophysical Research: Oceans* 124(6):3,645–3,663, https://doi.org/10.1029/2018JC014809.

Goes, M., S. Dong, G.R. Foltz, G. Goni, D.L. Volkov, and I. Wainer. 2024. Modulation of western South Atlantic marine heatwaves by meridional ocean heat transport. *Journal of Geophysical Research: Oceans* 129(3):e2023JC019715, https://doi.org/10.1029/2023JC019715.

Goni, G.J., J. Sprintall, F. Bringas, L. Cheng, M. Cirano, S. Dong, R. Domingues, M. Goes, H. Lopez, R. Morrow, and others. 2019. More than 50 years of successful continuous temperature section measurements by the global expendable bathythermograph network, its integrability, societal benefits, and future. *Frontiers in Marine Science* 6:452, https://doi.org/10.3389/fmars.2019.00452.

Good, S., E. Fiedler, C. Mao, M.J. Martin, A. Maycock, R. Reid, J. Roberts-Jones, T. Searle, J. Waters, J. While, and M. Worsfold. 2020. The current configuration of the OSTIA system for Operational Production of Foundation Sea Surface Temperature and Ice Concentration Analyses. *Remote Sensing* 2:720, https://doi.org/10.3390/rs12040720.

Mill, G.N., V.S. da Costa, N.D. Lima, M. Gabioux, L.A.A. Guerra, and A.M. Paiva. 2015. Northward migration of Cape São Tomé rings, Brazil. *Continental Shelf Research* 106:27–37, https://doi.org/10.1016/j.csr.2015.06.010.

Okubo, A. 1970. Horizontal dispersion of floatable particles in the vicinity of velocity singularities such as convergences. *Deep Sea Research and Oceanographic Abstracts* 17(3):445–454, https://doi.org/10.1016/0011-7471(70)90059-8.

ACKNOWLEDGMENTS

We thank the MCTI, NOAA/AOML, and the Cooperative Institute of the University of Miami, the Brazilian Navy, the UFRJ and FURG, the AX97 team, and all the volunteers who helped us collect the AX97 data during these 20 years. This research would not by possible without the support from the Petróleo Brasileiro S.A. (PETROBRAS), and the Brazilian Oil Regulatory Agency (ANP) for making the field campaigns possible using the Cooperation Terms SIGITEC 2018/00451-6, 2018/00452-2, and 2024/00240-6. We express our gratitude to the National Council for Scientific and Technological Development (CNPq) for their financial support of the National Ocean Observation and Monitoring Network (ReNOMO), grant number 409666/2022-0. Other important research grants from CNPq that also supported this research are grants numbers 475529/2012-0, 405908/2016-4, 310902/2018-5, 443262/2019-5, 420151/2023-0 and 441729/2024-0.

AUTHORS

Tayanne P. Ferreira (tayannepires.ufc@oceanica.ufrj.br), Ocean Engineering Program, COPPE/Federal University of Rio de Janeiro (UFRJ), Rio de Janeiro, Brazil. **Paula Marangoni G.M.P.**, Ocean Engineering Program, COPPE/UFRJ, Rio de Janeiro, Brazil. **Mauro Cirano**, Institute of Geosciences, UFRJ, Rio de Janeiro, Brazil. **Afonso M. Paiva**, Ocean Engineering Program, COPPE/UFRJ, Rio de Janeiro, Brazil. **Samantha B.O. Cruz**, Meteorology Program, UFRJ, Rio de Janeiro, Brazil. **Pedro P. Freitas**, Center for Marine Studies, Federal University of Paraná (UFPR), Pontal do Paraná, Brazil. **Marlos Goes**, Cooperative Institute for Marine and Atmospheric Studies, University of Miami, and NOAA/AOML, Miami, FL, USA. **Maurício M. Mata**, Institute of Oceanography, Federal University of Rio Grande (FURG), Rio Grande, Brazil.

ARTICLE DOI. https://doi.org/10.5670/oceanog.2025e113

FISHING FOR OCEAN DATA IN THE EAST AUSTRALIAN CURRENT

By Véronique Lago, Moninya Roughan, Colette Kerry, and Ian Knuckey

ABSTRACT

Knowledge of the three-dimensional structure and variability of ocean temperature is critical for understanding ocean circulation, heat uptake, marine extremes, and the abundance and distribution of marine life. While satellite technology offers near-global coverage of surface ocean temperatures, subsurface observations represent a big gap in the coastal ocean record. Here we present the first results from FishSOOP (Fishing Vessels as Ships of Opportunity Program), Australia's pilot program that uses commercial fishing gear to collect subsurface ocean data. Since early 2023, temperature and pressure data have been collected through the FishSOOP project across the Australian continental shelf and upper-slope waters. These new data provide insights into the development of marine heatwaves throughout the water column and new understanding of how the East Australian Current interacts with shelf water to produce nonuniform temperature changes. Comparison with the South East Australian Coastal Ocean Forecasting System (SEA-COFS) model indicates potential for improving forecasts of upper ocean heat content and subsurface temperatures by filling large gaps in observational data coverage. FishSOOP already provides a step change in the amount of open access temperature data available as well as ocean information critical to marine industries for operational decision-making, showing the value of using fishing vessels to observe challenging western boundary current regions.

INTRODUCTION

Western boundary currents (WBCs) such as the East Australian Current (EAC) are the heat engines of the ocean, transferring heat from low to high latitudes. They flow along the eastern sides of continents, often adjacent to large population centers. For example, 80% of Australia's population live along the east coast and are thus impacted by the EAC. WBCs impact our weather, climate, and the distribution and abundance of fish and other marine organisms. Therefore, changes and variations in WBCs impact our seafood security. In addition, WBCs are warming at a rapid rate (Li et al., 2022), yet due to their dynamic natures (swift currents that shed numerous eddies), WBCs are difficult to measure and model.

Satellite sensors provide observations of sea surface height and surface ocean temperature, while the Argo float program provides subsurface ocean data—but only for the open ocean. By design, Argo floats do not profile over continental shelves, and they are also advected rapidly out of WBCs. Hence, despite the 4,000 floats profiling globally, their data coverage remains relatively sparse in WBC regions. Using fishing vessels to crowdsource research-quality data is an effective way to collect valuable ocean information cost-effectively where the data matter most (Jakoboski et al., 2024).

Additionally, fishing vessels provide the opportunity for widespread data collection in coastal regions and over the continental shelf, and thus provide opportunities to fill data gaps (Van Vranken et al., 2023; Jakoboski et al., 2024) on a broad scale. Programs using fishing vessels for ocean data collection have thus been gaining in popularity worldwide, and FishSOOP (Fishing Vessels as Ships of Opportunity Program) is Australia's contribution to the international Fishing Vessel Ocean Observing Network (Van Vranken et al., 2023).

FishSOOP

FishSOOP is a collaborative project between research and industry. The proof-of-concept trial was co-funded by the Fisheries Research and Development Corporation (FRDC) and Australia's Integrated Marine Observing System (IMOS) to install temperature sensors on commercial fishing vessels off southeastern Australia. This region was chosen because of the variety of fishing methods used and because it is where the EAC is extending southward, warming the ocean surface at a rate four times the global average (Li et al., 2022). It is also where climatic extreme events, such as marine heatwaves (MHWs), are critically impacting fisheries. The project quickly expanded to all coastal states and territories of Australia, with co-investment from several industry partners (**Figure 1c,e**).

ZebraTech's Moana TD200 and TD1000 sensors and data transmission deck units were chosen for this project because the system, co-designed with fishers and purpose-built for deployment on fishing vessels, is extremely robust and easy to install and use; full sensor specifications and the data pathway are described in Jakoboski et al. (2024). The Moana sensors provide ±0.05°C initial accuracy with 0.001°C resolution for temperature, and ±0.5% initial accuracy with 0.1m resolution for the pressure sensor. The sensors send the data to the deck unit via Bluetooth, which in turns sends the data to a cloud server via a mobile network. When out of cell phone range, the data are sent when the

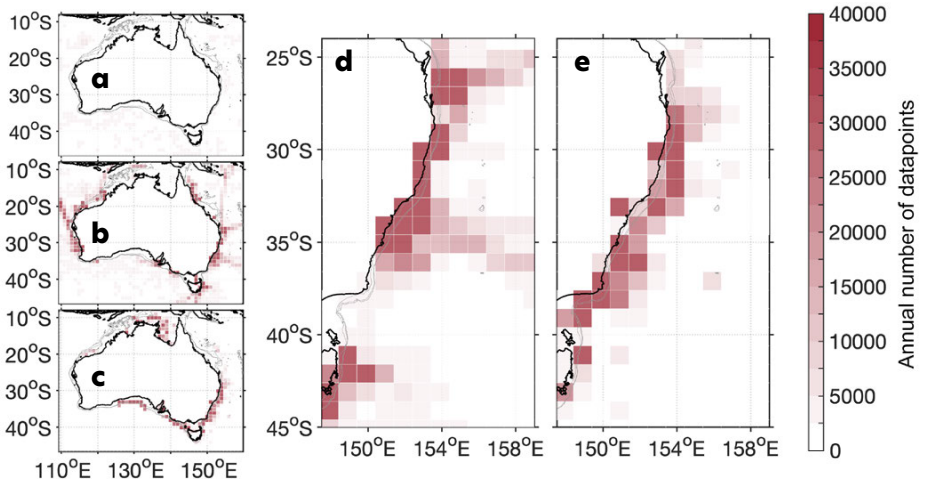

FIGURE 1. Annual average quantity of subsurface data points around Australia gridded to 1° resolution from (a) Argo, and (b) all available profiling data sources. (c) Quantity of data points from FishSOOP over a year (from August 2023 to July 2024) on a 1° resolution grid. (d) Annual average for all the available subsurface profiling sources of data available in the EAC region. (e) One year of FishSOOP data. The annual averages for the observations are from January 2000 to December 2022, drawn from the World Ocean Database (NOAA).

vessel is within range again. There is an option to connect the deck unit to the vessel Wi-Fi, which is preferable for vessels with extended operations further offshore. The data are returned in real time to the fishers who collected them, and an anonymized version is sent for open access archival on the Australian Ocean Data Network (AODN), currently accessible through the AODN THREDDS catalog.

During the trial phase of the program, 34 vessels were instrumented around Australia with a total of 53 sensors on a wide range of fishing gear types: prawn trawl, gillnet, demersal and pelagic longline, traps and pots, fish trawl, squid jig, and scallop dredge. Most vessels deployed one sensor, but some vessels deployed multiple sensors, either on different gear types (e.g., traps or pots) or spread over the length of the gear (e.g., longline). The trial yielded more than 3.3 million data points (from ~31,000 profiles) from the sea surface to 1,214 m depth, considerably expanding existing data records around Australia, including in waters previously poorly observed (Figure 1).

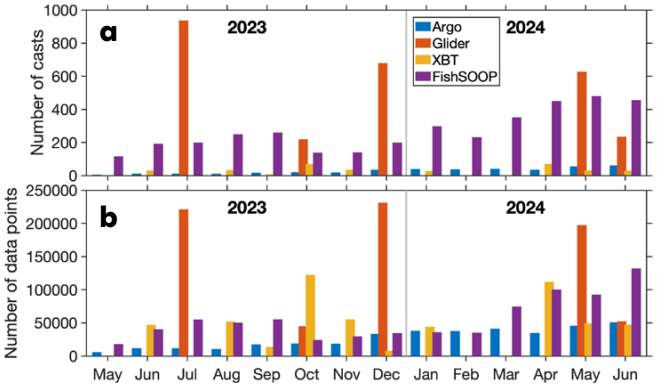

FIGURE 2. Comparison of (a) the quantity of casts, and (b) the quantity of data points collected by the FishSOOP program and other sources of near real time data in the East Australian Current (EAC). The downcasts and upcasts are counted separately in the number of casts. The EAC region is defined as shown in Figure 1d and e (24°S to 45°S and 147°E to 159.6°E. Argo, glider, and expendable bathythermograph (XBT) data were sourced from Australia's Integrated Marine Observing System (IMOS).

FILLING OBSERVATIONAL GAPS

Among WBCs, the EAC is considered fairly well observed (Ayoub et al., 2024) due to a concerted effort over the past 15 years by IMOS. This effort includes a network of 11 shelf moorings along the east coast of Australia from 28°S to 44°S, two high frequency (HF) radar systems (since 2012), more than 60 glider missions, repeat expendable bathythermograph (XBT) lines, Argo floats, surface drifters, and 10 years of deep transport observations at 28°S. And yet there are still vast data gaps along the length of this extensive coastline.

While the sustained moorings provide high resolution time series of climate-quality data, they are a sparse network comprised of 11 single points on the EAC shelf. Conversely, gliders provide high density data, but there are only four to five missions per year across the entire length of the EAC, and they are comparatively costly (Figure 2). Observations from FishSOOP complement this effort by providing cost-effective broad-scale, high-resolution, high-quality data across the shelf and upper slope in near-real time throughout the entire year (Figures 1d and 2).

Over the trial period, we deployed 35 Moana TD sensors from 16 vessels within the EAC region. We have surpassed the quantity of real-time data collected within the EAC region by all other sources combined within the same period (Figure 2). Due to annual variability in fishing effort, some months had more casts by gliders (e.g., July 2023, December 2023, and May 2024), but overall from May 2023 to June 2024 there were 2,699 casts from gliders (downcasts and upcasts) and 3,780 casts from the FishSOOP program (downcasts and upcasts; Figure 2a). After just 14 months of operation, we have filled extensive data gaps in the EAC and along the adjacent shelf.

CASE STUDY: FISHING INDUSTRY ENGAGEMENT

MHWs are discrete and quantifiable events of anomalously warm water above the 90th percentile for at least five consecutive days as defined by Hobday et al. (2016). Previous studies have shown that sea surface temperature (SST) data are not sufficient to predict the occurrence, duration, or intensity of MHWs below the surface (e.g., Schaeffer and Roughan, 2017). This is particularly true in regions of high variability, such as the warming shelf region of the EAC. However, MHWs are having a significant impact on the fishing industry and catchability of fish (Smith et al., 2023). One key aspect of FishSOOP is that the data are returned to the fishers in near-real time to inform fishing effort and potentially allow more efficient use of resources (e.g., fuel and time).

In January–February 2024, a severe MHW occurred in the northern EAC (Figure 3a–c) where a longline tuna vessel engaged in the FishSOOP program was actively fishing. This MHW lasted roughly three months, likely driven by anomalous advection of heat by the EAC, with SST anomalies showing that it was a strong MHW. Due to significant cloud cover, Figure 3a–c shows sea surface temperature only for February 4, making it hard to see the overall conditions for the vessel's remaining stay in the region (Figure 3d–f). However, FishSOOP data provided the first look below the surface where fishing was actively occurring. The temperature recorded was >28°C down to 80 m depth (Figure 3d). Over the following week, the vessel headed 500 km south while continuing to deploy fishing gear with the sensors attached until they reached colder waters. The sensor data clearly captured the temperature structure throughout the water column and showed the change in thermocline depth with latitude (Figure 3d,e). Finally, on February 14, the vessel encountered a cyclonic eddy inshore of the EAC separation where waters deeper than 60 m were <25°C (Figure 3f). By monitoring the near-real-time subsurface conditions, fishers were able to adjust the location and depth at which their fishing gear was deployed, seeking conditions that might optimize their catch rates. The sensors also alleviate the issue of patchy satellite SST data due to cloud cover. This highlights the value of obtaining direct observational data in real time where fishing occurs. The next step is to understand the relationship between ocean temperature at depth and catch composition and rates, and to provide ocean modeling products that might help improve fishing effort.

FINE-SCALE/SUBSURFACE DATA TO IMPROVE OCEAN MODELS

Ocean prediction requires the combination of numerical models and ocean observations, referred to as data assimilation, to correctly represent the timing and locations of fine-scale ocean features such as fronts and eddies. Here we present an example of surface and subsurface ocean representation from a data-assimilating model (part of the South East Australian Coastal Ocean Forecast System, SEA-COFS) along with observations from FishSOOP sensors (Figure 4). We compare a complex example of the western side of an anticyclonic eddy in the EAC adjacent to the continental shelf. The model is based on the data-assimilating

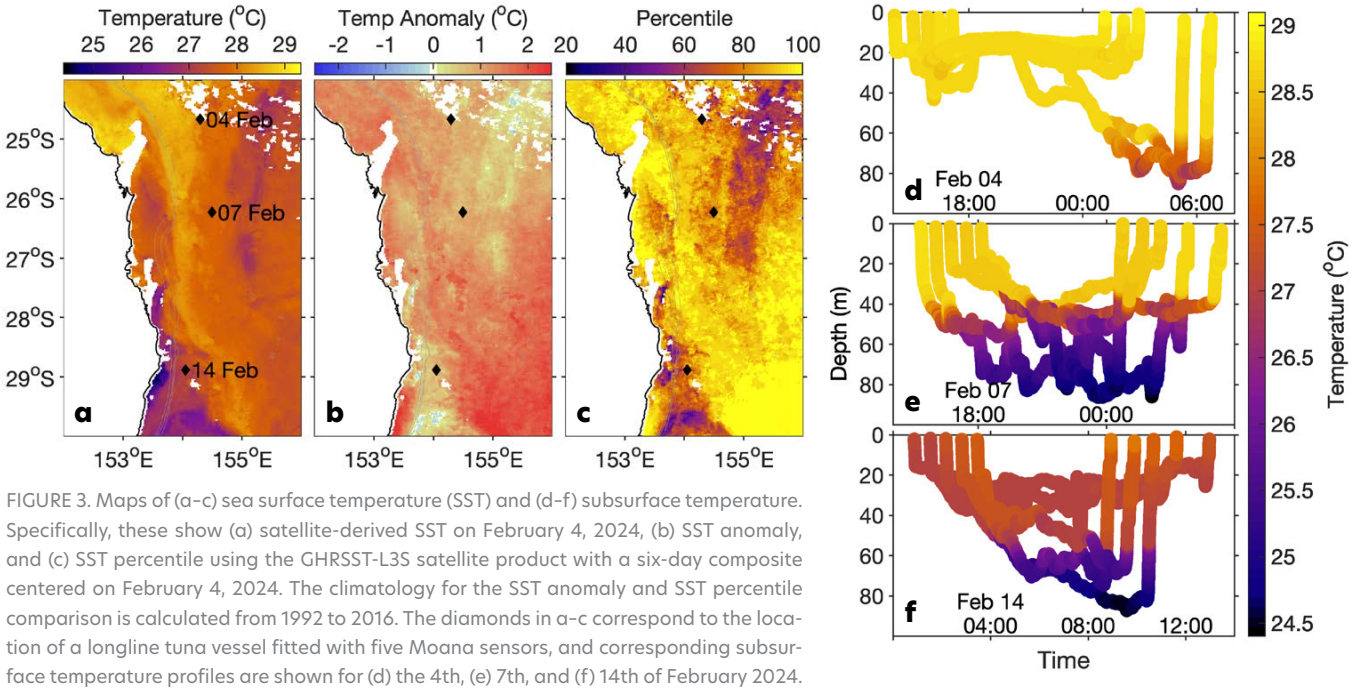

FIGURE 3. Maps of (a–c) sea surface temperature (SST) and (d–f) subsurface temperature. Specifically, these show (a) satellite-derived SST on February 4, 2024, (b) SST anomaly, and (c) SST percentile using the GHRSST-L3S satellite product with a six-day composite centered on February 4, 2024. The climatology for the SST anomaly and SST percentile comparison is calculated from 1992 to 2016. The diamonds in a–c correspond to the location of a longline tuna vessel fitted with five Moana sensors, and corresponding subsurface temperature profiles are shown for (d) the 4th, (e) 7th, and (f) 14th of February 2024.

Regional Ocean Modeling configuration of the EAC system (described in Kerry et al., 2016) and assimilates daily gridded satellite-derived sea surface height (SSH) data from Archiving, Validation, and Interpretation of Satellite Oceanographic Data (AVISO), satellite-derived SST observations and temperature and salinity from Argo profiling floats. The Moana sensor observations are not yet assimilated and represent independent observations.

The EAC separates from the coast at 32°S and wraps around a large anticyclonic eddy, while cold water is entrained between the separating EAC and the core of the anticyclonic eddy. The SST observations (Figure 4d) reveal a cold filament (east of the EAC core from 32°S to 33°S), but cloud coverage limits the availability of SST data extending south toward the vessel track. The subsurface observations from the Moana sensor (Figure 4f) indicate that the cold filament does indeed extend to the vessel track, showing shoaling of the isotherms associated with the cold filament between 153.5°E and 154°E. The model captures the cold-water entrainment (Figure 4c), but the model filament does not extend as far south as it does in reality; SST data that could resolve the filament are lacking, as are subsurface (Argo) data. The subsurface observations from the Moana sensor reveal both the complex structures of the front

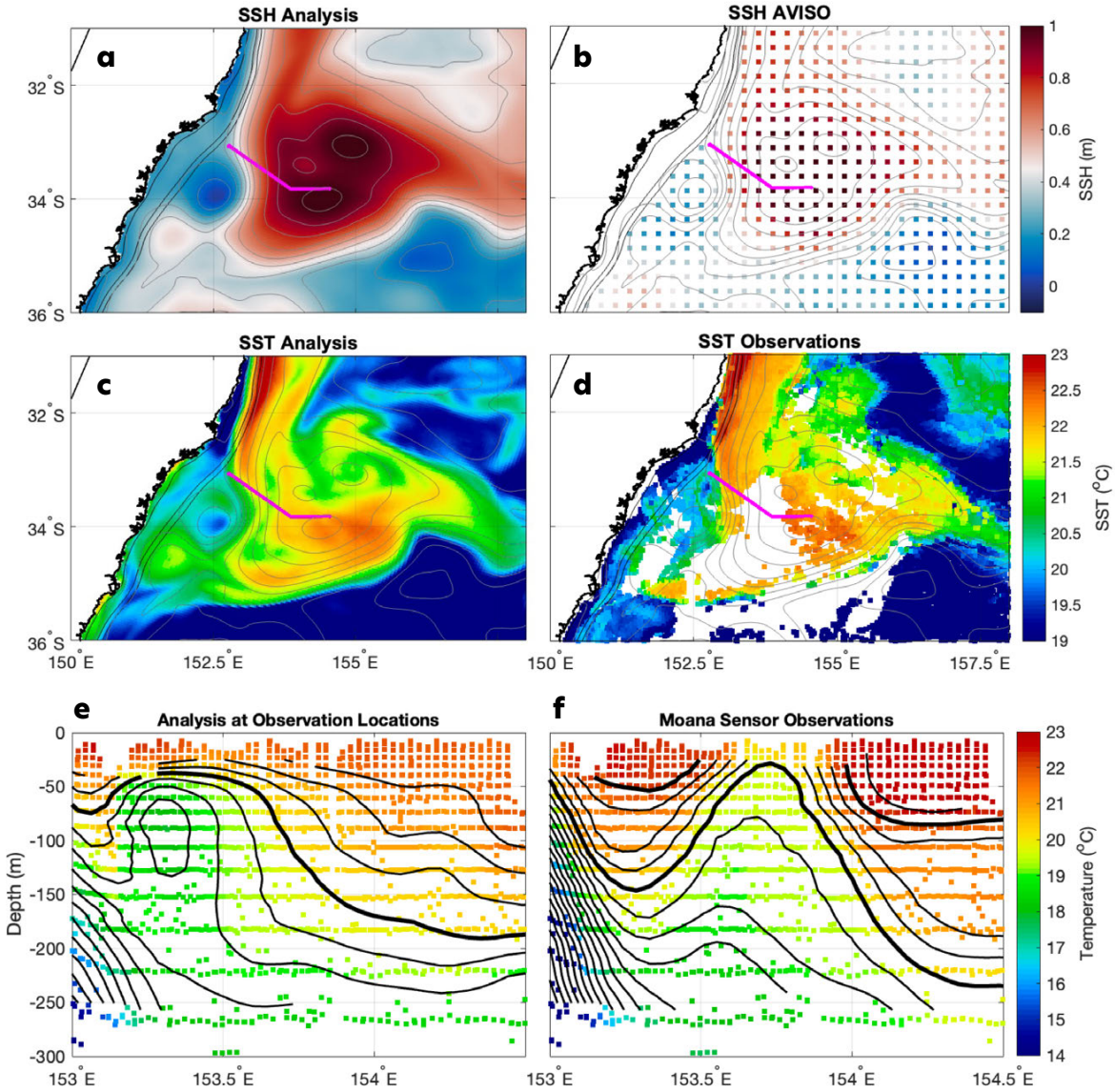

FIGURE 4. A comparison of a data-assimilating model solution with independent subsurface data from Moana sensors is plotted for October 12, 2023. (a) Modeled sea surface height (SSH). (b) AVISO SSH data. (c) Modeled sea surface temperature (SST). (d) SST observations. The magenta lines in panels a–d represent the path of the vessel from which the sensor was deployed. Black lines represent the 100 m, 400 m, and 1,000 m model bathymetry contours. (e) Model values at Moana sensor observation times and locations. (f) Moana sensor observations representing sections across the magenta lines in panels a–d. Bold black lines represent 20°C and 22°C isotherms, and the lighter black lines show isotherms separated by 0.5°C.

between the EAC and the shelf waters and the entrained cold filament between the EAC and the eddy. These comparisons highlight the potential value of subsurface observations from FishSOOP for improving model estimates below the surface, compared to existing models that typically assimilate satellite-derived surface observations and (usually sparse) profiles from Argo and XBTs. Model estimates of complex subsurface features are likely to benefit most.

SUMMARY

The FishSOOP project highlights the benefit of research-industry collaboration and has proven to be a reliable and cost-effective way to monitor the EAC and to fill in gaps in observations of Australian shelf and upper slope waters. By returning the data to the fishers in near-real time, we provide them with information that may enable them to target fish more efficiently while both collecting valuable subsurface data to improve ocean forecasting and providing a view of the EAC's three-dimensional temperature structure. This information is even more important and valuable for regions of high variability such as a WBC. Elsewhere, the value of including subsurface ocean observations in a regional model is clearly shown in depictions of shelf regions around New Zealand (Kerry et al., 2024) where there are considerable improvements in bottom temperature and heat content representation in shelf seas upon assimilation of FVON data.

Working with our international collaborators as part of FVON, we have been able to successfully build an Australia-wide operational program in a year. FVON has been endorsed by the UN Ocean Decade and as an emerging network in the Global Observing System, highlighting the global interest and need for such programs. FishSOOP data will also be assimilated into the SEA-COFS model, also endorsed by the UN Ocean Decade, and the project is a Global Ocean Observing System CoastPredict pilot program.

As FishSOOP grows, we are working with manufacturers to develop new sensors, notably a 2,000 m sensor and a fit-for-purpose, low-cost, hands-free salinity sensor. We are also looking to further develop tools and visualization methods useful to fishers and ocean forecasters for returning the data to them in real time. This will ensure effective, mutually beneficial collaboration for partnered growth to help fill ocean data gaps using informed observing system design and to sustainably manage fisheries into the future.

REFERENCES

Ayoub, N.K., M.P. Chidichimo, E. Dever, X. Guo, S.Y. Kim, M. Krug, B.M. Miquez, T. Morris, M. Roughan, J. Sprintall, and others. 2024. Observing ocean boundary currents: Lessons learned from six regions with mature observational and modeling systems. *Oceanography* 37(4):82–91, https://doi.org/10.5670/oceanog.2024.504.

Hobday, A., L.V. Alexander, S.E. Perkins, D.A. Smale, S.C. Straub, C.J. Oliver, J.A. Benthuysen, M.T. Burrows, M.G. Donat, M. Feng, and others. 2016. A hierarchical approach to defining marine heatwaves. *Progress in Oceanography* 141:227–238, https://doi.org/10.1016/j.pocean.2015.12.014.

Jakoboski, J., M. Roughan, J. Radford, J.M. Azevedo Correia de Souza, M. Felsing, R. Smith, N. Puketapu-Waite, M. Montaño Orozco, K.H. Maxwell, and C. Van Vranken. 2024. Partnering with the commercial fishing sector and Aotearoa New Zealand's ocean community to develop a nationwide subsurface temperature monitoring program. *Progress in Oceanography* 225:103278, https://doi.org/10.1016/j.pocean.2024.103278.

Kerry, C., B. Powell, M. Roughan, and P. Oke. 2016. Development and evaluation of a high-resolution reanalysis of the East Australian Current region using the Regional Ocean Modelling System (ROMS 3.4) and Incremental Strong-Constraint 4-Dimensional Variational (IS4D-Var) data assimilation. *Geoscientific Model Development* 9:3,779–3,801, https://doi.org/10.5194/gmd-9-3779-2016.

Kerry, C., M. Roughan, and J.M. Azevedo Correia de Souza. 2024. Assessing the impact of subsurface temperature observations from fishing vessels on temperature and heat content estimates in shelf seas: A New Zealand case study using Observing System Simulation Experiments. *Frontiers in Marine Science* 11:1358193, https://doi.org/10.3389/fmars.2024.1358193.

Li, J., M. Roughan, and C. Kerry. 2022. Drivers of ocean warming in the western boundary currents of the Southern Hemisphere. *Nature Climate Change* 12:901–909, https://doi.org/10.1038/s41558-022-01473-8.

Schaeffer, A., and M. Roughan. 2017. Subsurface intensification of marine heatwaves off southeastern Australia: The role of stratification and local winds. *Geophysical Research Letters* 44(10):5,025–5,033, https://doi.org/10.1002/2017GL073714.

Smith, K.E., M.T. Burrows, A.J. Hobday, N.G. King, P.J. Moore, A. Sen Gupta, M.S. Thomsen, T. Wernberg, and D.A. Smale. 2023. Biological impacts of marine heatwaves. *Annual Review of Marine Science* 15:119–145, https://doi.org/10.1146/annurev-marine-032122-121437.

Van Vranken, C., J. Jakoboski, J.W. Carroll, C. Cusack, P. Gorringe, N. Hirose, J. Manning, M. Martinelli, P. Penna, M. Pickering, and others. 2023. Towards a global Fishing Vessel Ocean Observing Network (FVON): State of the art and future directions. *Frontiers in Marine Science* 10:1176814, https://doi.org/10.3389/fmars.2023.1176814.

ACKNOWLEDGMENTS

This work was partially supported by the Australian government through the Fisheries Research and Development Corporation (FRDC), the Integrated Marine Observing System (IMOS), the University of New South Wales (UNSW), and the Australian Research Council (ARC). FishSOOP is now part of Australia's Integrated Marine Observing System (IMOS), enabled by the National Collaborative Research Infrastructure Strategy (NCRIS). It is operated by a consortium of institutions as an unincorporated joint venture, with the University of Tasmania as Lead Agent. We thank all the fishing industry participants who helped facilitate this work, including fleet managers, vessel skippers and crew, and Russell Hudson (Fishwell Pty Ltd), who instrumented the vessels in SE Australia. Phil Ravanello from Tuna Australia and Kylie Scales from the University of the Sunshine Coast are acknowledged for their efforts to help instrument tuna vessels in the EAC.

AUTHORS

Véronique Lago (v.lago@unsw.edu.au), **Moninya Roughan**, and **Colette Kerry**, Coastal and Regional Oceanography Lab, School of Biological Earth an Environmental Sciences, University of New South Wales, Sydney, Australia. **Ian Knuckey**, Fishwell Pty Ltd, Queenscliff, Victoria, Australia.

ARTICLE DOI. https://doi.org/10.5670/oceanog.2025e105

COORDINATED OBSERVING AND MODELING OF THE WEST FLORIDA SHELF WITH HARMFUL ALGAL BLOOM APPLICATION

By Robert H. Weisberg and Yonggang Liu

ABSTRACT

The central portion of the west Florida continental shelf is the epicenter for blooms of the harmful alga *Karenia brevis*, which tends to form at mid-shelf under nutrient depleted, or oligotrophic, conditions. Whether or not the shelf is conducive to such bloom formation in any given year appears to be related to when and where the Gulf of Mexico Loop Current, a western boundary current, interacts with the shelf slope. If this occurs in the southwest corner, where shallow isobaths wrap around the Florida Keys at the Dry Tortugas, then the entire west Florida shelf may be set into a protracted upwelling circulation that can both reset water properties and transport mid-shelf materials to the shoreline within the bottom Ekman layer. The 2018 *K. brevis* bloom provides one such example, as described via a coordinated program of coastal ocean observing and modeling. Both the elevation of *K. brevis* cell counts along the coast and their eventual cessation may be largely accounted for by the coastal ocean circulation, as driven, in part, by the Loop Current's interaction with the shelf slope.

THE LOOP CURRENT AND PRODUCTIVITY ALONG THE WEST FLORIDA SHELF

Often considered to be oligotrophic, the west Florida continental shelf (WFS) supports abundant fisheries, and at times it is beset by copious quantities of the harmful alga *Karenia brevis*, raising the question of how it is possible for an oligotrophic shelf to be so productive. The answer is that the WFS is not always oligotrophic. To understand why this is so and to appreciate the ecological consequences, we must consider how the WFS is forced, in particular, by the adjacent western boundary current—the Gulf of Mexico Loop Current (LC).

The first consideration is the geometry of the eastern Gulf of Mexico (Figure 1), where we observe that the gently sloping WFS is as wide as the dry land mass of the Florida peninsula. The LC abuts the WFS slope region at times, entering the Gulf of Mexico through the Yucatán Strait and exiting through the Straits of Florida as the Florida Current and the Gulf Stream. While in the Gulf of Mexico, the Loop Current/Florida Current/Gulf Stream system penetrates northward before looping around to exit, occasionally shedding a large anticyclonic eddy and retracting back to the south. Within its penetrating, eddy-shedding, and retraction evolutionary process (e.g., Nickerson et al., 2022), the LC often interacts with the WFS slope at various locations. Figure 1 includes an example of such eddy shedding.

Geophysical fluid dynamical constraints are such that a sea surface height displacement (or pressure perturbation) imposed upon the shelf slope can only penetrate landward by a distance equal to a Rossby radius of deformation (about 30 km for the WFS, given the local Coriolis parameter and water properties) and that such a perturbation may also propagate with shallow water to its right (i.e., northward along the WSF slope). Thus, LC effects on the WFS are limited to the outer shelf except when the LC impacts the shelf slope at its southernmost extent near the Dry Tortugas. Because the Dry Tortugas are the westernmost islets in the Florida Keys chain, all isobaths of about 20 m and deeper must wrap around the Dry Tortugas. Hence, if the LC contacts the shelf slope near the Dry Tortugas, its impact (by contacting shallow isobaths within a Rossby radius of deformation) can extend across the entire WFS,

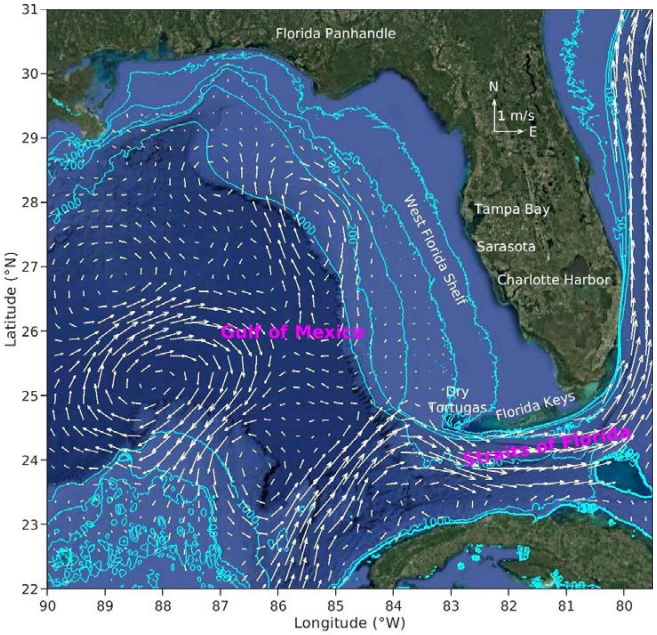

FIGURE 1. The configuration of the Loop Current system within the Gulf of Mexico, as estimated for September 15, 2018, using AVISO satellite altimetry. The arrows denote the surface geostrophic currents in m s^{-1} calculated from the height gradients. The contours are the 25 m, 50 m, 100 m, 200 m, and 1,000 m isobaths. Regions of discussion are labeled. Note the separation of an anticyclonic eddy from the parent Loop Current and the subsequent contact by the Loop Current with the southwest corner of the west Florida shelf near the Dry Tortugas, the region referred to as the pressure point.

thereby setting up a shelf-wide upwelling circulation. This circulation enables upper shelf slope water (with elevated inorganic nutrient concentrations) to flow over the shelf break and transit across the shelf toward the shore within the bottom Ekman layer. The companion works of Weisberg and He (2003) and Walsh et al. (2003) demonstrate this occurrence and its effect on phytoplankton ecology.

K. BREVIS BLOOM PREDICTION

Subsequent analyses by Liu et al. (2016), using a growing set of observations (*K. brevis* cell counts, LC position via satellite altimetry, long-term velocity and water property observations from moorings, plus glider and shipboard transects), led to the development of a seasonal prediction scheme regarding whether a major *K. brevis* bloom would materialize along the WFS in any given year. *K. brevis* is a slow growing dinoflagellate that can only outcompete faster growing diatoms under oligotrophic conditions, which in most years are limited to the mid-shelf, away from either nutrient inputs by land drainage, as occurs nearshore, or deeper-ocean nutrient inputs, as occurs at the outer shelf. This mid-shelf, oligotrophic scenario changes in years when the LC makes protracted contact with the shelf slope near the Dry Tortugas, a location we refer to as the WFS pressure point. If this occurs prior to the spring to summer phytoplankton bloom period, then diatoms are favored over *K. brevis*, negating a nearly annual occurrence of such a harmful algae bloom. Exceptions do occur to this simple scenario; nonetheless, for the years subsequent to 1993, when joint cell count and satellite altimetry observations exist, the simplistic pressure point hypothesis prediction score card has a winning record.

K. brevis blooms do not depend only on mid-shelf nutrient conditions; they also require a delivery mechanism from the mid-shelf to the nearshore to become a nuisance bloom. Transport within the bottom Ekman layer under upwelling conditions was confirmed via observations for the 2012 bloom event (Weisberg et al., 2016). Combined, the nutrient and delivery mechanisms result in considerable interannual variations in nearshore red tide bloom onsets, intensities, and durations. Some years are truly disruptive, whereas others are not. The *K. brevis* bloom of 2018 provides a case study for which cell count and glider and moored instrumentation observations, coordinated with numerical circulation model simulations, demonstrate locations, sequencing of intensities, and eventual abatement of what was arguably the worst of the red tide blooms to affect Florida in recent decades.

2018 *K. BREVIS* BLOOM

As described in Weisberg et al. (2019), the LC remained in a penetrative state without any WFS slope contact until around mid-July of 2018. This changed once the LC shed an eddy, allowing the LC to sidle eastward to interact with the pressure point, an interaction that lasted through the end of December 2018. Figure 1 shows the LC configuration for September 15, 2018. A glider survey conducted from August 24 through September 17, 2018, documented the water properties of the mid-WFS, identifying near-bottom, upwelled water with high chlorophyll (identified as being *K. brevis* related) located roughly between the 30 m to 40 m isobaths. A subsequent numerical circulation model simulation (employing the West Florida Coastal Ocean Model, an adaptation of the Finite Volume Community Ocean Model of Chen et al. [2003] nested in the HYbrid Coordinate Ocean Model of Chassignet et al. [2009]), with neutrally buoyant particles initialized along the glider track, then demonstrated the fluid pathways for the glider sampled water parcels to the nearshore (Figure 2). This helped to explain (1) an elevation in cell concentration from what had

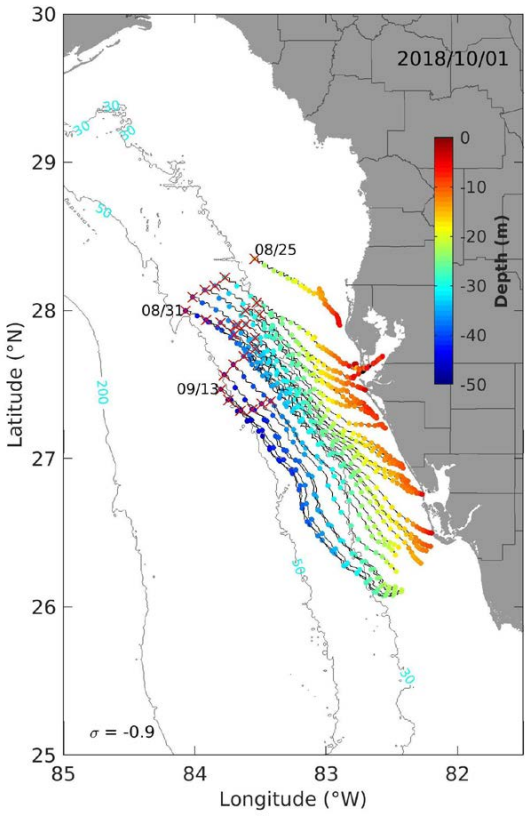

FIGURE 2. Modeled isopycnic trajectories for particles initialized along the glider track (marked by red Xs) from August 24, 2018, to September 17, 2018, and run through October 1, 2018, for totals of two to five weeks. Isobaths are shown at 30 m, 50 m, and 200 m; the glider sampled between 25 m and 55 m. The initial vertical location for all these particles was the near-bottom (model) level, and the daily color-coding provides the simulated particle depth (m) while en route. *Figure from Weisberg et al. (2019)*

been a lingering 2017 bloom (Figure 3) after the LC made its pressure point contact, and (2) a substantial increase in bloom intensity in the Tampa Bay region. These transport findings were also consistent with the timing of *K. brevis* cells appearing off Florida's panhandle and east coasts, as explained in Weisberg et al. (2019).

Given such a nexus between the observed, mid-shelf, near-bottom formation region and the subsequent delivery to the nearshore, is it possible to employ the same coastal ocean circulation argument to account for the eventual cessation of such a *K. brevis* bloom? To address this question, Liu et al. (2022) posed the following: How long might it take for a continuing upwelling circulation to flush the nearshore situated cells back out to sea once an offshore source is depleted? This is a physically reasonable question to ask because we know from Weisberg et al. (2019) that nearshore cells were transported offshore to eventually be entrained into the LC and thus transported to Florida's east coast. A numerical experiment was performed by initializing a normalized tracer concentration (equal to 1.0) at all of the model grid cells (surface to bottom) located inshore of the 10 m isobath from just north of Tampa Bay to Naples, Florida, and then running the model with available local forcing information, including winds, heat fluxes, and river inflows, plus deeper-ocean forcing by LC interaction at the pressure point and elsewhere along the shelf slope. The tracer concentration as a function of time was then compared with the observed cell concentration, with the results showing a qualitative consistency with the observed *K. brevis* cell concentrations (Figure 4).

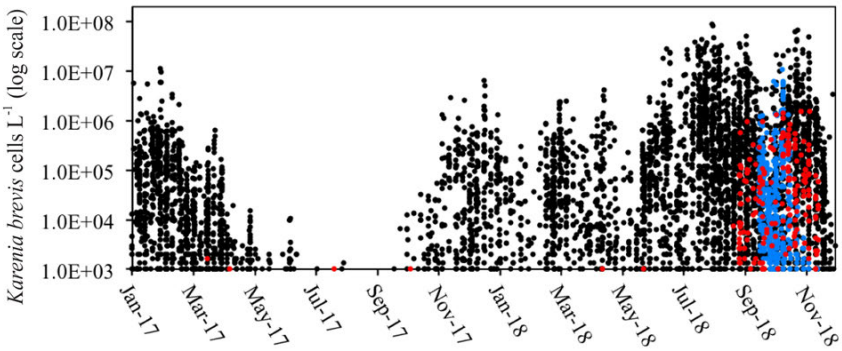

FIGURE 3. *K. brevis* cell counts, plotted using a log scale from January 1, 2017, through December 16, 2018, show the persistence of the *K. brevis* bloom from 2017 through the spring 2018, the increase in intensity in the central west Florida shelf epicenter region in summer 2018 (black dots), and the durations of bloom conditions on the Florida panhandle coast (red dots) and on the Florida east coast (blue). Only samples with ≥10^3 cells per liter are shown. Data source: Florida Fish and Wildlife Conservation Commission - Fish and Wildlife Research Institute HAB monitoring database. *Figure from Weisberg et al. (2019)*

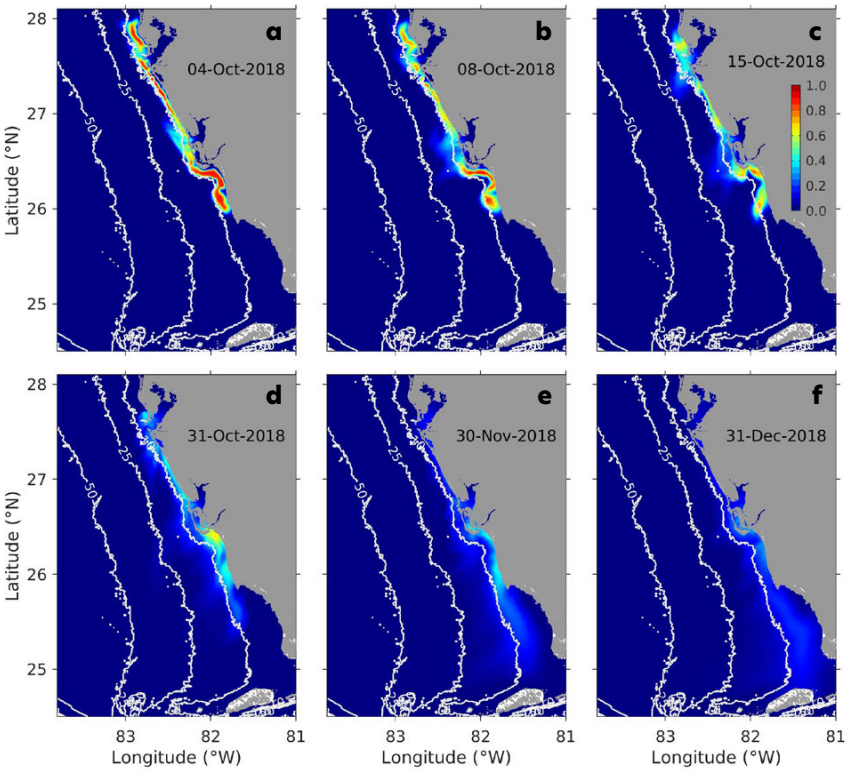

FIGURE 4. Snapshots of model-simulated surface tracer concentrations for the central to southern west Florida shelf relative to the 10 m, 25 m, and 50 m isobaths. The snapshots are sampled after the initial release at (a) three days, (b and c) one and two weeks, respectively, and (d–f) one, two and three months, respectively. The color-coding shows the decrease in tracer concentration. *Adapted from Liu et al. (2022)*

BROADER IMPLICATIONS

While our discussions here focus on the WFS, our findings have broader implications. Whereas all continental shelves respond to both local and deeper-ocean forcing influences, their individual geometries may make these influences less discernible than those for the WFS. For instance, the WFS width enables us to distinguish between inner-shelf and outer-shelf regions and hence the relative imprints imposed by local and deeper-ocean forcings. Additionally, regions like the Dry Tortugas, where shallow isobaths are approachable by adjacent boundary currents, are not limited to the WFS. Cape Hatteras presents an opportunity for the Gulf Stream to impact the entire South Atlantic Bight, and similar situations may occur wherever boundary currents and their associated eddies may come into contact with wide continental shelves at locations where the shelf may narrow down to a Rossby radius of deformation.

CONCLUSION

It would be an oversimplification to say that ocean circulation physics fully controls *K. brevis* bloom evolution, but it is fair to say that ocean circulation physics are on an equal footing with the organism's biology in determining *K. brevis* bloom inception and duration. Subsequent experiments with biological elements added to the otherwise purely physical transport mechanism are yielding modifications, but none that would negate the basic finding that by determining the water properties in which *K. brevis* may, or may not, thrive, plus the mechanism by which *K. brevis* may be transported, the ocean circulation forms an integral part of interdisciplinary harmful algal bloom studies.

What applies to harmful algae should also apply more generally to all matters of coastal ocean ecology. By recognizing that the coastal ocean (whether at the WFS or elsewhere) is driven by a combination of local and deeper ocean forcing factors and that to study these requires coordination between both long-term observations and model simulations, we will collectively continue to advance our knowledge of what controls this essential region where society meets the sea.

REFERENCES

Chassignet, E.P., H.E. Hurlburt, E.J. Metzger, O.M. Smedstad, J. Cummings, G.R. Halliwell, R. Bleck, R. Baraille, A.J. Wallcraft, C. Lozano, and others. 2009. US GODAE: Global Ocean Prediction with the HYbrid Coordinate Ocean Model (HYCOM). *Oceanography* 22:48–59, https://doi.org/10.5670/oceanog.2009.39.

Chen, C.S., H. Liu, and R.C. Beardsley. 2003. An unstructured, finite-volume, three-dimensional, primitive equation ocean model: Application to coastal ocean and estuaries. *Journal of Atmospheric and Oceanic Technology* 20:159–186, https://doi.org/10.1175/1520-0426(2003)020<0159:AUGFVT>2.0.CO;2.

Liu, Y., R.H. Weisberg, J.M. Lenes, L. Zheng, K. Hubbard, and J.J. Walsh. 2016. Offshore forcing on the "pressure point" of the West Florida Shelf: Anomalous upwelling and its influence on harmful algal blooms. *Journal of Geophysical Research: Oceans* 121:5,501–5,515, https://doi.org/10.1002/2016JC011938.

Liu, Y., R.H. Weisberg, L. Zheng, C.A. Heil, and K.A. Hubbard. 2022. Termination of the 2018 Florida red tide event: A tracer model perspective. *Estuarine, Coastal and Shelf Science* 272:107901, https://doi.org/10.1016/j.ecss.2022.107901.

Nickerson, A., R.H. Weisberg, and Y. Liu. 2022. On the evolution of the Gulf of Mexico Loop Current through its penetrative, ring shedding and retracted states. *Advances in Space Research* 69:4,058–4,077, https://doi.org/10.1016/j.asr.2022.03.039.

Walsh, J.J., R.H. Weisberg, D.A. Dieterle, R. He, B.P. Darrow, J.K. Jolliff, K.M. Lester, G.A. Vargo, G.J. Kirkpatrick, K.A. Fanning, and others. 2003. Phytoplankton response to intrusions of slope water on the West Florida Shelf: Models and observations. *Journal of Geophysical Research: Oceans* 108(C6), https://doi.org/10.1029/2002JC001406.

Weisberg, R.H., and R. He. 2003. Local and deep-ocean forcing contributions to anomalous water properties on the West Florida Shelf. *Journal of Geophysical Research: Oceans* 108(C6), https://doi.org/10.1029/2002JC001407.

Weisberg, R.H., L. Zheng, Y. Liu, A.A. Corcoran, C. Lembke, C. Hu, J.M. Lenes, and J.J. Walsh. 2016. *Karenia brevis* blooms on the West Florida Shelf: A comparative study of the robust 2012 bloom and the nearly null 2013 event. *Continental Shelf Research* 120:106–121, https://doi.org/10.1016/j.csr.2016.03.011.

Weisberg, R.H., Y. Liu, C. Lembke, C. Hu, K. Hubbard, and M. Garratt. 2019. The coastal ocean circulation influence on the 2018 West Florida Shelf *K. brevis* red tide bloom. *Journal of Geophysical Research: Oceans* 124:2,501–2,512, https://doi.org/10.1029/2018JC014887.

ACKNOWLEDGMENTS

Current support for this work is by the Southeast Coastal Ocean Observing Regional Association (SECOORA) as a pass-through from NOAA IOOS (award #NA21NOS0120097), a cooperative agreement between NOAA's Office of Coast Survey and the University of South Florida through the Center for Ocean Mapping and Innovative Technologies (COMIT, award #NA20NOS4000227), NOAA National Centers for Coastal Ocean Science Competitive Research Program (award #NA19NOS4780183) for which this is ECOHAB contribution #1114, and the State of Florida through FWC/FWRI (agreement #20035).

AUTHORS

Robert H. Weisberg (weisberg@usf.edu) and **Yonggang Liu**, College of Marine Science, University of South Florida, St. Petersburg, FL, USA.

ARTICLE DOI. https://doi.org/10.5670/oceanog.2025e107

TECHNOLOGICAL SOLUTIONS FOR AN ACCESSIBLE DEEP OCEAN

UNRAVELING MAJOR QUESTIONS IN MICRONEKTON ECOLOGY AND THEIR ROLE IN THE BIOLOGICAL CARBON PUMP THROUGH INTEGRATIVE APPROACHES AND AUTONOMOUS MONITORING

By Pavanee Annasawmy, Guillaume Chandelier, and Thomas Le Mézo

Micronekton consist of crustaceans, cephalopods, gelatinous organisms, and fishes that are 2–20 cm in size (Figure 1). These organisms have unique functional traits that impact their vertical migration patterns and ecosystem processes (Aparecido et al., 2023). Our understanding of their potential carbon transport and sequestration from the epipelagic (upper 200 m) to mesopelagic zones (200–1,000 m) or deeper (e.g., Boyd et al., 2019; Le Moigne, 2019; Cavan et al., 2019) is limited by the tools traditionally used to assess their biomass, diversity, and varied migration patterns (e.g., Annasawmy et al., 2019, 2024; Barbin et al., 2024; Eduardo et al., 2024). These knowledge gaps are notable considering that micronekton are ubiquitous throughout the world ocean.

MAJOR UNCERTAINTIES IN MICRONEKTON RESEARCH

After 200 years of oceanography, the answers to the following major questions remain incomplete due to the limitations of existing conventional approaches used to investigate micronekton such as trawl (and net) sampling and active acoustics:

- What is the global biomass of micronekton?
- What are their ecological patterns, including species richness, functional diversity, and vertical migration?
- What is their role in the biological carbon pump?

Biomass and biodiversity estimates of mesopelagic communities in the ocean vary by an order of 5 to 58 (e.g., Kloser et al., 2009; Irigoien et al., 2014; Dornan et al., 2022) because of net selectivity and catchability limitations (Annasawmy et al., 2019; Kwong et al., 2022; Barbin et al., 2024) and because active acoustics lack taxonomic resolution and do not give direct biomass measurements. Novel eDNA methods offer the potential to fill in knowledge gaps in micronekton diversity and distribution left by traditional tools. However, variations in eDNA sampling collection and analysis methods may influence results and conclusions (Govindarajan et al., 2023a). To bridge the current methodological gaps and for global-scale comparisons, it is crucial to construct open access micronekton DNA reference libraries, establish consensus on optimal primers for detecting micronekton, and integrate eDNA with active acoustics and trawls.

Although contemporary eDNA methods can detect species presence and absence (Govindarajan et al., 2023b), they often rely on ship-based platforms (similar to ship-borne active acoustics and nets) that offer only limited temporal and spatial sampling resolutions. When autonomous platforms are used, knowledge and expertise are currently restricted to larger, northern institutions, generally limiting scientists from the Global South from participating as leaders in deep-sea research (Bell et al., 2023). Research on the biological carbon pump is primarily focused on planktonic organisms and concentrated in the Global North (Pacific and Atlantic Oceans), leaving substantial geographical gaps in the Southern Hemisphere (Kwong et al., 2022; Yang et al., 2024). Technological and geographical gaps in deep-sea research constitute major knowledge gaps, resulting in significant uncertainties regarding the role of micronekton in the biological carbon pump, and, consequently, in climate regulation (Pillar et al., 2024).

FIGURE 1. Examples of micronekton organisms shown here include mesopelagic fishes, cephalopods, gelatinous organisms, and crustaceans. *Photo credit: Gildas Roudaut, Institut de Recherche pour le Développement, Brest, France*

CASE STUDY: PROJECT NEAT AND THE INTEGRATION OF TRADITIONAL AND CONTEMPORARY TOOLS

The project NEAT, funded by the European Marine Research Network (EuroMarine), investigates micronekton ecology in the Western Indian Ocean. Samples were collected in April to May 2022 during the RESILIENCE (fRonts, EddieS and marIne LIfe in the wEstern iNdian oCEan) cruise (Figure 2). The project objective was to integrate the eDNA, acoustic, and trawl data collected to investigate the diversity, abundance, biomass, and distribution of micronekton in the Western Indian Ocean. Migration patterns of the different species were not assessed due to the unbalanced trawl and eDNA sampling designs.

Micronekton specimens were collected using a Mesopelagos trawl net (mean vertical opening: 7 m; horizontal opening: 12 m; mouth area: 65 m^2; length: 44 m; mesh nettings: 30 mm at the front and 4 mm at the cod end) towed at a ship speed of approximately 1.2 knots for a fishing duration of 30 min and at a maximum depth of 70 m. Specimens were divided into four broad categories: fishes, crustaceans, cephalopods, and gelatinous. Wet weight measurements of each broad category were recorded. Organisms are being identified to the lowest taxonomic level possible at the CITEB laboratory (Centre technique, de recherche et de valorisation des milieux aquatiques,

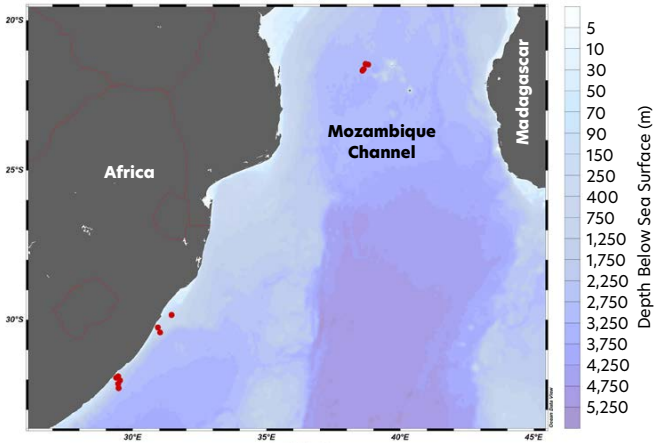

FIGURE 2. With land masses shown in gray, red dots indicate Western Indian Ocean sites where samples were collected during the RESILIENCE cruise, plotted on GEBCO's (General Bathymetric Chart of the Oceans) gridded bathymetric dataset (relative depth below the sea surface in meters; GEBCO_2024 grid) in Ocean Data View software (Schlitzer, 2024).

Reunion Island). Organism abundance (A, ind. m^{-2}) was calculated using the number of individuals captured in each tow (N), volume of water filtered (VF; m^{-3}), and the thickness of the scattering layer (SL thickness of 20 m) according to Kwong et al. (2022):

$$A = \frac{N}{VF} \times SL\ thickness.$$

Dry mass was calculated from wet mass using the percentage water content from each broad category according to Cotté et al. (2022): 75% for fishes and crustaceans, 80% for cephalopods, and 94% for gelatinous organisms. The percentage of C in dry mass was also calculated for each group according to Cotté et al. (2022) as follows: 50% for fishes, 40% for crustaceans, 35% for cephalopods, and 15% for gelatinous organisms. The biomass (mgC m^{-2}) was calculated using the total biomass (B_t) of each broad category per net tow, VF and SL thickness according to Kwong et al. (2022):

$$B = \frac{B_t}{VF} \times SL\ thickness.$$

Seawater from the trawl net cod end was filtered on Millipore cellulose filters of 47 mm diameter and 0.45 µm pore size. The filters were stored at −80°C before being analyzed using the "MiFish-E" primer amplifying a 170 bp fragment of the 12S rRNA gene (Miya et al., 2015), and the "mlCOIintF" primer targeting a 313 bp fragment of the COI (mitochondrial Cytochrome c Oxidase subunit I) gene (Leray et al., 2013). Metabarcoding analyses were conducted at the ADNId laboratory (Montpellier, France). Bioinformatics were conducted using the FROGS pipeline (Escudié et al., 2017; Figure 3). Sequences were clustered into operational taxonomic units (OTUs) using the SWARM v2.1.10 algorithm (Mahe et al., 2015).

In an effort to identify the organisms reflecting the transmitted sound waves, and layers of scattering organisms, a backscatter classification approach based on pairwise frequency differences (S_{v18-38}, S_{v70-38}, and $S_{v120-38}$), called the Ellipsoid score (Escore) algorithm, was developed and used to classify the multifrequency acoustic data (18, 38, 70, 120 kHz) collected using a shipborne SIMRAD EK80

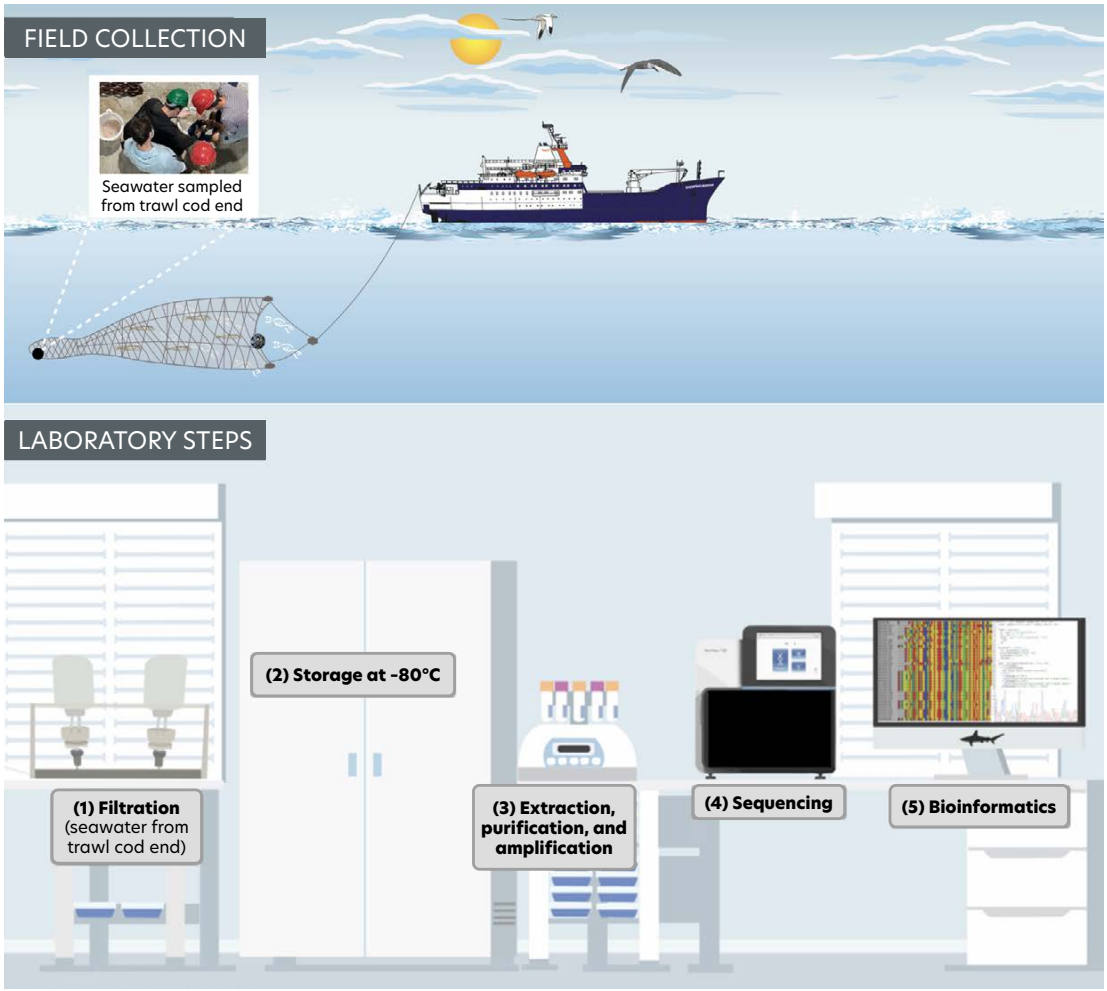

FIGURE 3. Schematic shows apparatus for eDNA field collection and laboratory analyses during the NEAT project. *Image credit: Guillaume Chandelier*

echosounder (Annasawmy et al., 2024). Annasawmy et al. (2024) describe the Escore algorithm in more detail, and the open access code and manual for its implementation are available through the IRD (Institut de recherche pour le développement) Forge website.

The Escore algorithm classified the RESILIENCE cruise acoustic backscatter into groups corresponding to zooplankton-like organisms (echo-class 1); small gelatinous organisms (e.g., siphonophores with pneumatophores) and small gas-bearing fishes of juvenile stages (echo-class 2); organisms with gas bubbles, siphonophores with pneumatophores, and gas-filled swimbladdered mesopelagic fish (echo-class 3); and siphonophores of small sizes (echo-class 4) (Annasawmy et al., 2024; Figure 4).

Fishes were well represented by the Escore algorithm, trawl relative abundance and biomass estimates, and the trawl net cod end eDNA analyses (Figure 4). Cephalopods, although caught in very low numbers, accounted for the majority of the trawl net biomass estimates. In contrast, crustaceans were abundant in the net but contributed the least to the overall biomass estimates. Cephalopods were underrepresented by the Escore algorithm and minimally detected in the eDNA analyses with the primers used in this study. Crustaceans and gelatinous organisms were also completely overlooked in the metabarcoding analyses, despite gelatinous organisms being a dominant group detected by both the Escore algorithm and in trawl net samples.

Future work will investigate species richness from the eDNA samples compared to trawl data. Although cephalopods are often underrepresented in acoustics, trawl, and eDNA data, biomass estimates, and bioenergetic and trait-based models of carbon transport (Aumont et al., 2018; Woodstock et al., 2022), they are significant contributors to carbon transport, as this study demonstrates. The use of a cephalopod-specific universal primer set could enhance the detection of cephalopods in eDNA samples. To be able to estimate cephalopod biomass, it is crucial to improve trawl net sampling and acoustic backscatter classification techniques because squids are weak scatterers and distribute sparsely under natural conditions (Chen et al., 2014).

Biomass and abundance estimations from trawls are limited by net efficiency. Future work will refine biomass estimates by classifying captured organisms into acoustic groups based on their backscattering properties using established acoustic backscattering models for "gas-bearing," "fluid-like," and "elastic-shelled" categories. The relative abundance of each group, determined from net catches, will be used to assess their contribution to water

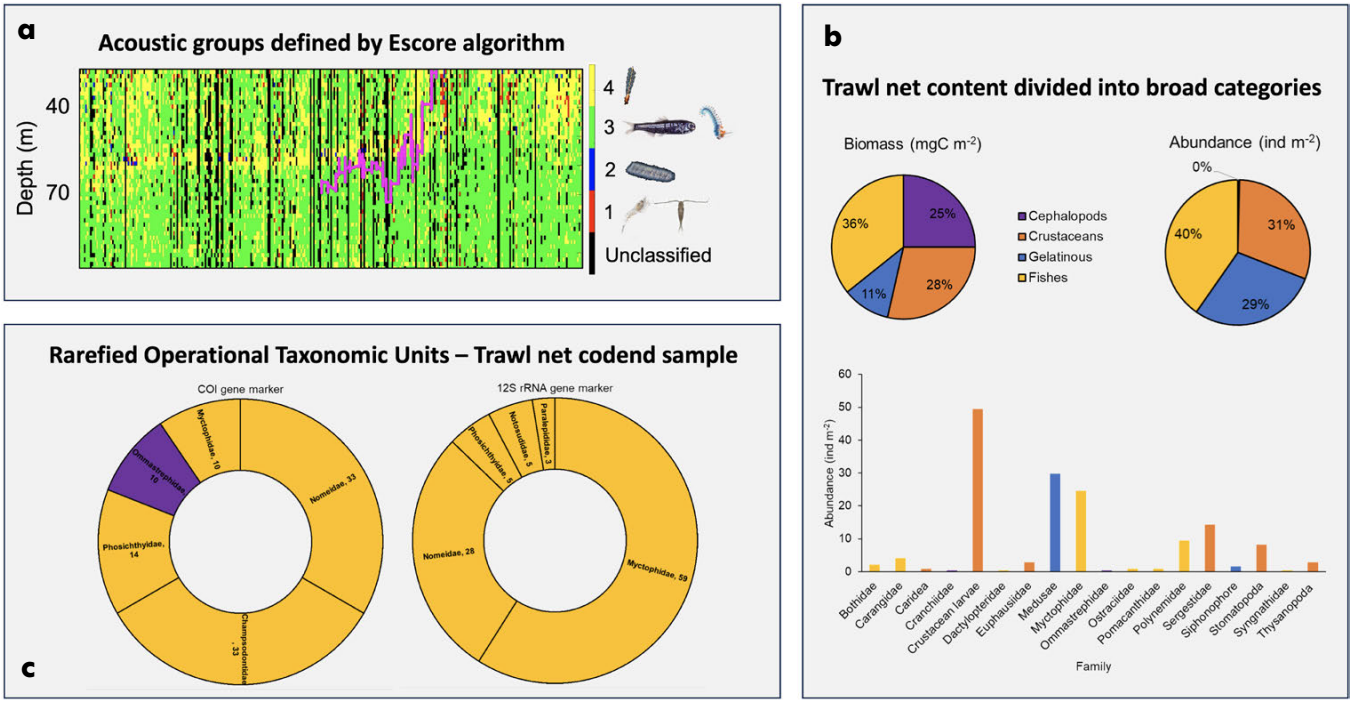

FIGURE 4. (a) One nighttime trawl path of the RESILIENCE cruise (magenta) is plotted here showing the echo classes determined by the Escore algorithm and labeled 1 through to 4. Unclassified acoustic backscatter is shown in black. (b) Analysis of the trawl contents revealed these relative biomass and abundance estimates of cephalopods, crustaceans, gelatinous organisms, and mesopelagic fishes. (c) Plots show percentages of rarefied operational taxonomic units from the trawl net cod end sample for each DNA marker.

column backscattering. Sonar observations will permit the extrapolation of abundances based on actual measured backscattering levels. Biomass will be estimated by combining these abundance estimates with the average wet weight from net catches. Some parameters used to model the organisms' echoes are not known at the species level. The literature offers various hypotheses such as the shape of gas inclusions, the orientation of organisms, and the density contrast with the surrounding medium. To address these uncertainties, scattering models will be run using bootstrapping (1,000 iterations), randomly varying these parameters. Accurate biomass estimations are the major limiting factor in trait-based, bioenergetic, and ecosystemic models of micronekton carbon transport. The approach described above will enhance the accuracy of biomass estimations for micronekton communities, including those underrepresented in trawl samples, while identifying sources of variability and quantifying uncertainties, a necessary first step in quantifying the role of micronekton in the biological carbon pump.

By integrating eDNA, acoustics, and trawl data, NEAT is an example of how traditional tools such as active acoustics and trawls could be used in conjunction with novel eDNA methods to provide information on species presence and absence, abundance, biomass, and distribution in the deep ocean.

PUSHING MICRONEKTON RESEARCH PAST THE CURRENT BOTTLENECKS

While NEAT represents a significant step forward in integrating traditional and novel technologies and addressing key methodological and knowledge gaps, substantial geographical gaps remain because observations have been vessel-based in a localized region of the Indian Ocean and limited to the year 2022. The next step should be to develop a fleet of cost-effective autonomous underwater vehicles (AUVs) each equipped with "acoustic intelligence" (i.e., a computer to process and transmit acoustic data in real time), a camera, and an autonomous eDNA sampler for daily monitoring of micronekton (**Figure 5**). Commercial autonomous samplers are often not cost-effective due to high proprietary costs. Our approach aims to bypass the expense of commercially developed vehicles by investing in research-driven prototypes that could offer greater sensor flexibility, autonomy, and spatio-temporal sampling capacity, allowing for tailored solutions that better serve specific research needs (Le Mézo et al., 2020).

The use of cost-effective AUVs could achieve finer spatial and temporal sampling resolutions by increasing the density of measurements in areas of interest, allowing for year-round investigation of diversity and migration patterns of micronekton taxonomic groups, which has never before been accomplished. Presently, we do not know how the biomass, migration patterns, and carbon transport by micronekton varies year-round. Existing sampling approaches are limited by the high cost of data acquisition, resulting in small temporal sampling resolution with insufficient day-night, monthly, seasonal, or multi-year sampling frequency at any single location done aboard research vessels. Existing models of carbon transport do not incorporate micronekton's migration patterns, accurate biomass estimates, and diets. Development of cost-effective AUVs that integrate active acoustics, optical, and eDNA sensors is crucial for advancing micronekton research in order to address the major questions related to their biomass, diversity, and migration. Answering these questions is a necessary step before tackling more complex issues, such as their role in carbon transport out of the euphotic zone.

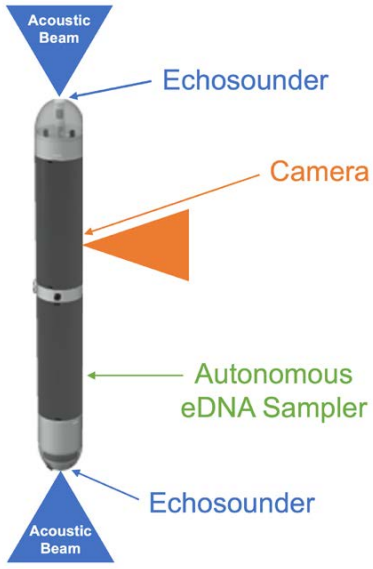

FIGURE 5. Schematic of an idealized autonomous underwater vehicle for micronekton studies.

REFERENCES

Annasawmy, P., J.-F. Ternon, P. Cotel, Y. Cherel, E.V. Romanov, G. Roudaut, A. Lebourges-Dhaussy, F. Ménard, and F. Marsac. 2019. Micronekton distributions and assemblages at two shallow seamounts of the south-western Indian Ocean: Insights from acoustics and mesopelagic trawl data. *Progress in Oceanography* 178:102161, https://doi.org/10.1016/j.pocean.2019.102161.

Annasawmy, P., G. Roudaut, and A. Lebourges Dhaussy. 2024. Impact of an eddy dipole of the Mozambique channel on mesopelagic organisms, highlighted by multifrequency backscatter classification. *PLoS ONE* 19(9):e0309840, https://doi.org/10.1371/journal.pone.0309840.

Aparecido, K.C., T. Frédou, L.N. Eduardo, M.M. Mincarone, R.S. Lima, M.F.D.S. Morais, and B. Mérigot. 2023. Living in darkness: Functional diversity of mesopelagic fishes in the western tropical Atlantic. *Frontiers in Marine Science* 10:1117806, https://doi.org/10.3389/fmars.2023.1117806.

Aumont, O., O. Maury, S. Lefort, and L. Bopp. 2018. Evaluating the potential impacts of the diurnal vertical migration by marine organisms on marine biogeochemistry. *Global Biogeochemical Cycles* 32:1,622–1,643, https://doi.org/10.1029/2018GB005886.

Barbin, L., A. Lebourges-Dhaussy, V. Allain, A. Receveur, P. Lehodey, J. Habasque, E. Vourey, A. Portal, G. Roudaut, and C. Menkes. 2024. Comparative analysis of day and night micronekton abundance estimates in west Pacific between acoustic and trawl surveys. *Deep Sea Research Part I* 204:104221, https://doi.org/10.1016/j.dsr.2023.104221.

Bell, K.L.C., M.C. Quinzin, D. Amon, S. Poulton, A. Hope, O. Sarti, T.E. Cañete, A.M. Smith, H.I. Baldwin, D.M. Lira, and others. 2023. Exposing inequities in deep-sea exploration and research: Results of the 2022 Global Deep-Sea Capacity Assessment. *Frontiers in Marine Science* 10:1217227, https://doi.org/10.3389/fmars.2023.1217227.

Boyd, P.W., H. Claustre, M. Levy, D.A. Siegel, and T. Weber. 2019. Multi-faceted particle pumps drive carbon sequestration in the ocean. *Nature* 568:327–335, https://doi.org/10.1038/s41586-019-1098-2.

Cavan, E.L., E.C. Laurenceau-Cornec, M. Bressac, and P.W. Boyd. 2019. Exploring the ecology of the mesopelagic biological pump. *Progress in Oceanography* 176:102125, https://doi.org/10.1016/j.pocean.2019.102125.

Chen, G.B., J. Zhang, J. Yu, J.T. Fan, and L.C. Fang. 2014. Hydroacoustic scattering characteristics and biomass assessment of the purple-back flying squid (*Sthenoteuthis oualaniensis*) from the deep water area of the South China Sea. Pp. 49–62 in *Progress in the Application of Acoustics in Inland and Estuarine Fishery Research*. H. Rosenthal, Q. Wei, and P. Bronzi, eds, World Conservation Society, Special Publication no. 6, Books on Demand, Norderstedt, Germany.

Cotté, C., A. Ariza, A. Berne, J. Habasque, A. Lebourges-Dhaussy, G. Roudaut, B. Espinasse, B.P.V. Hunt, E.A. Pakhomov, N. Henschke, and others. 2022. Macrozooplankton and micronekton diversity and associated carbon vertical patterns and fluxes under distinct productive conditions around the Kerguelen Islands. *Journal of Marine Systems* 226:103650, https://doi.org/10.1016/j.jmarsys.2021.103650.

Dornan, T., S. Fielding, S.A. Saunders, and M.J. Genner. 2022. Large mesopelagic fish biomass in the Southern Ocean resolved by acoustic properties. *Proceedings of the Royal Society B* 289:20211781, https://doi.org/10.1098/rspb.2021.1781.

Eduardo, L.N., M.M. Mincarone, T. Sutton, and A. Bertrand. 2024. Deep-pelagic fishes are anything but similar: A global synthesis. *Ecology Letters* 27(9):e14510, https://doi.org/10.1111/ele.14510.

Escudié, F., L. Auer, M. Bernard, M. Mariadassou, L. Cauquil, K. Vidal, S. Maman, G. Hernandez-Raquet, S. Combes, and G. Pascal. 2017. FROGS: Find, Rapidly, OTUs with Galaxy Solution. *Bioinformatics* 34:1,287–1,294, https://doi.org/10.1093/bioinformatics/btx791.

Govindarajan, A.F., A. Adams, E. Allan, S. Herrera, A. Lavery, J. Llopiz, L. McCartin, D.R. Yoerger, and W. Zhang. 2023a. Advances in environmental DNA sampling for observing ocean twilight zone animal diversity. Pp. 80–86 in *Frontiers in Ocean Observing: Emerging Technologies for Understanding and Managing a Changing Ocean*. E.S. Kappel, V. Cullen, M.J. Costello, L. Galgani, C. Gordó-Vilaseca, A. Govindarajan, S. Kouhi, C. Lavin, L. McCartin, J.D. Müller, B. Pirenne, T. Tanhua, Q. Zhao, and S. Zhao, eds, *Oceanography* 36(Supplement 1), https://doi.org/10.5670/oceanog.2023.s1.27.

Govindarajan, A.F., J.K. Llopiz, P.E. Caiger, M.J. Jech, A.C. Lavery, H. McMonagle, P.H. Wiebe, and W. Zhang. 2023b. Assessing mesopelagic fish diversity and diel vertical migration with environmental DNA. *Frontiers in Marine Science* 10:1219993, https://doi.org/10.3389/fmars.2023.1219993.

Irigoien, X., T.A. Klevjer, A. Røstad, U. Martinez, G. Boyra, J.L. Acuña, A. Bode, F. Echevarria, J.I. Gonzalez-Gordillo, S. Hernandez-Leon, and S. Agusti. 2014. Large mesopelagic fishes biomass and trophic efficiency in the open ocean. *Nature Communications* 5(1):3271, https://doi.org/10.1038/ncomms4271.

Kloser, R.J., T.E. Ryan, J.W. Young, and M.E. Lewis. 2009. Acoustic observations of micronekton fish on the scale of an ocean basin: Potential and challenges. *ICES Journal of Marine Science* 66(6):998–1,006, https://doi.org/10.1093/icesjms/fsp077.

Kwong, L.E., A.A. Bahl, and E.A. Pakhomov. 2022. Variability in micronekton active carbon transport estimates on the Southwest Coast of Oahu using three different sampling gears. *Frontiers in Marine Science* 9:948485, https://doi.org/10.3389/fmars.2022.948485.

Le Mézo, T., G. Le Maillot, T. Ropert, L. Jaulin, A. Ponte, and B. Zerr. 2020. Design and control of a low-cost autonomous profiling float. *Mechanics & Industry* 21:512, https://doi.org/10.1051/meca/2020037.

Le Moigne, F.A.C. 2019. Pathways of organic carbon downward transport by the oceanic biological carbon pump. *Frontiers in Marine Science* 6:634, https://doi.org/10.3389/fmars.2019.00634.

Leray, M., J.Y., Yang, C.P. Meyer, S.C. Mills, N. Agudelo, V. Ranwez, J.T. Boehm, and R.J. Machida. 2013. A new versatile primer set targeting a short fragment of the mitochondrial COI region for metabarcoding metazoan diversity: Application for characterizing coral reef fish gut contents. *Frontiers in Zoology* 10:34, https://doi.org/10.1186/1742-9994-10-34.

Mahe, F., T. Rognes, C. Quince, C. De Vargas, and M. Dunthorn. 2015. Swarm v2: Highly-scalable and high-resolution amplicon clustering. *PeerJ* 3:e1420, https://doi.org/10.7717/peerj.1420.

Miya, M., Y. Sato, T. Fukunaga, T. Sado, J.Y. Poulsen, K. Sato, T. Minamoto, S. Yamamoto, H. Yamanaka, H. Araki, and others. 2015. MiFish, a set of universal PCR primers for metabarcoding environmental DNA from fishes: Detection of more than 230 subtropical marine species. *Royal Society Open Science* 2:150088, https://doi.org/10.1098/rsos.150088.

Pillar, H.R., E. Hetherington, L.A. Levin, L. Cimoli, J.M. Lauderdale, J.M.A. van der Grient, K. Johannes, P. Heimbach, L. Smith, C.I. Addey, and others. 2024. Future directions for deep ocean climate science and evidence-based decision making. *Frontiers in Climate Science* 6:1445694, https://doi.org/10.3389/fclim.2024.1445694.

Schlitzer, R. 2024. Ocean Data View, http://odv.awi.de.

Woodstock, M.S., T.T. Sutton, and Y. Zhang. 2022. A trait-based carbon export model for mesopelagic fishes in the Gulf of Mexico with consideration of asynchronous vertical migration, flux boundaries, and feeding guilds. *Limnology and Oceanography* 7(7):1,443–1,455, https://doi.org/10.1002/lno.12093.

Yang, N., D. Jin, and A.F. Govindarajan. 2024. Applying environmental DNA approaches to inform marine biodiversity conservation: The case of the Ocean Twilight Zone. *Marine Policy* 165:106151, https://doi.org/10.1016/j.marpol.2024.106151.

ACKNOWLEDGMENTS

We thank the anonymous reviewers for their careful reading of our manuscript and their many insightful comments and suggestions. The authors acknowledge the captain, crew, and scientific staff of R/V *Marion Dufresne* for their assistance during the research cruise RESILIENCE. The chief scientist, Jean-François Ternon (IRD, Sète, France), and co-principal investigators, Margaux Noyon (Nelson Mandela University, South Africa), Steven Herbette (Laboratoire d'Oceanographie Physique et Spatiale, Brest, France) and Pierrick Penven (IRD, Brest, France) are further acknowledged for their support and assistance with biological and environmental data acquisition during the cruise. We extend our gratitude to Arthur Blanluet (University of Queensland, Australia), Anne Lebourges Dhaussy (IRD, Brest, France), and the master's students from the ISblue (Interdisciplinary graduate School for the blue planet) floating university (Université de Bretagne Occidentale, Université du Littoral Côte d'Opale, Université Côte d'Azur) and their coordinators, for their help with the trawl and acoustic data collection. Micronekton taxonomic identification is being conducted by Evgeny Romanov (CITEB, Reunion Island). The RESILIENCE oceanographic cruise was supported by the French National Oceanographic Fleet, by the Belmont Forum Ocean Front Change project, implemented through the French National Research Agency (ANR-20-BFOC-0006-04), by the ISblue project, Interdisciplinary graduate school for the blue planet (ANR-17-EURE-0015) and co-funded by a grant from the French government under the program Investissements d'Avenir embedded in France 2030. The eDNA analyses were partly supported by the French National program LEFE (Les Enveloppes Fluides et l'Environnement) coordinated by the CNRS (Centre national de la recherche scientifique) through a grant awarded in 2022. The eDNA analyses were also supported by EuroMarine Association, through its 2023 funding programme for Cooperation Projects led by Early Career Researchers, managed by OYSTER (Orienting Young ScienTists of EuromaRine).

AUTHORS

Pavanee Annasawmy (angelee-pavanee.annasawmy@ird.fr), Foundation for Biodiversity Research-Center for the Synthesis and Analysis of Biodiversity (FRB-CESAB), Montpellier, France. **Guillaume Chandelier**, Florida International University, Marine Conservation Ecology Lab, North Miami, FL, USA. **Thomas Le Mézo**, École Nationale Supérieure de Techniques Avancées (ENSTA), LabSTICC M3, Bretagne, Brest, France.

ARTICLE DOI. https://doi.org/10.5670/oceanog.2025e118

REAL-TIME DATA CONNECTIVITY TO DEEP AUTONOMOUS SEAFLOOR INSTRUMENTATION IN ADVERSE FLOW CONDITIONS

By Christopher Ewert, Romain Heux, Noah Howins, Matthias Lankhorst, Gaston Manta, and Uwe Send

INTRODUCTION

Many straits and passages between ocean basins or regional seas exhibit strong flows that are difficult to observe yet represent important controls or exchange mechanisms for the adjacent regions. Examples are the Denmark Strait in the North Atlantic, the Indonesian Throughflows between the Pacific and Indian Oceans, the Strait of Gibraltar at the entrance of the Mediterranean, and the Yucatán Channel as the source region of the Loop Current in the Gulf of Mexico. In most cases, the subsurface structures of these flows are important, as is density or temperature layering, and in some cases, there is a clear two-layer separation between inflow and outflow layers. These important interior conditions are usually not observable from space or with other remote-sensing methods. Thus, in situ instruments are required.

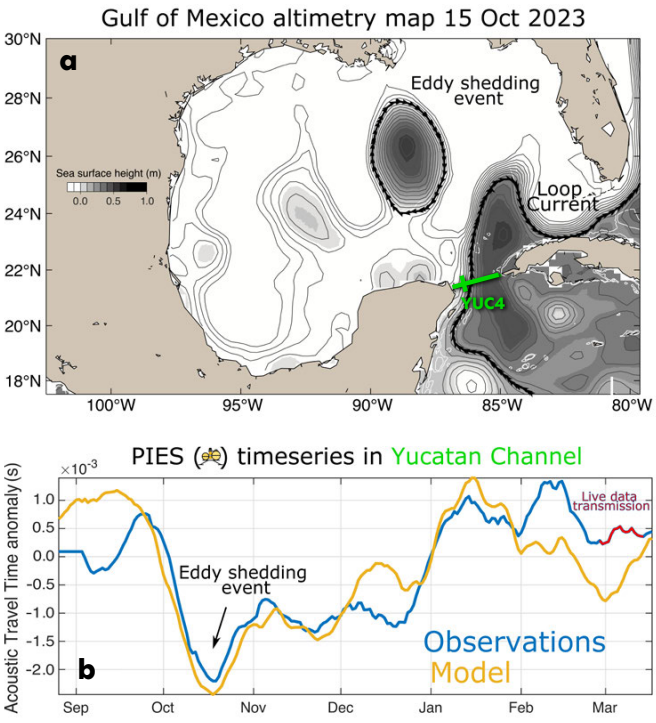

FIGURE 1. (a) Gulf of Mexico altimetry map during October 15, 2023, after an eddy-shedding event from the Gulf of Mexico's Loop Current. Contours show sea surface height (m), and bold black contours show the Loop Current, the eddy, and eddy surface currents. (b) Time series of vertical acoustic travel time anomaly measured by the bottom-mounted pressure-sensing inverted echosounder (PIES) at site YUC4 in the Yucatán Channel (at marked location on the green line in panel a) and retrieved acoustically (blue), and Hybrid Coordinate Ocean Model (HyCOM) output for the same quantity (yellow). The period of live data transmission with the test mooring is shown in red (the remaining data were retrieved acoustically from a small boat). The eddy-shedding event moment shown in (a) is marked with a black arrow in the time series. This study was conducted using EU Copernicus Marine Service Information, https://doi.org/10.48670/moi-00148.

One example is the application discussed here, the use of bottom-mounted pressure-sensing inverted echosounders (PIESs) to track the vertical structure and the horizontal displacement of the Yucatán Current, where the lateral position is needed with higher temporal resolution than, for example, satellite altimetry can provide. The horizontal displacement of the Loop Current has been related to its growth/decay downstream, westward displacement being associated with Loop Current growth (Manta et al., 2023). Modeling studies show that the deep flow within the Loop Current below 1,000 m, which is not measurable by surface sensing, may also be predictable (Vazquez et al., 2023).

Figure 1a shows a snapshot of the Gulf of Mexico after an eddy-shedding event. Such eddies represent intense flow anomalies that are important for predicting the security of oil rigs operating in the Gulf. In the Yucatán Channel, PIESs measure bottom pressure and vertical acoustic travel time between the seafloor and the sea surface. Preliminary data from a test deployment there show that roughly two weeks before the shedding event, the PIESs measured a continuous reduction in acoustic travel time (Figure 1b). The use case here demonstrates that if real-time data from PIESs were available and fed into numerical models, such event predictions are possible.

Due to cost and personnel availability, crewed ships are not an option for continuous, year-round data collection on these flows. Equally, autonomous vehicles such as underwater gliders, Wave Gliders, and Saildrones cannot hold position in strong currents. It is also difficult to anchor and maintain a surface buoy in extreme current conditions. The challenge is to find an approach that enables real-time data delivery from subsurface instruments in such strong-flow regimes. Other than laying a cable on the seafloor, the most feasible technology in deep ocean data acquisition is acoustic telemetry. This requires a surface platform to perform underwater telemetry and to relay the data to shore via satellite. Here, we present a simple solution that was developed for currents exceeding 4 knots and demonstrate that data telemetry from bottom-mounted PIESs in such environments is possible.

The application described here is an array of five PIESs spanning the Yucatán Channel at approximately 21°40'N, ranging in depth from 250 m to 1,800 m. This is a challenging environment due to strong currents (often 3–4 kts), the presence of a major shipping lane, and the prevalence of *Sargassum* seaweed.

MOORING DESIGN

Given these conditions and the possibility of losing the float (e.g., from ship strikes, fish bites, fishing line entanglement), the Yucatán Channel mooring design needed to be simple, low-cost, and easy to deploy, and the surface float had to minimize drag and shed *Sargassum*. A long cylinder, tapered at both ends, was chosen as the float design because it can tilt in strong currents and is likely to shed *Sargassum* when horizontal at the surface.

To maximize the use of off-the-shelf components and minimize cost, our design uses several 14-inch fishing trawl floats protected and streamlined by a large 16-inch industrial PVC pipe. The electronics and transmitters are housed under a UV-protective plastic cone at the top of the float, and the acoustic modem is installed inside a self-poured polyurethane cone at the bottom. The Iridium antenna inside the Delrin transmitter pressure case is angled so that it roughly points upward during typical float tilts, and the float has a ballasting weight designed to rotate into the desired orientation. The use of these parts allows for cheap and quick turnaround, as almost everything is made in-house, eliminating potentially long lead times and outsourcing costs. Overall, the final material and machining to produce a single (unloaded) telemetry float cost just under $6,000. With all instruments and electronics (portable acoustic modem, controller, Iridium transmitter, and GPS beacon), the total expenditure was about $27,000. These costs are expected to decrease as more moorings are built, because the largest expenses were incurred for single prototype runs of custom parts or pressure cases. Figure 2 shows the current design for deployment with our custom payload. All components are designed to withstand depths of more than 300 m, because we expect the surface float to be pulled underwater for short periods in the most intense currents phases. This could also help to shed *Sargassum*.

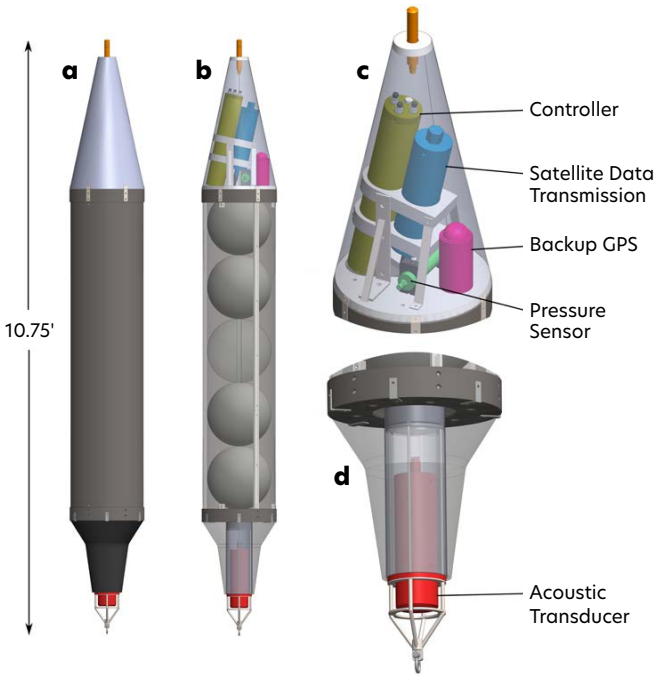

FIGURE 2. (a) CAD rendering of the second version of the float. (b) A transparent view shows the payloads at the top and bottom of the float and five trawl floats inside the PVC pipe between them. Close-ups illustrate the modular payloads at the top (c) and bottom (d) of the float.

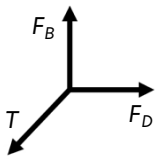

For a steady-state orientation of a mooring surface float in the current, the horizontal drag force (F_D) induced by the currents can only be compensated by the horizontal component of the tension (T) on the mooring line below the float. This (downward) tension is determined by the combination of drag and (upward) buoyancy force (F_B). Therefore, a small buoyancy will lead to a more horizontal mooring line, making it difficult to keep the float at the surface. Because we had already used the largest available trawl floats, buoyancy could only be increased by lengthening the float. However, both the drag and the volume of a (vertical) cylinder in constant flow scale linearly with length. Therefore, the angle of the mooring line is not changed by increasing the cylinder length (only line tension changes). Simulations with a static mooring design program (IMP, updated from Helmbrecht, 2001) confirmed that performance did not change much between using, for example, nine trawl floats or five. Detailed simulations suggested that five floats were a good option. This gave a net float buoyancy with all electronics and hardware installed of 63 kg (80 kg without electronics).

To minimize the drag on the remaining mooring components, we use thin synthetic line (1/8-inch Amsteel) wherever possible. Because the currents in the Yucatán Channel are surface intensified with the strongest currents in the upper 150–200 m, standard 17-inch glass floats can be added below the strong currents without adding too much drag, helping to keep the mooring vertical. Given the drag-buoyancy ratio of the top float, a large mooring tilt of order 70° results, which requires a long line to cover the uppermost water column. The resulting design is outlined in Figure 3 for the test deployment (see below) in 1,650 m water depth. The drag forces are substantial: order 150 kg for the top float, and the tension near the anchor can approach 500 kg. Therefore, the required anchor weight varies between 600 kg and 1,000 kg, depending on water depth.

TEST DEPLOYMENT

In August 2024, the mooring was deployed for four weeks in 1,650 m of water near a PIES in the Yucatán Channel (Figure 3). This site was next to the YUCi5 mooring of the Canek current meter array established in 1999 (Sheinbaum et al., 2002; Candela et al., 2019). The float typically surfaced twice per day and remained at the surface approximately 75% of the time, despite the Yucatán Current being near peak strength. When the float was knocked down by strong currents, data were still retrieved acoustically, stored, and then transmitted once the float returned to the surface. The float's ability to reach the surface in strong currents was likely due to tides, which periodically weaken even in the strongest currents. The rate of transmission matched the rate of data collection, giving a truly real-time delivery of PIES data with latencies of fewer than 24 hours. This deployment followed a previous successful test in 500 m of water that showcased the moorings' ability to perform in varying depths. The two moorings were nearly identical in design, only needing to be scaled up by increasing mooring line length and adding mid-mooring flotation via additional 17-inch glass spheres. The maximum deployment duration of a PIES is four years; we present energy and transmission budgets for the remote modem for this duration below. For shorter deployments, more data can be transmitted.

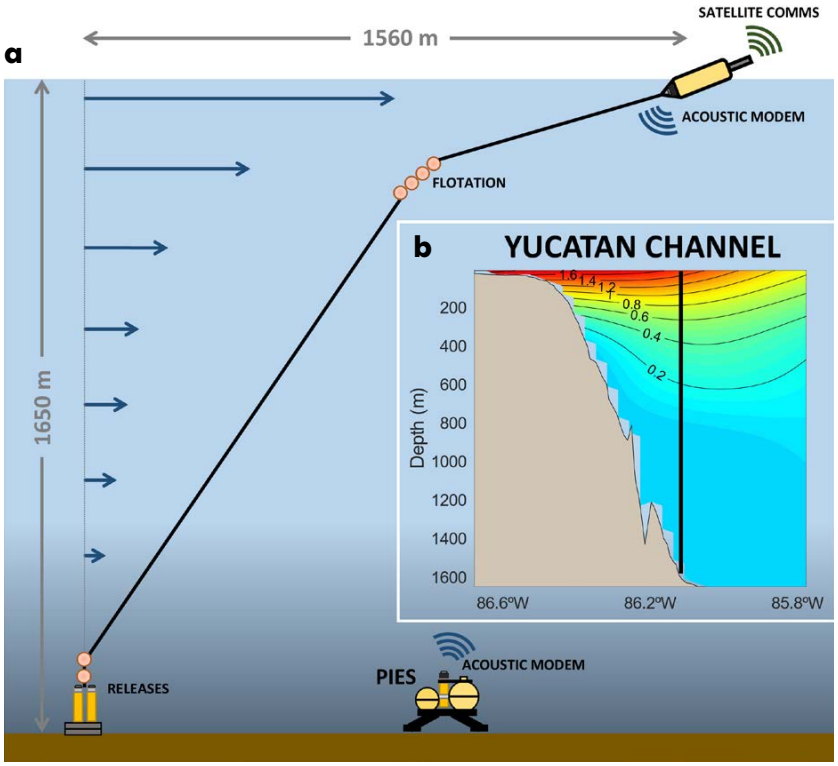

FIGURE 3. (a) A conceptual layout of the mooring design shows the relative positioning and proximity of the float and the PIES to one another for the 1,650 m deep test deployment. The vertical/horizontal aspect ratio is true and shows the actual geometry. (b) The western part of the Yucatán Channel with northward currents in m s^{-1} contoured for a typical strong-flow situation mapped from the Canek current meter array (Sheinbaum et al., 2002; Ochoa et al., 2003; Candela et al., 2019). The heavy vertical line shows the location of the 1,650 m deep PIES for the test deployment.

PIES DATA TRANSMISSION: DATA RATES AND ENERGY BUDGET

Here, we present a data rate and energy budget for the deployment described above to illustrate the capabilities and limitations of typical acoustic modems, using PIESs as an example. These instruments are made by the University of Rhode Island (Kennelly et al., 2022), with a custom modification to output data through a serial port installed in the glass sphere. A Teledyne Benthos acoustic modem (ATM-9 series) with a low-frequency transducer is attached to each PIES so that data can be recovered acoustically via an underwater glider (Send et al., 2013), from a surface vessel, or via a mooring. The PIES takes one sample every 10 minutes (one pressure and four acoustic travel time readings) and stores the single samples internally, but only sends the last value obtained at the end of every hour to the acoustic modem. This amounts to 597 bytes per day or 217,905 bytes per year. These data are stored permanently in the modem memory and can be downloaded at any time by another acoustic modem located within 8–10 km.

In our application, there will be a mooring with a surface expression that contains a controller interfaced with an acoustic modem and a satellite modem. The controller uses the acoustic modem to download data from the remote PIES acoustic modem, and the data are then both stored internally and sent through the satellite system (Iridium using RUDICS protocol). Each byte takes about 2.12 J to be stored and sent acoustically in average conditions (30 bytes per second selected download speed with a 300 baud setting in the modem), maximum transmission power, and a transmission success rate of 67%. During deployment, the remote modem is in one of four different states, each requiring the following energy over four years (values are given for daily downloads and for downloads every four days):

1. Data storing, when receiving data from a PIES via RS-232 (609 kJ per day/609 kJ per four days)

2. Link establishment, when a remote modem tries to start an acoustic communication with the PIES modem at the beginning of each download (852 kJ/213 kJ)
3. Data transmission, when sending data over the acoustic link to the buoy modem (902 kJ/1,027 kJ)
4. Quiescent/sleep mode (1,766 kJ/1,766 kJ)

This energy output would result in about 95% (daily) or 83% (every four days) of the entire lithium battery pack capacity for storing and sending data after four years. In addition, the time needed for sending commands and handshaking reduces the effective download speed, depending on:

1. Distance between the acoustic modems
2. Retry rate
3. Packet size (a data request command needs to be sent for each data packet)

This effective download speed can be estimated as (assuming 1,500 m s^{-1} average sound speed and 3 s total time for each command to be internally processed by the modems):

$$effective\ speed = \frac{packet\ size}{\left(\frac{packet\ size}{theoretical\ speed} + \frac{distance\ to\ PIES}{1{,}500} * 2 + 3\right)} \div retry\ rate$$

For a typical setup on the Yucatán Channel PIESs, where we conservatively achieve a 30 B s^{-1} theoretical speed, a distance of 4,000 m, a packet size of 500 bytes, and a retry rate of 1.5, we get an effective speed of 13 B s^{-1}, so less than half the theoretical speed. If we reduce the packet size to 250 bytes, we get only 10 B s^{-1}, one-third of the theoretical speed.

DISCUSSION

Although still in a preliminary design stage, this simple telemetry mooring has demonstrated its potential with several successful test deployments in 500 m and 1,650 m of water, while successfully sending data that have been used for Loop Current predictions. Even in peak flow conditions in Yucatán Channel, the float reached the surface typically twice per day, likely when tidal flows reduced the current speeds a bit. The float is designed for low cost, in terms of both construction and operation, allowing for deployments in larger numbers or with frequent replacements. The entire mooring can be deployed by hand from a smaller boat (the anchor can be tipped into the water with a simple wooden platform). The float also allows for both hardware and software customization to, for example, accommodate different sensor types such as CTDs or pumped optical sensors like fluorometers or oxygen optodes. In the ongoing project in the Yucatán Channel, we have already added data transmission from additional bottom-mounted temperature/salinity sensors, and are considering adding telemetry from bottom-mounted current meters to better characterize the channel's throughflow. Given the current success, a future cruise has been scheduled for August 2025 to deploy three more floats at various water depths along with current profilers to complete the array and to permit real-time transmission of all our PIES data. While this new design is still being tested and improved, it has successfully demonstrated remote data acquisition in harsh environments with modest hardware investment: near-continuous, real-time data from far beneath the strongest ocean currents can indeed be collected. This advancement opens the door for real-time data applications from deep-water sites that were previously inaccessible.

REFERENCES

Candela, J., J. Ochoa, J. Sheinbaum, M. Lopez, P. Perez-Brunius, M. Tenreiro, E. Pallàs-Sanz, G. Athié, and L. Arriaza-Oliveros. 2019. The flow through the Gulf of Mexico. *Journal of Physical Oceanography* 49(6):1,381–1,401, https://doi.org/10.1175/JPO-D-18-0189.1.

Helmbrecht, L. 2001. Entwicklung einer Verankerungssimulation als Designhilfe und zur Verbesserung der Datenanalyse. Academic thesis paper, Mathematisch-Naturwissenschaftliche Fakultät, Christian-Albrechts-Universität, Kiel, Germany, 118 pp., https://oceanrep.geomar.de/id/eprint/5943.

Kennelly, M., K.L. Tracey, K.A. Donohue, and D.R. Watts. 2022. *PIES and CPIES Data Processing Manual*. Physical Oceanography Technical Reports, Paper 38, University of Rhode Island, Narragansett, RI, https://digitalcommons.uri.edu/physical_oceanography_techrpts/38.

Manta, G., G. Durante, J. Candela, U. Send, J. Sheinbaum, M. Lankhorst, and R. Laxenaire. 2023. Predicting the Loop Current dynamics combining altimetry and deep flow measurements through the Yucatan Channel. *Frontiers in Marine Science* 10:1156159, https://doi.org/10.3389/fmars.2023.1156159.

Send, U., L. Regier, and B. Jones. 2013. Use of underwater gliders for acoustic data retrieval from subsurface oceanographic instrumentation and bi-directional communication in the deep ocean. *Journal of Atmospheric and Oceanic Technology* 30(5):984–998, https://doi.org/10.1175/JTECH-D-11-00169.1.

Sheinbaum, J., J. Candela, A. Badan, and J. Ochoa. 2002. Flow structure and transport in the Yucatan Channel. *Geophysical Research Letters* 29(3):10-1–10-4, https://doi.org/10.1029/2001GL013990.

Vazquez, H.J., G. Gopalakrishnan, and J. Sheinbaum. 2023. Impact of Yucatan Channel subsurface velocity observations on the Gulf of Mexico state estimates. *Journal of Physical Oceanography* 53(1):361–385, https://doi.org/10.1175/JPO-D-21-0213.1.

ACKNOWLEDGMENTS

This work was supported by the Gulf Research Program of the National Academies of Sciences, Engineering, and Medicine under award numbers 2000011057 and 200013145.

AUTHORS

Christopher Ewert (cewert@ucsd.edu), **Romain Heux**, **Noah Howins**, **Matthias Lankhorst**, **Gaston Manta**, and **Uwe Send**, Scripps Institution of Oceanography, University of California San Diego, La Jolla, CA, USA

ARTICLE DOI. https://doi.org/10.5670/oceanog.2025e119

INTERFEROMETRIC SYNTHETIC APERTURE SONAR: A NEW TOOL FOR SEAFLOOR CHARACTERIZATION

By John W. Jamieson, Caroline Gini, Craig Brown, and Katleen Robert

Interferometric synthetic aperture sonar (InSAS) is an emerging sonar technology for high-resolution mapping and imaging of the seafloor. This technology is increasingly utilized for defense- and commercial-related applications. However, its application for scientific and environmental purposes remains limited. In this article, we describe the development of InSAS as a tool for seafloor characterization. We discuss the potential applications for InSAS that extend its use beyond traditional defense and offshore infrastructure related surveys to applications for habitat classification, environmental monitoring, and seafloor geological characterization.

SEAFLOOR EXPLORATION

Exploration of the deep seafloor commonly involves the acquisition of two different types of data: direct imaging from optical surveys and geophysical remote sensing using sonar-based surveys. Optical, or visual, surveys use cameras mounted on underwater vehicles or towed platforms, and, more recently, lidar and other laser-based systems. These types of surveys provide the most detail so that when using cameras, a "true" image of the seafloor is obtained. However, optical surveys are limited by the very restricted field of view (meters to maybe tens of meters) in front of or below the camera or laser system, making these types of surveys impractical for covering large areas of the seafloor.

Acoustic-based surveys, such as a multibeam echosounders or side-scan sonars, produce digital elevation models and associated backscatter intensity maps of the seafloor using sonar systems mounted on surface vessels or on underwater and towed vehicles. Sonar systems rely on the effective propagation of sound through water over large distances, compared to optical surveys that rely on light, which attenuates quickly in water. Sonar systems can therefore cover much wider areas (up to several kilometers on either side of a survey line for deep water systems) to measure seafloor bathymetry (depth) and associated backscatter intensity maps (in the case of multibeam surveys) or backscatter-based acoustic images of the seafloor (in the case of side-scan sonar surveys).

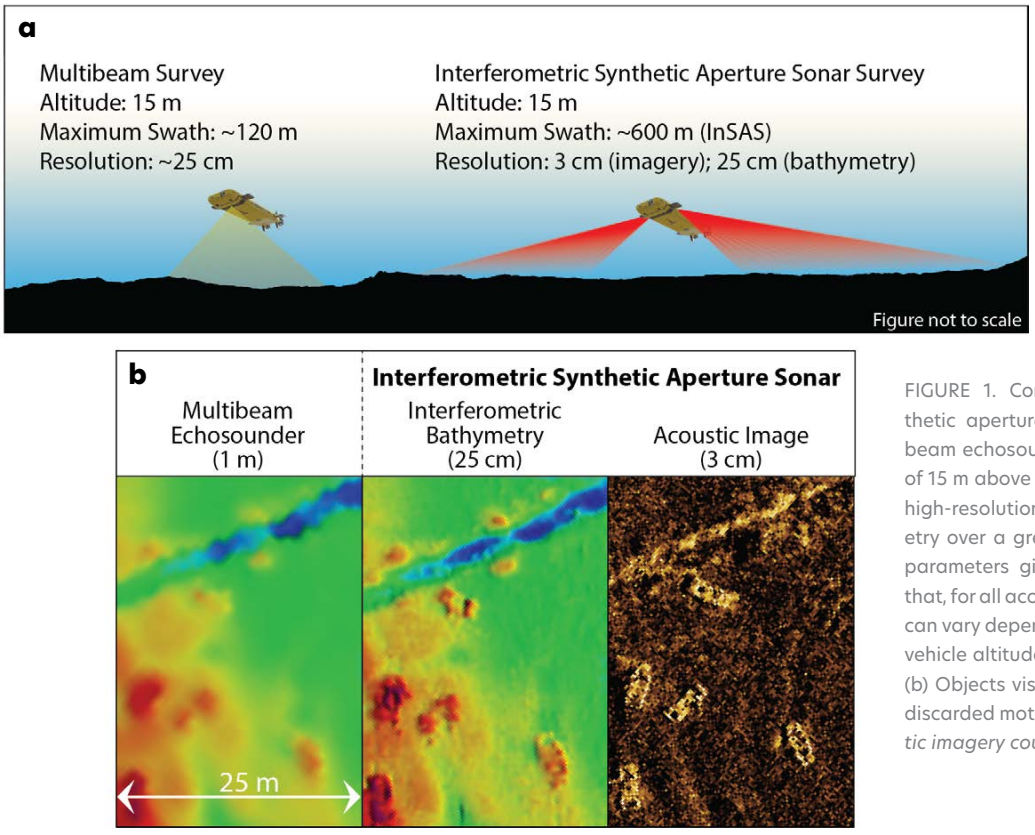

FIGURE 1. Comparison of interferometric synthetic aperture sonar (InSAS) surveys to multibeam echosounder surveys, flown at an altitude of 15 m above seafloor. (a) InSAS surveys provide high-resolution acoustic imagery and bathymetry over a greater swath. Note that the survey parameters given here are examples only and that, for all acoustic surveys, resolution and swath can vary depending on the sonar frequency used, vehicle altitude, beam angles, and survey speed. (b) Objects visible on seafloor in the images are discarded motor vehicles. *Bathymetry and acoustic imagery courtesy of Kraken Robotics*

The spatial advantages of sonar-based surveys, relative to optical surveys, are offset by the lower resolution of the resulting data, which can range from less than 10 cm horizontal resolution for near-seafloor surveys obtained using autonomous underwater vehicles to as much as 100 m horizontal resolution for deep water surveys acquired from surface vessels. It is this trade-off of resolution versus coverage area that must be considered when designing a seafloor survey to fulfill its objectives. InSAS can achieve a horizontal resolution of 3 cm (or better with post-processing) for backscatter imagery and ~25 cm for derived bathymetry, combined with a survey swath that can range from 100 m to ~400 m on either side of the sensor platform (wider swaths can be achieved but at lower horizontal resolutions). InSAS therefore provides a significant improvement on the trade-off between data resolution and spatial coverage (Figure 1). The ranges of possible resolutions and survey swaths reflect the fact that, for all types of acoustic surveys, these parameters are also controlled by the sonar frequency used, vehicle altitude, beam angles, and survey speed.

INTERFEROMETRIC SYNTHETIC APERTURE SONAR

Synthetic aperture sonar is similar to traditional side-scan sonar in that it produces an acoustic image of the seafloor. The primary difference is that, unlike regular side-scan sonar, for which the resolution of the image decreases laterally with distance from the sensor platform as sound propagates and spreads, the resolution of InSAS imagery remains constant over the entire survey swath (Figure 2). The swath itself is also wider than that of a typical near-seafloor multibeam survey, resulting in greater survey coverage, although the side-looking geometry of the sonar does result in a data gap (nadir) below the vehicle (Figure 1).

The principles of InSAS are derived from the earlier development of synthetic aperture radar, which is widely used in satellite and aerial remote sensing to generate 2D and 3D images and topographic models of Earth's surface (Hansen, 2011). For sonar systems, the length, or "aperture," of the transducer that sends and receives the acoustic signals is a primary constraint on the resolution of the acquired data. The longer the aperture, the higher the possible resolution of the resulting data. For InSAS, a "synthetic" aperture is generated by using the along-track movement of the survey vehicle to create a longer simulated aperture than the physical transducer. Specialized signal processing allows for an object on the seafloor to be imaged by combining several sonar pings as the vehicle moves along the survey track, producing a higher resolution image. Because objects further away from the vehicle are imaged with a higher number of pings, the resulting image resolution remains constant and independent from the lateral distance to the vehicle.

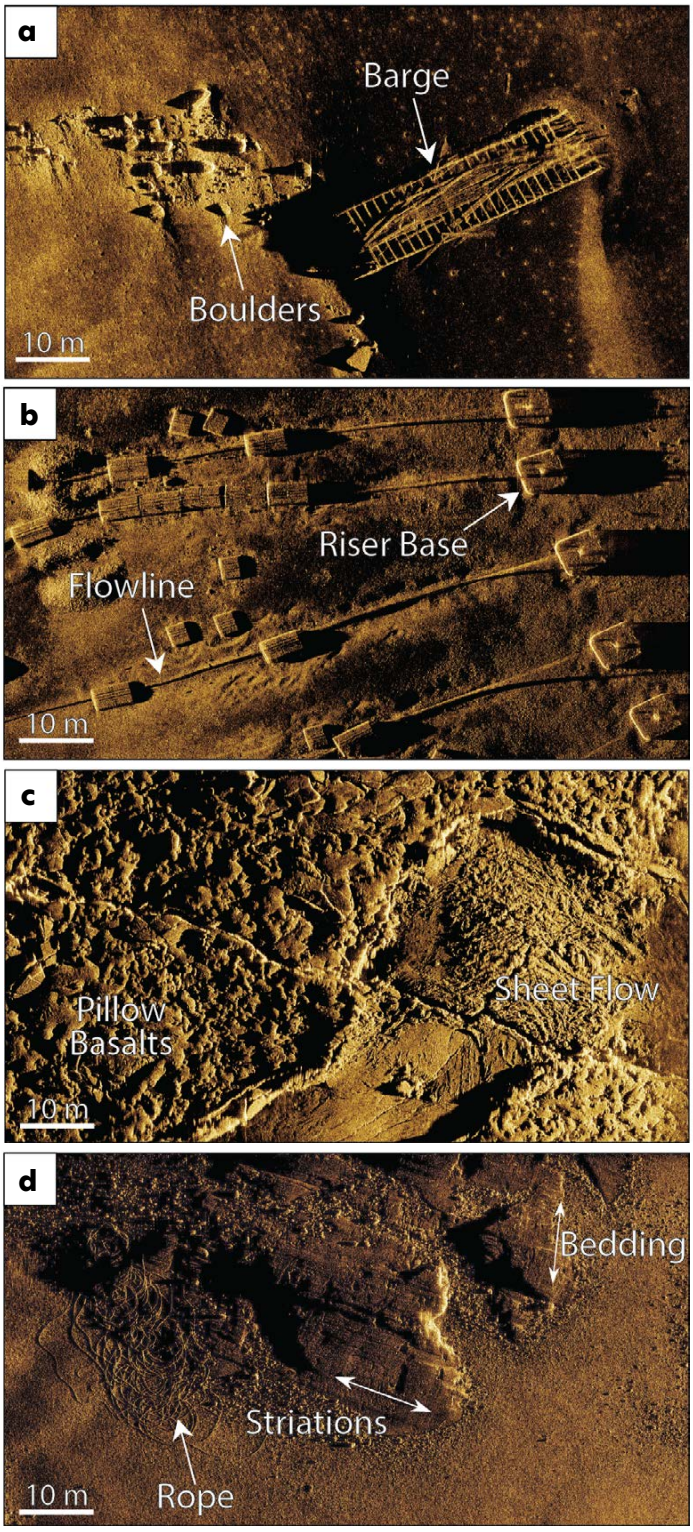

FIGURE 2. Interferometric synthetic aperture sonar images of the seafloor. (a) Wreck of a barge on a sediment substrate with boulders. (b) Offshore energy production infrastructure. (c) Fresh lava flows (pillow basalts, sheet flow with ropy lava texture) from a mid-ocean ridge. (d) Discarded rope next to bedrock outcrop and sand and gravel sediments. Both bedding planes and glacial striations are visible in the outcrop. Image resolution is 3 cm for all images. Data for images a, b, and d were collected using a Kraken Robotics MINSAS 180 system mounted on Kraken's *Katfish* towed vehicle. Data for image c was collected using a Kraken Robotics MINSAS 120 mounted on the Schmidt Ocean Institute remotely operated vehicle *SuBastian*.

For the "interferometry" aspect of InSAS, the phase difference of the return acoustic signals recorded at two vertically separated receivers is used to determine the height (or depth) of objects on the seafloor (Saebø, 2010). This information allows for a bathymetric grid to be simultaneously generated from the same data used to generate the acoustic backscatter image, thereby producing two datasets from a single survey. The resolution of the resulting bathymetric data (~25 cm) is similar to what can be achieved by a multibeam survey flown at the same altitude, but with a much wider swath (~600 m for InSAS at an altitude of 15 m, minus the nadir gap, versus <100 m for a multibeam system). Examples of InSAS sensors include Kraken Robotics's *MINSAS*, Kongsberg's *HISAS*, Exail's *Sams*, and Northrop Grumman's *mSAS*. Swath widths and resolutions vary, depending on system frequencies, survey speeds, and altitude (Figure 1). Sensors can be mounted on surface vehicles, towed vehicles, autonomous underwater vehicles, and remotely operated vehicles.

APPLICATIONS FOR SYNTHETIC APERTURE SONAR

The first applications of InSAS focused on defense-related deployments, primarily for mine countermeasures and reconnaissance, for which the wide swath and high-resolution imagery are ideally suited. The past decade has seen increasing applications of InSAS for commercial applications such as marine archeology and maritime searches for shipwrecks, aircraft, and lost cargo (Figure 2a), as well as pipeline, communications, and offshore energy infrastructure inspection and monitoring (Figure 2b). However, applications of InSAS as a tool for general seafloor characterization remain limited. Recent surveys on the continental shelf off the east coast of Canada and at the Galápagos Spreading Center, a volcanic ridge north of the Galápagos Islands, reveal the level of detail that can be derived from InSAS data with respect to substrate composition and textures, including specific seafloor lava flow morphologies (Figure 2c) and bedrock features such as bedding orientations and glacial striations (Figure 2d; Gini et al., 2023). The combined high-resolution and high coverage area of InSAS offers significant potential for various scientific, conservation, and spatial planning applications, including habitat mapping, geology, and environmental monitoring and baselines studies.

There are, however, limitations to where and how InSAS data can be successfully collected. The most significant limitation is data collection in topographically complex seafloor terrain. The synthetic aperture requires a high degree of vehicle stability along the survey track. The relatively low survey altitudes required for InSAS surveys (e.g., ~10–50 m) often necessitate changes in survey vehicle depth and direction to avoid obstacles and maintain constant altitude, introducing pitching and yawing of the vehicle that can easily exceed the stability limits required to generate high-resolution images (Gini et al., 2023). Low survey altitudes further result in the potential for the occurrence of significant acoustic shadows behind objects or terrain features that create data gaps. Future development and testing of InSAS should focus on improving its versatility for surveys over complex seafloor topography.

Looking forward, deep-sea mining for polymetallic nodules on deep abyssal plains has the potential to become the next large-scale human activity to impact the seafloor. With its wide swath and resolution high enough to detect potato-sized nodules on the relatively flat seafloor, InSAS is the ideal tool for nodule exploration and resource assessment, as well as impact monitoring and pre- and post-mining environmental assessment.

REFERENCES

Gini, C., K. Robert, J.W. Jamieson, S. Steele, and R. Charron. 2023. Interferometric synthetic aperture sonar for centimeter scale mapping and imaging of seafloor geology on the Scotian Shelf, Canada. Abstract on p. 32 in *Proceedings of the 2023 International Symposium on Marine Geological and Biological Habitat Mapping (GeoHab '23).* H.C. Cawthra and R. Devillers, eds, Saint-Gilles-Les-Bains, La Réunion, France, May 8–12, 2023, https://doi.org/10.5281/zenodo.7890332.

Hansen, R.E. 2011. Introduction to synthetic aperture sonar. Pp. 3–28 in *Sonar Systems*. N.Z. Kolev, ed, Intech.

Saebø, T.O. 2010. *Seafloor Depth Estimation by Means of Interferometric Synthetic Aperture Sonar.* PhD Dissertation, University of Tromsø, Norway, 202 pp.

ACKNOWLEDGMENTS

This work was supported by the Ocean Frontier Institute Benthic Ecosystem Mapping and Engagement (BEcoME) Project. JJ and KR acknowledge funding support from the Canada Research Chairs program. CG acknowledges funding support from the Mitacs Accelerate Fellowship. The authors thank Kraken Robotics for providing the InSAS data from the Scotian Shelf and for supporting InSAS data collection along the Galápagos Spreading Center. The Galápagos data were collected as part of a Schmidt Ocean Institute (SOI)-supported expedition (FKt231024) on R/V *Falkor (too)*, and SOI is acknowledged for providing the ship time and remotely operated vehicle for this project. The Galápagos expedition was further supported by Stuart Banks at the Charles Darwin Research Station and the Charles Darwin Foundation, the Galápagos National Park Directorate, and the Instituto Oceanográfico y Antártico de la Armada de Ecuador (INOCAR).

AUTHORS

John W. Jamieson (jjamieson@mun.ca) and **Caroline Gini**, Department of Earth Sciences, Memorial University of Newfoundland, St. John's, NL, Canada. **Craig Brown**, Department of Oceanography, Dalhousie University, Halifax, NS, Canada. **Katleen Robert**, Marine Institute, Memorial University of Newfoundland, St. John's, NL, Canada.

ARTICLE DOI. https://doi.org/10.5670/oceanog.2025e121

THE POTENTIAL OF LOW-TECH TOOLS AND ARTIFICIAL INTELLIGENCE FOR MONITORING BLUE CARBON IN GREENLAND'S DEEP SEA

By Narissa Bax, John Halpin, Stephen Long, Chris Yesson, Joseph Marlow, and Nadescha Zwerschke

OVERVIEW: SEAFLOOR MONITORING IN GREENLAND

Arctic environments are changing rapidly. To assess climate change impacts and guide conservation, there is a need to effectively monitor areas of high biodiversity that are difficult to access, such as the deep sea. Greenland (Kalaallit Nunaat), like many remote countries with large deep-sea exclusive economic zones (EEZs), lacks consistent access to the funding and logistics required to maintain advanced and expensive technologies for seafloor exploration. To fill this need, video and camera imaging technologies have been adapted to suit the unique requirements of Arctic environments and the social and economic needs of Greenland. Since 2015, a benthic monitoring program carried out by the Greenland Institute of Natural Resources (GINR) has provided the only large-scale, comprehensive survey in this region, including collection and analysis of photos and GoPro video footage recorded as deep as 1,600 m (Blicher, and Arboe, 2021). In line with the "collect once, use many times" principle, GINR is exploring the versatility of these data, which were originally designated for monitoring and evidence-based management. A potential research avenue for these data is polar blue carbon—the carbon stored and sequestered in ocean habitats—including benthic communities that either live on the seafloor (such as corals and sponges) or are transported there by ocean currents (such as algal detritus). This paper outlines Greenland's affordable deep-sea technology, based on a towed camera system (Yesson, 2023), and its potential application to rapid, standardized artificial intelligence (AI)-based analysis.

GREENLAND'S LOW-TECH TOWED CAMERA SYSTEM

A practical, relatively low cost and effective way to monitor the seafloor is with a simple towed camera system that can be deployed from most vessels with an A-frame and that is not dependent on a dynamic positioning system or fiber-optic capabilities. Greenland's towed camera system consists of an oblique angled centrally mounted video camera, lights, scaling lasers, and an echo sounder unit on a steel frame (Figure 1). It has been successfully deployed since 2017.

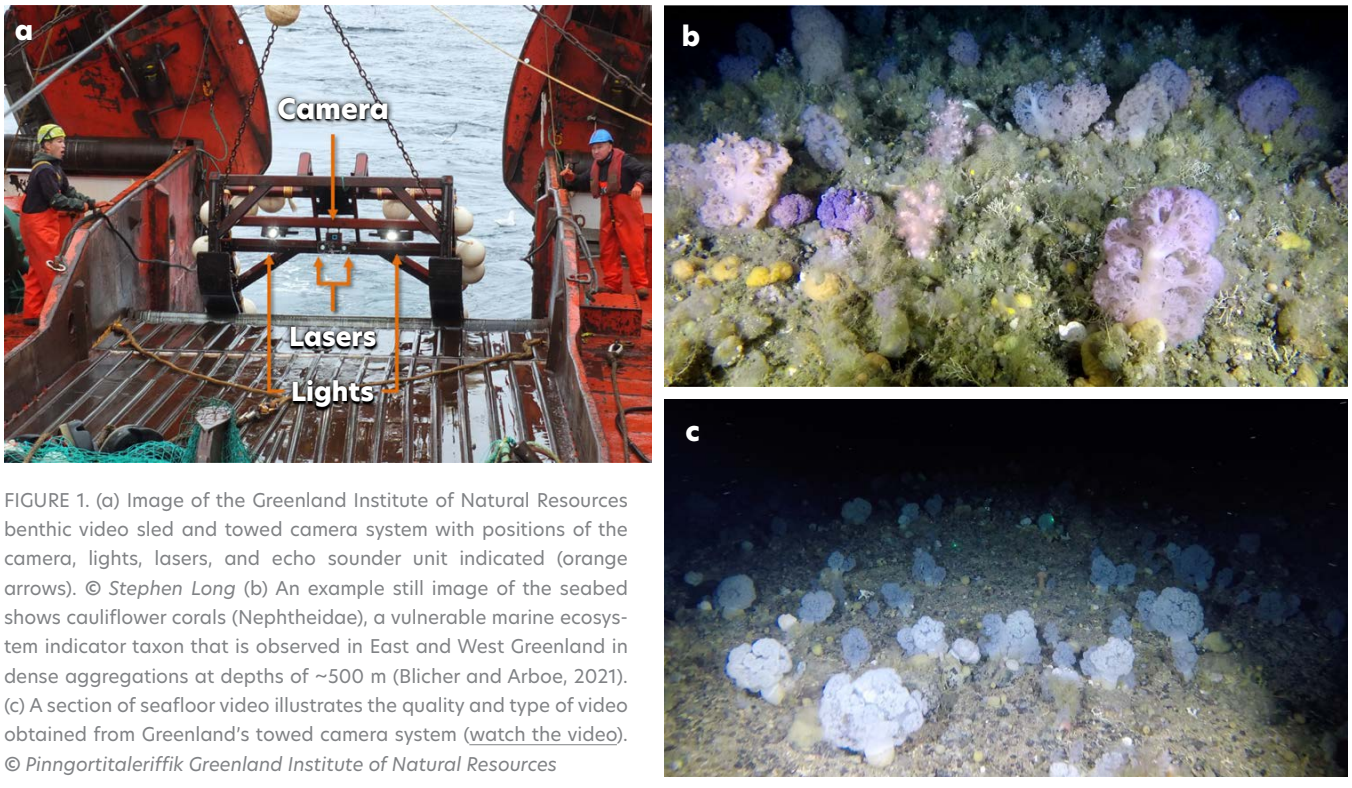

FIGURE 1. (a) Image of the Greenland Institute of Natural Resources benthic video sled and towed camera system with positions of the camera, lights, lasers, and echo sounder unit indicated (orange arrows). © *Stephen Long* (b) An example still image of the seabed shows cauliflower corals (Nephtheidae), a vulnerable marine ecosystem indicator taxon that is observed in East and West Greenland in dense aggregations at depths of ~500 m (Blicher and Arboe, 2021). (c) A section of seafloor video illustrates the quality and type of video obtained from Greenland's towed camera system (watch the video). © *Pinngortitaleriffik Greenland Institute of Natural Resources*

Two Group-Binc Nautilux 1,750 m LED light sources are positioned either side of the camera and angled slightly inward. Two Z-Bolt lasers (515 nm wavelength) in custom-made housings provide scale (20 cm). Position and orientation of the sled is monitored in real time using a Marport Trawl Eye Explorer. Video is collected using a GoPro5 action camera in a Group-Binc housing. The camera is positioned 0.55 m above the seabed. The camera angle is adjustable but typically set at 28.8 ° down from horizontal. The camera is set to record at 2,704 × 1,520 pixel resolution using the "medium" field of view (FOV) setting.

The sled is lowered to the seabed on a winch cable whose length is approximately 1.2–1.5 times the seabed depth. Tow speed is 0.8–1.0 knots. Typical transect time is 15–30 minutes, which covers ~500–1,000 m, creating a swept area of ~0.75–1.5 km^2. Battery life, reduced by Arctic temperatures, is the main limitation on deployment time. Sled deployment requires a relatively flat seabed, but the sled is robust enough to manage areas with small boulders and gentle slopes.

These sled attributes result in an average observed seafloor area of approximately 8.23 m^2 and a horizontal midline span of 1.49 m (based on the camera height and angle above). Image area calculations can be performed using the "TowedCameraTools development version" R package (Yesson, 2023).

The initial setup cost of this system ranges between EUR 15,000 and EUR 20,000, with a yearly maintenance fee of approximately EUR 500. Its advantages are that it does not require trained personnel for deployment or repairs, that it exhibits few technical malfunctions and is not prone to getting stuck or lost on the seabed, and that its significant depth range is 50 m to 1,600 m.

So far, still images and videos have been analyzed in the BIIGLE (Bio-Image Indexing and Graphical Labelling Environment) video and still image annotation platform to identify, describe, and map benthic habitats, as well as quantify and measure the heights of epibenthic megafauna. Yet, this is a costly and time-consuming process.

AI FOR COST-EFFECTIVE ANALYSIS OF DEEP-SEA IMAGERY

The need for practical, low-cost "cheap and deep" technology extends beyond data collection to include a cost-effective method of analyzing benthic imagery/footage. Fortunately, developments in computer vision and AI have made this possible. Deep learning-based models using either vision transformers or convolutional neural networks can be trained using consumer grade hardware to offer performance that can match or indeed beat (by certain criteria) a human annotator. Critically, they can do this at speeds far exceeding those of human annotators, allowing for the efficient analysis of spatially extensive survey data.

The success of computer vision models depends on effective training, and the model's ability to differentiate between similar taxa largely hinges on the human annotator's accuracy in providing the training data. Automated species IDs and occurrence information hinge on accurate taxonomic reference systems and generally work best on data that are similar to training imagery. For example, by determining benthic assemblages—such as dense aggregations of cauliflower corals (Nephtheidae) and sponges (*Geodia* spp.)—AI workflows can estimate habitat-specific carbon storage potential (**Figures 1 and 2**), although subtle morphological differences often impede reliable species-level identification from images. Consequently, the key to successful AI recognition lies in building taxonomically robust and well-annotated training sets that accurately represent the survey data in terms of image quality, benthic composition, and habitat type, and ensuring researcher-led validation remains integral to refining automated classification tools.

Figure 2 shows a complete workflow for automatic identification from footage of a Greenlandic *Geodia* spp. sponge bed. The dataset consisted of only 46 images, but the network was able to produce tolerable levels of precision/recall after 10 minutes of training. The metrics available to researchers for extracting from this analysis depend upon both the computer vision method and the given research question. A common metric for extracting from object detection is density, but this requires image scaling to allow for identification counts per unit area. We have developed two approaches to this: automatic detection of paired laser spots so that each image can be automatically scaled or the combination of positional information with object tracking, allowing for counts per unit area. The combination of computer vision and image scaling also allows for size measurements of a given taxa, either approximate measurements in the case of object detection, or highly accurate measurements when using semantic or panoptic segmentation methods. These can be combined with three-dimensional workflows to produce accurate estimates of epibenthic biomass (Marlow et al., 2024) or potentially even carbon content.

FUTURE AI-INFORMED BLUE CARBON RESEARCH

The combination of benthic footage from Greenland's towed camera system and the AI workflow for automated taxon identification is an ideal use case for future blue carbon assessments. With suitable training sets, the technology would enable fast and economical analyses of large quantities of benthic survey footage at ecologically relevant

spatial scales. For example, the role of benthic invertebrates and macroalgae in blue carbon assessments has been controversial, partially due to uncertainties about the fate of carbon on the seafloor and a lack of systematic assessment. AI could help clarify this issue by linking in situ observations from videos with carbon content data from key seafloor taxa, such as sponge, coral, and seaweed specimens recorded in benthic images and collected during benthic monitoring surveys. Three collaborative projects undertaken by the coauthors represent practical applications: (1) BlueCea, tracing the fate of macroalgae with a focus on blue carbon processes in sub-Arctic North Atlantic fjord ecosystems, (2) POMP, Polar Ocean Mitigation Potential, and (3) SES, Seabed Ecosystem Survey. These projects aim to apply this novel AI approach to almost 10 years of imagery data across Greenland to better understand the blue carbon storage potential of Greenland's shelf system. The combination of tools that were developed to simplify, standardize, and accelerate monitoring and identification of vulnerable marine ecosystems, habitats, and taxa is expected to contribute significantly to cutting-edge research. This work may also be relevant in other remote locations worldwide that rely on low budget solutions.

REFERENCES

Blicher, M.E., and N.H. Arboe. 2021. *Atlas of Vulnerable Marine Ecosystem (VME) Indicators Observed on Bottom Trawl Surveys in Greenland Waters During 2015-2019*. Technical Report no. 113, Greenland Institute of Natural Resources, 26 pp.

Marlow, J., J.E. Halpin, and T.A. Wilding. 2024. 3D photogrammetry and deep-learning deliver accurate estimates of epibenthic biomass. *Methods in Ecology and Evolution* 15(5):965–977, https://doi.org/10.1111/2041-210X.14313.

Yesson, C. 2023. Towed Camera Tools R Package, development version, https://github.com/cyesson/TowedCameraTools.

ACKNOWLEDGMENTS

We thank the staff and crew of R/V *Tarajoq* for their invaluable support. This work has been funded by Granskingarráðið for the BlueCea project (grant number 8014), the Government of Greenland's partnership agreement with the European Commission under the so-called Green Growth Programme, the Aage V. Jensen Charity Foundation, the EU Horizon POMP Project (grant agreement 101136875), and the NERC UK-Greenland Bursary, and through Research England support for ZSL research staff. Image and video data from the GINR benthic monitoring program contributes to the BlueCea, POMP, and SES projects.

AUTHORS

Narissa Bax (narissa.bax@gmail.com), Pinngortitaleriffik, Greenland Institute of Natural Resources, Greenland Climate Research Centre, Nuuk, Greenland. **John Halpin**, Scottish Association for Marine Science, Oban, UK. **Stephen Long** and **Chris Yesson**, Institute of Zoology, Zoological Society of London, UK, and University College London, UK. **Joseph Marlow**, Scottish Association for Marine Science, Oban, UK. **Nadescha Zwerschke**, Pinngortitaleriffik, Greenland Institute of Natural Resources, Greenland Climate Research Centre, Nuuk, Greenland.

ARTICLE DOI. https://doi.org/10.5670/oceanog.2025e112

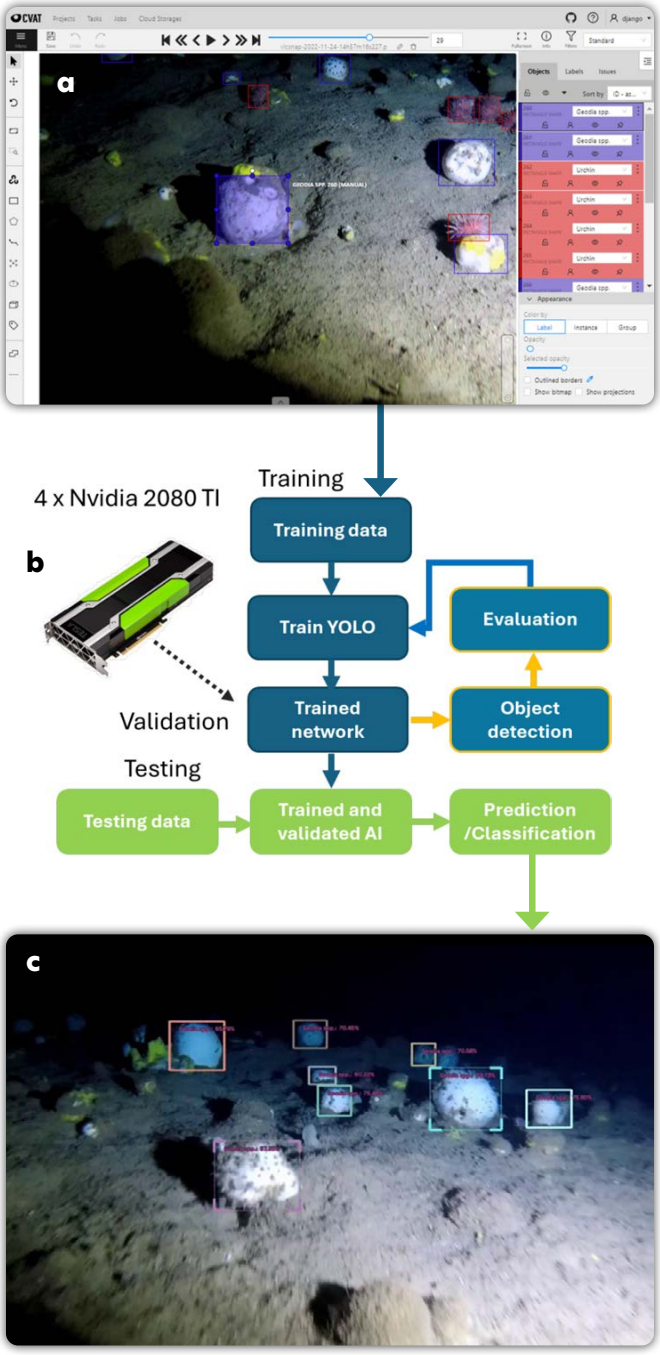

FIGURE 2. (a) As part of the workflow (see panel b), a training set was first generated using the Computer Vision Annotation Tool, but many alternative tools are available, for example, BIIGLE (Bio-Image Indexing and Graphical Labelling Environment). (b) The complete workflow for artificial intelligence (AI) auto identification of Greenlandic benthos. (c) The dataset was then exported in a YOLO (You Only Look Once) format and used to train a YOLO V5 large object detection model, and object detection predictions were applied to frames from seafloor footage. See the animated GIF illustrating AI detection of massive sponges such as the VME indicator taxa *Geodia* spp., identified in East Greenland in high densities that exceed trawl bycatch weights of >1,000 kg at depths from 300 m to 1,450 m (Blicher and Arboe, 2021) © *Pinngortitaleriffik Greenland Institute of Natural Resources*

ATLANTIC ARC LANDER MONITORING (ALaMo): AN EMERGING NETWORK OF LOW-COST LANDER ARRAYS FOR OCEAN BOTTOM OBSERVATIONS

By Cesar González-Pola, Caroline Cusack, Ignacio Robles-Urquijo, Rocio Graña, Luis Rodriguez-Cobo, Ricardo F. Sánchez-Leal, Glenn Nolan, and A. Miguel Piecho-Santos

THE NEED

The need to establish a sustained Global Ocean Observing System (GOOS) has long been recognized by the international ocean science community. Established in 1991 and led by the Intergovernmental Oceanographic Commission of the United Nations Educational, Scientific, and Cultural Organization (IOC-UNESCO), GOOS develops guidelines and coordinates regional alliances across the world's ocean basins to evolve the system. The need to sustainably expand GOOS has recently gained urgency as expressed in the United Nations Decade of Ocean Science for Sustainable Development (2021–2030) Challenge 7: Ensure a sustainable ocean observing system across all ocean basins that delivers accessible, timely, and actionable data and information to all users.

Developing "innovative in situ, autonomous and cost-effective technologies" is flagged as a pillar for the sustainable expansion of GOOS (Miloslavich et al., 2024). Technological developments that will enhance sustained monitoring systems include advances in sensors (increased accuracy and stability) and in the autonomous robotic systems (e.g., Argo floats and gliders) that carry such sensors across the world ocean. Improvements in batteries and memory will support longer deployments of stand-alone sensors, benefiting the Eulerian component of GOOS.

Although tracking climate-induced changes in the deep ocean and at the seafloor is a fundamental requirement for managing the ocean and the services it provides and for informing decisions about active climate remediation (Levin, 2021), accessing the deep sea remains a challenge. A well-established approach for gathering Eulerian measurements at the seafloor is through the use of benthic stations or landers. An oceanographic lander is any structure designed for placement on the seabed to host a variety of sensors for autonomous operation (Jahnke, 2003). Landers have been in use for decades, but the high cost of their recovery systems, typically based on fitting the landers with buoyancy modules, releases, and expendable ballast, have so far prevented widespread use and development of monitoring strategies based on benthic station arrays or swarms, with a few costly exceptions.

Development of a system for cost-effective deployment and recovery of landers would help implement distributed networks of high-temporal-resolution Eulerian nodes at the seafloor. International environmental monitoring commitments, including management plans for deep marine protected areas (MPAs) or, in the particular case of Europe, collecting baseline line data for the Marine Strategy Framework Directive, specifically require sustained collection of essential ocean variables (EOVs) at the seafloor. In addition, lander swarms offer an invaluable tool for supporting targeted scientific studies. Circulation and dynamics at complex topographic sites such as canyons or seamounts, where notable deep-sea ecosystems typically thrive, cannot be properly quantified without simultaneous measurement at several sites. Likewise, understanding shelf-slope currents, critical for margin exchange processes and meridional mass and heat transports, requires distributed measurement spots. In addition to physical oceanography instruments, the landers can host other types of sensors, making fleets of landers a truly multidisciplinary research tool.

LanderPick SYSTEM

Targeting this technological challenge, development of the LanderPick system has been underway as a series of proof-of-concept projects by the Spanish Institute of Oceanography (IEO-CSIC) since 2020. Continuous advances in vessel dynamic positioning systems as well as improvements in subsea vehicle positioning and tracking systems (typically ultra short baseline [USBL] technology), has made feasible the control of a remotely operated towed vehicle (ROTV) accurately enough to approach a lander sitting on the seafloor with sub-meter accuracy. This is the unconventional idea of the LanderPick approach.

The LanderPick concept entails (1) development of a specific, cost-effective, and compact ROTV capable of transporting a lander for placement/hitching, with visual assistance, at/from the seafloor, and (2) development of landers provided with built-in metal "cobweb" structures for easy hitching (Figure 1). Two vehicle prototypes, LanderPick-2000 and LanderPick-6000 (operational depths of 2,000 and 6,000 m), have been constructed. Outfitting of each of

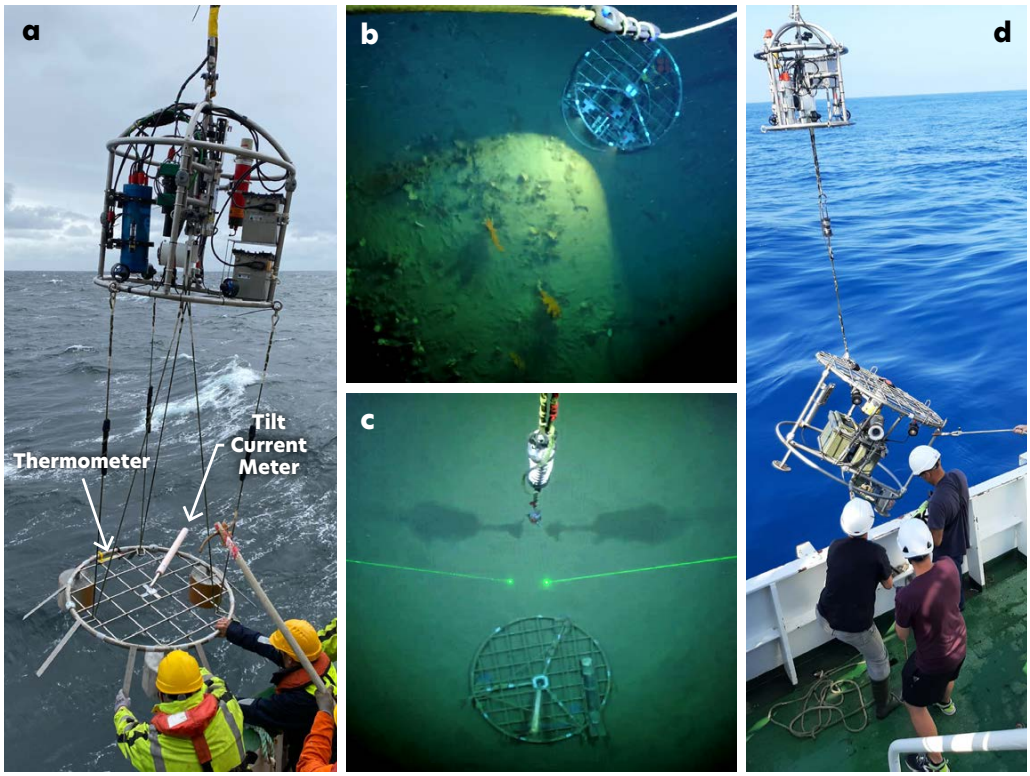

FIGURE 1. (a) Deployment from R/V *Celtic Explorer* of a disk-type LanderPick-suited lander with "cobweb" metal structure design. The lander, hanging from the LanderPick-6000 remotely operated towed vehicle, carries low-cost physics sensors consisting of a Lowell TCM-3 tilt current meter and an RBR SoloT thermometer. (b) This photo shows a cylindrical time lapse image lander just deployed from the LanderPick vehicle on the top of a coral mound. The lander lights are switched on to take a photograph. (c) The LanderPick vehicle makes a final approach for recovery of a disk-type lander equipped with a tilt current meter and a hydrophone. (d) The image lander shown in (b) comes onboard during recovery.

these vehicles includes a high-definition underwater camera, spotlights, a heavy-load mechanical release, and thrusters. During the landing process, auxiliary cords facilitate the connection between the release mechanism and the lander. Once the landing is visually confirmed at the target location, these cords are disengaged. Lander recovery requires use of the ship's dynamic positioning system, which serves as the primary navigational tool directing the LanderPick ROTV to the target location. Aided in the final stages by the LanderPick camera and propellers, a grapnel hooks the lander "cobweb."

CURRENT TESTING AND OPERATIONS

Among the lander designs conceived and built, the simplest features a circular recapture "cobweb" mesh with three ballasted legs (disk-type) specifically arranged to accommodate economic tilt-current meters and other small instruments as thermometers (Figure 1a,c). Cylindrical lander units allow for the installation of many more instruments (Figure 1b,d). Nearly 200 successful LanderPick operations from shallow waters to 1,500 m depth demonstrate system robustness and an operational time on the order of tens of minutes. A few failures have also occurred: three lander recovery attempts in shallow areas were aborted due to high turbidity that prevented visual operation when ship time was available. Because expectations are that these landers are still in place, further recovery attempts will be sought in the future. One lander was trawled and returned by a fishing vessel, with some instruments damaged. Although standard landers are deployed with a service horizon of one year, some deployments have exceeded 18 months.

A fleet of about 40 landers is currently operating in Spanish waters (Northwest Iberia, Gulf of Cádiz, Canaries, and Mediterranean Sea; Figure 2). Small landers provide distributed basic EOV monitoring (hydrography and currents) of the seafloor along the continental shelf and slope, currently only at trawl-free sites. Cylindrical landers are mostly located in Spanish MPAs to track environmental variables during the periods between ship-based monitoring cruises (i.e., serving as sentinels). These landers incorporate additional instruments, including biogeochemical sensors for pH and hydrophones for ambient noise and/or marine mammal tracking, and some units add time-lapse image systems (Figure 1b,d). Specific short-term experiments, supported by arrays of landers, have been conducted to pursue complex hydrodynamic processes, in particular, the breaking of internal tides at canyon heads, overflow downstream of Gibraltar Strait, recirculation patterns at seamount rims, and coherence of shelf-slope currents across wider regions (Figure 3).

The initial investment for the LanderPick ROTV prototype system is approximately $150,000, which is comparable to or cheaper than other ROTVs. The total cost of a LanderPick-compatible lander is about an order of magnitude lower

than conventional landers that use buoyancy, ballast, and release mechanisms. Without these expensive recovery mechanisms, LanderPick-compatible landers cost between $3,000 and $5,000, depending on payload size and configuration. For example, in late 2024, a steel-fabricated lander equipped with a tilt current meter and temperature sensor for shelf work (≤300 m) cost $2,908, while a deep-water lander (≤3,000 m) cost $5,315.

The lander technology has demonstrated robust performance with minimal maintenance requirements. Furthermore, the LanderPick deployment and recovery procedures have proven to be more time efficient than servicing standard landers, resulting in significant ship-time savings. This efficiency is particularly advantageous, as lander servicing is typically conducted as an ancillary activity within routine environmental monitoring or scientific expeditions. Consequently, the LanderPick system can be regarded as a cost-effective complementary solution for oceanographic research and monitoring operations.

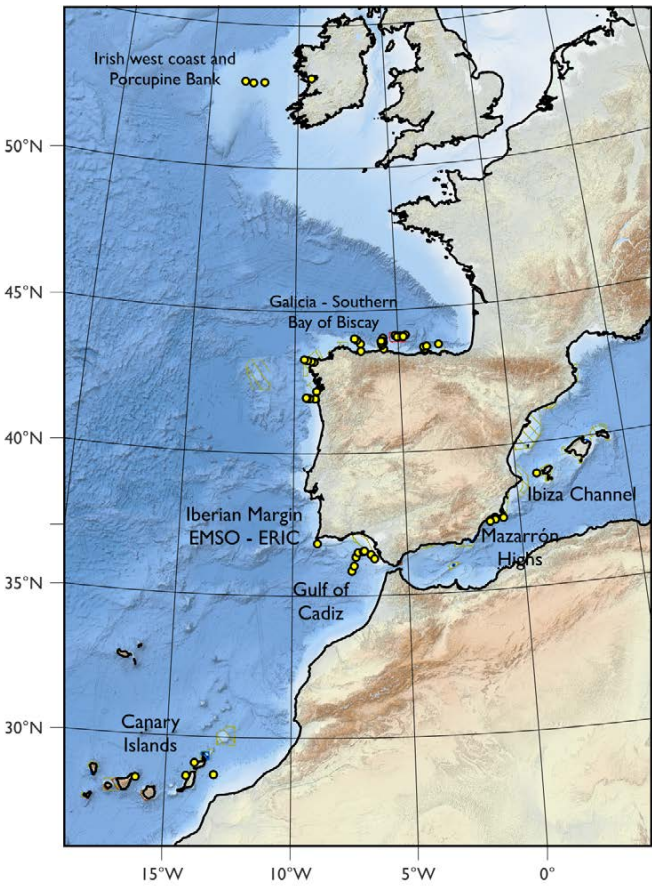

FIGURE 2. Dots indicate sites where LanderPick-suited landers have been deployed in Spanish and Irish waters since 2021 and the Iberian margin EMSO (European Multidisciplinary Seafloor and Water Column Observatory) site (Portugal) scheduled for deployment by April 2025. About one-quarter of landers shown in Spanish waters are set as "sentinel landers" that are intended to be permanent observing systems.

THE FUTURE

The current fleet of landers operated by the LanderPick system in Spain has formally become part of a sustained ocean observing system that supports environmental management commitments. Since 2023, and especially in 2024, the volume of data coming from the lander arrays has begun to be significant, making it necessary to implement protocols and procedures for transferring it to data centers following FAIR (findable, accessible, interoperable, and reusable) principles, as required by most funding agencies. Currently, data are being incorporated into Spanish marine repositories as part of bulk databases assembled from cruises employed for (but not dedicated to) recovery. Specific treatment of lander records is still being designed.

While the system can now be considered operational, future refinements are being addressed under ongoing projects. The LanderPick-6000 has been designed to operate at great depths, but the lack of appropriate cable has so far prevented it from surpassing 1,500 m. Testing the system in the 2,000–5,000 m depth range is a major near-future objective. Another challenge is gathering data at the continental shelf where trawling activity occurs; a LanderPick-suited anti-trawl lander is being designed for testing in summer 2025. Additional goals include continuing to lower the cost of simple lander units and ensuring that landers can measure for longer periods (well over a year). Real-time data transmission from landers, a declared desire of the oceanographic community, will be possible depending on future developments in underwater communication systems, in terms of both cost and reliability.

International collaboration to further develop the system and transfer the LanderPick technology began in 2022, driven by the need for coordination among ocean observing systems in neighboring regions. Scientists from the Irish Marine Institute and the Portuguese Instituto Português do Mar e da Atmosfera joined a Spanish cruise on board R/V *Ramón Margalef* in July 2023 to deploy an array of 20 landers across the north and northwestern Spanish continental shelf and upper slope (Figure 3). In April 2024, Spanish scientists participated in an Irish cruise around Porcupine Bank on board R/V *Celtic Explorer*, successfully deploying four landers (Figure 2). This provided an opportunity to test the LanderPick-6000 vehicle on a different vessel, which was equipped with fiber-optic cable capabilities, and demonstrated the feasibility of technology transfer. Recovery of this set of landers is expected in early May 2025.

Under a proposal to access EMSO (European Multidisciplinary Seafloor and Water Column Observatory) sites, at least two landers will be deployed in April 2025 around the Iberian Margin EMSO site (Figure 2) from the Portuguese R/V *Mario Ruivo*. Successful deck testing of the

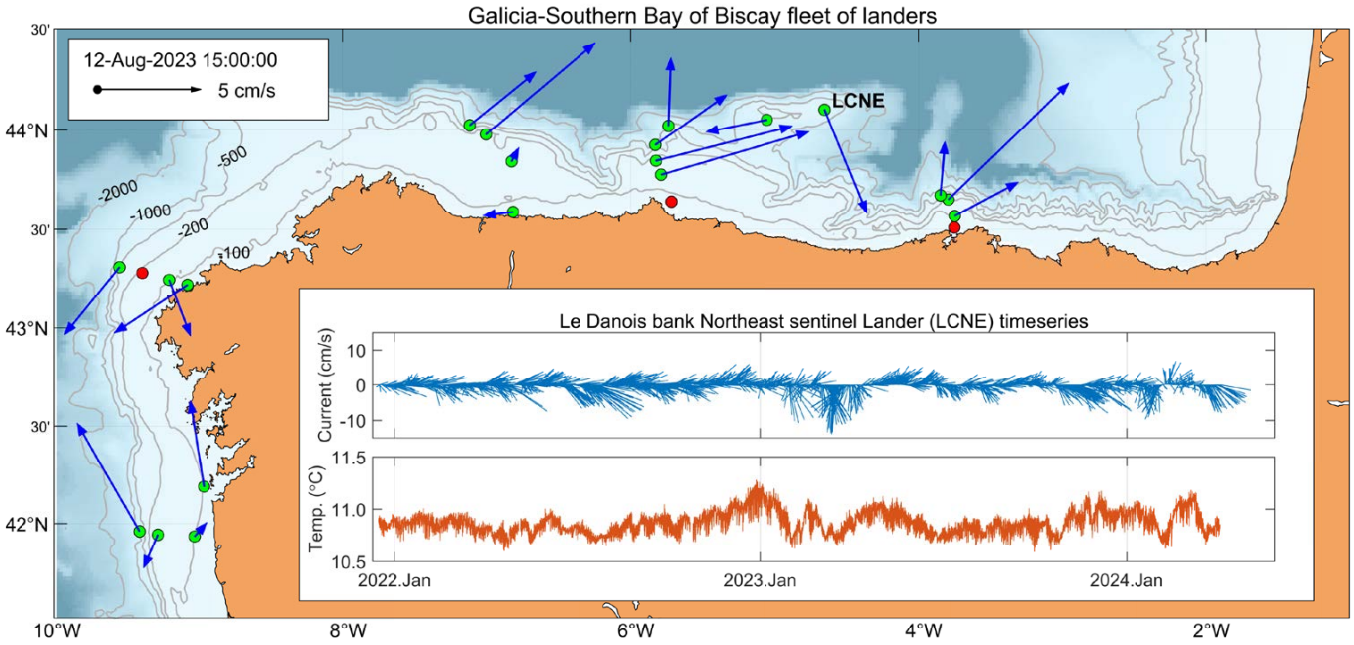

FIGURE 3. Snapshot of benthic currents on August 12, 2023, 15:00 UTC, from all active landers off the Galician coast-Southern Biscay region. Most of the landers were of disk-type design and equipped with sensors that measured only physical data (see Figure1a). Of the 23 landers deployed, 20 were successfully recovered with complete data records (green dots). For the three remaining landers (red dots), one was recovered successfully but with a malfunctioning current meter, another was lost to trawling (and later returned), and the third has yet to be recovered because water visibility was low at the time of retrieval operations. The inset shows bottom water current and temperature time series data recorded since late 2021 at a sentinel lander called LCNE (Spanish acronym for Le Danois bank Northeast, marked on the map), scheduled for its next service in May 2025. A low-pass filter (Butterworth filter with 30-hour cutoff period) was applied to current data records.

system on this vessel has already taken place.

These international cooperation experiences lay the foundation for what we hope will become a coordinated network of cost-effective lander arrays for sustained seafloor monitoring across Western Europe in an effort called Atlantic Arc Lander Monitoring (ALaMo). The network aims to contribute to the development of "innovative in situ, autonomous, and cost-effective technologies" highlighted in the UN Ocean Decade white paper (Miloslavich et al., 2024). Lessons learned from the operation of the system in our three countries will provide refined procedures and protocols for using the system on several oceanographic vessels. The joint effort will also improve analysis, exploitation, and transfer of the data gathered by lander systems. Figure 2 shows that a first piece of the ALaMo network across the Northeast Atlantic boundary is already in place. Further deployments along Portuguese and Irish coasts are planned, followed by expansion into French and Moroccan waters.

REFERENCES

Jahnke, R. 2009. Platforms: Benthic flux landers. Pp. 485–493 in *Encyclopedia of Ocean Sciences*, 2nd ed. John H. Steele, ed., Elsevier, https://doi.org/10.1016/b978-012374473-9.00731-1.

Levin, L.A. 2021. IPCC and the deep sea: A case for deeper knowledge. *Frontiers in Climate* 3:720755, https://doi.org/10.3389/fclim.2021.720755.

Miloslavich, P., J. O'Callaghan, E. Heslop, T. McConnell, M. Heupel, E. Satterthwaite, L. Lorenzoni, I. Schloss, M. Belbeoch, N. Rome, and others. 2024. Ocean Decade Vision 2030 White Papers – Challenge 7: Sustainably Expand the Global Ocean Observing System. The Ocean Decade Series, 51.7., UNESCO-IOC, Paris, France, 22 pp., https://doi.org/10.25607/brxb-kr45.

ACKNOWLEDGMENTS

The LanderPick system was developed under the LanderPick, LanderPick-2, and LanderPick-3 projects by the Pleamar Program (Fundación Biodiversidad, MITECO, UE EMFF funds) and grant TED2021-132887B-I00 by MCIN/AEI, NextGenerationEU. The participation of AMPS on the R/V *Ramón Margalef* cruise received Portuguese national funds from the Foundation for Science and Technology (FCT) through projects UIDB/04326/2020 and LA/P/0101/2020. The authors declare no conflicts of interest.

AUTHORS

Cesar González-Pola (cesar.pola@ieo.csic.es), Spanish Institute of Oceanography-Consejo Superior de Investigaciones Científicas (IEO-CSIC), Gijón, Spain. **Caroline Cusack**, Marine Institute, Oranmore, County Galway, Ireland. **Ignacio Robles-Urquijo**, Environmental Smart Devices, Cantabria, Spain. **Rocio Graña**, IEO-CSIC, Gijón, Spain. **Luis Rodriguez-Cobo**, Environmental Smart Devices, Cantabria, Spain. **Ricardo F. Sánchez-Leal**, IEO-CSIC, Cádiz, Spain. **Glenn Nolan**, Marine Institute, Oranmore, County Galway, Ireland. **A. Miguel Piecho-Santos**, Instituto Português do Mar e da Atmosfera (IPMA), Algés, Portugal, and Centre of Marine Sciences (CCMAR), University of Algarve, Faro, Portugal.

ARTICLE DOI. https://doi.org/10.5670/oceanog.2025e117

VIDEOMODULE TOWED SYSTEM: ACQUISITION AND ANALYSIS OF VIDEO IMAGING DATA FOR BENTHIC SURVEYS

By Ivan Anisimov, Andrey Lesin, Valeriya Muravya, Anna Zalota, and Maxim Zalota

SCIENTIFIC MOTIVATION

Ecological studies require two types of primary information: qualitative (what species are present in the study area) and quantitative (e.g., number, biomass, size structure). Such information is difficult to gather for underwater communities, especially in the deep sea, where scuba diving for census-taking is impossible. Traditionally, tools such as grabs and trawls have been used, but they have their limitations: grabs sample small areas, and the location of trawl samples is imprecise. In addition, these tools damage both the organisms and their habitats.

Still photography and video footage have been used for effectively decades to study underwater species (Mallet and Pelletier, 2014), as these tools are used to identify organisms that live above the substrate. Benthic video surveys are carried out with various underwater vehicles including remotely operated and autonomous underwater vehicles and towed camera systems that allow researchers to observe and document habitats and species in their natural settings without significant disturbance. Towed camera systems in particular offer advantages that enhance the effectiveness of benthic video surveys. Towed systems can efficiently cover extensive areas of the seafloor to provide a broad spatial context that is difficult to achieve with classic sampling methods or other types of vehicles. The connection of these towed systems to the vessel facilitates the estimation of transect distance and area covered. Towed systems operate at consistent speeds and depths, ensuring uniform data collection and reducing variability in the footage. Additionally, towed cameras are adaptable to various depth ranges, from shallow coastal waters to the deep sea, making them suitable for diverse marine environments. A comprehensive overview of such systems can be found in Durden et al. (2016).

Currently, numerous groups around the world are working to develop automatic identification systems for organisms using machine learning methods (ML; Li et al., 2023). Most ML efforts and error assessments are concerned with species identification: effectively finding an object in the footage and accurately identifying it and its taxonomic level. Very little attention is paid to the quantitative parameters. In machine learning, there are no standard technical or analysis parameters to account for the differences in underwater vehicles, such as in camera quality and distortion, water transparency, light level, and measurement methods, making comparative studies unreliable. Even multiple surveys of the same area using the same apparatus can result in significant differences in the quality of video footage due to, for example, different water transparency conditions. Therefore, the number of observed specimens may be undercounted because of actual changes in the assemblage or simply lower visibility in the water column.

We aim to develop an underwater vehicle and analysis tool that can minimize technical and environmental factors affecting video footage quality and quantify errors in the comparative quantitative analysis of underwater objects.

VIDEOMODULE TOWED SYSTEM

A towed system called *Videomodule* was designed at the Shirshov Institute of Oceanology for benthic research at depths of up to 6,000 m (**Figure 1**). *Videomodule* operates at a standard towing speed of approximately 0.5 knots and maintains an average height of 1.5 m above the seafloor. At this speed, the system is situated beneath the A-frame of the vessel, thereby facilitating system positioning. Eight 30 kg weights are distributed in a manner that minimizes pitch during towing. Stabilizers are mounted in the rear of the system to eliminate roll and course rotations.

Videomodule is equipped with a video camera, a still camera, a side-scan sonar, and various auxiliary sensors, including a depth gauge, an altimeter, and an inclinometer. The system uses six 30 W LED lights and a 200 W strobe light for optimal illumination. Two parallel red lasers fixed 20 cm apart are mounted next to the camera to provide a scale for the frame. The video camera is a 4K IP surveillance camera with a Sony Exmor R sensor that provides 6 MP resolution and a 76° field of view underwater. The down-looking camera captures a bird's-eye view of the seafloor to identify the best possibilities for quantitative analysis of examined species. At a standard height above the seabed, organisms approximately 1 cm in size can be distinguished in the video. The photo system is based on a consumer-grade Sony ILCE 7RM2 digital photo camera with 24.3 MP resolution and a 56° field of view under water, enabling the study of smaller organisms (less than 1 mm). For operational purposes, two analog TV cameras, one down-looking and one tilted, transmit low latency video onboard, allowing operators to avoid obstacles on the seafloor. The side-scan sonar operates at a frequency of 240 kHz, enabling high-resolution imaging of a 300 m wide strip of seabed.

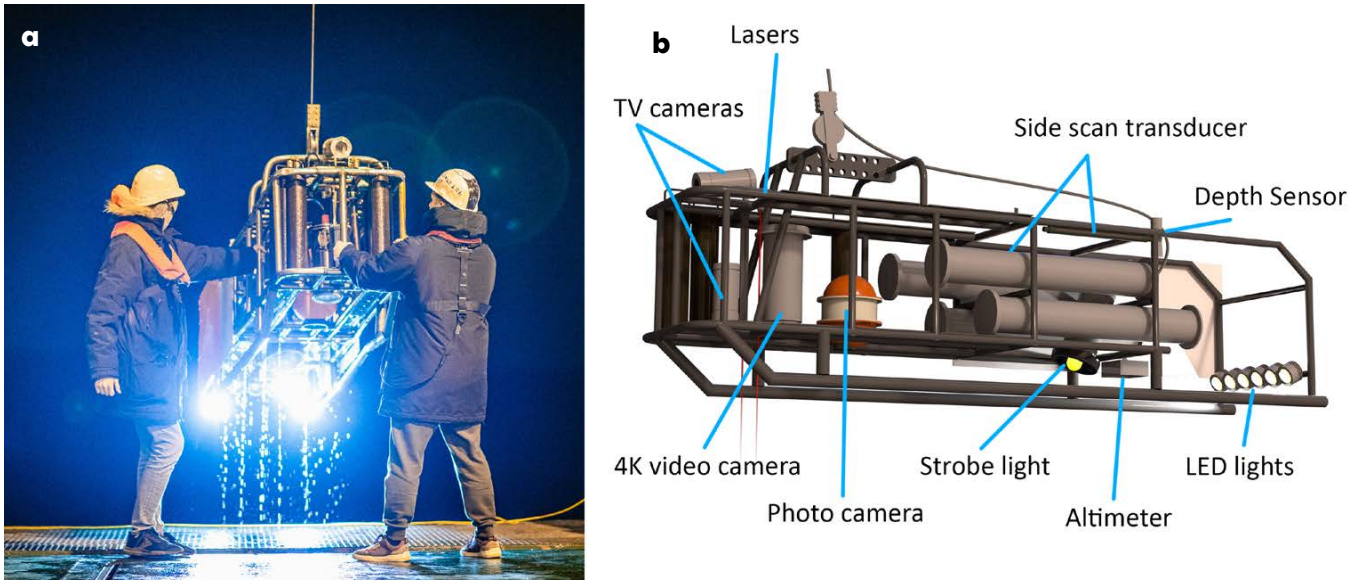

FIGURE 1. *Videomodule* towed system designed at the Shirshov Institute of Oceanology. (a) *Videomodule* is recovered here during the 85th expedition of R/V *Akademik Mstislav Keldysh* in 2021. *Photo credit: Ivan Potylicin* (b) Schematic shows *Videomodule* equipment including cameras, side-scan sonar, and auxiliary sensors.

Videomodule is connected to the research vessel via a fiber-optic cable, allowing real-time data transmission to a computer on board the vessel. The system is powered by two LiFePO4 batteries that provide sufficient power for surveys lasting up to 12 hours at full load without recharging.

Surveys conducted with *Videomodule* are typically organized into 500–600 m transects. Each transect yields approximately 40 minutes of video footage, 80–100 photographs, and a single side-scan stripe image. Comprehensive metadata, including system depth, distance from the seafloor, pitch, roll, heading, and vessel coordinates, are recorded in a log file at one-second intervals. These metadata are also embedded in the video's captions and photos to facilitate analysis.

IMAGE ANALYSIS

Two main groups of software tools that have been developed for analysis of underwater video data (1) generate three-dimensional models of the seafloor based on photos and video sequences, and (2) provide tools for direct analysis of the images themselves using laser marks as references. The latter group is simpler and faster but is typically better suited for analyzing images of relatively flat seafloor areas. Another issue to consider when using such methods is the need for constant camera tilt to avoid perspective distortions (Istenič et al., 2020).

Image distortion can reduce the accuracy of species measurements. To address this issue, the camera's radial distortion coefficients were evaluated and corrections were made. In addition, we developed a novel method of perspective correction. Although similar methods are widely used in computer vision systems (e.g., self-driving cars), as far as we are aware, this method has not yet been applied to underwater image analysis. Our approach involves estimating the correspondence between consecutive images, triangulating three-dimensional points, and approximating them with a plane. This plane is then virtually reoriented to align with the image plane, thereby reducing measurement errors. At 1.5 m above the seafloor, we achieve an average measurement uncertainty of 6 mm (Anisimov, 2023).

For quantitative analysis of images aided by software applications, researchers primarily work with still images rather than continuous video data (Gomes-Pereira et al., 2016). The usual method for generating sets of still images from video involves extracting frames at fixed time intervals. However, this approach can result in gaps between or overlaps with subsequent frames, which can cause errors in the analysis. Some organisms may be counted multiple times, leading to inaccuracies in biomass and quantity estimates. To address this issue, we developed a Python-based program (available on GitHub) that analyzes the movement of objects in video sequences and calculates the displacement between two frames, referred to as "drift." The program can estimate the optimal time intervals for capturing frames to place seafloor images side by side without overlapping by determining the drift between frames. These non-overlapping frames are referred to as "seafloor fragments." Afterward, each seafloor fragment's distance between red laser marks is calculated to provide a scale. There is an option to manually adjust the drifts and laser mark positions if the program evaluates them incorrectly.

The program provides tools for marking different organisms (Figure 1a) and calculating their linear dimensions (Figure 2b). Every marked organism is associated with the corresponding seafloor fragment. Because the analysis is done using video rather than independent seafloor fragments, users can switch between video frames to select the best lighting and perspective for estimating dimensions without changing the seafloor fragment with which the organism is associated. As a result, we can increase the accuracy of identification and measurements of the organisms in a fixed area of the seafloor. These areas are stacked next to each other, forming the entire transect.

APPLICATION IN THE KARA SEA: SPREAD OF INVASIVE SNOW CRABS

Benthic surveys using *Videomodule* were conducted in the Arctic's Kara Sea, among other polar regions. The software was developed for and used extensively to study the spread of the large predatory snow crab *Chionoecetes opilio* into the Kara Sea (Zalota et al., 2019, 2020; Udalov et al., 2024). Unlike still images, long video transects supplied information on the size structure dynamics of the growing invasive crab population and its density on the seafloor in different regions of the Kara Sea. The software allowed us to use all video footage for the analysis rather than just random fragments, increasing the accuracy of identification by providing views of objects from different angles as the camera passes over, and increasing the accuracy of objects' measurements by using images with the most accurate angle of view in addition to distortion and pitch and tilt corrections. We observed that crabs rarely notice the vehicle and generally do not flee from it. The size structure of crab assemblages calculated from the video is less detailed than that of physical specimens caught by bottom trawls. This is due to measurement errors, which we strive to minimize, and biological factors such as sexual dimorphism that cannot be accounted for in the video. However, the dominant size groups are easily identified from video data and correspond to those observed from trawl data (Zalota et al., 2019). Unlike bottom trawls, video data have allowed us to calculate crab densities in different regions of the sea and observe changes in these densities as the invasion progresses. In addition, no apparent clustering of crabs has been observed. Rather, they are evenly distributed on the flat Kara seafloor unless it has been disturbed. After bottom trawling, crabs gather around the trench created by it, possibly to consume unearthed burrowing organisms.

Videomodule has also been used to investigate the dynamics of benthic communities in response to the invasion of this active predator (Udalov et al., 2024). Research on this topic has been ongoing for more than 10 years, resulting in the collection and analysis of a substantial amount of data on benthic assemblages. The towed camera system has allowed diverse and long-term monitoring of large areas of the seafloor, revealing significant changes in the ecosystem due to the snow crab invasion.

FUTURE WORK

In the absence of standardized methodologies for evaluating the quality of images captured via benthic video surveys, there is a significant gap in our ability to accurately identify organisms. Variations in light conditions, water turbidity, the height of the camera above the seafloor, sensor resolution, and image compression can substantially influence the visibility of organisms. The size, texture, and color of the organisms play crucial roles in this regard. Our objective is to develop criteria that ensure the reliability and comparability of benthic organism analysis under diverse conditions

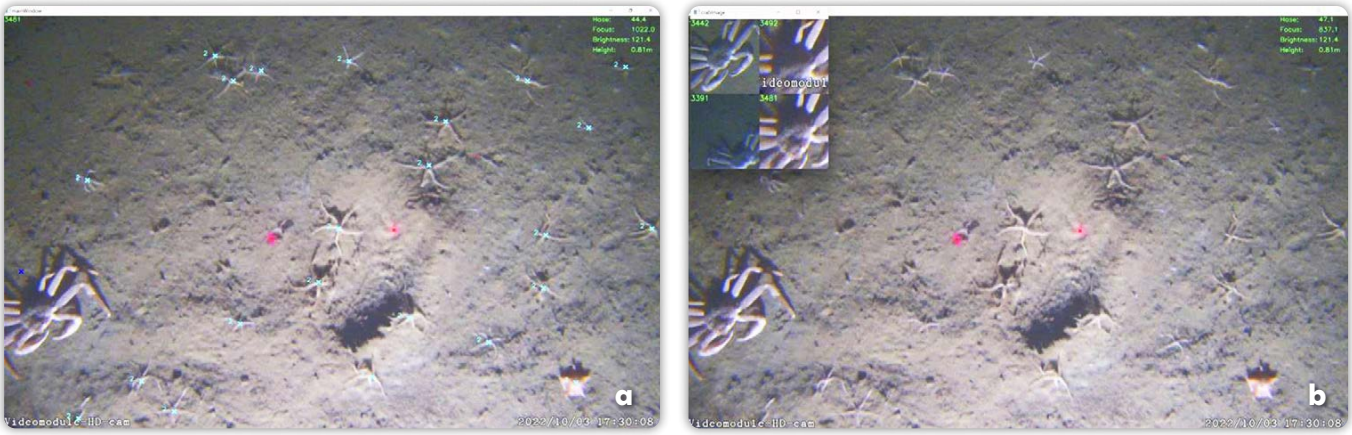

FIGURE 2. Two windows show the interface of *Videomodule*'s Python-based program for video data analysis. (a) The window for marking species in the frame. Light blue dots indicate marked species. Two red dots in the center are laser marks 20 cm apart. (b) The window for carrying out measurements. A dialog box at top right allows selection of optimal measurements for various organisms.

by assessing the impacts of these variables on image quality. At present, we can only reliably compare large organisms under different conditions; however, with such criteria, we could understand size limitations of organisms studied and the associated range of errors.

REFERENCES

Anisimov, I.M. 2023. Improving the accuracy of measuring seabed objects using video images with a laser scaler. [In Russian] *Underwater Investigations and Robotics* 4(46):16–28.

Durden, J.M., T. Schoening, F. Althaus, A. Friedman, R. Garcia, A.G. Glover, J. Greinert, N.J. Stout, D.O.B. Jones, A. Jordt, and others. 2016. Perspectives in visual imaging for marine biology and ecology: From acquisition to understanding. *Oceanography and Marine Biology: An Annual Review* 54:9–80, https://doi.org/10.1201/9781315368597.

Gomes-Pereira, J.N., V. Auger, K. Beisiegel, R. Benjamin, M. Bergmann, D. Bowden, P. Buhl-Mortensen, F.C. De Leo, G. Dionísio, J.M. Durden, and others. 2016. Current and future trends in marine image annotation software. *Progress in Oceanography* 149:106–120, https://doi.org/10.1016/j.pocean.2016.07.005.

Istenič, K., N. Gracias, A. Arnaubec, J. Escartín, and R. Garcia. 2020. Automatic scale estimation of structure from motion based 3D models using laser scalers in underwater scenarios. *ISPRS Journal of Photogrammetry and Remote Sensing* 159:13–25, https://doi.org/10.1016/j.isprsjprs.2019.10.007.

Li, J., W. Xu, L. Deng, Y. Xiao, Z. Han, and H. Zheng. 2023. Deep learning for visual recognition and detection of aquatic animals: A review. *Reviews in Aquaculture* 15(2):409–433, https://doi.org/10.1111/raq.12726.

Mallet, D., and D. Pelletier. 2014. Underwater video techniques for observing coastal marine biodiversity: A review of sixty years of publications (1952–2012). *Fisheries Research* 154:44–62, https://doi.org/10.1016/j.fishres.2014.01.019.

Udalov, A.A., I.M. Anisimov, A.B. Basin, G.V. Borisenko, S.V. Galkin, V.L. Syomin, S.A. Shchuka, M.I. Simakov, A.K. Zalota, and M.V. Chikina. 2024. Changes in benthic communities in Blagopoluchiya Bay (Novaya Zemlya, Kara Sea): The influence of the snow crab. *Biological Invasions* 26:3,455–3,473, https://doi.org/10.1007/s10530-024-03388-1.

Zalota, A.K., O.L. Zimina, and V.A. Spiridonov. 2019. Combining data from different sampling methods to study the development of an alien crab *Chionoecetes opilio* invasion in the remote and pristine Arctic Kara Sea. *PeerJ* 7:e7952, https://doi.org/10.7717/peerj.7952.

Zalota, A.K., V.A. Spiridonov, S. Galkin and A.A. Pronin. 2020. Population structure of alien snow crabs (*Chionoecetes opilio*) in the Kara Sea (trawl and video sampling). *Oceanology* 60(1):83–88, https://doi.org/10.1134/S0001437020010257.

ACKNOWLEDGMENTS

The study was carried out within the state task of IO RAS (topic no. FMWE-2024-0024). In situ data acquisition was conducted with support of the Russian Science Foundation (grant No. 23-17-00156).

AUTHORS

Ivan Anisimov (oceanbreak@gmail.com), **Andrey Lesin**, **Valeriya Muravya**, and **Anna Zalota**, Shirshov Institute of Oceanology of the Russian Academy of Sciences, Moscow, Russia. **Maxim Zalota**, WhoTalks.app, Westbrook, CT, USA.

ARTICLE DOI. https://doi.org/10.5670/oceanog.2025e114

FRONTIERS IN
OCEAN OBSERVING

BE SURE TO CHECK OUT THE COMPLETE ONLINE COLLECTION

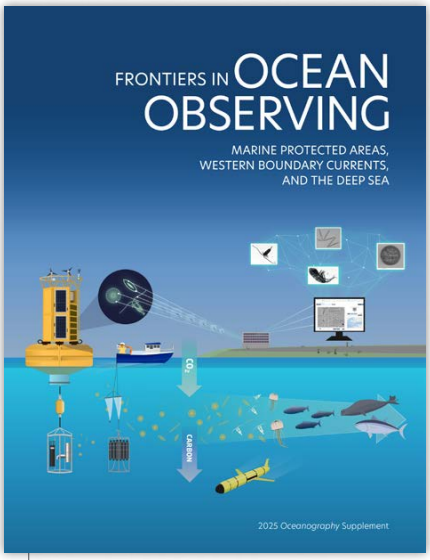

2025 Supplement
Marine Protected Areas, Western Boundary Currents, and the Deep Sea

> Individual Articles
> Full Flipbook

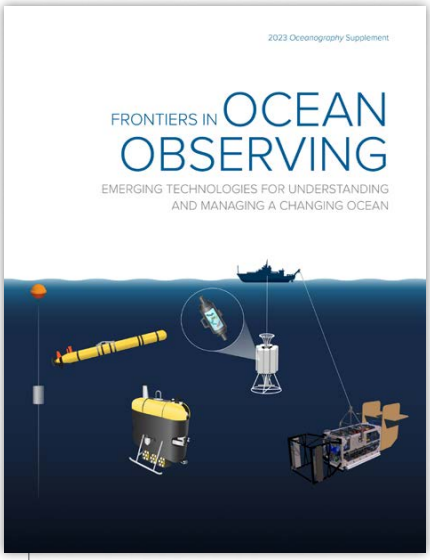

2023 Supplement
Emerging Technologies for Understanding and Managing a Changing Ocean

> Individual Articles
> Full Flipbook

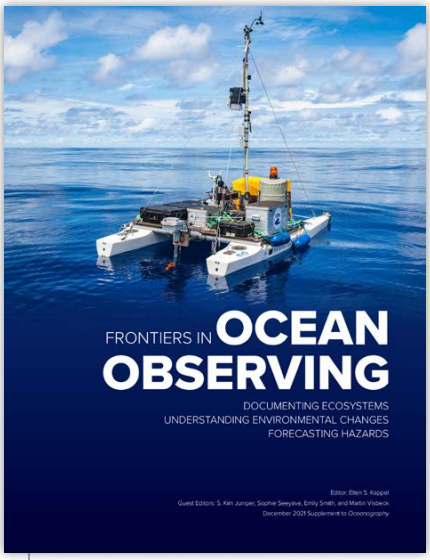

2021 Supplement
Documenting Ecosystems, Undersanding Environmental Changes, Forecasting Hazards

> Individual Articles
> Full Flipbook

PUBLISHER

The Oceanography Society

1 Research Court, Suite 450-117
Rockville, MD 20850 USA
https://tos.org

SPONSORS

Support for this publication is provided by Ocean Networks Canada, the National Oceanic and Atmospheric Administration's Global Ocean Monitoring and Observing Program, and the Partnership for Observation of the Global Ocean.